doi.org/10.26434/chemrxiv.8870324.v2

Functionalized and Degradable Polyphthalaldehyde Derivatives

J. Patrick Lutz, Oleg Davydovich, Matthew Hannigan, Jeffrey S. Moore, Paul M. Zimmerman, Anne McNeil

Submitted date: 22/08/2019 • Posted date: 22/08/2019

Citation information: Lutz, J. Patrick; Davydovich, Oleg; Hannigan, Matthew; Moore, Jeffrey S.; Zimmerman, Paul M.; McNeil, Anne (2019): Functionalized and Degradable Polyphthalaldehyde Derivatives. ChemRxiv. Preprint.

Polymers that depolymerize back to monomers can be repeatedly chemically recycled, thereby reducing their environmental impact. Polyphthalaldehyde is a metastable polymer that is rapidly and quantitatively depolymerized due to its low ceiling temperature. However, the effect of substitution on the physical and chemical properties of polyphthalaldehyde derivatives has not been systematically studied. Herein, we investigate the cationic polymerization of seven distinct o-phthalaldehyde derivatives and demonstrate that judicious choice of substituents results in materials with a wide range of ceiling temperatures (from < −60 to 106 °C) and decomposition temperatures (109–196 °C). We anticipate that these new polymers and their derivatives will enable researchers to access degradable materials with tunable thermal, physical, and chemical properties.

File list (2)

Functionalized and Degradable Polyphthalaldehyde Derivatives

J. Patrick Lutz[†], Oleg Davydovich[§], Matthew D. Hannigan[†], Jeffrey S. Moore[§], Paul M. Zimmerman[†], and Anne J. McNeil[†*]

[†]Department of Chemistry and Macromolecular Science and Engineering Program, University of Michigan, Ann Arbor, Michigan 48109-1055, United States

[§]Department of Chemistry and Beckman Institute for Advanced Science and Technology, University of Illinois at Urbana–Champaign, Urbana, Illinois 61801, United States

ABSTRACT: Polymers that depolymerize back to monomers can be repeatedly chemically recycled, thereby reducing their environmental impact. Polyphthalaldehyde is a metastable polymer that is rapidly and quantitatively depolymerized due to its low ceiling temperature. However, the effect of substitution on the physical and chemical properties of polyphthalaldehyde derivatives has not been systematically studied. Herein, we investigate the cationic polymerization of seven *o*-phthalaldehyde derivatives and demonstrate that judicious choice of substituents results in materials with a wide range of ceiling temperatures (< –60 to 106 °C) and decomposition temperatures (109–196 °C). We anticipate that these new polymers and their derivatives will enable researchers to access degradable materials with tunable thermal, physical, and chemical properties.

While much progress has been made in synthesizing polymers with diverse structures, considerably less attention has been paid to their fates after use. Low–ceiling temperature (T_c) polymers are a class of metastable materials that are readily triggered to depolymerize back to monomers at temperatures above their T_c (Scheme 1).[1,2] Such materials have the potential to address a grand challenge in sustainability by facilitating recycling through repeated depolymerization/repolymerization cycles, extending their useful lifetimes.[3,4] Depolymerizable polymers also have important applications in areas such as lithography,[5] triggered release,[6] and transient electronics.[7]

Polyphthalaldehyde (PPA) is among the most thoroughly studied depolymerizable polymers.[8,9] Linear or cyclic PPA (cPPA) can be obtained via anionic or cationic polymerization (respectively) of *o*-phthalaldehyde (*o*PA) below its T_c of –36 °C.[10,11] While end-capped linear PPA and cPPA are kinetically stable at room temperature, solution-phase exposure to acid results in complete depolymerization at rates too rapid to measure using standard analytical techniques (< 1 min; Scheme 1).[1] The thermodynamic instability of PPA is key to its depolymerization, but this same property has led to challenges in polymer processing.[12] For example, PPA requires plasticizers to improve its processability because its glass transition temperature (T_g) is *above* its thermal degradation temperature.[13]

A small number of substituted polyphthalaldehydes have been reported, primarily for the purpose of increasing thermal stabilities. For example, researchers at IBM found that polyphthalaldehydes bearing 4-bromo, 4-chloro, and 4-trimethylsilyl substitution exhibited higher thermal degradation temperatures than unsubstituted PPA, making them more suitable for photolithographic applications.[14] In related work, Phillips and co-workers showed that end-capped linear poly(4,5-dichlorophthalaldehyde) displayed a similar effect.[15] Poly(4-methylphthalaldehyde) has also been synthesized as a mechanistic probe, [16] but no other PPA derivatives have been reported.

Scheme 1. Low Ceiling Temperature (T_c) Cyclic Polymers

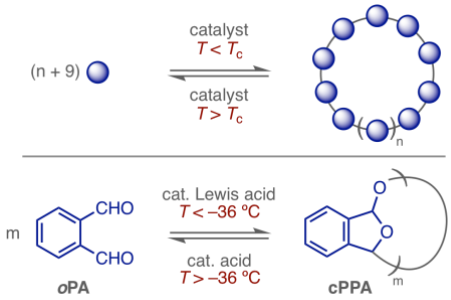

This relative lack of PPA derivatives results in part from the perception that synthesizing substituted *o*-phthalaldehydes is prohibitively challenging, relying on a few established, but often low-yielding, synthetic routes.[8] Furthermore, it is still unclear *a priori* whether a specific phthalaldehyde is polymerizable under experimentally accessible conditions due to a lack of quantitative data on the ceiling temperatures of known PPA derivatives. To address these deficiencies, we set out to synthesize a range of substituted *o*PA derivatives and evaluate their Lewis acid–catalyzed polymerizations. As a result of these studies, we identified four new cPPA derivatives with ceiling temperatures ranging from –23 to +106 °C and demonstrated that their thermal degradation temperatures positively correlate with their T_c. We anticipate that these new polymers will significantly expand the

versatility of the PPA scaffold and that the structure–property relationships will serve as a roadmap for researchers to develop other PPA-based materials with varied physical and chemical properties.

Computational T_c Estimation. To estimate the ceiling temperatures for substituted phthalaldehyde derivatives, a literature method[17] was adapted. Specifically, the acetalization of *o*PA with MeOH was used as the model reaction (Scheme 2, R = H). Density functional theory (B3LYP/6-31++G**)[18] was used to calculate the heat of formation for each reaction component, enabling us to determine the overall enthalpy (ΔH) for the equilibrium (SI pgs S100–S122). Using our measured T_c for *o*PA of –36 °C (vida infra), we computed the entropy (ΔS) from Eq. 1:

$$T_c = \frac{\Delta H}{\Delta S} \qquad (1)$$

We next assumed that the ΔS determined for *o*PA would be similar for the substituted derivatives, given that the changes in bonding are similar for each reaction. With this assumption, the ceiling temperature was estimated by calculating the ΔH for each *o*PA derivative and solving Eq. 1 for T_c. We chose to focus exclusively on symmetrically substituted derivatives because nonsymmetrically substituted *o*PAs would have electronically distinct acetal linkages, making it difficult to disentangle the effects of different substituents.

Scheme 2. Model Reaction for Phthalaldehyde Polymerization

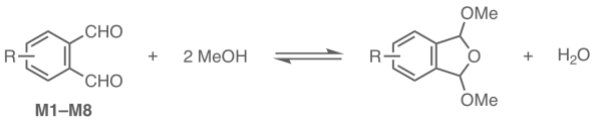

Our computations suggested that simple changes to *o*PA yield monomers with ceiling temperatures ranging from –122 °C to +98 °C (Table 1). As expected, electron-donating substituents resulted in a predicted T_c below that of *o*PA (**M1**–**M3**), while electron-withdrawing substituents led to higher T_c values (**M6**–**M8**), in line with these substituents' relative abilities to impact aldehyde electrophilicity.[15,17]

Monomer Synthesis and Homopolymerization. We devised and executed 2–5 step synthetic routes to substituted *o*PAs **M1**–**M4** and **M6**–**M8** (SI pgs S4–S24). Notably, during purification, monomers **M6**–**M8** underwent carbonyl hydrate formation and oligomerization to varying extents on silica, suggesting that their ceiling temperatures were near or above room temperature. In each of these cases, the dialdehyde was obtained via vacuum sublimation.[19]

We next subjected each monomer to $SnCl_4$-catalyzed cationic polymerization conditions at –78 °C in DCM. The reactions were quenched by adding pyridine to sequester the Lewis acid, then the polymers were precipitated into MeOH and isolated by vacuum filtration.[10] As a baseline, the reaction of unsubstituted *o*PA (**M5**) produced cPPA (**P5**) in 35% isolated yield (Table 1, entry 5). Propoxy-substituted **M1**, butylthio-substituted **M2**, and hexyl-substituted **M3** all possess estimated ceiling temperatures < –78 °C and were therefore not expected to generate polymer under these conditions. Consistent with the predictions, these monomers failed to generate isolable polymers; ^{1}H NMR spectroscopic analysis following attempted precipitation from MeOH and solvent removal revealed mixtures of monomer and the corresponding dimethyl acetals (entries 1–3; see also Figure S25). In contrast to **M1**–**M3**, the estimated T_c of hexynyl-substituted **M4** (–60 °C) suggested that its polymerization was feasible. Indeed, **P4** was isolated in 64% yield (entry 4). Methyl ester–substituted **M6**, phthalimide derivative **M7**, and tetrafluorophthalaldehyde **M8** had predicted ceiling temperatures substantially higher than that of *o*PA, and all three were effectively polymerized at –78 °C (entries 6–8).

Table 1. Cationic Polymerization of *o*PA Derivatives[a]

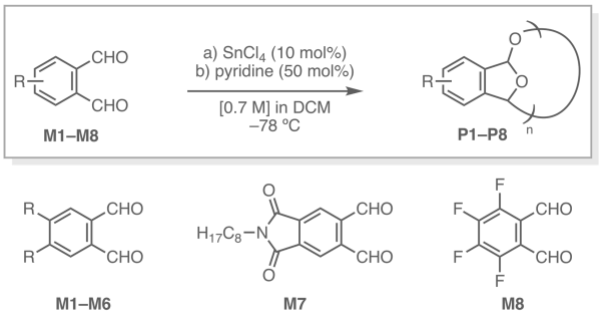

monomer	R =	est. T_c[b] (°C)	Yield[c] (%)	M_n (kg/mol)	Đ
M1	OPr	–122	0	–	–
M2	SBu	–86	0	–	–
M3	*n*-C_6H_{13}	–80	0	–	–
M4	C≡CBu	–60	64	12.3	2.2
M5	H	–36[d]	35	3.2	2.2
M6	CO_2Me	–2	48	11.7	1.7
M7	–	+43	83	25.1	1.9
M8	–	+98	53	16.2	2.0

[a]Entries 4–8 represent the average of two runs. [b]At 1 M. [c]Isolated yield. [d]Experimentally determined.

Ceiling Temperature Measurement and Thermal Analysis. While the results of the polymerizations were qualitatively consistent with our T_c estimations, we sought to evaluate these predictions quantitatively. To do so, a variable-temperature ^{1}H NMR spectroscopic method was adapted from a protocol by Kohl and co-workers (SI pgs 72–97).[20] Solutions with known initial concentrations of monomer ($[M]_0$) and catalyst were prepared. Then, the monomer concentration ([M]) was measured at different temperatures by integrating the aldehyde C–H resonance versus an internal standard. Consistent with the predicted ceiling temperatures, we observed dramatic differences in monomer conversion based on the phthalaldehyde substitution: hexyl-substituted **M3** showed <5% conversion at –60 °C, whereas tetrafluorophthalaldehyde **M8** reached >95% conversion at rt (Figure 1). In the absence of a Lewis basic quenching agent, the polymerizations were reversible; warming the reactions to the starting temperatures

regenerated the dialdehyde monomers.

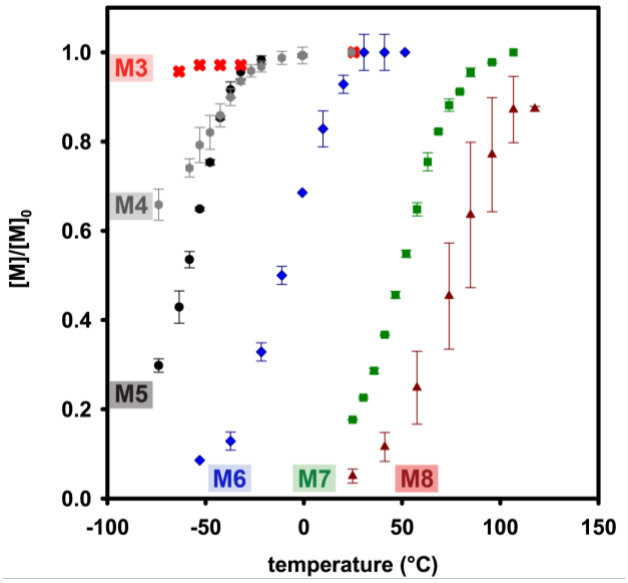

Figure 1. Plot of the normalized monomer concentrations versus temperature in the presence of 10 mol% $SnCl_4$. ([**M6**]$_0$ = 0.35 M; [M]$_0$ = 0.70 M for all other monomers.)

To quantitatively determine the ceiling temperature, the data from each reaction were plotted as $R \bullet \ln[M]$ versus $1/T$, where R is the universal gas constant. The slope and intercept of the resulting line correspond respectively to the ΔH and ΔS for the polymerization. From these two values, Eq. 2 was used to calculate the experimental T_c.[21] Performing this analysis on *o*PA provided a ceiling temperature of –36 °C (Table 2, entry 5), in close agreement with the results of Kohl and co-workers.[20] We could not measure T_c values for **M1**–**M3** due to the limited temperature range of the NMR probe; however, –60 °C provides an upper limit (entries 1–3).

$$T_c = \frac{\Delta H}{\Delta S + R \bullet \ln[M]_0} \qquad (2)$$

Hexynyl-substituted **M4** displayed a T_c of –23 °C, slightly *above* that of *o*PA. This result is consistent with the weak electron-withdrawing nature of alkynyl groups[22] (σ_m = 0.21, σ_p = 0.03 for –C≡CMe).[23] Ester-substituted **M6** exhibited a T_c of 13 °C, in line with the stronger electron-withdrawing abilities of esters (σ_m = 0.36, σ_p = 0.45 for $-CO_2Me$).[24] Both phthalimide **M7** and tetrafluorophthalaldehyde **M8** had ceiling temperatures significantly higher than room temperature (74 and 106 °C, respectively) due to the even stronger resonance- and inductive-withdrawing effects of these substituents.

While our estimations of ceiling temperatures were qualitatively accurate and useful in identifying a range of substrates to examine, there are substantial quantitative differences between computed and experimental values. Examining the thermodynamic parameters in Table 2 reveals that a contributing factor in this discrepancy was our flawed assumption that the ΔS would remain approximately constant for the different monomers. In fact, a ~7-fold difference in ΔS was observed for **M4** versus **M8**.[25]

Table 2. Thermodynamic Parameters for Polymerizing M1–M8[a]

monomer	est. T_c[b] (°C)	ΔH (kcal/mol)	ΔS (cal/mol•K)	expt. T_c (°C)
M1[d]	–122	–	–	< –60
M2[d]	–86	–	–	< –60
M3[d]	–80	–	–	< –60
M4[d]	–60	–0.90	–2.9	–23
M5[d]	n/a	–3.0	–11.9	–36
M6[e]	–2	–4.9	–14.9	+13
M7[f]	+43	–7.0	–19.3	+74
M8[f]	+98	–7.9	–20.1	+106

[a]Entries 4–8 represent the average of two runs. [b]At 1 M. [c]Corrected to 1 M. [d]CD_2Cl_2 solvent. [e]$CDCl_3$ solvent. [d]1,1,2,2-Tetrachloroethane-d_2 solvent.

Following purification,[12] the polymers' thermal decomposition temperatures (T_d) were measured by differential scanning calorimetry (DSC; SI pgs S49–S71).[26] A positive relationship between T_c and T_d was apparent, with T_d ranging from 109 °C for **M5** to 196 °C for **M8** (Figure 2A). Interestingly, polymer **P8** was the only polymer to exhibit a glass transition *below* its decomposition temperature (Figure 2B), suggesting that **P8** could have processing advantages over unsubstituted PPA.

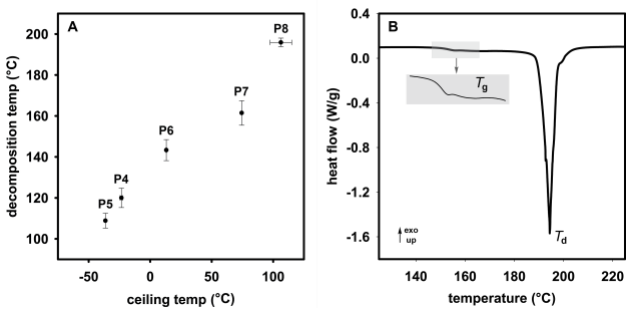

Figure 2. (A) Plot of decomposition temperature (via DSC) versus the experimental ceiling temperature for **P4**–**P8** (via ^{1}H NMR spectroscopy). (B) DSC thermogram for **P8**.

Cationic Copolymerization. To elucidate the impact of copolymer composition on thermal stabilities, we copolymerized **M5** with **M6** at feed ratios ranging from 0–100 mol% **M6** (SI pgs S54–S62).[27] Following purification, the cumulative copolymer composition was estimated via ^{1}H NMR spectroscopy. A linear trend between copolymer composition and feed ratio was evident (Figure 3A), suggesting either an alternating or statistical sequence. Thermal analysis of the copolymers revealed a near-linear relationship between copolymer composition and T_d (Figure 3B). The slight non-linearity is likely a result of differing levels of residual Lewis acid remaining in the (co)polymers after purification.[12,28] A similar trend in decomposition temperature has been reported for copolymers of *o*PA with ethyl glyoxylate.[13] These results demonstrate that PPA substitution patterns and incorporation ratios can be

rationally designed to obtain copolymers with targeted thermal properties, though improvements to the purification process will likely be required to ensure consistent results.

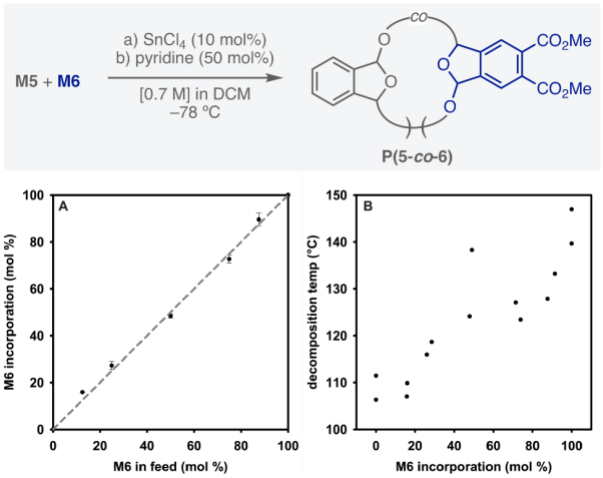

Figure 3. (A) Plot of **M6** incorporation in **P(5-*co*-6)** (via ^{1}H NMR spectroscopy) versus **M6** composition in the feed. The dashed line is for a 1:1 relationship. (B) Plot of decomposition temperature (via DSC) versus **M6** incorporation in **P(5-*co*-6)**.

Microcapsule fabrication. In previous work, cPPA was used to form triggerable core–shell microcapsules.[29] The new PPA derivatives described herein could generate capsules that exhibit different surface functionalities, specific ion coactivators,[29b] and rates of payload release. For a preliminary study, **P6** was prepared on gram scale in 76% yield (SI pg S71) and subjected to the previously described microencapsulation conditions optimized for unsubstituted cPPA (SI pgs S98–S99).[29a] Briefly, oil-in-water emulsions comprised of **P6**/jojoba oil/DCM in aqueous poly(vinyl alcohol) were generated via a microfluidic flow focusing device. Rapid evaporation of the DCM followed by filtering and washing furnished microcapsules with an average diameter of 228 ± 5 µm. Scanning electron microscopy (SEM) confirmed these capsules exhibited a core–shell architecture, with an estimated shell-wall thickness of 11 µm (Figure 4). These **P6** microcapsules represent a potential starting point to generate anionic, cationic, and labelled depolymerizable capsules via post-encapsulation functionalization reactions.

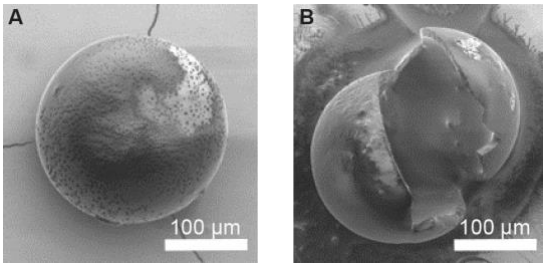

Figure 4. SEM images of (A) intact and (B) ruptured **P6** microcapsules.

To summarize, seven substituted *o*-phthalaldehyde derivatives were synthesized and subjected to cationic polymerization conditions. As predicted computationally, several of these compounds were unreactive at –78 °C due to their low ceiling temperatures; however, four new polyphthalaldehydes bearing alkyne, ester, imide, and fluorine substituents were successfully synthesized due to their higher ceiling temperatures. Remarkably, poly(tetrafluorophthalaldhyde) is both highly stable and likely thermally processable. We anticipate that these (co)polymers, as well as derivatives synthesized via post-polymerization modification, will enable researchers to access degradable materials with tunable thermal, physical, and chemical properties. Moreover, the combined computational and experimental method to predict and measure ceiling temperatures should help guide the synthesis of new PPA derivatives.

ASSOCIATED CONTENT

Supporting Information. Experimental details, characterization data, synthetic procedures.

AUTHOR INFORMATION

Corresponding Author

*ajmcneil@umich.edu

ORCID

J. Patrick Lutz 0000-0002-5795-5049

Oleg Davydovich 0000-0002-1096-7034

Matthew D. Hannigan 0000-0002-2267-1388

Jeffrey S. Moore 0000-0001-5841-6269

Paul M. Zimmerman 0000-0002-7444-1314

Anne J. McNeil 0000-0003-4591-3308

ACKNOWLEDGMENT

We (AJM and JSM) gratefully acknowledge the National Science Foundation for supporting this work through a Phase I Center for Chemical Innovation Grant (CHE–1740597) as well as the Department of Defense for a National Defense Science and Engineering Graduate Fellowship for MDH.

REFERENCES

[1] Kaitz, J.A.; Lee, O.P.; Moore, J.S. Depolymerizable Polymer: Preparation, Applications, and Future Outlook. *MRS Communications* **2015**, *5*, 191–204.

[2] Yardley, R.E.; Kenaree, A.R.; Gillies, E.R. Triggering Depolymerization: Progress and Opportunities for Self-Immolative Polymers. *Macromolecules* doi: 10.1021/acs.macromol.9b00965.

[3] Hong, M.; Chen, E.Y.-X. Chemically Recyclable Polymers: A Circular Economy Approach to Sustainability. *Green Chem.* **2017**, *19*, 3692–3706.

[4] Lloyd, E.M.; Hernandez, H.L.; Feinberg, A.M.; Yourdkhani, M.; Zen, E.K.; Mejia, E.B.; Sottos, N.R.; Moore, J.S.; White, S.R. Fully Recyclable Metastable Polymers and Composites. *Chem. Mater.* **2019**, *31*, 398–406.

[5] Bowden, M.J.; Thompson, L.F. Electron Irradiation of Poly(olefin sulfones). Application to Electron Beam Resists. *J. Appl. Polym. Sci.* **1973**, *17*, 3211–3221.

[6] Esser-Kahn, A.P.; Odom, S.A.; Sottos, N.R.; White, S.R.; Moore, J.S. Triggered Release from Polymer Capsules. *Macromolecules* **2011**, *44*, 5539–5553.

[7] Fu, K.K.; Wang, Z.; Dai, J.; Carter, M.; Hu, L. Transient Electronics: Materials and Devices. *Chem. Mater.* **2016**, *28*, 3527–3539.

[8] Wang, F.; Diesendruck, C.E. Polyphthalaldehyde: Synthesis, Derivatives, and Applications. *Macromol. Rapid Commun.* **2018**, *39*, 1700519.

[9] (a) Aso, C.; Tagami, S. Cyclopolymerization of *o*-Phthalaldehyde. *J. Polym. Sci. Part B: Polym. Lett.* **1967**, *5*, 217–220. (b) Aso, C.; Tagami, S.; Kunitake, T. Polymerization of Aromatic Aldehydes. II. Cationic Cyclopolymerization of Phthalaldehyde. *J. Polym. Sci. Part A: Polym. Chem.* **1969**, *7*, 497–511. (c) Aso, C.; Tagami, S. Polymerization of Aromatic Aldehydes. III. The Cyclopolymerization of Phthalaldehyde and the Structure of the Polymer. *Macromolecules* **1969**, *2*, 414–419.

[10] Kaitz, J.A.; Diesendruck, C.E.; Moore, J.S. End Group Characterization of Poly(phthalaldehyde): Surprising Discovery of a Reversible, Cationic Macrocyclization Mechanism. *J. Am. Chem. Soc.* **2013**, *135*, 12755–12761.

[11] Ceiling temperatures ranging from –35 to –43 °C have been reported for PPA. We use our own experimentally determined temperature of –36 °C throughout this manuscript.

[12] Feinberg, A.M.; Lopez Hernandez, H.; Plantz, C.L.; Mejia, E.B.; Sottos, N.R.; White, S.R.; Moore, J.S. Cyclic Poly(phthalaldehyde): Thermoforming a Bulk Transient Material. *ACS Macro. Let.* **2018**, *7*, 47–52.

[13] Kaitz, J.A.; Moore, J.S. Copolymerization of *o*-Phthalaldehyde and Ethyl Glyoxylate: Cyclic Macromolecules with Alternating Sequence and Tunable Thermal Properties. *Macromolecules* **2014**, *47*, 5509–5513.

[14] (a) Ito, H.; Schwalm, R. Thermally Developable, Positive Resist Systems with High Sensitivity. *J. Electrochem. Soc.* **1989**, *136*, 241–245. (b) Ito, H.; Ueda, M.; Renaldo, A.F. Thermally Developable, Positive Tone, Oxygen RIE Barrier Resist for Bilayer Lithography. *J. Electrochem. Soc.* **1989**, *136*, 245–249.

[15] (a) DiLauro, A.M.; Phillips, S. T. End-Capped Poly(4,5-dichlorphthalaldehyde): A Stable Self-Immolative Poly(aldehyde) for Translating Specific Inputs into Amplified Outputs, Both in Solution and the Solid State. *Polym. Chem.* **2015**, *6*, 3252–3258. (b) DiLauro, A.M.; Lewis, G.G.; Phillips, S.T. Self-Immolative Poly(4,5-dichlorophthalaldehyde) and its Applications in Multi-Stimuli-Responsive Macroscopic Plastics. *Angew. Chem. Int. Ed.* **2015**, *54*, 6200–6205.

[16] Kaitz, J.A.; Diesendruck, C.E.; Moore, J.S. Dynamic Covalent Macrocyclic Poly(phthalaldehyde)s: Scrambling Cyclic Homopolymer Mixtures Produces Multi-Block and Random Cyclic Copolymers. *Macromolecules* **2013**, *46*, 8121–8128.

[17] Kaitz, J.A.; Moore, J.S. Functional Phthalaldehyde Polymers by Copolymerization with Substituted Benzaldehydes. *Macromolecules* **2013**, *46*, 608–612.

[18] Shao, Y.; Gan, Z.; Epifanovsky, E.; Gilbert, A.T.B.; Wormit, M.; Kussmann, J.; Lange, A.W.; Behn, A.; Deng, J.; Feng, X.; Ghosh, D.; Goldey, M.; Horn, P.R.; Jacobson, L.D.; Kaliman, I.; Khaliullin, R.Z.; Kús, T.; Landau, A.; Liu, J.; Proynov, E.I.; Rhee, Y.M.; Richard, R.M.; Rohrdanz, M.A.; Steele, R.P.; Sundstrom, E.J.; Woodcock III, H.L.; Zimmerman, P.M.; Zuev, D.; Albrecht, B.; Alguire, E; Austin, B.; Beran, G.J.O.; Bernard, Y.A.; Berquist, E.; Brandhorst, K.; Bravaya, K.B.; Brown, S.T.; Casanova, D.; Chang, C.-M.; Chen, Y.; Chien, S.H.; Closser, K.D.; Crittenden, D.L.; Diedenhofen, M.; DiStasio Jr., R.A.; Dop, H.; Dutoi, A.D.; Edgar, R.G.; Fatehi, S.; Fusti-Molnar, L.; Ghysels, A.; Golubeva-Zadorozhnaya, A.; Gomes, J.; Hanson-Heine, M.W.D.; Harbach, P.H.P.; Hauser, A.W.; Hohenstein, E.G.; Holden, Z.C.; Jagau, T.-C.; Ji, H.; Kaduk, B.; Khistyaev, K.; Kim, J.; Kim, J.; King, R.A.; Klunzinger, P.; Kosenkov, D.; Kowalczyk, T.; Krauter, C.M.; Lao, K.U.; Laurent, A.; Lawler, K.V.; Levchenko, S.V.; Lin, C.Y.; Liu, F.; Livshits, E.; Lochan, R.C.; Luenser, A.; Manohar, P.; Manzer, S.F.; Mao, S.-P.; Mardirossian, N.; Marenich, A.V.; Maurer, S.A.; Mayhall, N.J.; Oana, C.M.; Olivares-Amaya, R.; O'Neill, D.P.; Parkhill, J.A.; Perrine, T.M.; Peverati, R.; Pieniazek, P.A.; Prociuk, A.; Rehn, D.R.; Rosta, E.; Russ, N.J.; Sergueev, N.; Sharada, S.M.; Sharmaa, S.; Small, D.W.; Sodt, A.; Stein, T.; Stück, D.; Su, Y.-C.; Thom, A.J.W.; Tsuchimochi, T.; Vogt, L.; Vydrov, O.; Wang, T.; Watson, M.A.; Wenzel, J.; White, A.; Williams, C.F.; Vanovschi, V.; Yeganeh, S.; Yost, S.R.; You, Q.-Z.; Zhang, I.Y.; Zhang, X.; Zhou, Y.; Brooks, B.R.; Chan, G.K.L.; Chipman, D.M.; Cramer, C.J.; Goddard III, W.A.; Gordon, M.S.; Hehre, W.J.; Klamt, A.; Schaefer III, H.F.; Schmidt, M.W.; Sherrill, C.D.; Truhlar, D.G.; Warshel, A.; Xua, X.; Aspuru-Guzik, A.; Baer, R.; Bell, A.T.; Besley, N.A.; Chai, J.-D.; Dreuw, A.; Dunietz, B.D.; Furlani, T.R.; Gwaltney, S.R.; Hsu, C.-P.; Jung, Y.; Kong, J.; Lambrecht, D.S.; Liang, W.; Ochsenfeld, C.; Rassolov, V.A.; Slipchenko, L.V.; Subotnik, J.E.; Van Voorhis, T.; Herbert, J.M.; Krylov, A.I.; Gill, P.M.W.; Head-Gordon, M. Advances in Molecular Quantum Chemistry Contained in the Q-Chem 4 Program Package. *Mol. Phys.* **2015**, *113*, 184–215.

[19] Monomer **M8** was isolated in ~80% purity, presumably due to oligomerization during vacuum sublimation as a result of its high electrophilicity.

[20] Schwartz, J.M.; Engler, A.; Phillips, O.; Lee, J.; Kohl, P.A. Determination of Ceiling Temperature and Thermodynamic Properties of Low Ceiling Temperature Polyaldehydes. *J. Polym. Sci. Part A: Polym. Chem.* **2017**, *56*, 221–228.

[21] Dainton, F.S.; Ivin, K.J. Reversibility of the Propagation Reaction in Polymerization Processes and its Manifestation in the Phenomenon of a 'Ceiling Temperature.' *Nature* **1948**,*162*, 705–707.

[22] Bizier, N.P.; Wackerly, J.Wm.; Braunstein, E.D.; Zhang, M.; Nodder, S.T.; Carlin, S. M.; Katz, J.L. An Alternative Role for Acetylenes: Activation of Fluorobenzenes toward Nucleophilic Aromatic Substitution. *J. Org. Chem.* **2013**, *78*, 5987–5998.

[23] Charton, M. Electrical Effect Substituent Constants for Correlation Analysis. In *Progress in Physical Organic Chemistry*; Taft, R.W., Ed.; Wiley: New York, 1981; Vol. 13; pp 119–251.

24 Little, W.F.; Reilley, C.N.; Johnson, J.D.; Lynn, K.N.; Sanders, A.P. Chronopotentiometric Studies of Ferrocene Derivatives. I.

Determination of Substituent Constants with Substituted Phenylferrocenes. *J. Am. Chem. Soc.* **1964**, *86*, 1376–1381.

[25] The rationale for this large entropy difference is unclear at this time.

[26] Thermogravimetric analysis was unsuitable, as the T_d for some polymers was above or similar to the monomer volatilization temperature.

[27] Copolymers of *o*PA with monoaldehydes have been reported. See refs. 13, 17, and (a) Schwartz, J.M.; Gourdin, G.; Phillips, O.; Engler, A.; Lee, J.; Abdulkadir, N.R.; Miller, R.C.; Sutlief, A.; Kohl, P.A. Cationic Polymerization of High-Molecular Weight Phthalaldehyde–Butanal Copolymer. *J. Appl. Polym. Sci.* **2019**, *136*, 46921. (b) Engler, A.; Phillips, O.; Miller, R.C.; Tobin, C.; Kohl, P.A. Cationic Copolymerization of *o*-Phthalaldehyde and Functional Aliphatic Aldehydes. *Macromolecules* **2019**, *52*, 4020–4029.

[28] Schwartz, J.M.; Phillips, O.; Engler, A.; Sutlief, A.; Lee, J.; Kohl, P.A. Stable, High-Molecular-Weight Poly(phthalaldehyde). *J. Polym. Sci. Part A: Polym. Chem.* **2017**, *55*, 1166–1172.

[29] (a) Tang, S.; Yourdkhani, M.; Possanza Casey, P.M.; Sottos, N.R.; White, S.R.; Moore, J.S. Low–Ceiling-Temperature Polymer Microcapsules with Hydrophobic Payloads via Rapid Emulsion-Solvent Evaporation. *ACS Appl. Mater. Interfaces* **2017**, *9*, 20115–20123. (b) Tang, S.; Tang, L.; Lu, X.; Liu, H.; Moore, J.S. Programmable Payload Release from Transient Polymer Microcapsules Triggered by a Specific Ion Coactivation Effect. *J. Am. Chem. Soc.* **2018**, *140*, 94–97.

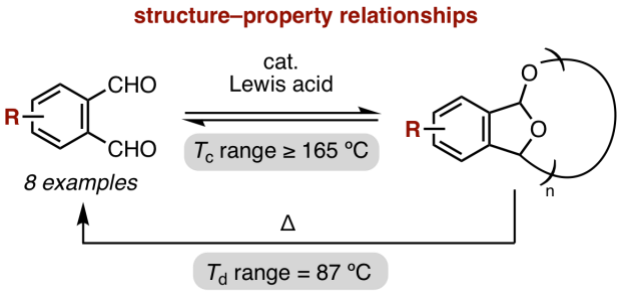
structure–property relationships
cat.
Lewis acid
R
CHO
CHO
8 examples
T_c range ≥ 165 °C
R
O
O
n
Δ
T_d range = 87 °C

Supporting Information for:

Functionalized and Degradable Polyphthalaldehyde Derivatives

J. Patrick Lutz[†], Oleg Davydovich[§], Matthew D. Hannigan[†], Jeffrey S. Moore[§], Paul M. Zimmerman[†], and Anne J. McNeil[†]*

[†]*Department of Chemistry and Macromolecular Science and Engineering Program, University of Michigan, Ann Arbor, Michigan, 48109-1055, United States*

[§] *Department of Chemistry and Beckman Institute for Advanced Science and Technology, University of Illinois at Urbana−Champaign, Urbana, Illinois 61801, United States*

Table of Contents

I. Materials

Flash chromatography was performed on SiliCycle silica gel (40–63 μm) using a Biotage Isolera One. Thin-layer chromatography was performed on Merck TLC plates (pre-coated with silica gel 60 F254). The glovebox in which specified procedures were carried out was an MBraun LABmaster 130 with a N_2 atmosphere.

ortho-Phthalaldehyde (*o*PA, **M5**) was purchased from Oakwood and recrystallized (x3) from dichloromethane/hexanes (5:2) for use in the ^{1}H NMR spectroscopic ceiling temperature measurements.[1] *o*PA used for the preparative-scale synthesis of **P5** and **P5-*co*-6** was purified by vacuum sublimation (120 ºC, ~0.1 torr).

Polyvinyl alcohol (13–23 kDa, 87–89% hydrolyzed) and jojoba oil used for the microencapsulation experiments were purchased from Aldrich.

CD_2Cl_2 and $CDCl_3$ used for the ^{1}H NMR spectroscopic ceiling temperature measurements were distilled, then freeze–pump–thawed (x3). Tetrahydrofuran (THF), toluene, and dichloromethane (DCM) were dried and deoxygenated using an Innovative Technology solvent purification system composed of activated alumina, copper catalyst, and molecular sieves. All other reagent-grade materials and solvents were purchased from Aldrich, Fisher, Strem, Santa Cruz Biotechnology, Scientific Polymer Products, or Oakwood and were used without further purification.

II. General Experimental

NMR Spectroscopy – Unless otherwise noted, ^{1}H, ^{13}C, and ^{19}F NMR spectra were acquired at rt. Chemical shift data are reported in units of δ (ppm) relative to tetramethylsilane (TMS); ^{1}H and ^{13}C spectra are referenced to residual solvent. Multiplicities are reported as follows: singlet (s), doublet (d), doublet of doublets (dd), triplet (t), quartet (q), multiplet (m).

High-Resolution Mass Spectrometry (HRMS) – High-resolution mass spectrometry data were obtained on a Micromass AutoSpec Ultima Magnetic Sector mass spectrometer.

Size-Exclusion Chromatography (SEC) – For SEC analysis, all polymers were dried under vacuum overnight, dissolved (~0.5 mg polymer/mL) in THF spiked with trace toluene (<1 vol%) with sonication if necessary, and filtered through a PTFE filter (0.2 μm). Polymer molecular weights were determined by comparison with polystyrene standards (Varian, EasiCal PS-2 MW 580–377, 400) at 40 °C in THF on a Malvern Viscotek GPCMax VE2001 equipped with two Viscotek LT-5000L 8 mm (ID) × 300 mm (L) columns and analyzed with Viscotek TDA 305, or on a Shimadzu LC-20AD equipped with two Styragel HT 7.8 mm (ID) x 300 mm (L) columns and a PSS Gram column 8 mm (ID) x 300 mm (L) and analyzed with Shimadzu SPD-M20A. Data presented correspond to the absorbance at 254 nm normalized to the highest peak, and data were obtained at a flow rate of 1 mL/min.

Fourier-Transform Infrared (FTIR) Spectroscopy – FTIR spectroscopy data were obtained on a Thermo-Nicolet IS-50 using the attenuated total reflectance (ATR) accessory on neat samples.

Differential Scanning Calorimetry (DSC) – DSC was performed under N_2 on a TA Instruments DSC Q2000 equipped with a TA RCS coolin accessory. Samples (~1–2 mg) were placed in aluminum pans (Tzero Low-Mass Hermetic) and sealed using a TA Instruments crimper. Samples were equilibrated at 40 ºC for 5 min, then heated to 300 ºC at a ramp rate of 5 ºC/min.

Elemental Analysis (EA) – EA was performed by Midwest Microlab.

Scanning Electron Microscopy (SEM) – SEM images were obtained on a FEI Quanta FEG 450 ESEM.

III. Monomer Syntheses

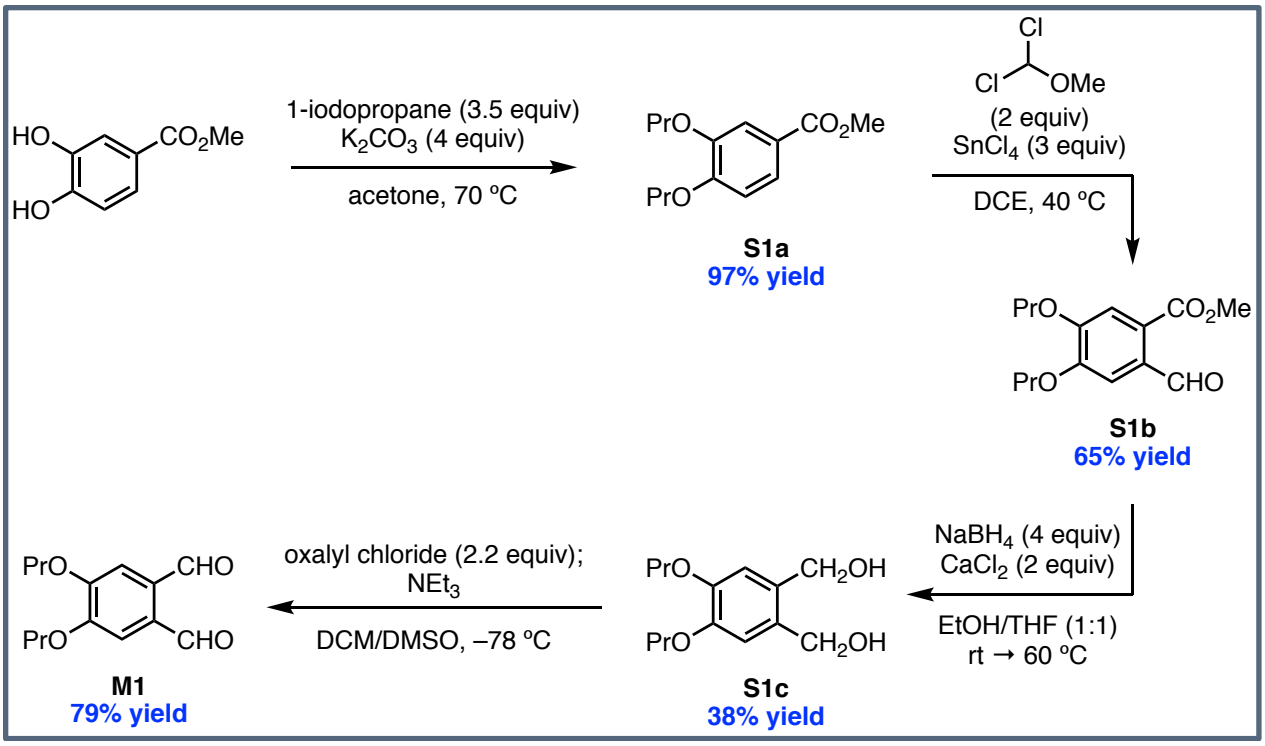

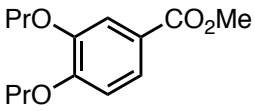

S1a

Methyl 3,4-dipropoxybenzoate (S1a).[2] A 500-mL round-bottomed flask was charged sequentially with methyl 3,4-dihydroxybenzoate (7.00 g, 41.6 mmol, 1.00 equiv), potassium carbonate (23.0 g, 166 mmol, 4.00 equiv), a stir bar, acetone (150 mL), and 1-iodopropane (12.2 mL, 125 mmol, 3.00 equiv). The flask was capped with a reflux condenser and stirred at 70 °C for 23 h, at which point TLC suggested a mixture of **S1a** and monoalkylated compound. An additional charge of 1-iodopropane (2.0 mL, 21 mmol, 0.49 equiv) was added, and stirring was continued at 70 °C for 4 h, at which point TLC indicated full conversion to **S1a**. The reaction was cooled to rt, then saturated aqueous $NaHCO_3$ (50 mL) and water (100 mL) were added. The mixture was extracted with ether (3 x 100 mL), and the combined organic extracts were washed with brine (50 mL), dried over $MgSO_4$, and filtered. The resulting solution was concentrated on the rotary evaporator and further dried under vacuum to yield **S1a** as a yellow solid (10.2 g, 40.4 mmol, 97% yield) that was used without further purification.

R_f: 0.64 in 30% EtOAc in hexanes.

FTIR (ATR): ν 2963.05 (m), 2947.19 (m), 2877.06 (m), 1715.54 (s), 1596.62 (m), 1585.10 (m), 1517.19 (m), 1467.85 (w), 1437.53 (s), 1424.84 (m), 1391.33 (m), 1349.79 (w), 1289.65 (s), 1268.37 (m), 1249.46 (m), 1216.27 (s), 1186.90 (m), 1137.16 (s), 1098.71 (s), 1060.14 (m),

1007.52 (m), 973.57 (s), 931.51 (w), 896.78 (m), 873.15 (m), 873.15 (m), 823.41 (m), 807.27 (m), 756.22 (s), 725.13 (m), 647.51 (m), 606.86 (w) cm^{-1}.

HRMS (ESI+): Calc'd for $C_4H_{21}O_4^+$ [M+H$^+$]: 253.1434; found: 253.1437.

NMR: See Figure S1 on pg S25.

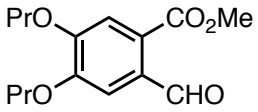

S1b

Methyl 2-formyl-4,5-dipropoxybenzoate (S1b).[3] A flame-dried, 200-mL recovery flask was charged with a stir bar and **S1a** (5.00 g, 19.8 mmol, 1.00 equiv), then evacuated and refilled with N_2 (x3). Anhydrous DCE (60 mL) and dichloromethyl methyl ether (3.6 mL, 40 mmol, 2.0 equiv) were added sequentially, and the reaction vessel was cooled to 0 °C in an ice/water bath. Neat $SnCl_4$ (7.0 mL, 59 mmol, 3.0 equiv) was added over the course of ~5 min. Following the addition, the reaction was transferred to an oil bath at 40 °C and stirred for 3 h, at which point TLC indicated full consumption of **S1a**. The reaction was transferred to an ice/water bath and carefully quenched with saturated aqueous $NaHCO_3$ (120 mL – caution: vigorous bubbling occurred). The organic/aqueous layers were separated, and the aqueous layer was extracted with DCM (3 x 50 mL). The combined organic fractions were washed with brine (50 mL), dried over $MgSO_4$, filtered, and concentrated on the rotary evaporator to provide a dark brown oil. The crude material was purified using automated column chromatography (100 g column, 1 → 30% EtOAc in hex) to afford **S1b** as an off-white solid (3.62 g, 19.8 mmol, 65% yield).

R_f: 0.51 in 30% EtOAc in hexanes.

FTIR (ATR): ν 2971.16 (w), 2883.46 (w), 1702.77 (s), 1676.99 (s), 1579.19 (s), 1520.81 (m), 1471.73 (m), 1433.10 (m), 1389.56 (w), 1354.12 (m), 1258.11 (s), 1212.57 (s), 1185.83 (s), 1154.83 (s), 1130.94 (s), 1069.02 (m), 1040.24 (m), 1015.69 (s), 997.45 (s), 964.72 (m), 906.51 (m), 886.01 (m), 796.98 (m), 779.89 (m), 771.41 (m), 775.80 (s), 730.04 (w), 683.72 (w), 631.37 (w), 620.06 (w) cm^{-1}.

HRMS (ESI+): Calc'd for $C_{15}H_{21}O_5^+$ [M+H$^+$]: 281.1384; found: 281.1383.

NMR: See Figure S2 on pg S26.

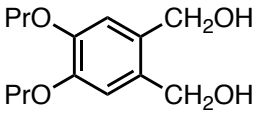

S1c

(4,5-Dipropoxy-1,2-phenylene)dimethanol (S1c).[4] A 200-mL recovery flask was charged sequentially with a stir bar, **S1b** (3.50 g, 12.5 mmol, 1.00 equiv), anhydrous THF (25 mL), $CaCl_2$ (2.77 g, 25.0 mmol, 2.00 equiv), absolute EtOH (25 mL), and $NaBH_4$ (1.89 g, 49.9 mmol, 4.00 equiv). The reaction mixture was stirred at rt for 3.75 h, then capped with a reflux

condenser and heated in an oil bath at 60 °C for 17.25 h. The reaction was removed from the oil bath and cooled to rt, then water (100 mL) was added and the mixture was extracted with DCM (3 x 60 mL). The combined organic fractions were washed with brine (50 mL), dried over $MgSO_4$, filtered, and concentrated on the rotary evaporator to give a tan solid. The crude material was purified by automated column chromatography (100 g column, 5 → 80% EtOAc in hexanes) to provide **S1c** (1.21 g, 4.78 mmol, 38% yield) as a white powder. The corresponding lactone was also isolated (1.02 g, 4.08 mmol, 33% yield) and could be converted to diol **S1c** in 64% yield by resubjection to the reaction conditions.

R_f: 0.04 in 50% EtOAc in hexanes.

FTIR (ATR): ν 3266.34 (w, br), 2962.85 (m), 2933.96 (m), 2874.57 (m), 1604.52 (m), 1520.92 (m), 1464.43 (m), 1435.98 (m), 1397.04 (m), 1337.57 (m), 1278.62 (s), 1247.77 (m), 1233.58 (m), 119746 (m), 1108.71 (s), 1062.13 (m), 1008.55 (m), 996.63 (m), 982.91 (s), 955.50 (s), 922.38 (m), 870.83 (s), 783.46 (m), 739.91 (m), 613.22 (m) cm^{-1}.

HRMS (ESI+): Calc'd for $C_{14}H_{22}NaO_4^+$ [M+Na^+]: 277.1410; found: 277.1411.

NMR: See Figure S3 on pg S27.

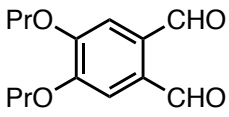

M1

4,5-Dipropoxyphthalaldehyde (M1).[5] An oven-dried 100-mL round-bottomed flask was charged with a stir bar and evacuated and refilled with N_2 (x3). Anhydrous DCM (16 mL) was added and the reaction vessel was cooled to –78 °C in a dry ice/acetone bath. Oxalyl chloride (1.1 mL, 13 mmol, 2.2 equiv) was added, then anhydrous DMSO (2.0 mL) was added dropwise. After stirring for 20 min at –78 °C, a solution of **S1c** (1.50 g, 5.90 mmol, 1.00 equiv) in anhydrous DCM (6 mL) was added and the reaction was stirred at –78 °C for 2 h. Triethylamine (15 mL) was added and the reaction was removed from the cold bath and stirred at rt for 1 h. Water (100 mL) was added, and the diluted reaction mixture was extracted with DCM (3 x 40 mL). The combined organic fractions were washed with brine (50 mL), dried over $MgSO_4$, filtered, and rotovapped to afford an orange solid. The crude material was purified via automated column chromatography (100 g column, 1 → 15% EtOAc in hexanes) and dried under vacuum to afford **M1** (1.17 g, 4.69 mmol, 79% yield) as a brown oil.

R_f: 0.55 in 50% EtOAc in hexanes.

FTIR (ATR): ν 2965.42 (m), 2938.67 (w), 2878.68 (w), 1692.61 (m), 1672.60 (m). 1580.35 (m), 1565.23 (s), 1523.99 (m), 1464.89 (m), 1405.13 (w), 1383.32 (m), 1348.70 (m), 1284.15 (m), 1277.64 (m), 1190.51 (m), 1134.08 (w), 1097.96 (s), 1040.36 (m), 1005.19 (m), 960.66 (m), 904.43 (w), 875.16 (m), 856.20 (w), 813.87 (m), 783.78 (w), 763.72 (w), 744.80 (w), 730.49 (w), 661.77 (w), 616.00 (w) cm^{-1}.

HRMS (ESI+): Calc'd for $C_{14}H_{19}O_4^+$ [M+H^+]: 251.1278; found: 251.1277.

NMR: See Figure S4 on pg S28.

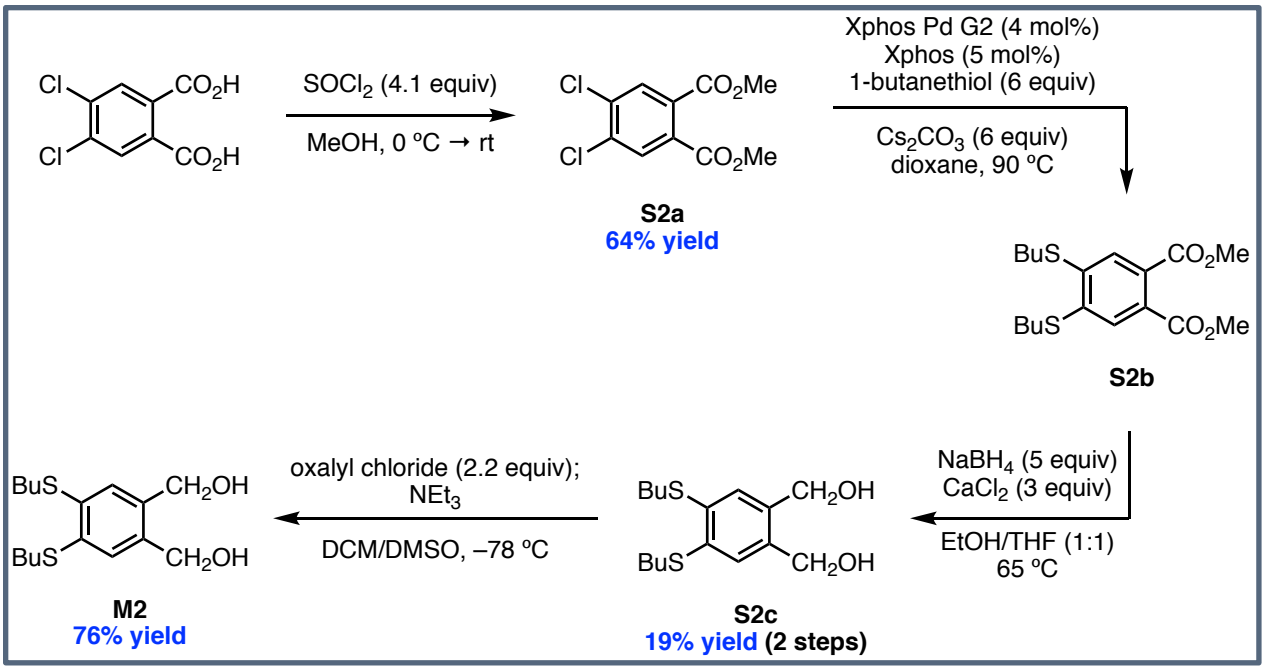

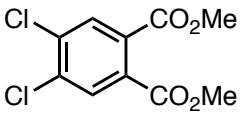

S2a

Dimethyl 4,5-dichlorophthalate (S2a).[6] A 500-mL round-bottomed flask was charged sequentially with 4,5-dichlorophthalic acid (15.00 g, 63.82 mmol, 1.00 equiv), a stir bar, and MeOH (120 mL). The solution was cooled to 0 °C in an ice/water bath and thionyl chloride (19.0 mL, 262 mmol, 4.10 equiv) was added. The reaction mixture was stirred for 30 min at 0 °C, then for 15 h at rt. The solution was concentrated on the rotary evaporator to afford a yellow-brown oil that was redissolved in EtOAc (120 mL) and washed successively with water (50 mL), saturated aqueous $NaHCO_3$ (50 mL), and brine (50 mL). The organic layer was dried over $MgSO_4$, filtered, and rotovapped to yield a brown oil. This crude material was purified via automated chromatography (100 g column, 5 → 30% EtOAc in hexanes) and dried under vacuum to provide **S2a** (10.64 g, 40.63 mmol, 64% yield) as a white solid.

R_f: 0.33 in 30% EtOAc in hexanes.

FTIR (ATR): ν 3092.63 (w), 2957.41 (w), 1725.43 (s), 1590.57 (m), 1550.68 (w), 1439.99 (w), 1427.34 (m), 1362.93 (w), 1288.66 (s), 1235.68 (s), 1224.37 (s), 1148.81 (w), 1121.55 (s), 1085.10 (s), 968.66 (s), 920.80 (m), 906.54 (w), 884.43 (s), 824.98 (w), 982.19 (s), 958.85 (s), 694.00 (w), 681.48 (m), 637.97 (w), 617.31 (m) cm^{-1}.

HRMS (ESI+): Calc'd for $C_{10}H_9Cl_2O_4^+$ [M+H$^+$]: 262.9872; found: 262.9870.

NMR: See Figure S5 on pg S29.

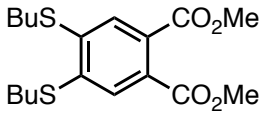

S2b

Dimethyl 4,5-bis(butylthio)phthalate (S2b).[7] An oven-dried, 250-mL, 3-neck round-bottomed flask was charged sequentially with a stir bar, cesium carbonate (22.39 g, 68.71 mmol, 6.00 equiv), **S2a** (3.00 g, 11.5 mmol, 1.00 equiv) Xphos Pd G2 (360.4 mg, 0.4581 mmol, 0.04 equiv), and Xphos (245.7 mg, 0.5153 mmol, 0.0500 equiv). The flask was capped with a reflux condenser and evacuated and refilled with N_2 (x3). Anhydrous dioxane (60 mL) was added, and the suspension was stirred in an oil bath at 90 °C for 20 min. 1-Butanethiol (7.4 mL, 69 mmol, 6.0 equiv) was added via syringe and stirring was continued at 90 °C for 15 h, at which point the reaction vessel was removed from the oil bath and cooled to rt. Water (150 mL) was added, and the reaction mixture was extracted with ether (4 x 70 mL). The combined organic fractions were washed with brine (50 mL), dried over $MgSO_4$, filtered, and concentrated on the rotary evaporator to afford an orange liquid. The crude material was purified via automated column chromatography (two sequential 100 g columns, 1 → 15% EtOAc in hexanes) and dried under vacuum to afford **S2b** (1.16 g, 3.14 mmol, 27% yield) as a yellow solid. ^{1}H NMR spectroscopic analysis indicated the presence of ~9 mol% of the monothiolated compound, but this mixture was used without further purification.

R_f: 0.53 in 30% EtOAc in hexanes.

FTIR (ATR): ν 2956.89 (w), 2924.26 (w), 2859.24 (w), 1728.69 (s), 1718.07 (s), 1575.19 (w), 1542.14 (w), 1464.36 (w), 1429.59 (m), 1300.31 (m), 1270.24 (m), 1253.17 (s), 1221.67 (m), 1193.16 (m), 1135.21 (m), 1116.92 (m), 1086.68 (s), 956.29 (m), 917.64 (w), 891.19 (m), 867.45 (m), 834.70 (m), 784.62 (s), 757.21 (m), 735.21 (w), 709.15 (w), 687.29 (w), 639.56 (w), 610.98 (w) cm^{-1}.

HRMS (ESI+): Calc'd for $C_{18}H_{27}O_4S_2^+$ [M+H$^+$]: 371.1345; found: 371.1348.

NMR: See Figure S6 on pg S30.

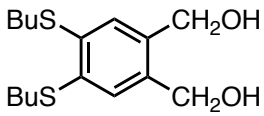

S2c

(4,5-Bis(butylthio)-1,2-phenylene)dimethanol (S2c).[4] A 100-mL round-bottomed flask was charged with a stir bar and a solution of **S2b** (1.00 g, 2.71 mmol, 1.00 equiv) in anhydrous THF (20 mL). Calcium chloride (902.2 mg, 8.129 mmol, 3.00 equiv), absolute EtOH (20 mL), and sodium borohydride (512.5 mg, 13.55 mmol, 5.00 equiv) were added sequentially, and the reaction was capped with a reflux condenser and stirred in an oil bath at 65 °C for 41 h. The reaction vessel was removed from the oil bath and allowed to cool to rt before water (100 mL) and DCM (30 mL) were added. Portions of 1 M HCl (~25 mL total) were added until the solids dissolved and a biphasic solution was formed. The layers were separated and the aqueous fraction was extracted with DCM (3 x 30 mL). The combined organic fractions were washed with brine (50 mL), dried over $MgSO_4$, filtered, and concentrated on the rotary evaporator to afford a

yellow oil. The crude material was purified via automated column chromatography (100 g column, 1 → 35% EtOAc in hexanes) and dried under vacuum to provide **S2c** (604.8 g, 1.923 mmol, 71% yield) as clear, colorless oil.

R_f: 0.13 in 50% EtOAc in hexanes (streaky).

FTIR (ATR): ν 3308.41 (w, broad), 2955.18 (m), 2926.76 (m), 2870.31 (m), 1456.35 (m), 1376.38 (m), 1266.17 (m), 1220.20 (m). 1005.01 (s), 940.76 (m), 893.76 (m), 872.47 (m), 731.22 (m) cm^{-1}.

HRMS (ESI+): Calc'd for $C_{16}H_{27}O_2S_2^+$ [M+H$^+$]: 315.1447; found: 315.1451.

NMR: See Figure S7 on pg S31.

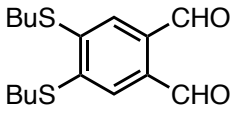

M2

4,5-Bis(butylthio)phthalaldehyde (M2).[5] An oven-dried 50-mL round-bottomed flask was charged with a stir bar and evacuated and refilled with N_2 (x3). Anhydrous DCM (5 mL) was added and the reaction vessel was cooled to –78 °C in a dry ice/acetone bath. Oxalyl chloride (0.34 mL, 3.9 mmol, 2.20 equiv) was added, then anhydrous DMSO (1.4 mL) was added dropwise. After stirring for 20 min at –78 °C, a solution of **S2c** (559.1 mg, 1.778 mmol, 1.00 equiv) in anhydrous DCM (2 mL) was added and the reaction was stirred at –78 °C for 2 h. Triethylamine (4.5 mL) was added and the reaction was removed from the cold bath and stirred at rt for 2 h. Water (50 mL) was added, and the diluted reaction mixture was extracted with DCM (3 x 30 mL). The combined organic fractions were washed with brine (50 mL), dried over $MgSO_4$, filtered, and rotovapped to afford a yellow solid. The crude material was purified via automated column chromatography (50 g column, 1 → 15% EtOAc in hexanes) and dried under vacuum to afford **M2** (421.3 mg, 1.357 mmol, 76% yield) as a yellow solid.

R_f: 0.53 in 30% EtOAc in hexanes.

FTIR (ATR): ν 2958.54 (m), 2930.06 (m), 2871.84 (w), 2862.23 (w), 1691.75 (m), 1680.81 (m), 1669.79 (s), 1554.30 (s), 1533.48 (s), 1456.39 (m), 1429.28 (m), 1418.05 (m), 1377.52 (w), 1340.22 (m), 1308.05 (w), 1263.80 (m), 1210.64 (s), 1159.16 (m), 1134.64 (m), 1116.53 (s), 1095.13 (m), 1050.55 (m), 953.24 (s), 917.33 (m), 895.56 (m), 884.35 (m), 841.52 (m), 790.13 (w), 757.39 (w), 745.83 (w), 735.59 (m), 724.53 (m), 640.46 (m), 603.24 (m) cm^{-1}.

HRMS (ESI+): Calc'd for $C_{16}H_{23}S_2O_2^+$ [M+H$^+$]: 311.1134; found: 311.1132.

NMR: See Figure S8 on pg S32.

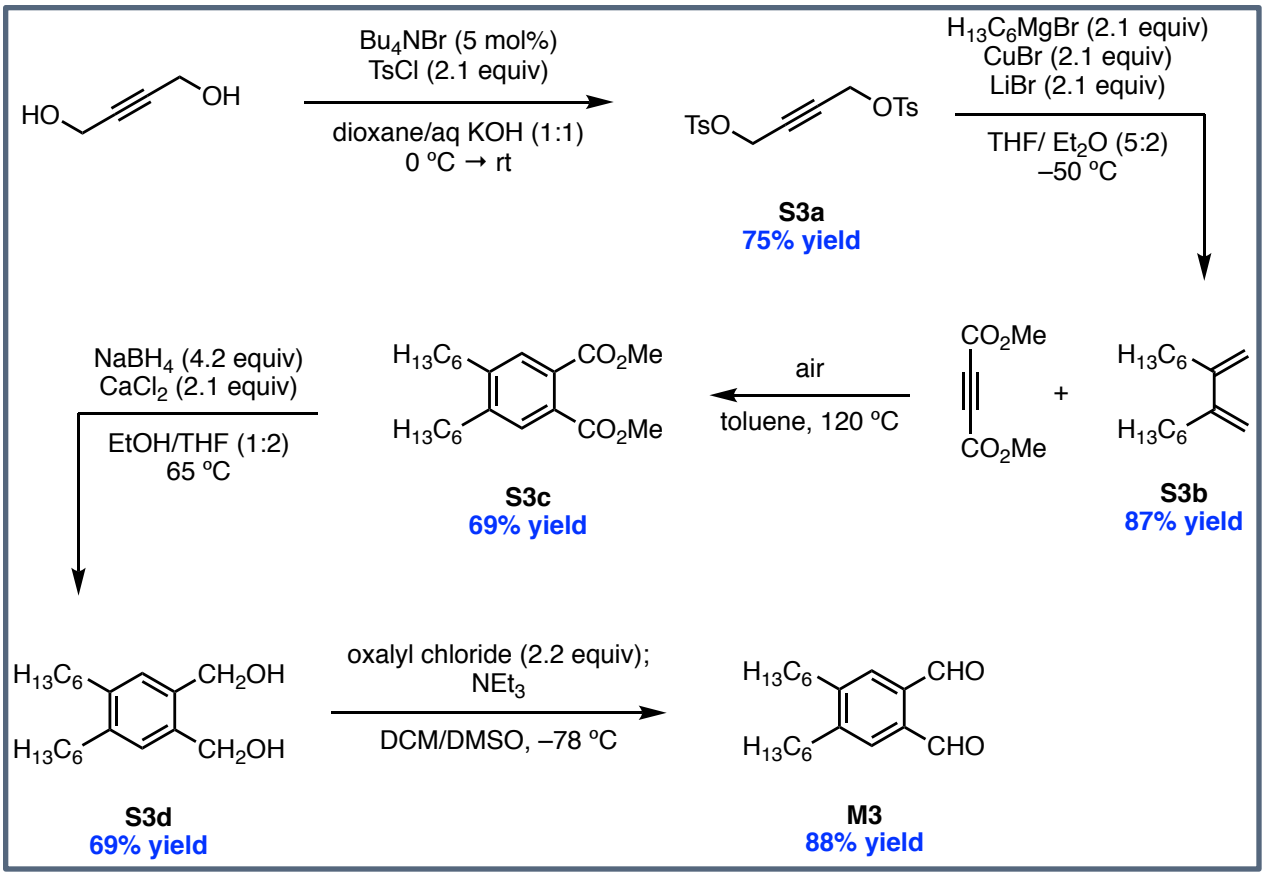

S3a

But-2-yne-1,4-diyl bis(4-methylbenzenesulfonate) (S3a).[8] A 500-mL round-bottomed flask was charged sequentially with 50 wt% aqueous KOH (45 mL), dioxane (45 mL), a stir bar, 2-butyne-1,4-diol (powdered in a mortar and pestle, 3.00 g, 34.9 mmol, 1.00 equiv), and tetrabutylammonium bromide (562 mg, 1.74 mmol, 0.0500 equiv). The reaction mixture was cooled to 0 °C in an ice/water bath and tosyl chloride (13.96 g, 73.22 mmol, 2.10 equiv) in dioxane (45 mL) was added with rapid stirring. The stirring reaction was allowed to warm to rt over 5 h, then diluted with water (100 mL). The aqueous and organic layers were separated, and the aqueous layer was extracted with ether (100 mL). The combined organic layers were washed with brine (50 mL), dried with $MgSO_4$, filtered, concentrated on the rotary evaporator, and further dried under vacuum overnight to yield **S3a** (10.33 g, 26.21 mmol, 75% yield) as a pale yellow powder that was used without further purification.

R_f: 0.68 in 30% EtOAc in hexanes.

FTIR (ATR): ν 2964.21 (w), 1717.26 (w), 1597.52 (m), 1495.31 (w), 1440.02 (w), 1369.54 (m), 1355.95 (m), 1339.81 (m), 1312.83 (w), 1291.94 (w), 1248.58 (w), 1214.29 (w), 1174.59 (s), 1137.63 (s), 1121.40 (s), 1095.45 (m), 1033.77 (m), 1011.86 (w), 929.85 (s), 813.31 (m), 799.84 (m), 755.84 (s), 703.01 (w), 679.58 (w), 663.36 (s), 632.97 (w), 606.57 (w) cm^{-1}.

HRMS (ESI+): Calc'd for $C_{18}H_{19}O_6S_2^+$ [M+H$^+$]: 395.0618; found: 395.0614.

NMR: See Figure S9 on pg S33.

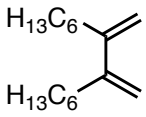

S3b

7,8-Dimethylenetetradecane (S3b).[9] A flame-dried, 200-mL recovery flask was charged sequentially with a stir bar, CuBr (5.37 g, 37.4 mmol, 2.00 equiv), and LiBr (3.47 g, 39.9 mmol, 2.10 equiv). The flask was sealed, then evacuated and refilled with N_2 (x3). Anhydrous THF (50 mL) was added, and the suspension was cooled to –50 °C in an acetone bath equipped with a Cryocool and stirred at this temperature for 15 min. Hexylmagnesium bromide (20 mL of a 2.0 M solution in ether, 40 mmol, 2.1 equiv) was added, and the reaction was stirred at –50 °C for 25 min. Compound **S3a** (7.50 g, 19.0 mmol, 1.00 equiv) was added as a solution in THF (50 mL) with cooling maintained at –50 °C, and the reaction mixture was stirred for 30 min. The flask was removed from the cold bath and stirred at rt for 17 h. The reaction was quenched by addition of sat. aq. NH_4Cl (150 mL) and extracted with ether (3 x 50 mL). The combined organic layers were dried over $MgSO_4$, filtered, and concentrated on the rotary evaporator to give a brown sludge, which was purified by automated column chromatography (100 g column, 1% EtOAc in hexanes) to provide a pale yellow oil (3.66 g, 16.5 mmol 87% yield). NMR analysis indicated the presence of minor impurities; however **S3b** was used without further purification.

R_f: 0.88 in 5% EtOAc in hexanes.

FTIR (ATR): ν 2955.76 (m), 2924.70 (s), 2856.03 (m), 1594.35 (m), 1466.32 (m), 1378.05 (w), 889.61 (s), 724.25 (w) cm^{-1}.

HRMS (EI): Calc'd for $C_{16}H_{30}^+$ [M$^+$]: 222.2342; found: 222.2351.

NMR: See Figure S10 on pg S34.

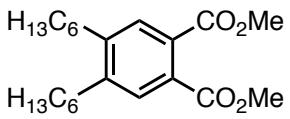

S3c

Dimethyl 4,5-dihexylphthalate (S3c).[10] A 250-mL, 3-neck, round-bottomed flask was charged sequentially with a stir bar, **S3b** (3.01 g, 13.5 mmol, 1.00 equiv), anhydrous toluene (25 mL), and dimethyl acetylenedicarboxylate (1.7 mL, 14 mmol, 1.00 equiv). The flask was capped with a reflux condenser and stirred in a 120 °C oil bath for 13.5 h. A long needle was used to bubble air through the reaction mixture and stirring was continued at 120 °C for an additional 47.5 h. Reaction progress was assessed by periodically analyzing aliquots of the reaction mixture using ^{1}H NMR spectroscopy until full conversion of the methylene peak of the intermediate cyclohexadiene (δ 2.95 ppm in $CDCl_3$) was observed. The reaction mixture was removed from the oil bath and cooled to rt, then concentrated on the rotary evaporator to provide a pale yellow oil. The crude material was purified via automated column chromatography (100 g column, 1 → 20% EtOAc in hexanes) and dried under vacuum to afford **S3c** (3.40 g, 9.37 mmol, 69% yield) as a clear, colorless oil.

R_f: 0.45 in 30% EtOAc in hexanes.

FTIR (ATR): ν 2952.87 (m), 2926.10 (m), 2855.91 (m), 1725.12 (s), 1433.39 (m), 1290.82 (s), 1213.14 (m), 1190.73 (m), 1130.92 (s), 1082.73 (w), 1036.03 (w), 972.39 (w), 910.55 (w), 910.14 (w), 767.61 (w), 724.50 (w) cm^{-1}.

HRMS (ESI+): Calc'd for $C_{22}H_{35}O_4^+$ [M+H$^+$]: 363.2530; found: 363.2535.

NMR: See Figure S11 on pg S35.

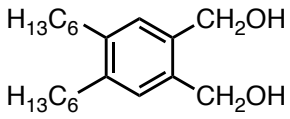

S3d

(4,5-Dihexyl-1,2-phenylene)dimethanol (S3d).[8] A 200-mL recovery flask was charged sequentially with **S3c** (2.91 g, 8.03 mmol, 1.00 equiv), a stir bar, anhydrous THF (30 mL), calcium chloride (1.87 g, 16.9 mmol, 2.10 equiv), absolute ethanol (15 mL), and sodium borohydride (1.28 g, 33.7 mmol, 4.20 equiv). The flask was capped with a reflux condenser and stirred at 60 °C in an oil bath for 22.25 h, then it was removed from the oil bath and cooled to rt. Water (200 mL) was added to the suspension, followed by 1 M HCl (~20 mL) until the solids dissolved. The resulting solution was extracted with DCM (3 x 100 mL) and the combined organic extracts were washed with brine (50 mL), dried over $MgSO_4$, filtered, and concentrated

on the rotary evaporator to provide a cloudy, colorless oil. The crude material was purified via automated column chromatography (25 g column, 5 → 70% EtOAc in hexanes) and dried under vacuum to afford **S3d** (1.70 g, 5.55 mmol, 69% yield) as a white solid.

R_f: 0.07 in 30% EtOAc in hexanes.

FTIR (ATR): ν 3295.72 (m, broad), 3194.40 (m, broad), 2954.97 (m), 2921.40 (s), 2871.53 (m), 2852.67 (m), 1482.39 (w), 1465.64 (m), 1455.40 (m), 1407.17 (w), 1345.74 (w), 1260.12 (m), 1094.16 (m), 1074.34 (s), 1047.35 (s), 1015.64 (s), 986.77 (m), 882.63 (w), 863.08 (m), 796.60 (m), 723.07 (s), 627.85 (m), 604.19 (m) cm^{-1}.

HRMS (ESI+): Calc'd for $C_{20}H_{34}NaO_2^+$ [M+Na^+]: 329.2451; found: 329.2453.

NMR: See Figure S12 on pg S36.

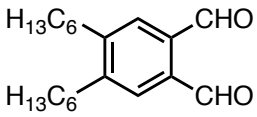

M3

4,5-Dihexylphthalaldehyde (M3).[5] An oven-dried 100-mL round-bottomed flask was charged with a stir bar and evacuated and refilled with N_2 (x3). Anhydrous DCM (16 mL) was added and the reaction vessel was cooled to –78 °C in a dry ice/acetone bath. Oxalyl chloride (0.84 mL, 9.8 mmol, 2.2 equiv) was added, then anhydrous DMSO (1.7 mL) was added dropwise. After stirring for 20 min at –78 °C, a solution of **S3d** (1.37 g, 4.47 mmol, 1.00 equiv) in anhydrous DCM (6 mL) was added and the reaction was stirred at –78 °C for 2 h. Triethylamine (11 mL) was added and the reaction was removed from the cold bath and stirred at rt for 1 h. Water (100 mL) was added, and the diluted reaction mixture was extracted with DCM (3 x 40 mL). The combined organic fractions were washed with brine (50 mL), dried over $MgSO_4$, filtered, and rotovapped to afford a brown oil. The crude material was purified via automated column chromatography (100 g column, 5 → 20% EtOAc in hexanes) and dried under vacuum to afford **M3** (1.19 g, 3.95 mmol, 88% yield) as a brown oil.

R_f: 0.69 in 30% EtOAc in hexanes.

FTIR (ATR): ν 2955.03 (m), 2925.30 (m), 2855.67 (m), 1687.97 (s), 1598.01 (m), 1557.71 (m), 1465.73 (w), 1377.95 (w), 1238.43 (m), 1184.92 (m), 1067.48 (w), 913.85 (w), 853.25 (w), 799.07 (w), 736.31 (m) cm^{-1}.

HRMS (ESI+): Calc'd for $C_{20}H_{30}NaO_2^+$ [M+Na^+]: 325.2138; found: 325.2142.

NMR: See Figure S13 on pg S37.

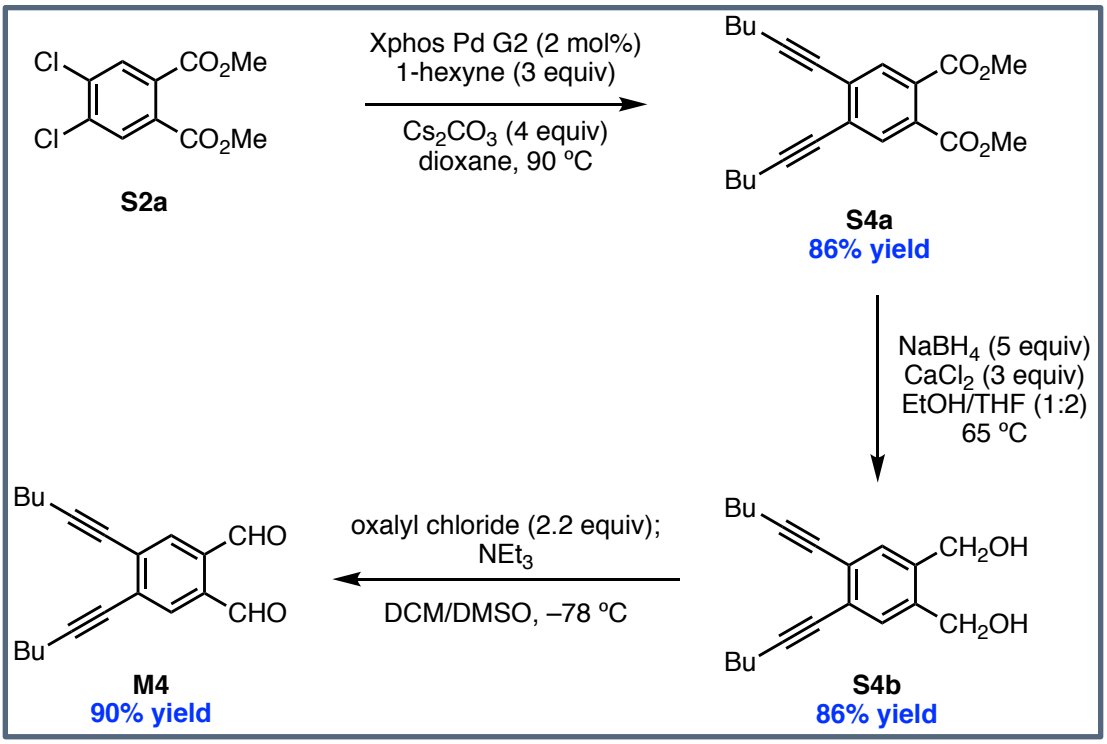

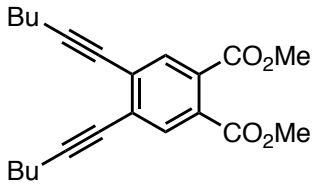

S4a

Dimethyl 4,5-di(hex-1-yn-1-yl)phthalate (S4a).[11] An oven-dried, 100-mL, 2-neck round-bottomed flask was charged sequentially with a stir bar, cesium carbonate (14.92 g, 45.81 mmol, 4.00 equiv), **S2a** (3.00 g, 11.5 mmol, 1.00 equiv), and Xphos Pd G2 (180.2 mg, 0.2290 mmol, 0.0200 equiv). The flask was capped with a reflux condenser and evacuated and refilled with N_2 (x3). Anhydrous dioxane (36 mL) was added, and the suspension was stirred for 30 min in a 90 °C oil bath. 1-Hexyne (3.9 mL, 34 mmol, 3.0 equiv) was added, and the reaction mixture was stirred at 90 °C for 14.25 h. The reaction vessel was removed from the oil bath and cooled to rt before water (100 mL) was added. The reaction mixture was extracted with ether (4 x 100 mL), and the organics were dried over $MgSO_4$, filtered, and concentrated on the rotary evaporator to afford a dark brown oil. The crude material was purified via automated column chromatography (two sequential 100 g columns, 1 → 15% EtOAc in hexanes) and dried under vacuum to provide **S4a** (3.50 g, 9.89 mmol, 86% yield) as a brown oil.

R_f: 0.55 in 30% EtOAc in hexanes.

FTIR (ATR): ν 2954.79 (w), 2932.14 (w), 2871.84 (w), 2862.32 (w), 2225.23 (w), 1726.67 (s), 1599.84 (w), 1537.33 (m), 1456.68 (w), 1433.30 (m), 1392.08 (w), 1379.58 (w), 1329.34 (w), 1307.37 (m), 1276.52 (m), 1263.29 (m), 1250.83 (s), 1195.17 (m), 1125.29 (s), 1068.22 (m),

968.89 (w), 915.53 (w), 888.73 (w), 874.44 (w), 845.68 (w), 821.59 (w), 784.03 (m), 758.49 (w), 734.59 (m), 702.91 (w), 633.32 (w), 639.97 (w), 611.39 (w), 602.93 (w) cm^{-1}.

HRMS (ESI+): Calc'd for $C_{22}H_{27}O_4^+$ [M+H$^+$]: 355.1904; found: 355.1908.

NMR: See Figure S14 on pg S38.

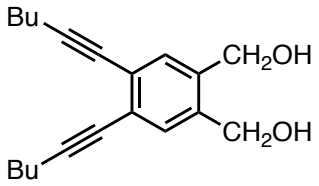

S4b

(4,5-Di(hex-1-yn-1-yl)-1,2-phenylene)dimethanol (S4b).[4] A 250-mL recovery flask was charged with a stir bar and a solution of **S4a** (3.11 g, 8.78 mmol, 1.00 equiv) in anhydrous THF (40 mL). Calcium chloride (3.92 g, 26.3 mmol, 3.00 equiv), absolute EtOH (20 mL), and sodium borohydride (1.66 g, 43.9 mmol, 5.00 equiv) were added sequentially, and the reaction was capped with a reflux condenser and stirred in an oil bath at 65 °C for 15 h. The reaction vessel was removed from the oil bath and allowed to cool to rt before water (100 mL) and DCM (50 mL) were added. Portions of 1 M HCl (~30 mL) were added until the solids dissolved and a biphasic solution was formed. The layers were separated and the aqueous fraction was extracted with DCM (3 x 50 mL). The combined organic fractions were washed with brine (50 mL), dried over $MgSO_4$, filtered, and concentrated on the rotary evaporator to afford an orange oil. The crude material was purified via automated column chromatography (100 g column, 5 → 60% EtOAc in hexanes) and dried under vacuum to provide **S4b** (1.52 g, 5.09 mmol, 58% yield) as an off-white solid.

R_f: 0.28 in 50% EtOAc in hexanes.

FTIR (ATR): ν 3227.34 (m, broad), 2956.69 (m), 2931.64 (m), 2871.38 (m), 2222.79 (w), 1491.16 (w), 1424.96 (m), 1401.37 (m), 1378.92 (w), 1357.80 (m), 1326.77 (w), 1270.20 (w), 1218.86 (w), 1239.62 (w), 1192.29 (m), 1122.57 (m), 1047.35 (s), 1025.88 (s), 997.06 (s), 893.58 (s), 804.59 (m), 728.38 (m), 668.05 (m) cm^{-1}.

HRMS (ESI+): Calc'd for $C_{20}H_{26}NaO_2^+$ [M+Na$^+$]: 321.1825; found: 321.1825.

NMR: See Figure S15 on pg S39.

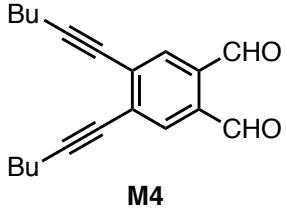

M4

4,5-Di(hex-1-yn-1-yl)phthalaldehyde (M4).[5] An oven-dried 100-mL round-bottomed flask was charged with a stir bar and evacuated and refilled with N_2 (x3). Anhydrous DCM (16 mL) was

added and the reaction vessel was cooled to –78 °C in a dry ice/acetone bath. Oxalyl chloride (0.94 mL, 11 mmol, 2.2 equiv) was added, then anhydrous DMSO (2.0 mL) was added dropwise. After stirring for 20 min at –78 °C, a solution of **S4b** (1.48 g, 4.99 mmol, 1.00 equiv) in anhydrous DCM (6 mL) was added and the reaction was stirred at –78 °C for 2 h. Triethylamine (12.5 mL) was added and the reaction was removed from the cold bath and stirred at rt for 1 h. Water (100 mL) was added, and the diluted reaction mixture was extracted with DCM (3 x 40 mL). The combined organic fractions were washed with brine (50 mL), dried over $MgSO_4$, filtered, and concentrated on the rotary evaporator to afford a brown solid. The crude material was purified via automated column chromatography (100 g column, 1 → 15% EtOAc in hexanes) and dried under vacuum to afford **M4** (1.31 g, 4.46 mmol, 90% yield) as a brown oil.

Note that a sample of **M4** stored in a refrigerator under air was observed to decompose on a time scale of weeks to months.

R_f: 0.55 in 50% EtOAc in hexanes.

FTIR (ATR): ν 2956.58 (w), 2930.99 (w), 2871.48 (m), 2862.01 (w), 2219.64 (w), 1689.87 (s), 1587.66 (m), 1535.45 (m), 1465.75 (w), 1374.87 (w), 1328.11 (w), 1302.12 (w), 1271.15 (m), 1209.65 (w), 1175.94 (m), 1122.49 (m), 810.80 (m), 894.52 (w), 851.71 (w), 828.29 (m), 745.06 (w), 726.65 (w) cm^{-1}.

HRMS (ESI+): Calc'd for $C_{20}H_{23}O_2^+$ [$M+H^+$]: 295.1693; found: 295.1694.

NMR: See Figure S16 on pg S40.

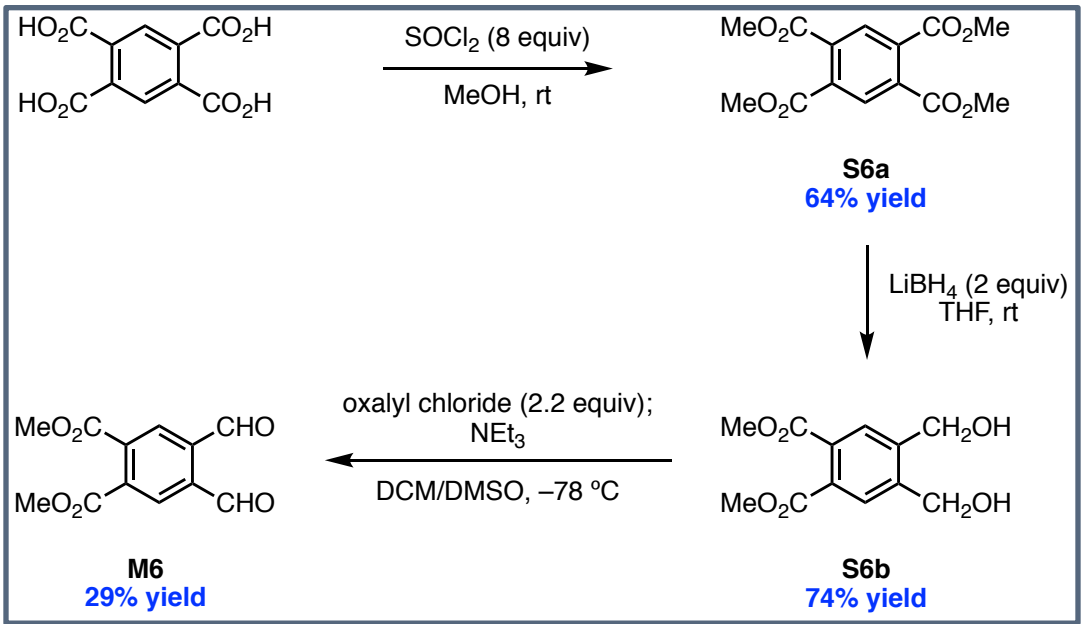

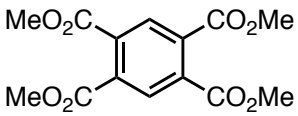

S6a

Tetramethyl benzene-1,2,4,5-tetracarboxylate (S6a).[6] A 1000-mL recovery flask was charged sequentially with a stir bar, benzene-1,2,4,5-tetracarboxylic acid (30.0 g, 118 mmol, 1.00 equiv), and MeOH (500 mL). The solution was cooled to 0 °C in an ice/water bath, and $SOCl_2$ (69.0 mL, 945 mmol, 8.00 equiv) was added dropwise via addition funnel over the course of ~1 h. The flask was removed from the cold bath and stirred at rt for 4.5 days, during which time a white precipitate crashed out of solution. The white precipitate was isolated by vacuum filtration, washed with MeOH, and dried under vacuum to provide **S6a** (29.4 g, 97.6 mmol, 83% yield), which was used without further purification.

R_f: 0.20 in 30% EtOAc in hexanes.

FTIR (ATR): ν 2955.70 (w), 1716.10 (s), 1503.65 (w), 1438.72 (m), 1368.51 (m), 1258.54 (s), 1193.95 (m), 1130.04 (m), 1905.07 (s), 1130.04 (m), 1095.07 (s), 951.74 (m), 918.99 (m), 850.64 (m), 809.14 (m), 794.54 (s), 740.03 (s), 661.99 (m), 608.51 (w) cm^{-1}.

HRMS (ESI+): Calc'd for $C_{14}H_{15}O_8^+$ [M+H$^+$]: 311.0761; found: 311.0761.

NMR: See Figure S17 on pg S41.

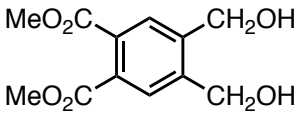

S6b

Dimethyl 4,5-bis(hydroxymethyl)phthalate (S6b).[12] A 500-mL round-bottomed flask was charged sequentially with a stir bar, **S6a** (10.0 g, 32.2 mmol, 1.00 equiv), anhydrous THF (140 mL), and $LiBH_4$ (1.40 g, 2.00 equiv). The reaction was stirred at rt for 15 h, then carefully quenched by addition of aq. 1 M HCl (~20 mL in 1-mL increments; caution – vigorous bubbling). A precipitate formed and was removed by vacuum filtration. The filtrate was diluted with water (100 mL) and extracted with DCM (3 x 100 mL). The combined organic extracts were dried over $MgSO_4$, filtered, and concentrated on the rotary evaporator to provide **S6b** (6.05 g, 23.8 mmol, 74% yield) as a white solid that was used without further purification.

R_f: 0.12 in 70% EtOAc in hexanes.

FTIR (ATR): ν 3257.82 (w, br), 2954.03 (w), 2907.06 (w), 2854.15 (w), 1716.44 (s), 1616.64 (w), 1433.35 (m), 1408.93 (w), 1357.65 (w), 1310.63 (m), 1283.40 (m), 1236.16 (m), 1205.30 (m), 1152.87 (w), 1133.47 (m), 1068.53 (w), 1047.12 (m), 1016.60 (w), 974.02 (m), 924.07 (w), 897.73 (m), 841.64 (w), 804.36 (m), 768.94 (m), 643.81 cm^{-1}.

HRMS (ESI+): Calc'd for $C_{12}H_{15}O_6^+$ [M+H$^+$]: 255.0863; found: 311.0761.

NMR: See Figure S18 on pg S42.

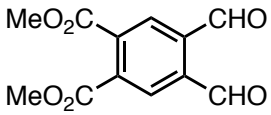

M6

Dimethyl 4,5-diformylphthalate (M6).[5] A flame-dried 500-mL round-bottomed flask was charged with a stir bar and evacuated and refilled with N_2 (x3), then charged with anhydrous DCM (50 mL), and cooled to –78 °C in a dry ice/acetone bath. Oxalyl chloride (5.8 mL, 68 mmol, 2.2 equiv) was added, followed by addition of anhydrous DMSO (10 mL) over the course of ~10 min. The reaction was stirred at –78 °C for 20 min, then a solution of **S6b** (7.84 g, 30.1 mmol, 1.00 equiv) in DCM/DMSO (1:1, 35 mL) was added. After stirring at –78 °C for 2 h, triethylamine (73 mL) was added. The reaction mixture was removed from the cold bath and stirred at rt for 14.5 h. The reaction was quenched with water (100 mL) and extracted with DCM (50 mL), and the organic extracts were dried over $MgSO_4$, filtered, and concentrated on the rotary evaporator to provide a brown oil. The crude material was purified via automated column chromatography (100 g column, 15 → 50% EtOAc in hexanes) and dried under vacuum

overnight to yield an orange solid. ^{1}H NMR spectroscopic analysis of this solid suggested a mixture of **M6** and oligomeric material. The solid was heated at 70 °C under vacuum (~0.1 torr) for 24 h to afford an orange solid (4.35 g) that was broken up with a spatula. A sample of this material (1.56 g) was further purified by subliming at 140 °C under vacuum (~0.1 torr) for 2 h to afford **M6** as a yellow solid (768.3 mg, 3.080 mmol, 29% yield).

R_f: 0.10 in 30% EtOAc in hexanes (very streaky).

FTIR (ATR): ν 3040.36 (w), 2957.93 (w), 1724.67 (s), 1709.59 (s), 1690.45 (s), 1559.15 (w), 1490.36 (w), 1436.62 (m), 1377.35 (w), 1297.29 (s), 1244.30 (s), 1194.37 (m), 1131.24 (s), 1027.72 (m), 972.31 (m), 938.22 (w), 914.56 (m), 847.82 (m), 814.24 (s), 801.87 (s), 792.64 (m), 762.48 (m), 696.39 (w), 664.84 (w) cm^{-1}.

HRMS (ESI+): Calc'd for $C_{12}H_{11}O_6^+$ [M+H$^+$]: 251.0550; found: 251.0545.

NMR: See Figure S19 on pg S43.

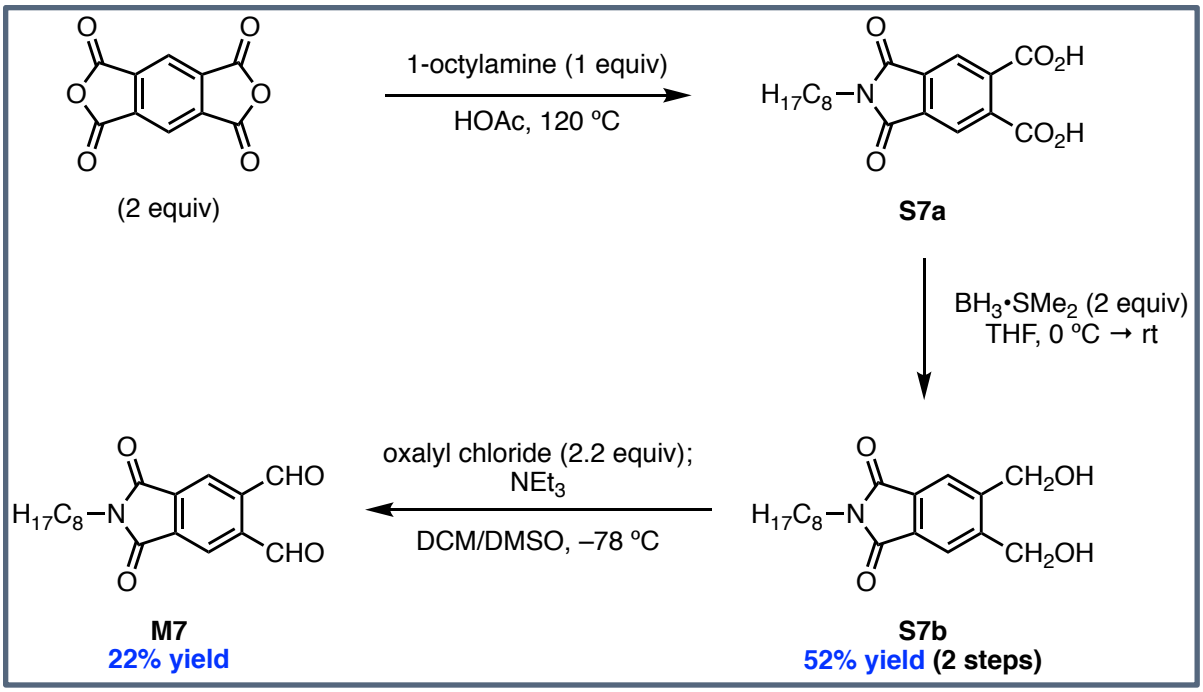

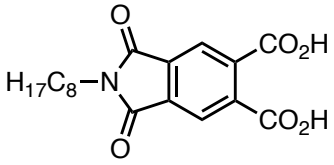

S7a

2-Octyl-1,3-dioxoisoindoline-5,6-dicarboxylic acid (S7a).[13] A 500-mL round-bottomed flask was charged sequentially with a stir bar, pyromellitic dianhydride (20.0 g, 91.7 mmol, 2.00 equiv), glacial acetic acid (200 mL), and octylamine (7.6 mL, 46 mmol, 1.00 equiv). The reaction flask was capped with a reflux condenser and stirred at 120 °C for 15.5 h, at which point it was removed from the oil bath and cooled to rt. The reaction mixture was poured into a 2-L round-bottomed flask containing a stir bar and DI water (1000 mL), then stirred at rt for 2 h, during which time a white precipitate crashed out. This precipitate was isolated by vacuum filtration and washed with DI water, then dried under vacuum at 60 °C for 17.5 h. ^{1}H NMR spectroscopic analysis of the resulting white solid (14.26 g) indicated a ~89:11 ratio of **S7a** to the corresponding diimide, but the material was used without further purification.

R_f: 0.17 in 50% EtOAc in hexanes.

FTIR (ATR): ν 2922.62 (m), 2850.85 (m), 1692.12 (s), 1430.22 (m), 1393.83 (m), 1372.86 (m), 1335.08 (w), 1283.78 (m), 1199.10 (m), 1145.31 (m), 1053.58 (m), 922.72 (w), 907.02 (m), 869.39 (w), 800.35 (m), 741.67 (m), 722.82 (m), 689.35 (m), 623.85 (m) cm^{-1}.

HRMS (ESI+): Calc'd for $C_{18}H_{22}NO_6^+$ [M+H$^+$]: 348.1442; found: 348.1436.

NMR: See Figure S20 on pg S44.

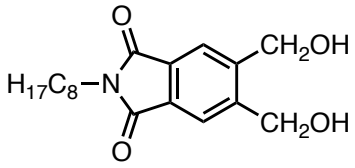

S7b

5,6-Bis(hydroxymethyl)-2-octylisoindoline-1,3-dione (S7b).[14] A flame-dried 500-mL round-bottomed flask was charged with **S7a** (6.00 g, 17.3 mmol, 1.00 equiv) and a stir bar. The flask was evacuated and refilled with N_2 (x3), then anhydrous THF (50 mL) was added. The reaction mixture was cooled to 0 °C in an ice/water bath and BH_3•SMe_2 (26.0 mL of a 2.0 M solution in THF, 51.8 mmol, 2.00 equiv) was added. After stirring at 0 °C for 20 min, the reaction was removed from the cold bath and stirred at rt for 18.25 h, then carefully quenched with aq. 1 M HCl (~10 mL – caution, vigorous bubbling). The reaction mixture was diluted with water (75 mL) and extracted with DCM (4 x 50 mL), and the combined organic extracts were dried over $MgSO_4$, filtered, and concentrated on the rotary evaporator to provide a white solid. The crude material was purified via automated column chromatography (100 g column, 5 → 60% EtOAc in hexanes) and dried under vacuum to afford **S7b** (3.22 g, 17.3 mmol, 52% yield over two steps) as a white solid.

R_f: 0.02 in 50% EtOAc in hexanes.

FTIR (ATR): ν 344.50 (m), 2923.10 (m), 2852.96 (m), 1770.24 (m), 1684.53 (s), 1618.73 (m), 1463.68 (m), 1438.25 (m), 1399.17 (s), 1367.82 (m), 1325.61 (m), 1284.58 (m), 1237.05 (m), 1204.54 (m), 1145.20 (m), 1088.43 (s), 10610.5 (s), 1029.18 (m), 1001.14 (m), 906.46 (m), 861.24 (m), 772.69 (m), 745.44 (s), 723.87 (m), 623.51 (m) cm^{-1}.

HRMS (ESI+): Calc'd for $C_{18}H_{26}NO_4^+$ [M+H^+]: 320.1856; found: 320.1858.

NMR: See Figure S21 on pg S45.

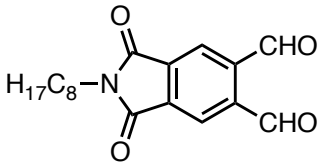

M7

2-Octyl-1,3-dioxoisoindoline-5,6-dicarbaldehyde (M7).[5] A flame-dried 250-mL round-bottomed flask was charged with a stir bar and evacuated and refilled with N_2 (x3), then charged

with anhydrous DCM (20 mL) and cooled to –78 °C in a dry ice/acetone bath. Oxalyl chloride (1.9 mL, 22 mmol, 2.2 equiv) was added, followed by addition of anhydrous DMSO (3.0 mL). The solution was stirred at –78 °C for 20 min, then a solution of **S7b** (3.22 g, 10.1 mmol, 1.00 equiv) in DCM (25 mL) was added. After stirring at –78 °C for 2 h, triethylamine (24 mL) was added. The reaction mixture was removed from the cold bath and stirred at rt for 5 h. The reaction was quenched with water (100 mL) and extracted with DCM (4 x 50 mL), and the combined organic extracts were dried over $MgSO_4$, filtered, and concentrated on the rotary evaporator to provide an orange oil. The crude material was purified via automated column chromatography (100 g column, 5 → 60% EtOAc in hexanes) and dried under vacuum for 6 h to yield an orange solid. ^{1}H NMR spectroscopic analysis of this solid suggested a mixture of **M7** and oligomeric material. The solid was heated at 90 °C under vacuum (~0.1 torr) for 13 h to afford an orange solid (2.16 g) that was broken up with a spatula. This material was further purified by subliming at 150–160 °C under vacuum (~0.1 torr) for 4 h to afford **M7** as a yellow solid (628.2 mg, 1.990 mmol, 22% yield).

R_f: 0.17 in 50% EtOAc in hexanes (very streaky).

FTIR (ATR): ν 2956.94 (w), 2917.26 (m), 2849.14 (m), 1709.35 (s), 1696.22 (s), 1686.08 (s), 1627.03 (w), 1466.81 (w), 1455.71 (w), 1438.41 (w), 1422.14 (w), 1403.00 (m), 1377.99 (m), 1333.92 (m), 1229.02 (m), 1209.94 (w), 1133.52 (m), 1095.42 (s), 1004.38 (w), 991.25 (w), 974.12 (w), 915.65 (m), 860.67 (w), 833.76 (m), 798.03 (w), 773.54 (w), 739.01 (s), 625.08 (m) cm^{-1}.

HRMS (EI+): Calc'd for $C_{18}H_{21}NO_4^+$ [M^+]: 315.1465; found: 315.1472.

NMR: See Figure S22 on pg S46.

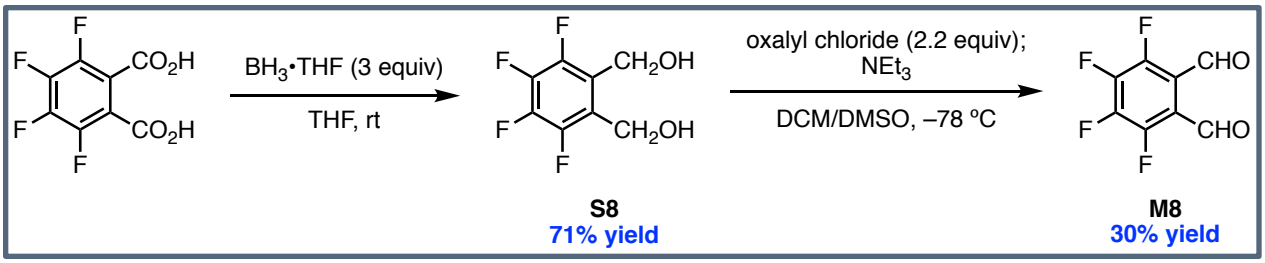

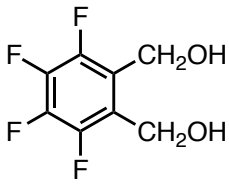

S8

(Perfluoro-1,2-phenylene)dimethanol (S8).[14] A 500-mL round-bottomed flask was charged with 3,4,5,6-tetrafluorophthalic acid (4.21 g, 17.7 mmol, 1.00 equiv), then evacuated and refilled with N_2 (x3). Anhydrous THF (40 mL) was added, and the flask was cooled to 0 °C in an ice/water bath. BH_3•THF (53.0 mL of a 1 M solution in THF, 53.0 mmol, 2.99 equiv) was added. The flask was removed from the cold bath, and the reaction mixture was stirred at rt for 14 h. The reaction was carefully quenched by adding 1 M HCl (~12 mL – caution, bubbling), followed by water (50 mL). The diluted reaction mixture was extracted with DCM (3 x 50 mL), washed with brine (50 mL), dried over $MgSO_4$, filtered via vacuum filtration, and concentrated on the rotary evaporator to afford a pale yellow oil. The crude material was purified via automated column chromatography (50 g column, 5 → 45% EtOAc in hexanes) and dried under vacuum to provide **S8** (2.64 g, 12.6 mmol, 71% yield) as a white solid.

R_f: 0.48 in 50% EtOAc in hexanes.

FTIR (ATR): ν 2339.99 (m), 2898.66 (w), 1706.33 (m), 1640.03 (w), 1510.84 (m), 1481.57 (s), 1456.19 (m), 1379.16 (s), 1311.38 (m), 1289.22 (m), 1234.24 (m), 1159.92 (w), 1108.28 (s), 1020.48 (w), 1049.52 (s), 983.32 (s), 952.34 (m), 922.49 (m), 893.37 (m), 833.39 (w), 810.53 (w), 774.00 (m), 701.81 (m), 682.53 (s), 661.35 (w), 624.49 (w) cm^{-1}.

EA: Found C, 46.0; H, 2.8. $C_8H_6F_4O_2$ requires C, 45.7, H, 2.9.

NMR: See Figure S23 on pg S47.

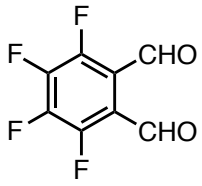

M8

3,4,5,6-Tetrafluorophthalaldehyde (M8).[5] An oven-dried 200-mL recovery flask was charged with a stir bar and evacuated and refilled with N_2 (x3), then charged with anhydrous DCM (40 mL) and cooled to –78 °C in a dry ice/acetone bath. Oxalyl chloride (4.2 mL, 50. mmol, 2.2 equiv) was added, followed by addition of anhydrous DMSO (10 mL). The solution was stirred at –78 °C for 20 min, then a solution of **S8** (4.73 g, 22.5 mmol, 1.00 equiv) in DMSO/DCM (2:1, 60 mL) was added. After stirring at –78 °C for 2 h, triethylamine (53 mL) was added. The reaction mixture was removed from the cold bath and stirred at rt for 2.5 h. The reaction was quenched with water (80 mL) and extracted with DCM (4 x 80 mL), and the combined organic extracts were dried over $MgSO_4$, filtered, and concentrated on the rotary evaporator to provide a brown oil. The crude material was purified via automated column chromatography (100 g column, 5 → 80% EtOAc in hexanes) and dried under vacuum for 2 days to yield a yellow solid (2.48 g). ^{1}H and ^{19}F NMR spectroscopic analysis of this solid suggested that the material was comprised primarily of oligomeric material. The solid was heated at 90 °C under vacuum (~0.1 torr) for 8 h. A portion of the resulting material (757.5 mg) was dissolved in anhydrous THF (2.0 mL) and polystyrene sulfonic acid (0.05 mL of an aqueous 18–22 wt% solution) was added as a nonvolatile acid catalyst to trigger deoligomerization at elevated temperature. The solution was concentrated on the rotary evaporator to afford a yellow solid, then heated at 90 ºC under vacuum (~0.1 torr) for 4 h. The resulting solid was sublimed at 150–160 ºC under vacuum (~0.1 torr) for 45 min. Before the cold finger could warm up, the deposited material was scraped off to provide a low-melting yellow solid (426.9 mg, 2.071 mmol, 30% yield). ^{1}H and ^{19}F NMR spectroscopic analysis indicated that the material was around 80% pure **M8**, with additional oligomeric material; however this material was used without further purification.

R_f: 0.69 in 80% EtOAc in hexanes.

FTIR (ATR): ν 3396.19 (w), 2898.98 (w), 1708,33 (s), 1694.78 (s), 1615.60 (m), 1510.70 (s), 1473.45 (s) 1394.52 (m), 1365.09 (s), 1309.53 (m), 1282.17 (m), 1134.45 (m) 1104.55 (s), 1017.83 (m), 945.13 (s), 899.14 (m), 805.01 (m), 743.80 (w), 690.29 (m), 647.05 (w), 608.61 (m) cm^{-1}.

HRMS (EI+): Calc'd for $C_8H_2F_4O_2^+$ [M^+]: 205.9991; found: 205.9986.

NMR: See Figure S24 on pg S48.

IV. Small Molecule NMR Spectra

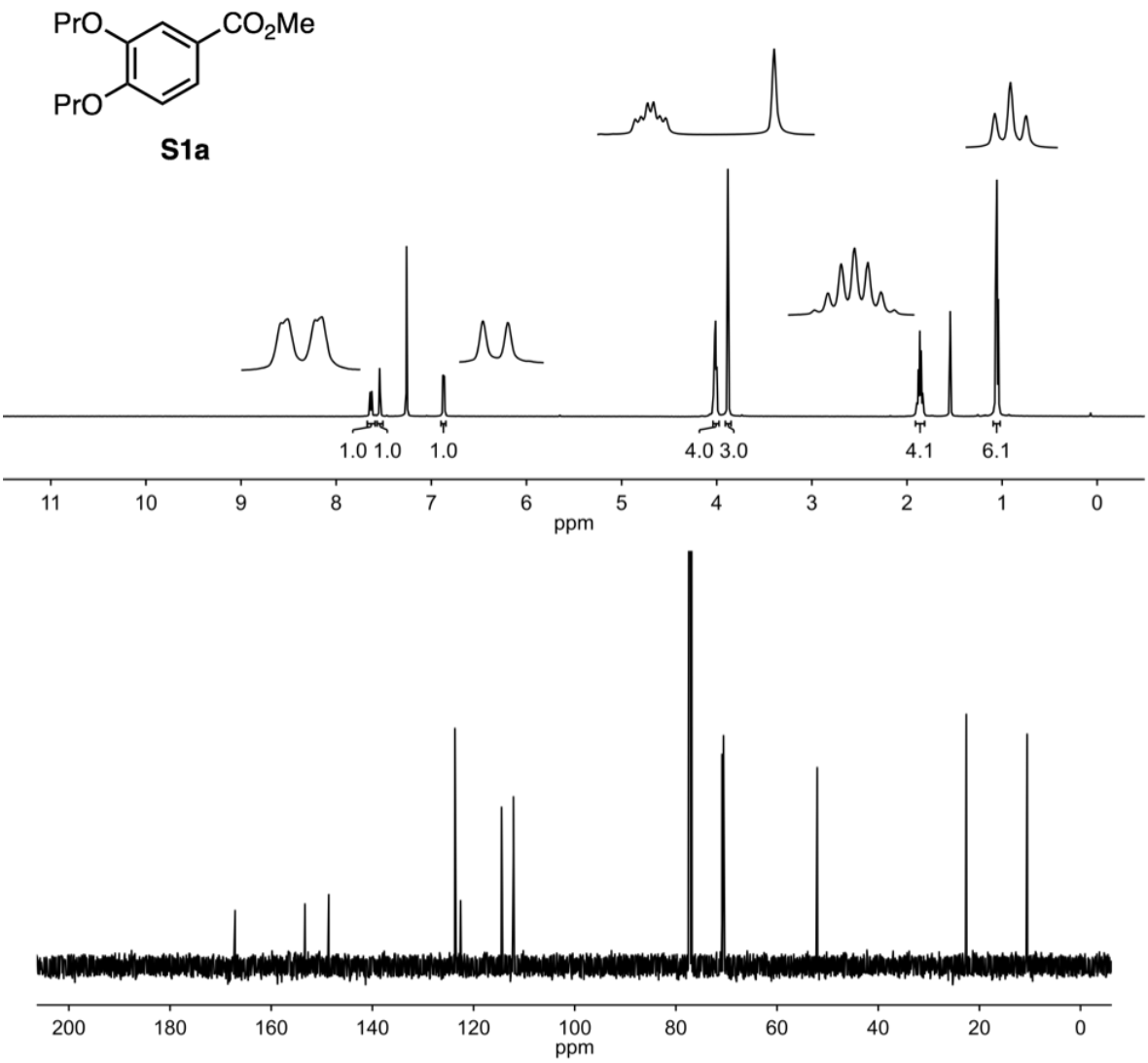

Figure S1. ^{1}H and ^{13}C NMR spectra of **S1a**.

^{1}H NMR (500 MHz, $CDCl_3$): δ 7.64 (dd, *J* = 8.4, 1.6 Hz, 1H), 7.54 (s, 1H), 6.87 (d, *J* = 8.4 Hz, 1H), 4.02 (td, *J* = 6.6, 3.1 Hz, 4H), 3.88 (s, 3H), 1.86 (app. hept, *J* = 7.0 Hz, 4H), 1.05 (t, *J* = 7.4 Hz, 6H) ppm.

^{13}C NMR (126 MHz, $CDCl_3$): δ 167.14, 153.33, 148.62, 123.68, 122.57, 114.46, 112.11, 70.88, 70.58, 52.05, 22.69, 22.60, 10.61, 10.57 ppm.

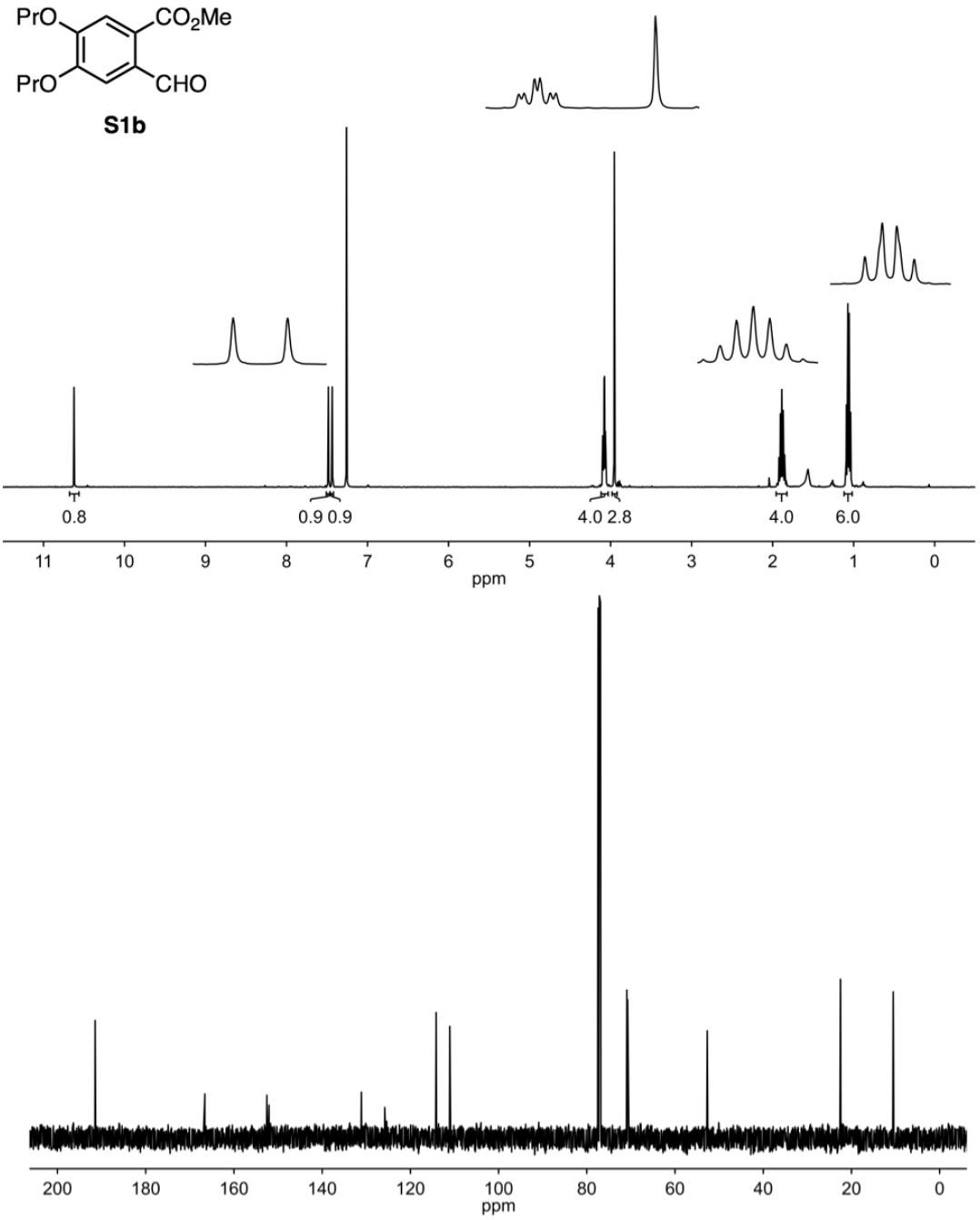

Figure S2. ^{1}H and ^{13}C NMR spectra of **S1b**.

^{1}H NMR (400 MHz, $CDCl_3$): δ 10.62 (s, 1H), 7.48 (s, 1H), 7.44 (s, 1H), 4.08 (app. td, *J* = 6.6, 2.3 Hz, 4H), 3.95 (s, 3H), 1.89 (app. hept, *J* = 7.1 Hz, 4H), 1.06 (app. q, *J* = 7.3 Hz, 6H) ppm.

^{13}C NMR (126 MHz, $CDCl_3$): δ 191.47, 166.59, 152.52, 152.06, 131.12, 125.81, 114.15, 111.07, 70.91, 70.74, 52.69, 22.53, 22.48, 10.55, 10.52 ppm.

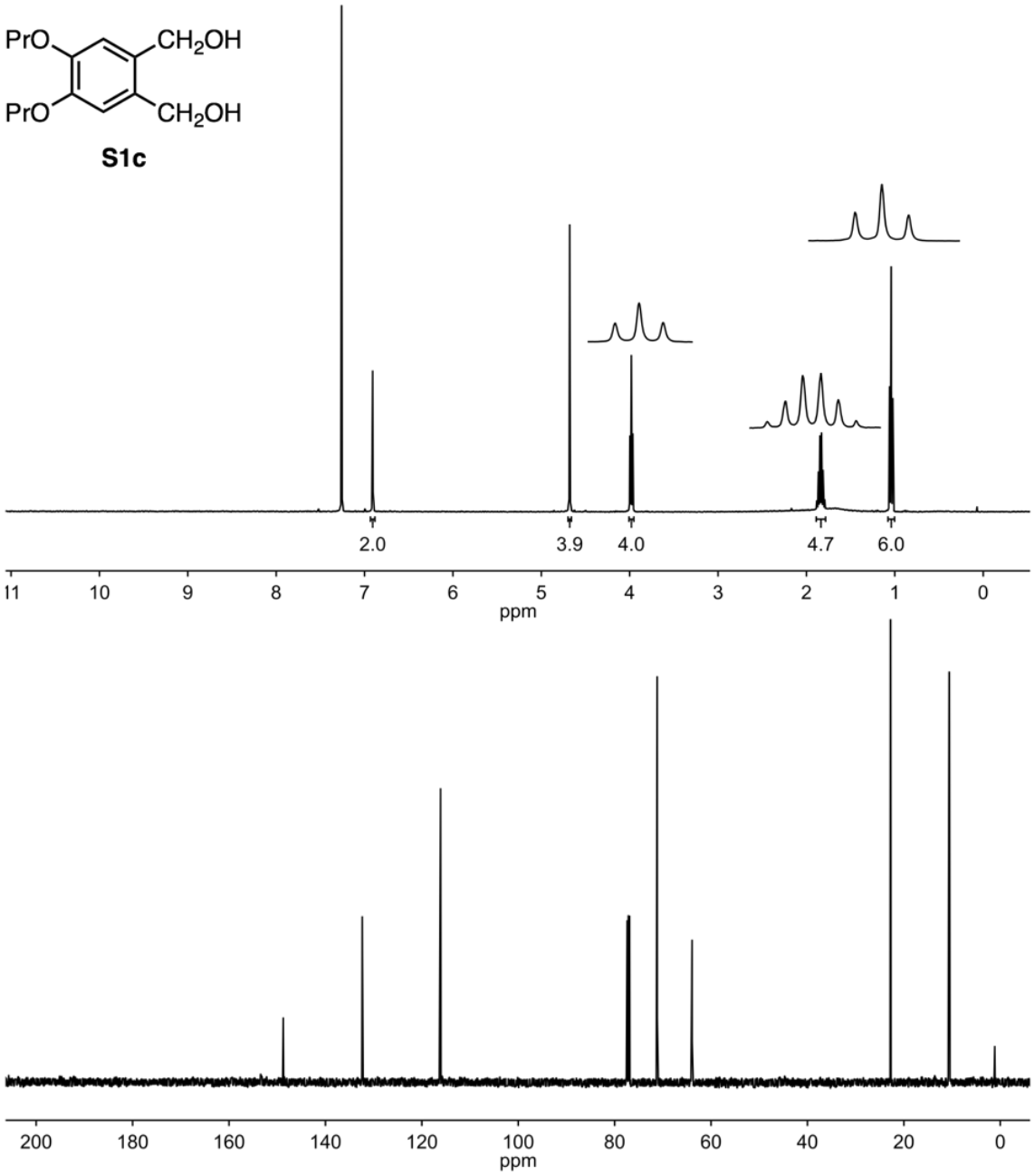

Figure S3. ^{1}H and ^{13}C NMR spectra of **S1c**.

^{1}H NMR (400 MHz, $CDCl_3$): δ 6.91 (s, 2H), 4.68 (s, 4H), 3.98 (t, *J* = 6.6 Hz, 4H), 1.84 (sext, *J* = 7.2Hz, 4H), 1.04 (t, *J* = 7.4 Hz, 6H) ppm.

^{13}C NMR (126 MHz, $CDCl_3$): δ 148.75, 132.36, 116.11, 71.16, 63.93, 22.77, 10.59 ppm.

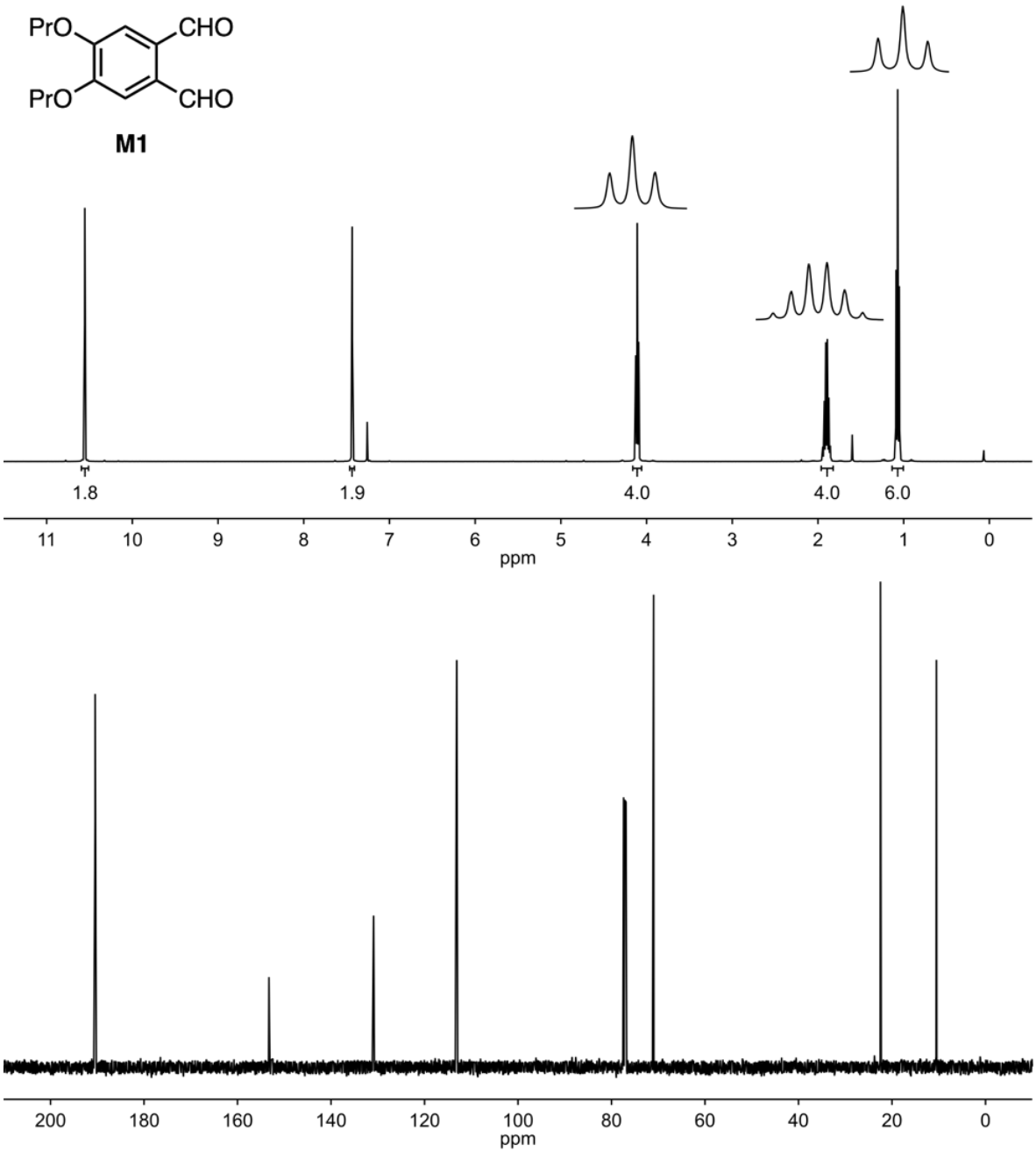

Figure S4. ^{1}H and ^{13}C NMR spectra of **M1**.

^{1}H NMR (400 MHz, $CDCl_3$): δ 10.55 (s, 2H), 7.43 (s, 2H), 4.11 (t, *J* = 6.6 Hz, 4H), 1.90 (sext, *J* = 7.2 Hz, 4H), 1.07 (t, *J* = 7.4 Hz, 6H) ppm.

^{13}C NMR (126 MHz, $CDCl_3$): δ 190.46, 153.28, 130.89, 113.10, 70.99, 22.48, 10.51 ppm.

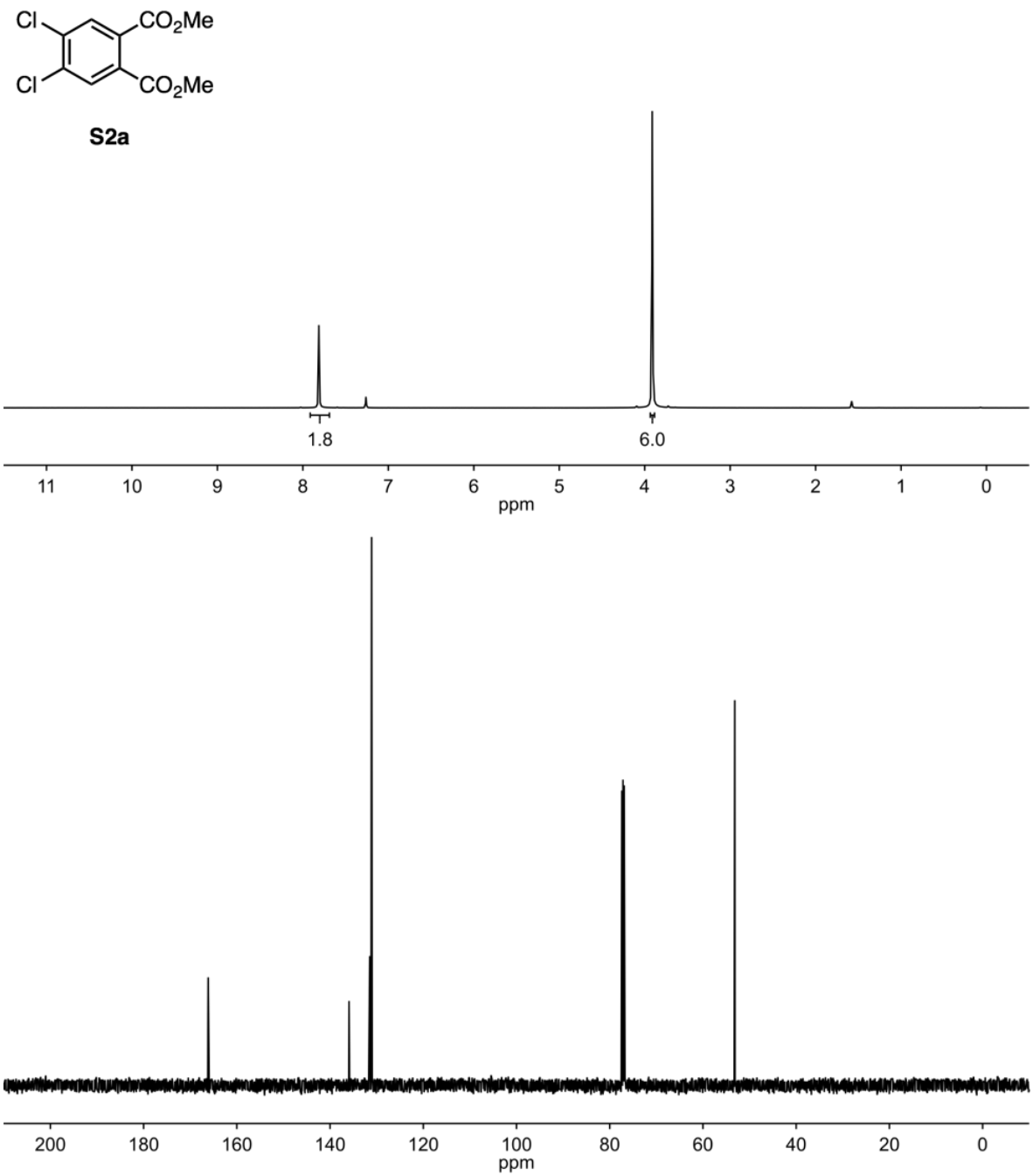

Figure S5. ^{1}H and ^{13}C NMR spectra of **S2a**.

^{1}H NMR (400 MHz, $CDCl_3$): δ 7.81 (s, 2H), 3.91 (s, 6H) ppm.

^{13}C NMR (126 MHz, $CDCl_3$): δ 166.14, 135.93, 131.50, 131.08, 53.18 ppm.

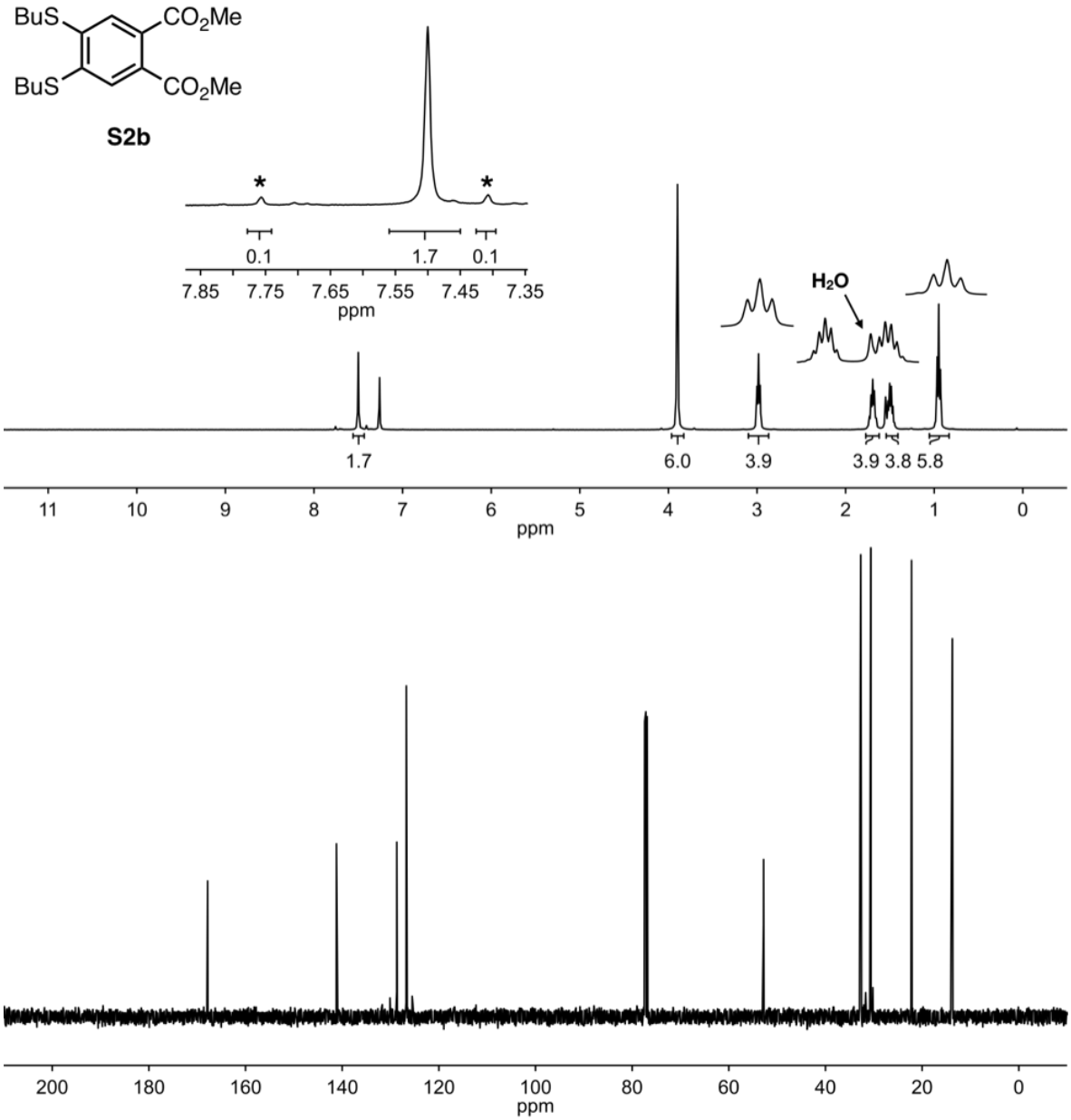

Figure S6. ^{1}H and ^{13}C NMR spectra of **S2b**.

^{1}H NMR (400 MHz, $CDCl_3$): δ 7.50 (s, 2H), 3.90 (s, 6H), 2.98 (t, *J* = 7.3 Hz, 4H), 1.69 (pent, *J* = 7.3 Hz, 4H), 1.49 (sext, *J* = 7.4 Hz, 4H), 0.95 (t, *J* = 7.3 Hz, 6H) ppm. The asterisks in the inset indicate diagnostic peaks for monothiolated compound.

^{13}C NMR (126 MHz, $CDCl_3$): δ 167.85, 141.19, 128.72, 126.73, 52.81, 32.71, 30.62, 22.19, 13.75 ppm.

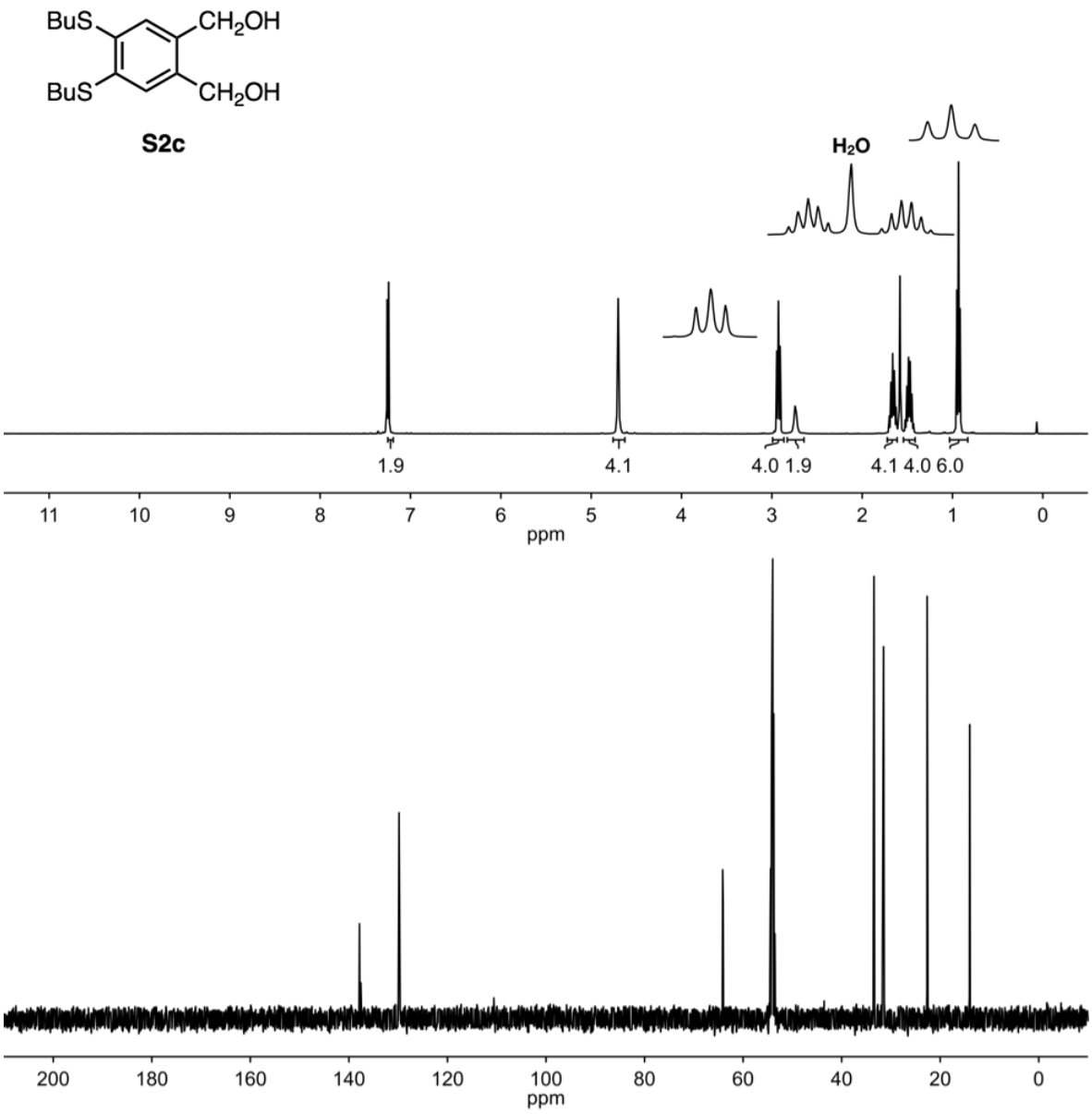

Figure S7. ^{1}H and ^{13}C NMR spectra of **S2c**.

^{1}H NMR (400 MHz, $CDCl_3$): δ 7.24 (s, 2H), 4.70 (s, 4H), 2.93 (t, *J* = 7.4 Hz, 4H), 2.74 (broad s, 2H), 1.66 (pent, *J* = 7.3 Hz, 4H), 1.48 (hept, *J* = 7.3 Hz, 4H), 0.93 (t, *J* = 7.3 Hz, 6H) ppm.

^{13}C NMR (126 MHz, CD_2Cl_2): δ 137.85, 137.56, 129.85, 64.08, 33.45, 31.50, 22.65, 14.00 ppm.

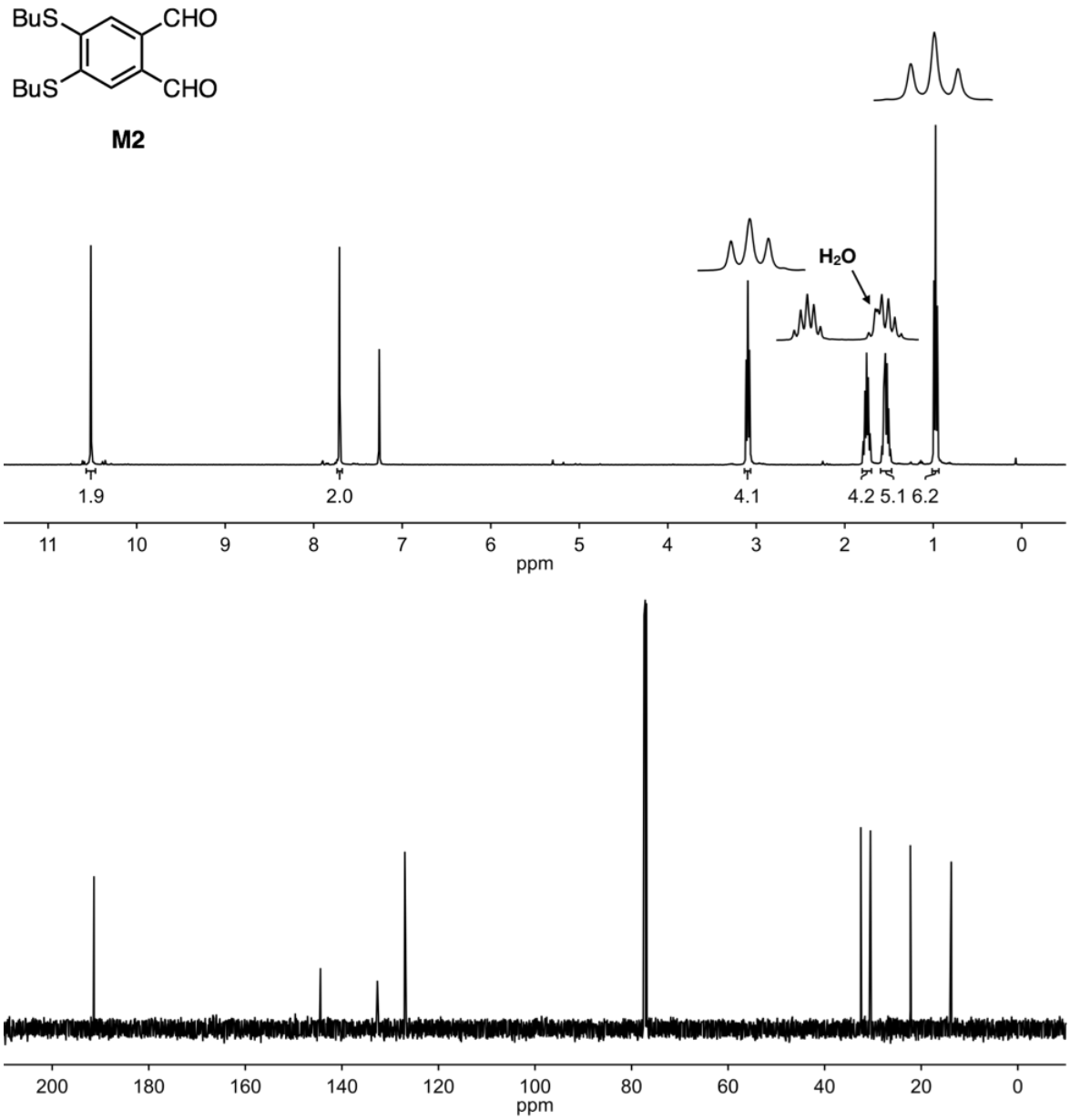

Figure S8. ^{1}H and ^{13}C NMR spectra of **M2**.

^{1}H NMR (400 MHz, $CDCl_3$): δ 10.52 (s, 2H), 7.71 (s, 2H), 3.09 (t, *J* = 7.3 Hz, 4H), 1.75 (pent, *J* = 7.3 Hz, 4H), 1.60–1.46 (m, 4H), 0.97 (t, *J* = 7.3 Hz, 6H) ppm.

^{13}C NMR (126 MHz, $CDCl_3$): δ 191.35, 144.43, 132.66, 126.97, 32.51, 30.52, 22.24, 13.78 ppm.

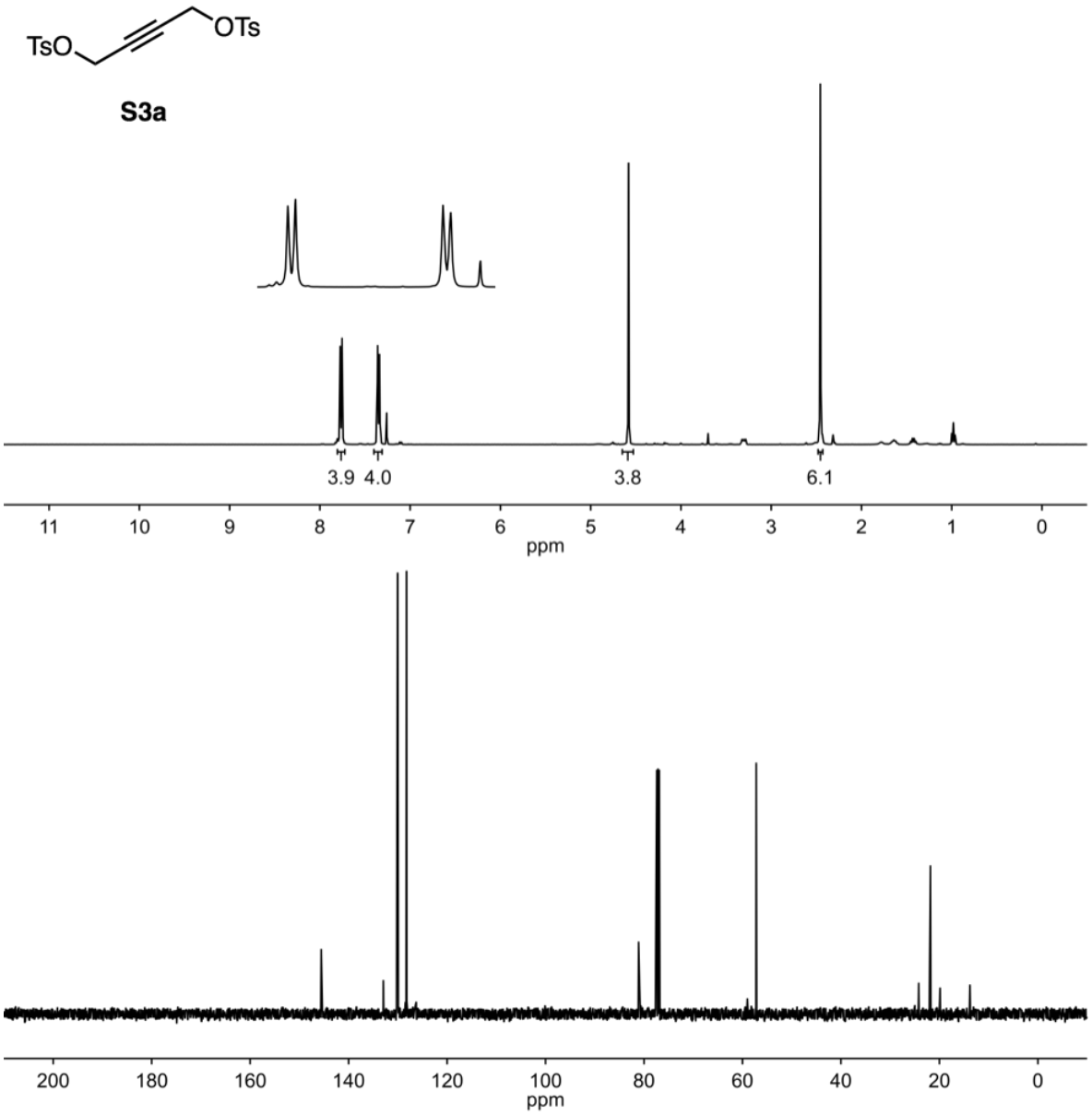

Figure S9. ^{1}H and ^{13}C NMR spectra of **S3a**.

^{1}H NMR (400 MHz, $CDCl_3$): δ 7.76 (d, *J* = 8.2 Hz, 2H), 7.35 (d, *J* = 8.2 Hz, 2H), 4.58 (s, 2H), 2.46 (s, 6H) ppm.

^{13}C NMR (126 MHz, $CDCl_3$): δ 145.56, 132.94, 130.04, 128.23, 81.10, 57.21, 21.82 ppm.

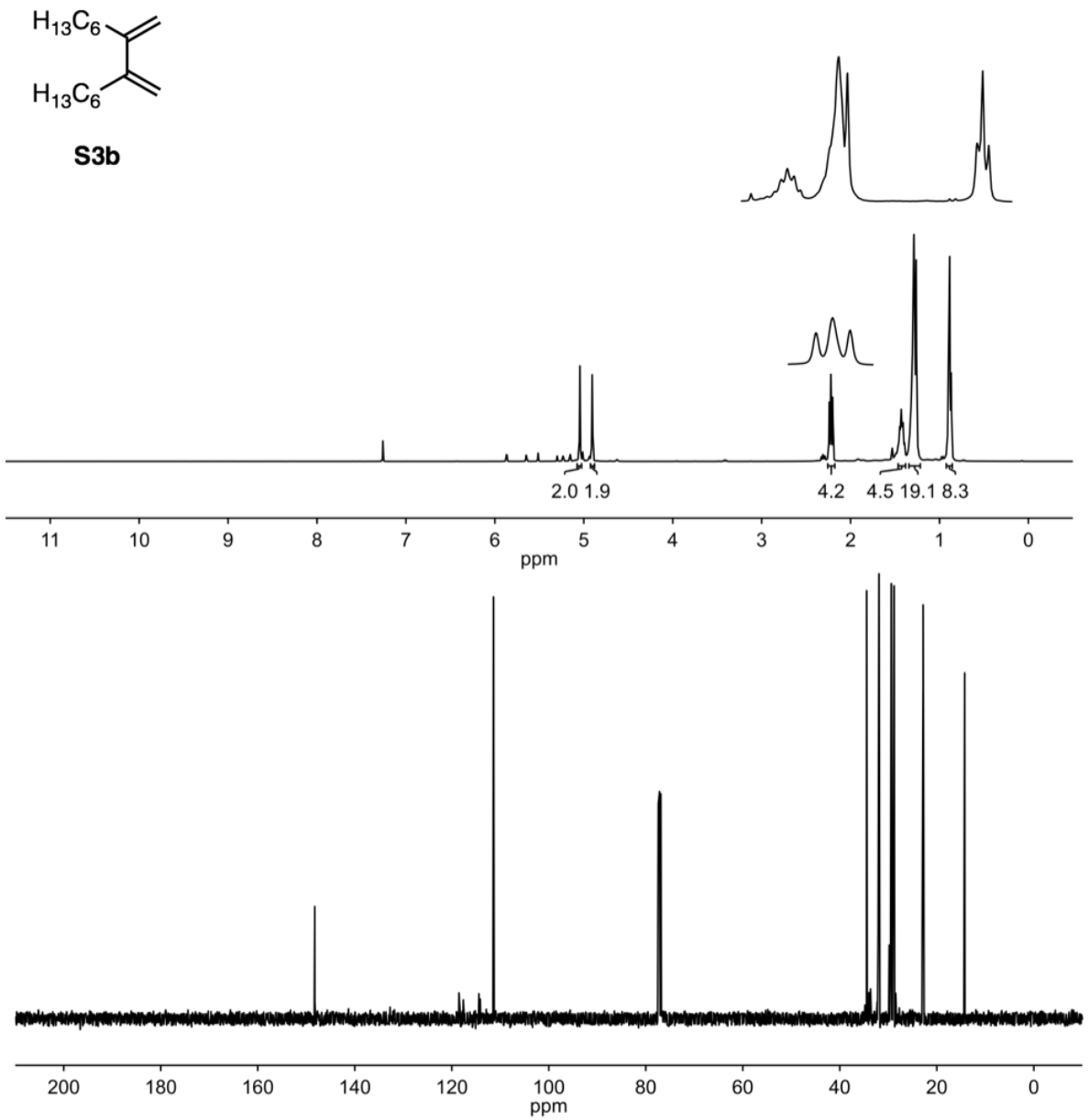

Figure S10. ^{1}H and ^{13}C NMR spectra of **S3b**.

^{1}H NMR (400 MHz, $CDCl_3$): δ 5.04 (s, 2H), 4.91 (s, 2H), 2.25–2.19 (m, 4H), 1.43 (pent, *J* = 7.1 Hz, 4H), 1.36–1.23 (m, 12H), 0.88 (t, *J* = 6.5 Hz, 6H) ppm.

^{13}C NMR (126 MHz, $CDCl_3$): δ 148.25, 111.39, 77.16, 34.47, 31.93, 29.38, 28.81, 22.82, 14.25 ppm.

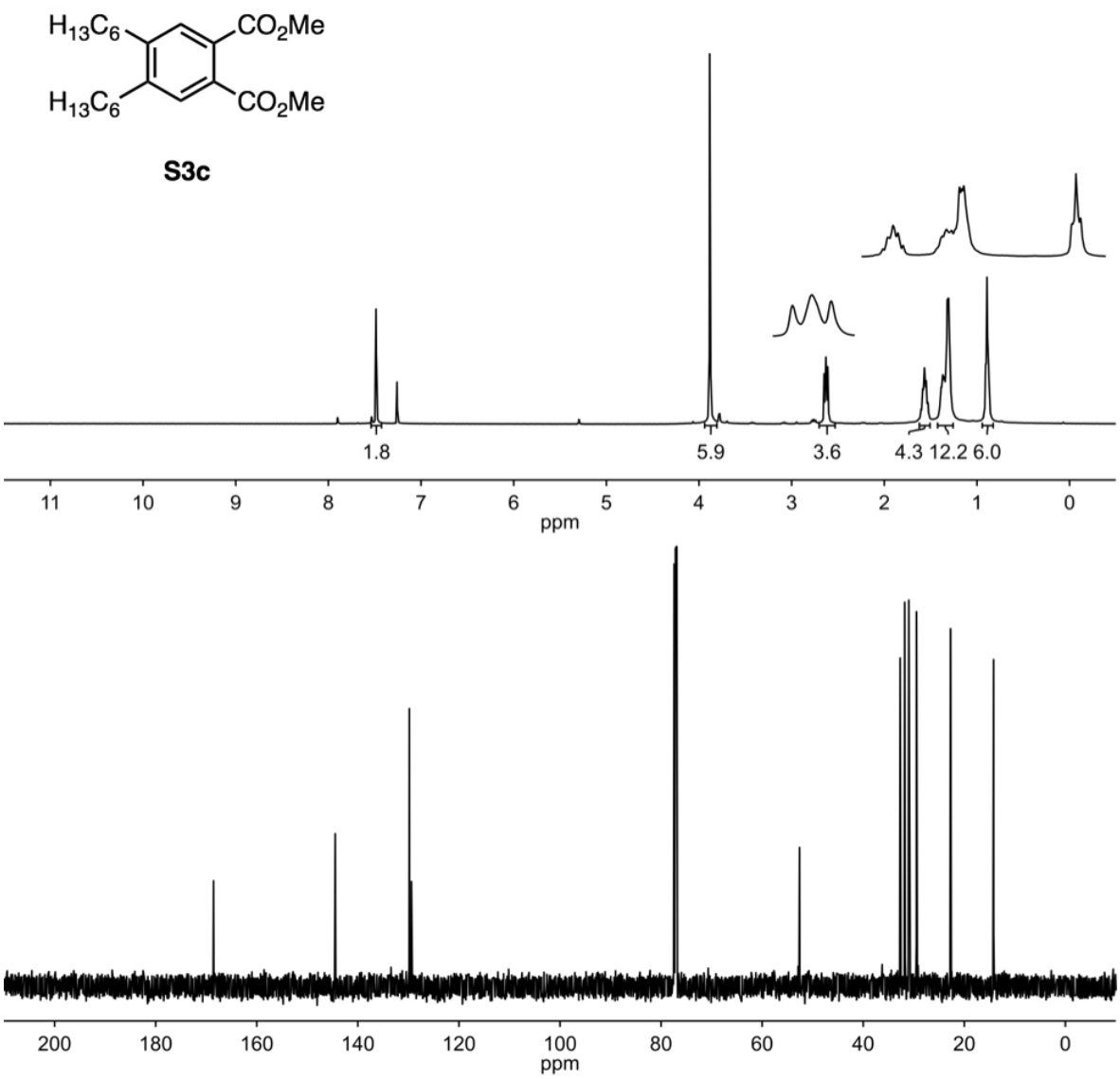

Figure S11. ^{1}H and ^{13}C NMR spectra of **S3c**.

^{1}H NMR (400 MHz, $CDCl_3$): δ 7.49 (s, 2H), 3.88 (s, 6H), 2.67–2.59 (m, 4H), 1.57 (pent, *J* = 7.6 Hz, 4H), 1.43–1.23 (m, 12H), 0.89 (t, *J* = 6.5 Hz, 6H) ppm.

^{13}C NMR (126 MHz, $CDCl_3$): δ 168.56, 144.47, 129.82, 129.39, 52.61, 32.69, 31.80, 30.98, 29.46, 22.72, 14.21 ppm.

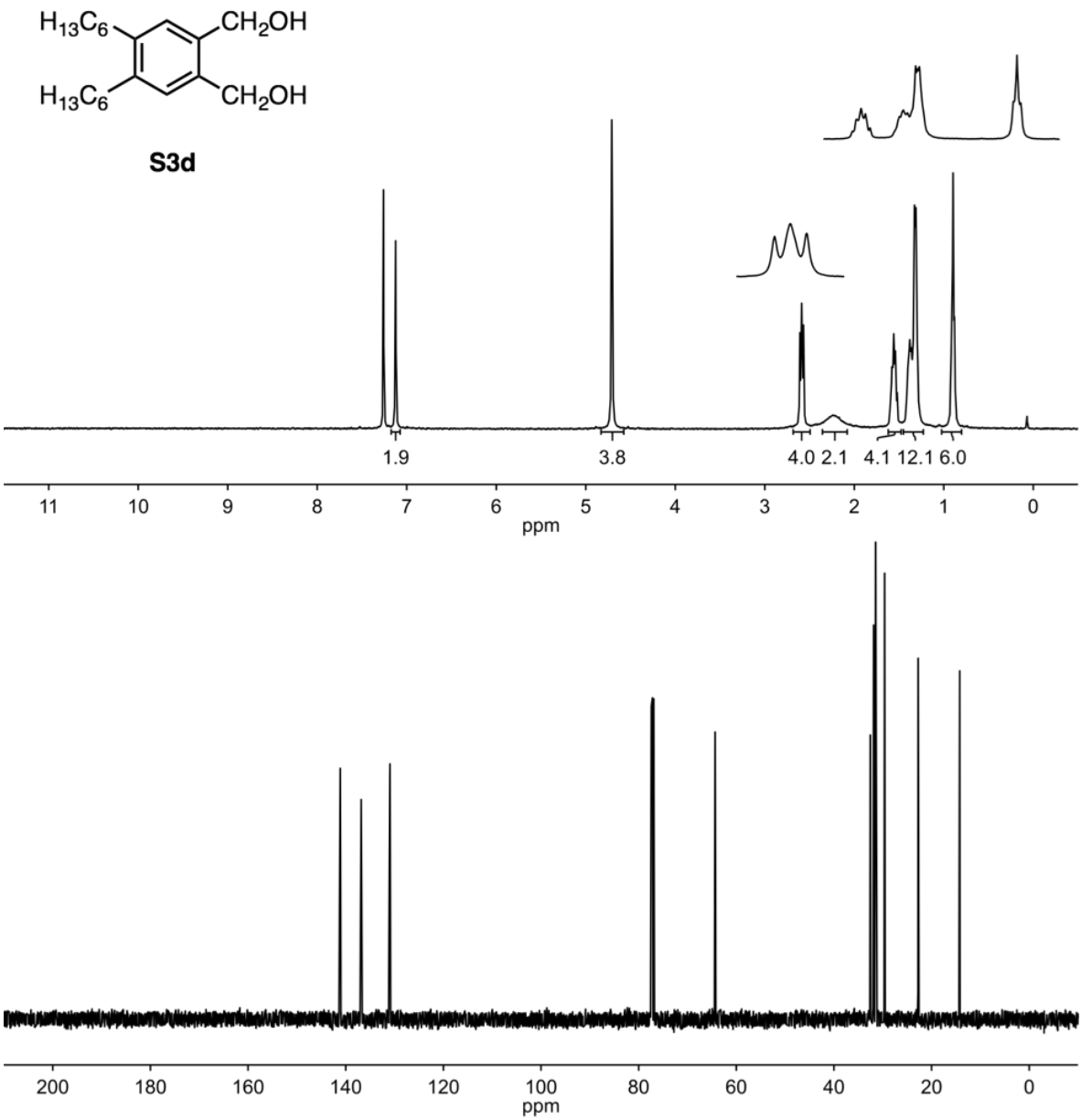

Figure S12. ^{1}H and ^{13}C NMR spectra of **S3d**.

^{1}H NMR (400 MHz, $CDCl_3$): δ 7.12 (s, 2H), 4.71 (s, 4H), 2.63–2.54 (m, 4H), 2.24 (broad s, 2H), 1.56 (pent, *J* = 7.9, 7.3 Hz, 4H), 1.44–1.24 (m, 12H), 0.90 (t, *J* = 6.4 Hz, 6H) ppm.

^{13}C NMR (126 MHz, $CDCl_3$): δ 141.12, 136.83, 130.96, 64.34, 32.55, 31.87, 31.48, 29.62, 22.76, 14.24 ppm.

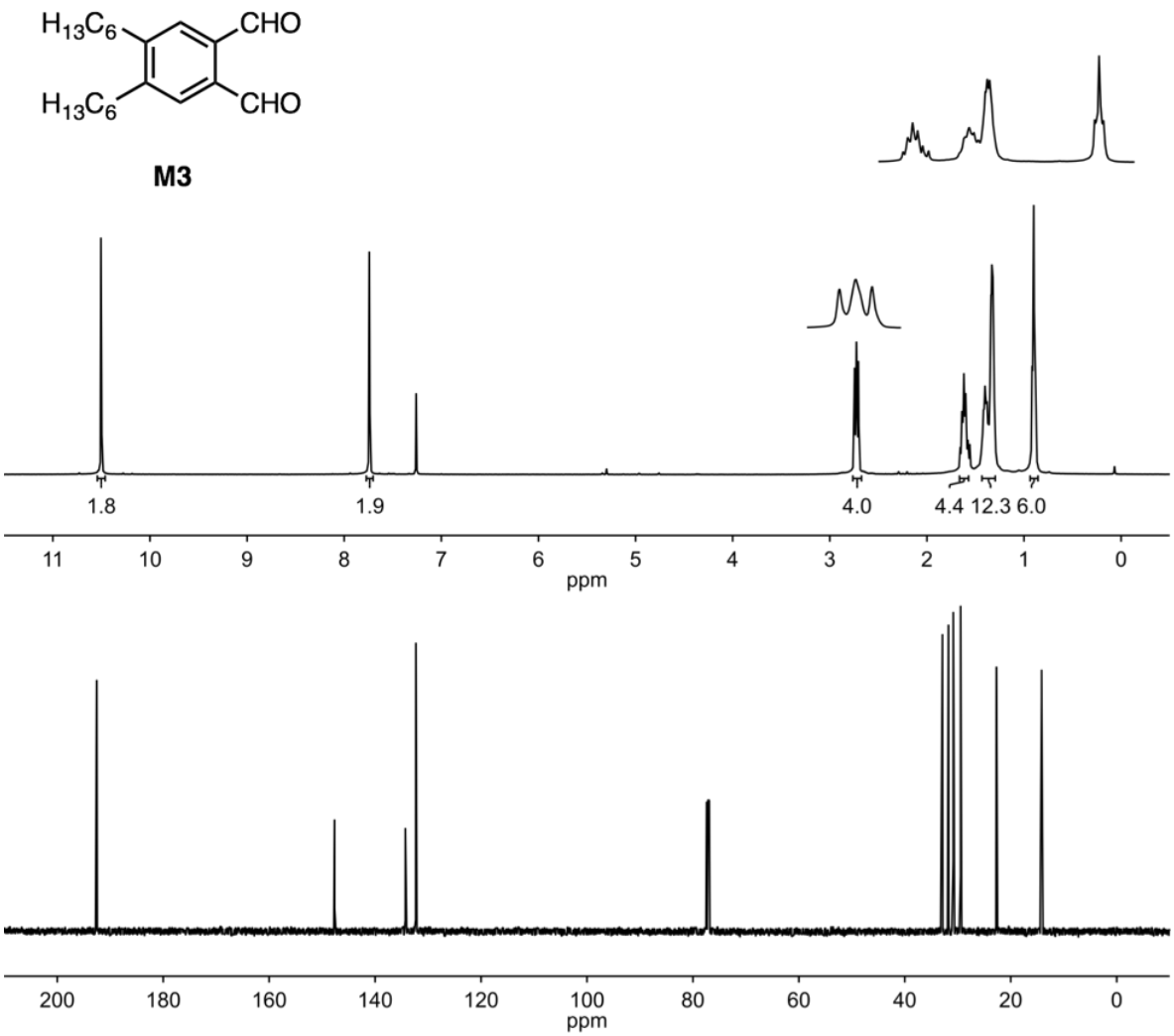

Figure S13. ^{1}H and ^{13}C NMR spectra of **M3**.

^{1}H NMR (400 MHz, $CDCl_3$): δ 10.50 (s, 2H), 7.74 (s, 2H), 2.80–2.64 (m, 4H), 1.62 (pent, *J* = 8.0, 7.5 Hz, 4H), 1.43–1.29 (m, 12H), 0.90 (t, *J* = 6.8 Hz, 6H) ppm.

^{13}C NMR (126 MHz, $CDCl_3$): δ 192.54, 147.66, 134.29, 132.31, 32.90, 31.76, 30.85, 29.46, 22.69, 14.18 ppm.

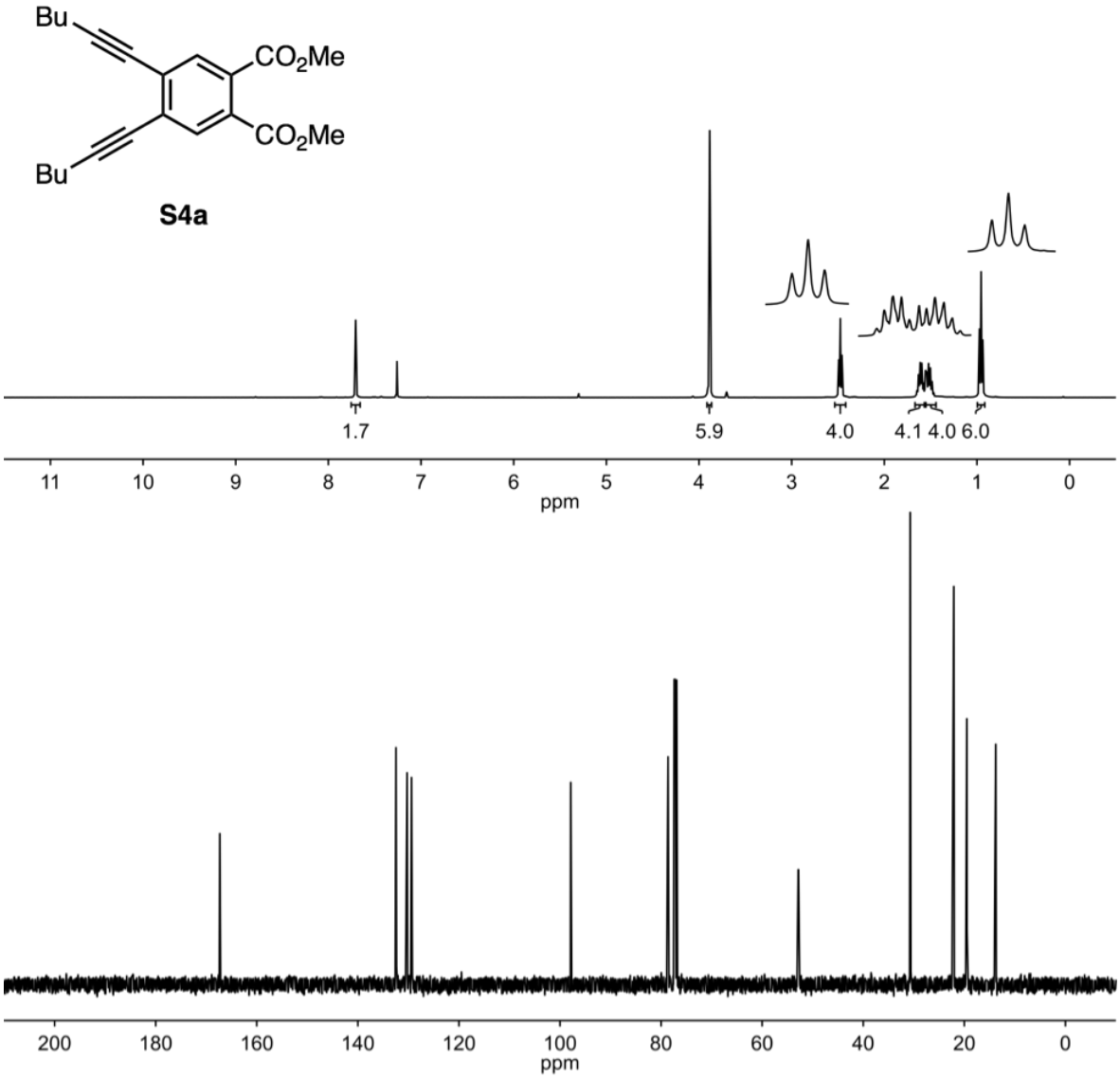

Figure S14. ^{1}H and ^{13}C NMR spectra of **S4a**.

^{1}H NMR (400 MHz, $CDCl_3$): δ 7.71 (s, 2H), 3.88 (s, 6H), 2.47 (t, *J* = 6.9 Hz, 4H), 1.67–1.57 (m, 4H), 1.55–1.44 (m, 4H), 0.96 (t, *J* = 7.2 Hz, 6H) ppm.

^{13}C NMR (126 MHz, $CDCl_3$): δ 167.30, 132.43, 130.25, 129.38, 97.87, 78.62, 52.87, 30.71, 22.08, 19.51, 13.78 ppm.

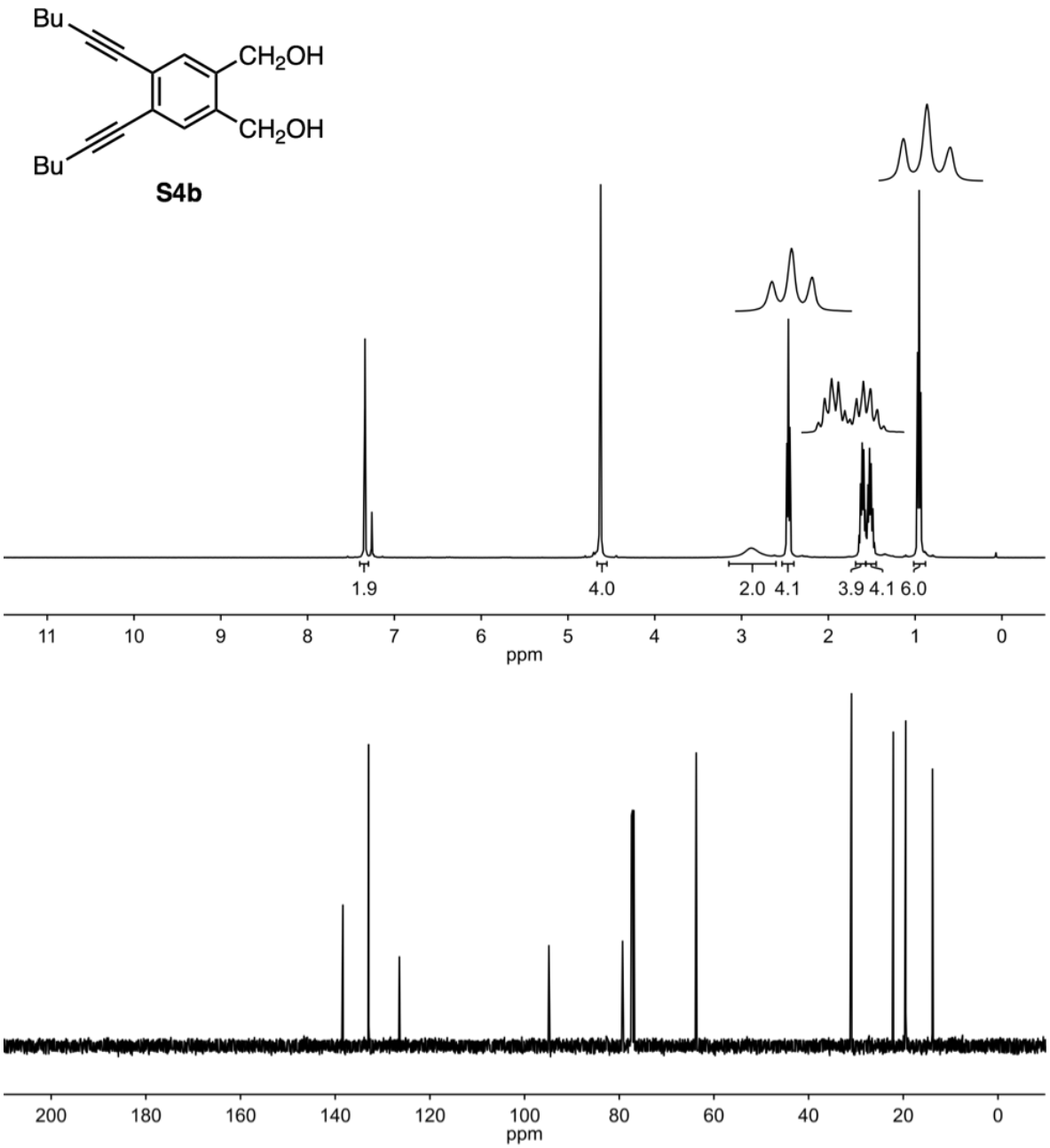

Figure S15. ^{1}H and ^{13}C NMR spectra of **S4b**.

^{1}H NMR (400 MHz, $CDCl_3$): δ 7.34 (s, 2H), 4.62 (s, 4H), 2.89 (broad s, 2H), 2.46 (t, *J* = 6.9 Hz, 4H), 1.61 (pent, *J* = 6.8 Hz, 4H), 1.57–1.45 (m, 4H), 0.95 (t, *J* = 7.2 Hz, 6H) ppm.

^{13}C NMR (126 MHz, $CDCl_3$): δ 138.37, 132.95, 126.45, 94.87, 79.30, 63.73, 30.94, 22.11, 19.48, 13.83 ppm.

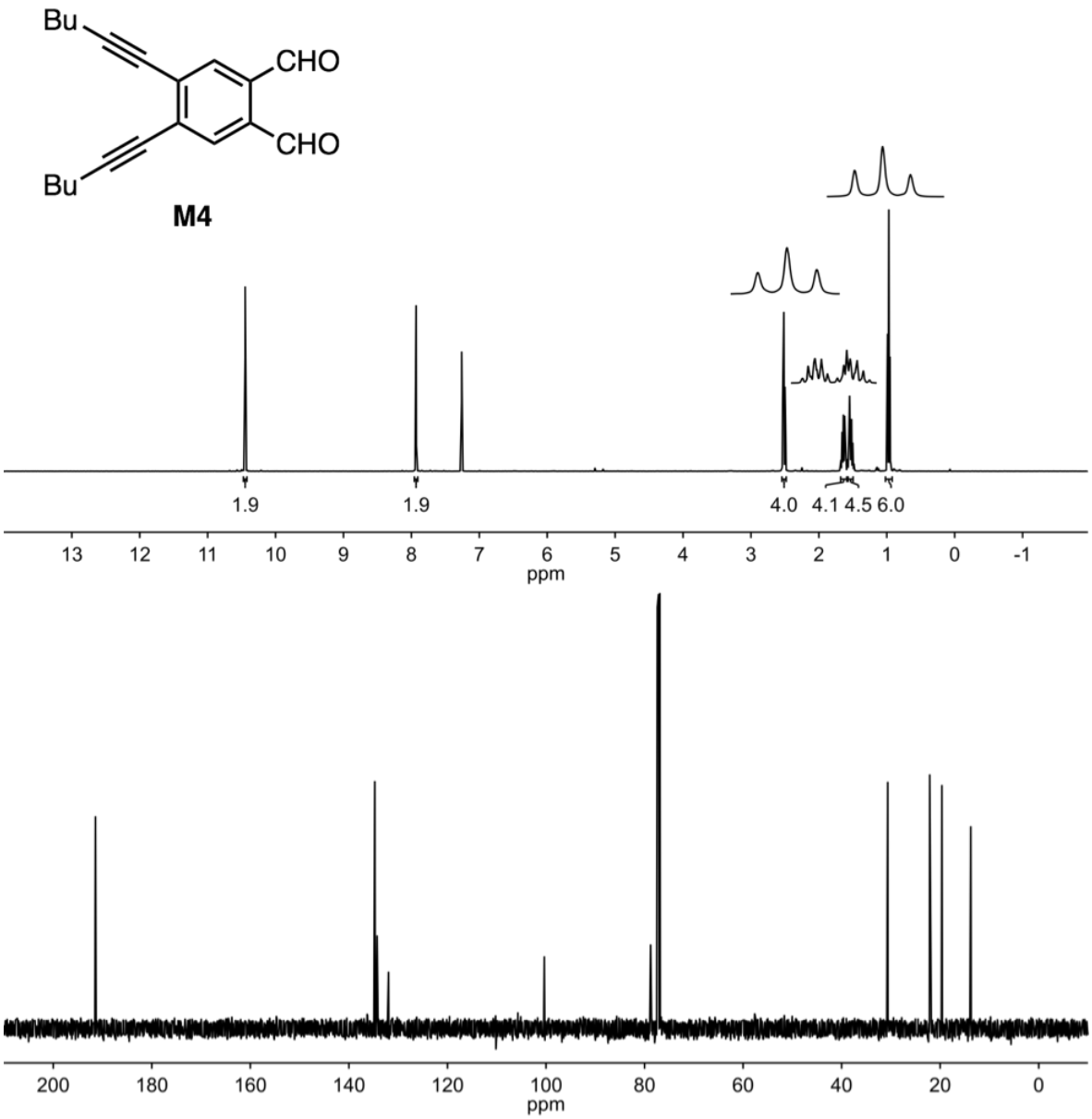

Figure S16. ^{1}H and ^{13}C NMR spectra of **M4**.

^{1}H NMR (400 MHz, $CDCl_3$): δ 10.45 (s, 2H), 7.93 (s, 2H), 2.52 (t, *J* = 6.9 Hz, 4H), 1.69–1.59 (m, 4H), 1.57–1.49 (m, 4H), 0.97 (t, *J* = 7.3 Hz, 6H) ppm.

^{13}C NMR (126 MHz, $CDCl_3$): δ 191.43, 134.74, 134.27, 131.96, 100.34, 78.77, 30.64, 22.12, 19.65, 13.79 ppm.

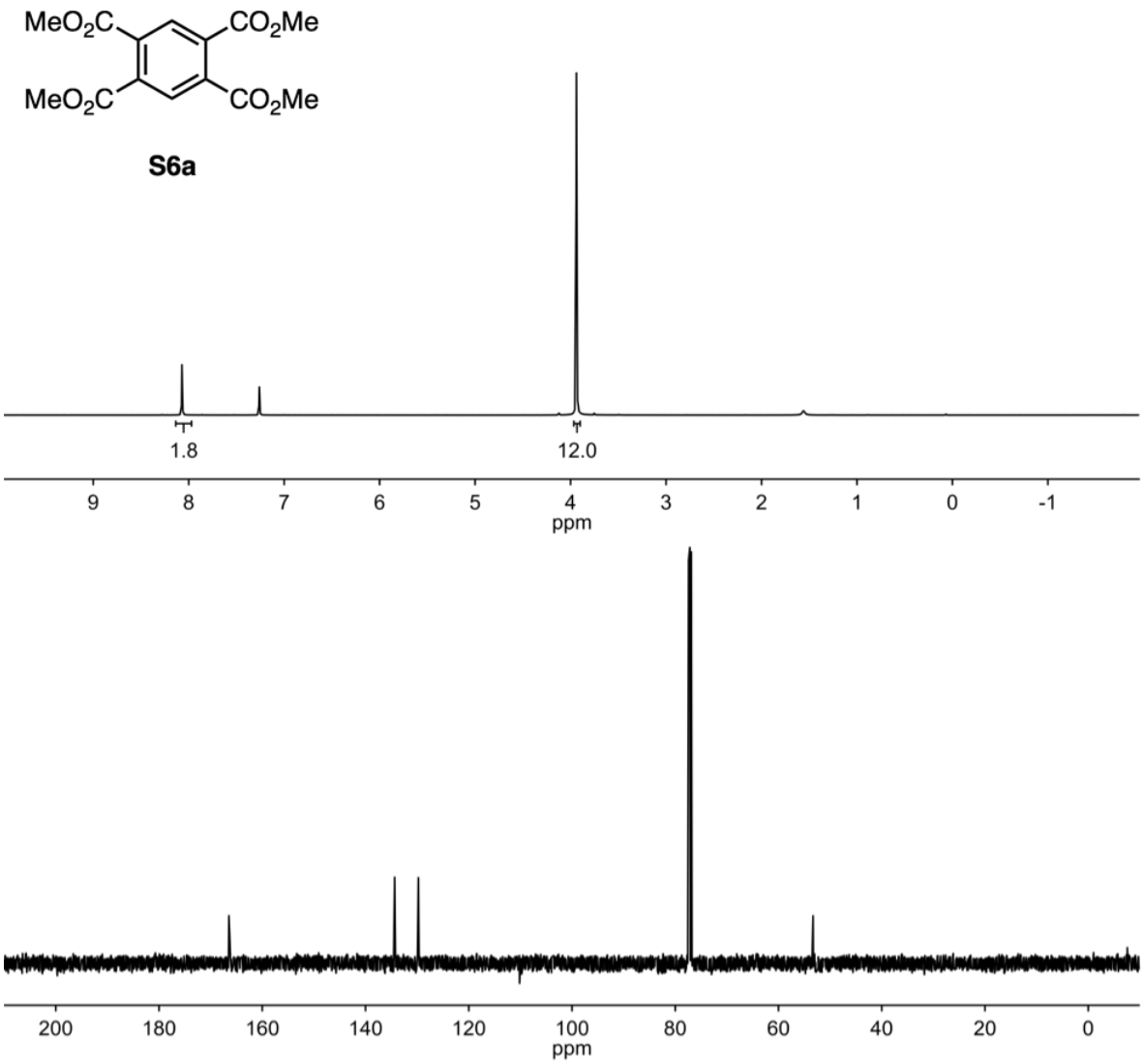

Figure S17. ^{1}H and ^{13}C NMR spectra of **S6a**.

^{1}H NMR (400 MHz, $CDCl_3$): δ 8.07 (s, 2H), 3.94 (s, 12H) ppm.

^{13}C NMR (126 MHz, $CDCl_3$): δ 166.46, 134.35, 129.78, 53.23 ppm.

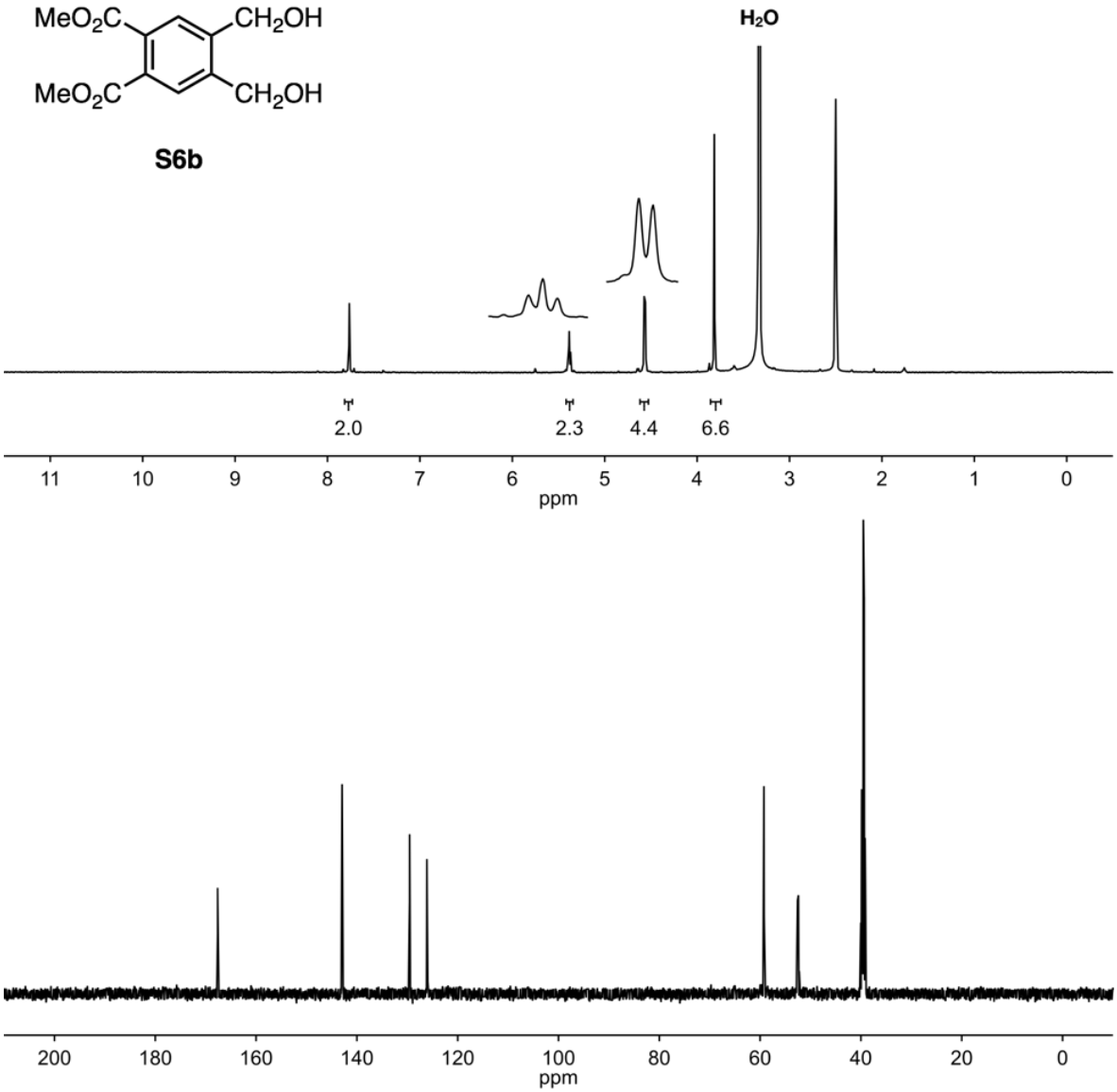

Figure S18. ^{1}H and ^{13}C NMR spectra of **S6b**.

^{1}H NMR (400 MHz, DMSO-d_6): δ 7.76 (s, 2H), 5.38 (t, *J* = 5.4 Hz, 2H), 4.57 (d, *J* = 5.5 Hz, 4H), 3.81 (s, 6H) ppm.

^{13}C NMR (126 MHz, DMSO-d_6): δ 167.63, 142.94, 129.54, 126.04, 59.25, 52.49 ppm.

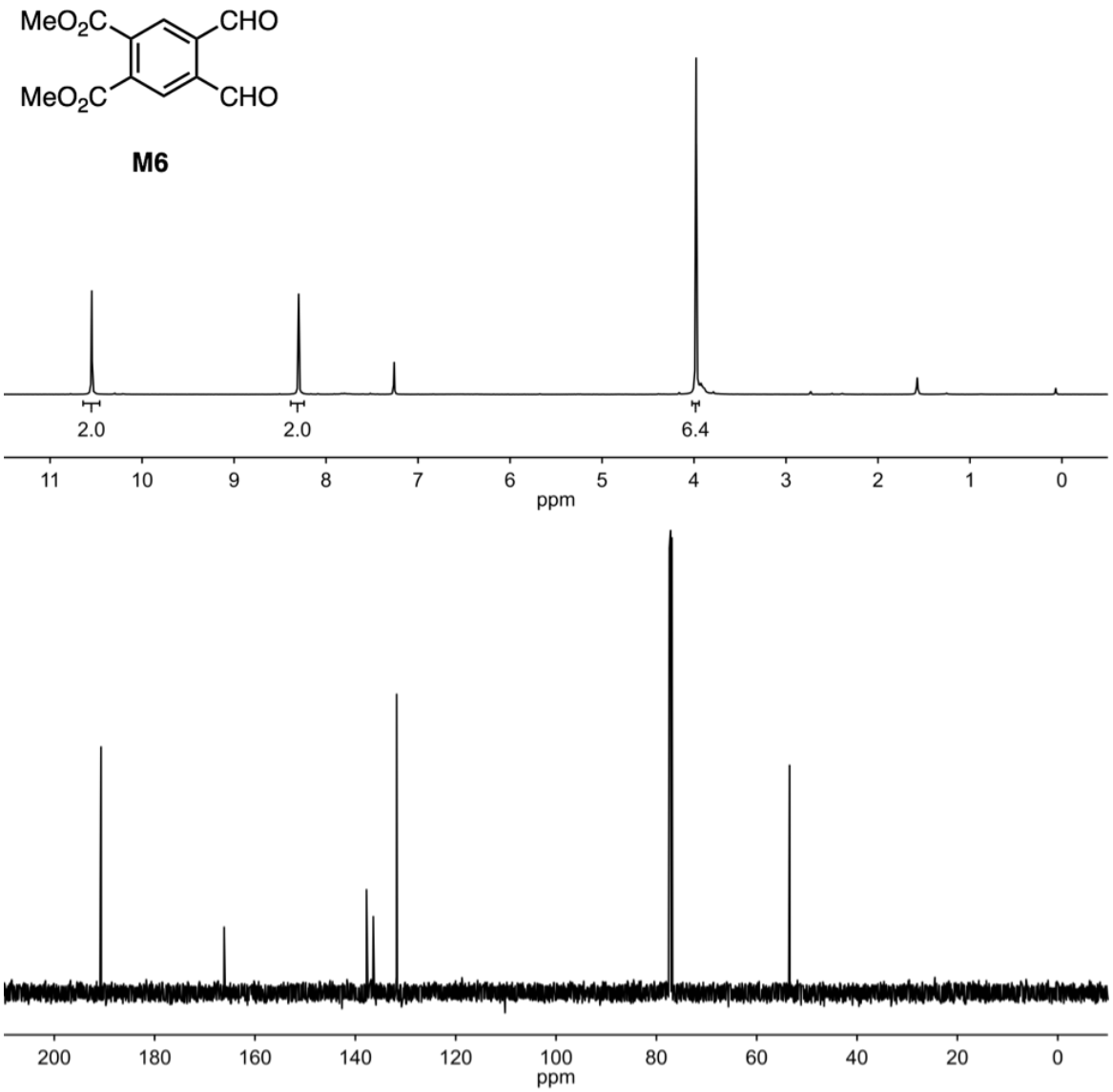

Figure S19. ^{1}H and ^{13}C NMR spectra of **M6**.

^{1}H NMR (400 MHz, $CDCl_3$): δ 10.55 (s, 2H), 8.30 (s, 2H), 3.98 (s, 6H) ppm.

^{13}C NMR (126 MHz, $CDCl_3$): δ 190.68, 166.14, 137.78, 136.42, 131.76, 53.45 ppm.

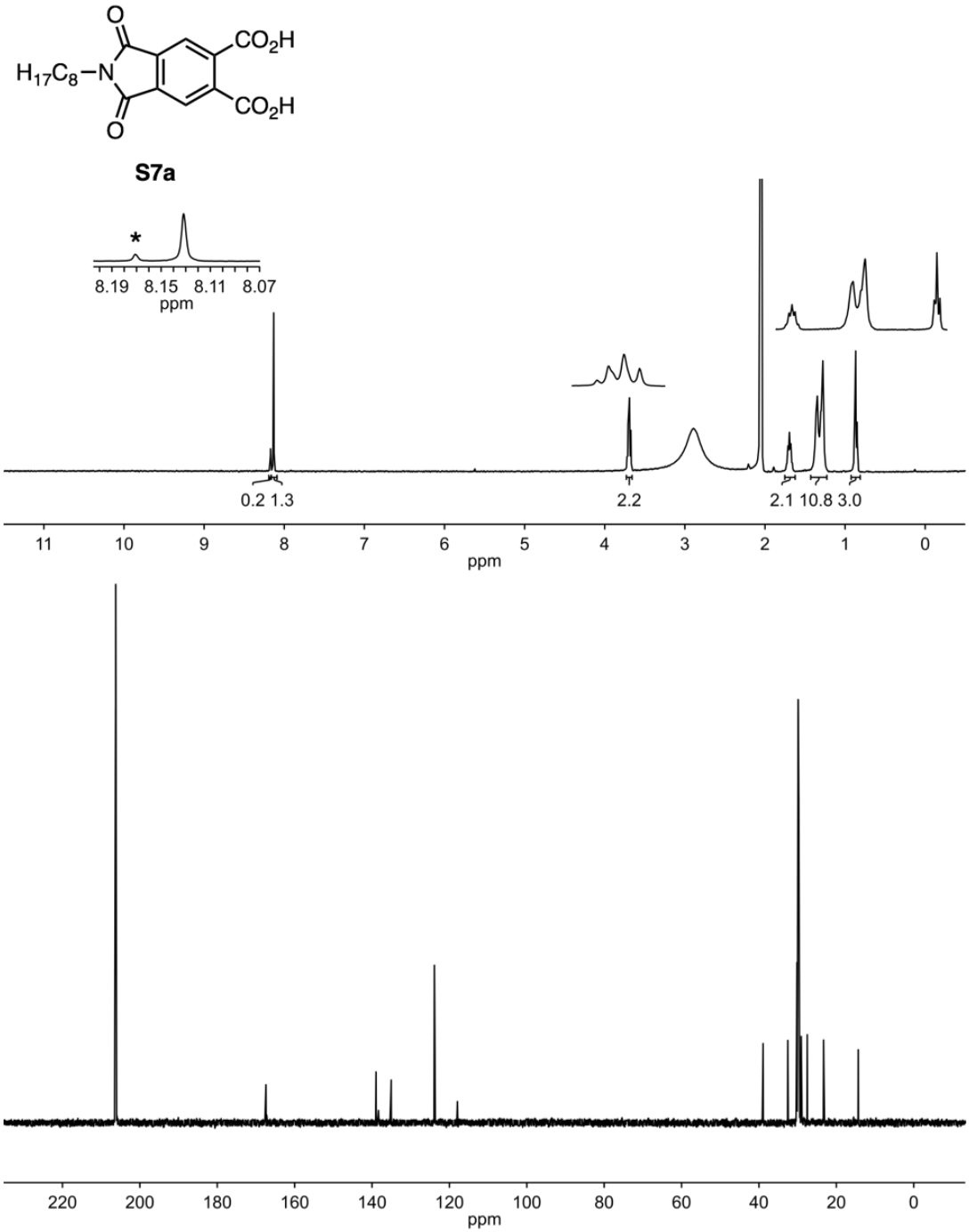

Figure S20. ^{1}H and ^{13}C NMR spectra of **S7a**.

^{1}H NMR (400 MHz, acetone-d_6): δ 8.13 (s, 2H), 3.69 (t, J = 7.1 Hz, 2H), 1.69 (p, J = 7.3 Hz, 2H), 1.45–1.21 (m, 10H), 0.92–0.82 (m, 3H) ppm. The asterisk in the inset indicates the diagnostic peak for the diimide.

^{13}C NMR (126 MHz, acetone-d_6): δ 167.46, 167.41, 138.96, 135.04, 123.88, 38.93, 32.53, 29.91, 29.08, 27.52, 23.30, 14.34 ppm. (One peak is obscured.)

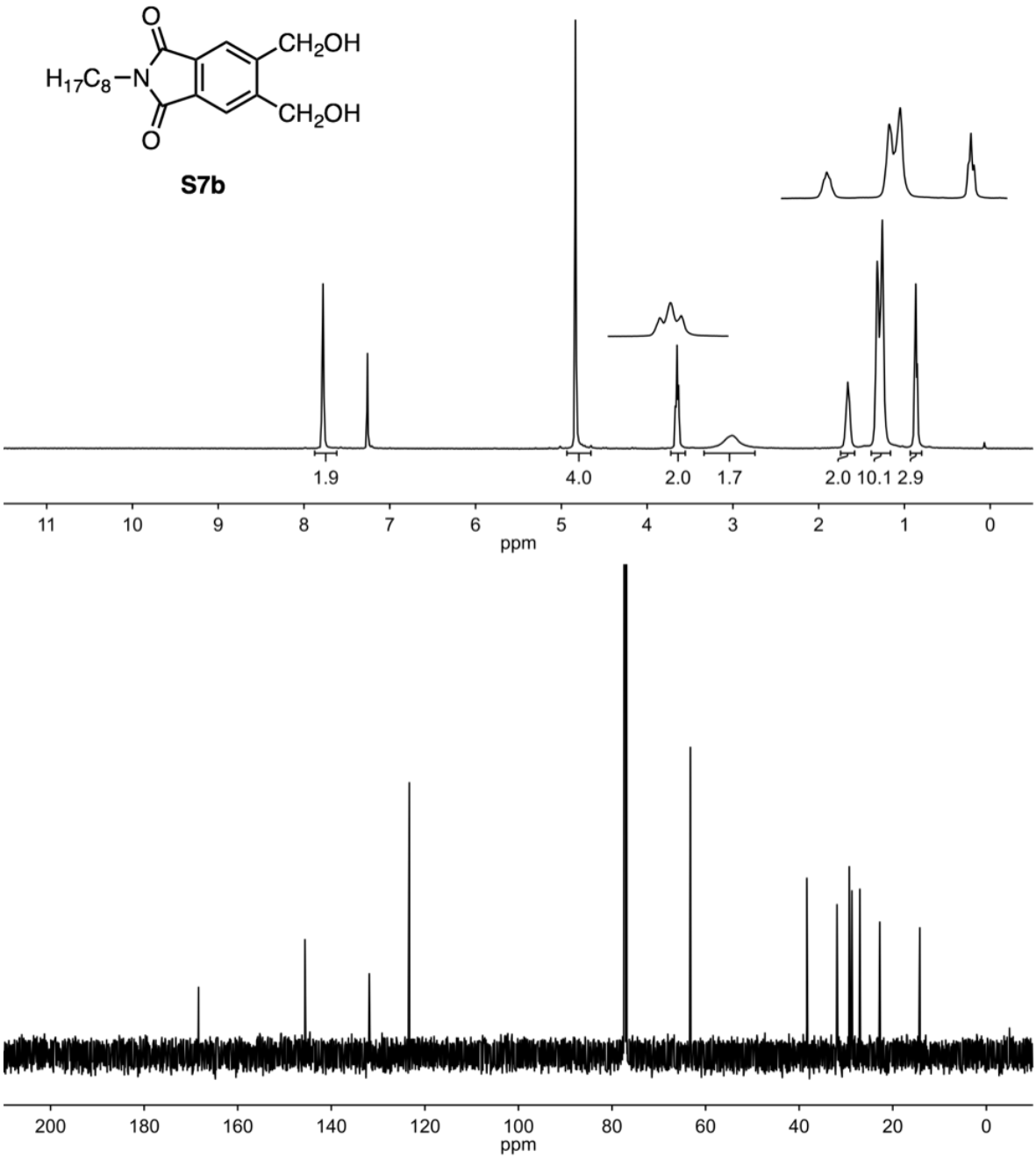

Figure S21. ^{1}H and ^{13}C NMR spectra of **S7b**.

^{1}H NMR (400 MHz, $CDCl_3$): δ 7.78 (t, *J* = 4.3 Hz, 2H), 4.84 (s, 4H), 3.65 (t, *J* = 7.3 Hz, 2H), 3.01 (br s, 1H), 1.74 – 1.59 (m, 2H), 1.29 (d, *J* = 24.0 Hz, 10H), 0.87 (t, *J* = 5.9 Hz, 3H) ppm.

^{13}C NMR (126 MHz, acetone-d_6): δ 168.37, 145.63, 131.89, 123.32, 63.26, 38.37, 31.91, 29.31, 29.29, 28.73, 27.03, 22.77, 14.22 ppm.

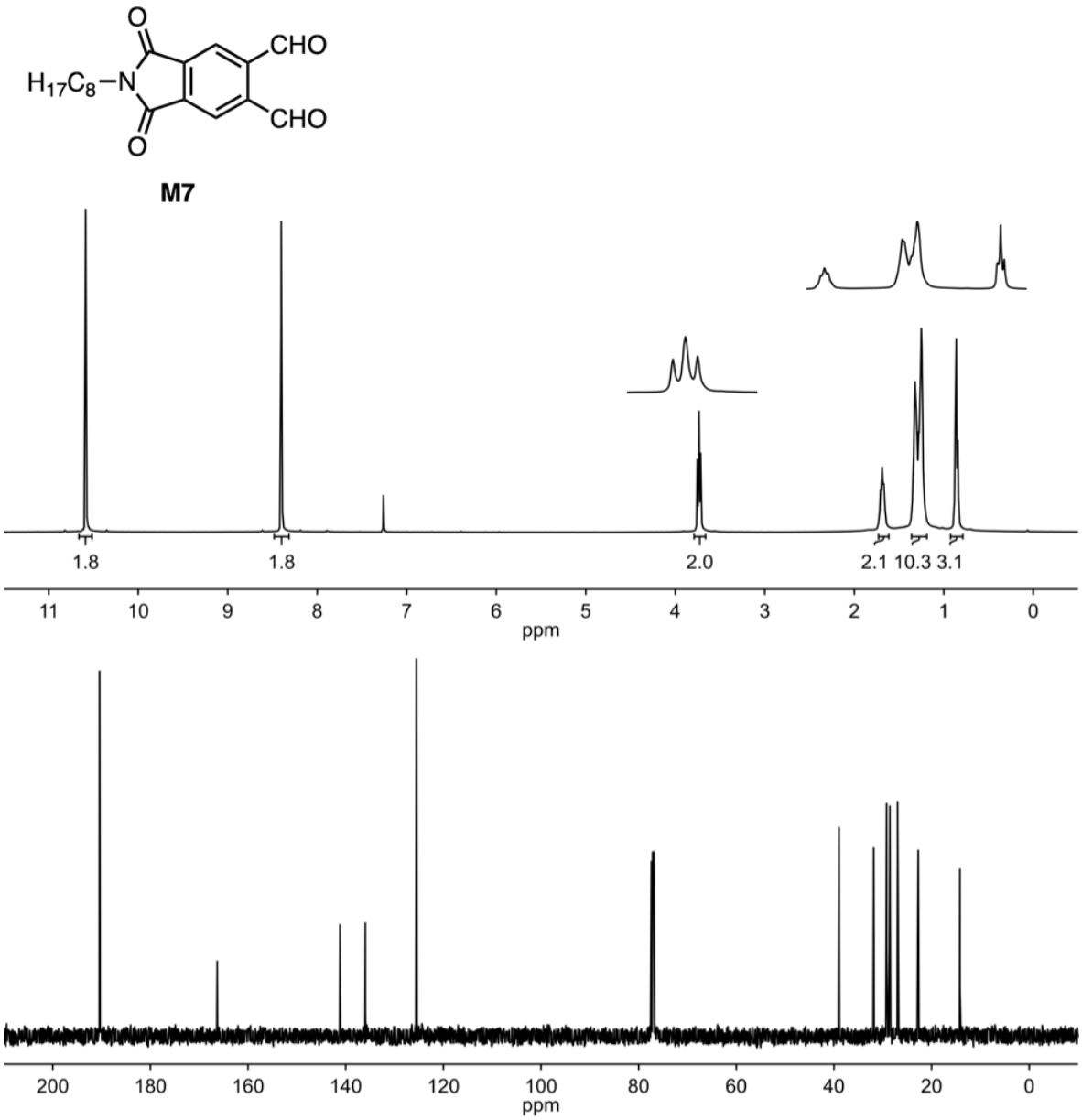

Figure S22. ^{1}H and ^{13}C NMR spectra of **M7**.

^{1}H NMR (400 MHz, $CDCl_3$): δ 10.59 (s, 2H), 8.40 (s, 2H), 3.73 (t, *J* = 7.3 Hz, 2H), 1.80–1.58 (m, 2H), 1.43 – 1.16 (m, 10H), 0.86 (t, *J* = 6.6 Hz, 3H) ppm.

^{13}C NMR (126 MHz, $CDCl_3$): δ 190.42, 166.32, 141.16, 135.98, 125.50, 38.97, 31.87, 29.25, 29.21, 28.56, 26.97, 22.74, 14.20 ppm.

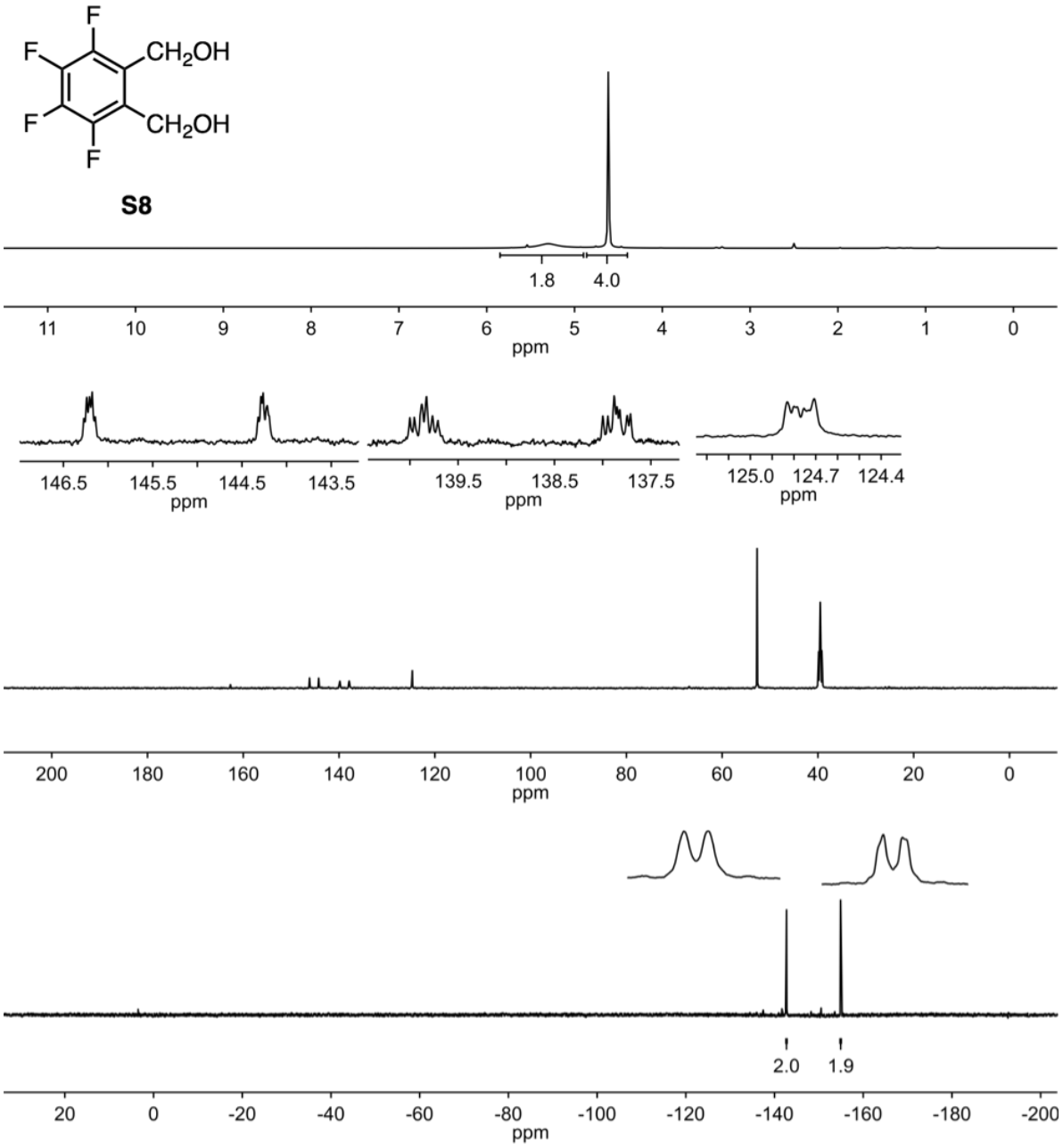

Figure S23. ^{1}H, ^{13}C, and ^{19}F NMR spectra of **S8**.

^{1}H NMR (500 MHz, DMSO-d_6): δ 5.82–4.88 (broad s, 2H), 4.62 (s, 4H) ppm.

^{13}C NMR (126 MHz, DMSO-d_6): δ 145.23 (ddt, J = 244.8, 8.3, 3.3 Hz), 140.11–137.45 (m), 124.89–124.62 (m), 52.70 (s) ppm.

^{19}F NMR (376 MHz, $CDCl_3$): δ –142.68 (d, J = 17.2 Hz, 2F), –154.91 (d, J = 14.9 Hz, 2F) ppm.

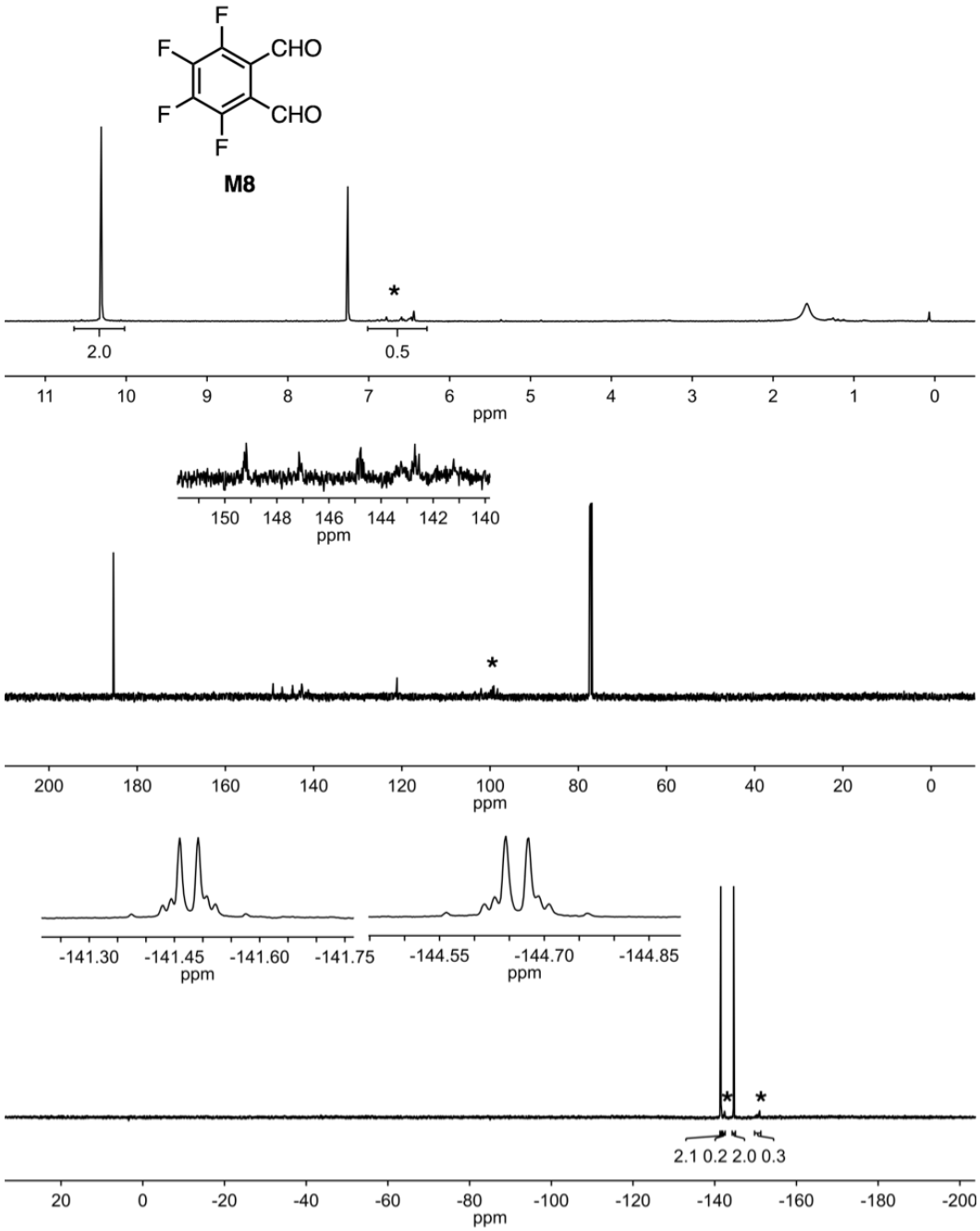

Figure S24. ^{1}H, ^{13}C, and ^{19}F NMR spectra of **M8**. The asterisks denote peaks attributed to oligomer.

^{1}H NMR (500 MHz, $CDCl_3$): δ 10.31 (s, 2H) ppm.

^{13}C NMR (126 MHz, $CDCl_3$): δ 185.39, 148.17 (m), 143.74 (m), 121.09 ppm.

^{19}F NMR (376 MHz, $CDCl_3$): δ –141.48 (m, 2F), –144.66 (m) ppm.

V. Polymerizations and Thermal Analysis

*Attempted Polymerizations of **M1–M3***

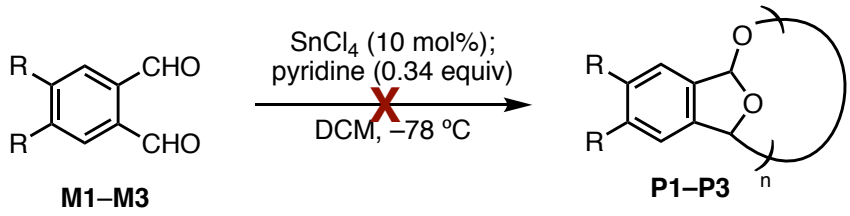

The following stock solutions were prepared in oven-dried 2-dram vials under N_2:

- $SnCl_4$ (0.080 mL, 0.68 mmol) in DCM (2.0 mL)
- pyridine (0.10 mL, 1.2 mmol) in DCM (1.0 mL)

Each of three oven-dried 2-dram vials were charged with a stir bar and **M1**, **M2**, or **M3**:

- vial A: **M1** (87.6 mg, 0.350 mmol)
- vial B: **M2** (108.7 mg, 0.3500 mmol)
- vial C: **M3** (105.9 mg, 0.3500 mmol)

The vials were sealed with a septum-lined cap, and evacuated and refilled with N_2 (x3). DCM (0.4 mL) was added to each vial, and the solutions were cooled to –78 ºC in a dry ice/acetone bath. $SnCl_4$ (0.10 mL of DCM stock solution, 0.034 mmol) was added, and the reactions were stirred at –78 ºC for 2 h. The reactions were quenched by adding pyridine (0.10 mL of DCM stock solution, 0.12 mmol), and stirring was continued at –78 ºC for an additional 2 h.

Each reaction was separately poured into MeOH (10 mL) in an attempt to precipitate polymer, but no precipitate formed. The MeOH solutions were concentrated on the rotary evaporator and subjected to ^{1}H NMR spectroscopic analysis. All three reactions had remaining monomer as well as signals attributed to dimethyl acetals formed by reaction with MeOH. No broad polymer peaks were evident.

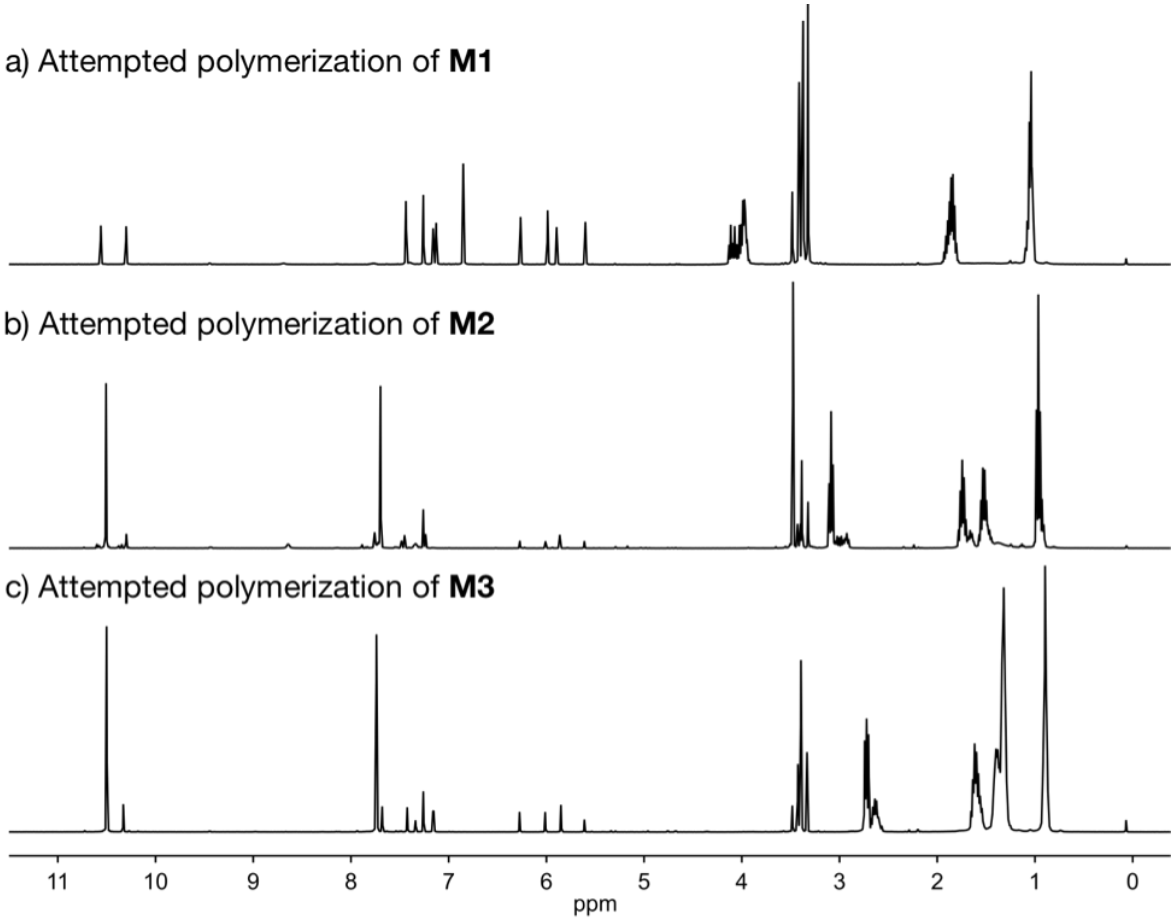

Figure S25. ^{1}H NMR spectra (400 MHz, $CDCl_3$) of concentrated reaction mixture following attempted polymerization of (a) **M1**, (b) **M2**, and (c) **M3**.

*Polymerization of **M4***

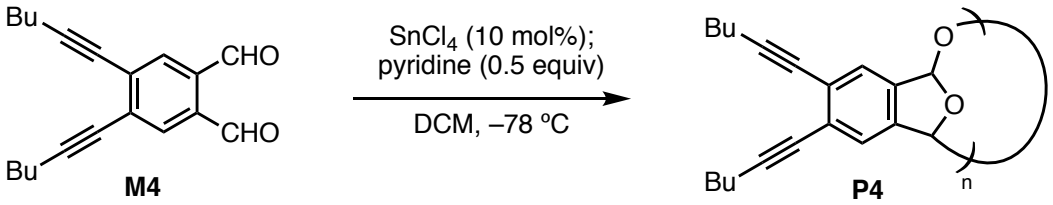

The following stock solutions were prepared in oven-dried 2-dram vials under N_2:

- $SnCl_4$ (0.080 mL, 0.68 mmol) in DCM (2.0 mL)
- pyridine (0.14 mL, 1.7 mmol) in DCM (1.0 mL)

An oven-dried 2-dram vial was charged with a stir bar and **M4** (103.0 mg, 0.3499 mmol), then sealed with a septum-lined cap and evacuated and refilled with N_2 (x3). DCM (0.4 mL) was added, and the solution was cooled to –78 ºC in a dry ice/acetone bath. $SnCl_4$ (0.10 mL of DCM stock solution, 0.034 mmol) was added, and the reaction was stirred at –78 ºC for 2 h. The reaction was quenched by adding pyridine (0.10 mL of DCM stock solution, 0.17 mmol), and stirring was continued at –78 ºC for an additional 2 h. The solution was poured into MeOH (10 mL), and a white precipitate immediately formed. The solid was isolated by vacuum filtration and dried under vacuum prior to SEC analysis.

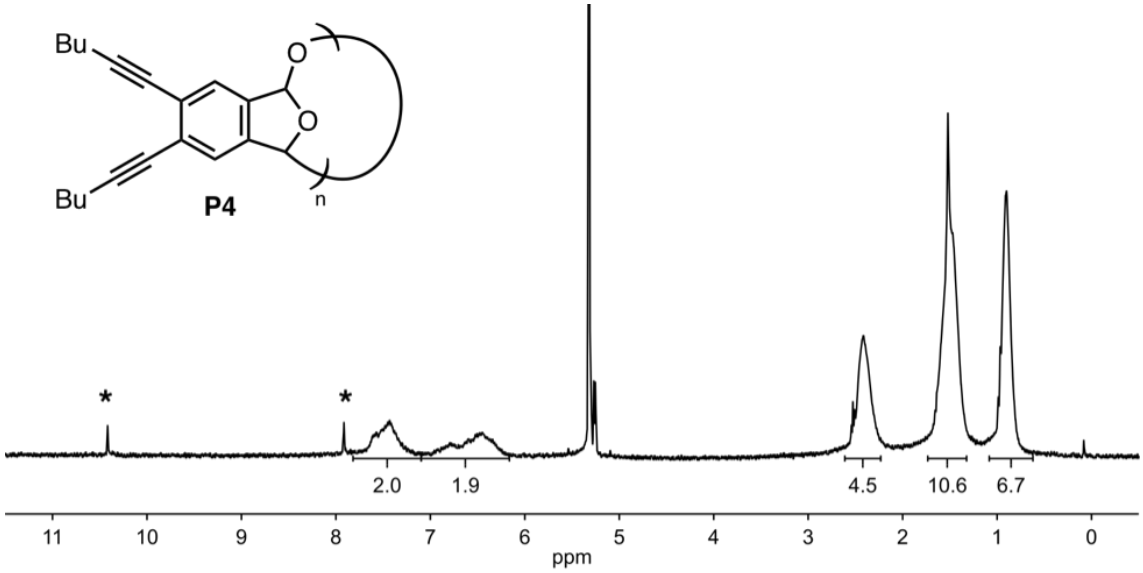

Figure S26. ^{1}H NMR spectrum of **P4** (400 MHz, CD_2Cl_2): δ 7.82–7.10 (2H), 7.10–6.16 (2H), 2.61–2.23 (4H), 1.73–1.32 (8H), 1.08–0.62 (6H) ppm. The asterisks denote residual **M4**.

Table S1. Yield and SEC data for crude **P4**.

run	mass isolated (mg)	yield (%)	M_n (kg/mol)	Đ
1	65.6	64	12.0	2.0
2	64.6	63	12.5	2.3

For purification, crude **P4** was dissolved in anhydrous DCM with sonication at a concentration of ~100 mg/mL and added dropwise to rapidly stirring ACS-grade MeOH (10 mL). Stirring was continued for 30 min at rt, then the precipitate was isolated by vacuum filtration and dried under vacuum.

Table S2. Recovery, SEC, and DSC data for purified **P4**.

run	mass used in purification (mg)	purified mass (mg)	recovery (%)	M_n (kg/mol)	Đ	T_d (ºC)
1	63.4	46.8	74	17.3	2.1	117
2	71.7	36.5	51	15.3	2.0	123

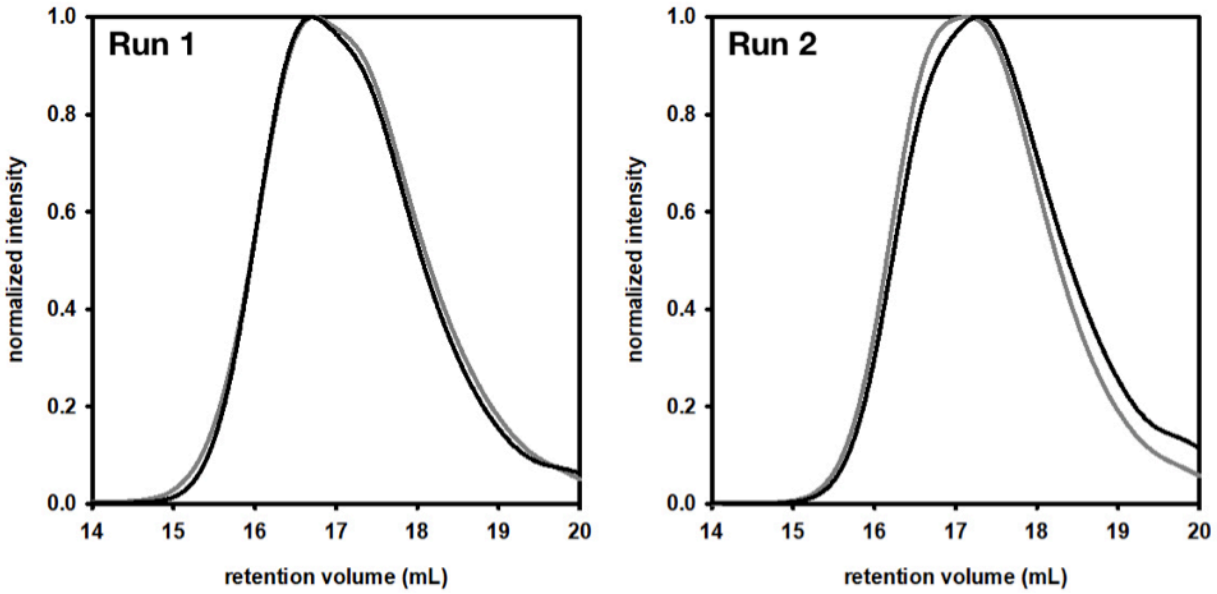

Figure S27. SEC traces for crude (black line) and purified (gray line) **P4**.

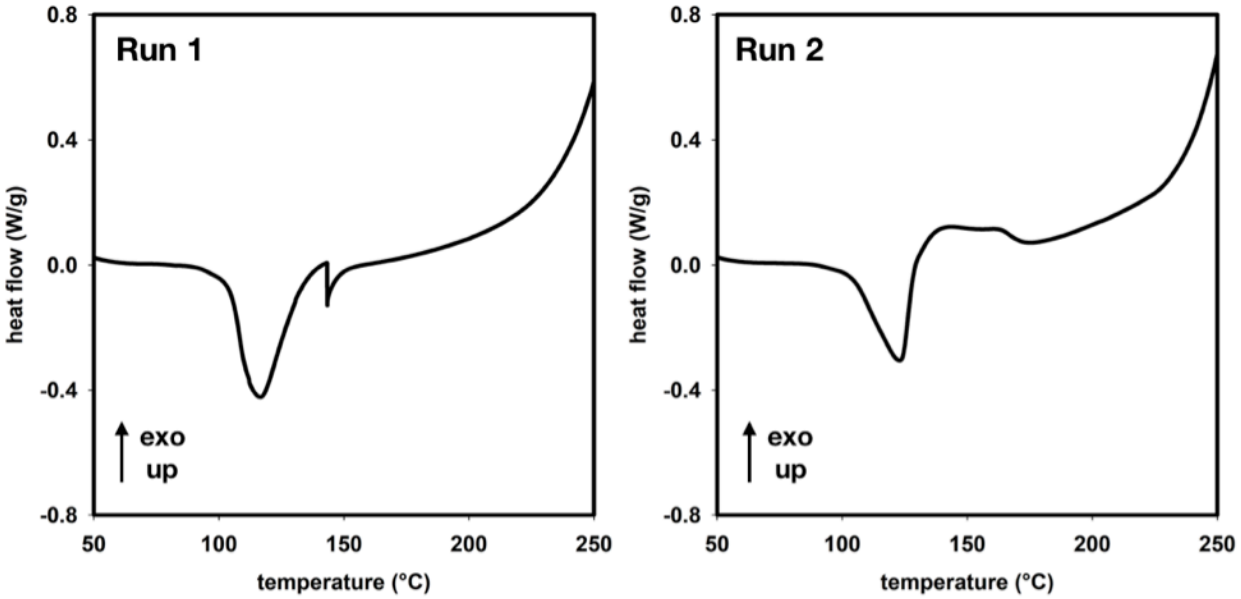

Figure S28. DSC heating thermograms for **P4**.

*Homo- and Copolymerization of **M5** and **M6***

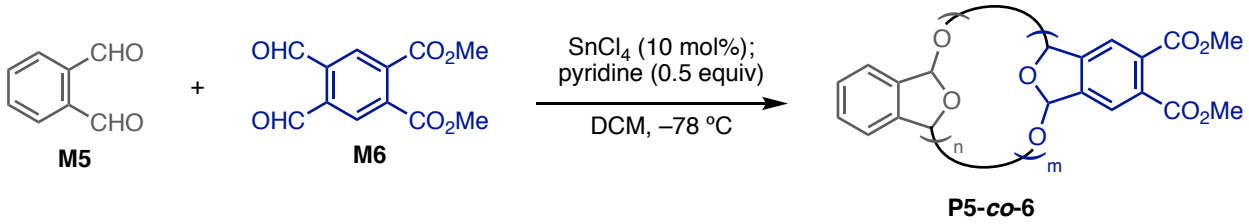

The following stock solutions were prepared in oven-dried 2-dram vials in a N_2-filled glovebox:

- **M5** (374.4 mg, 2.79 mmol) in DCM (3.2 mL)
- **M6** (700.8 mg, 2.81 mmol) in DCM (3.2 mL)

Each of seven oven-dried 2-dram vials were charged with a stir bar and **M5** and **M6** stock solutions (0.80 mL total volume, 0.70 mmol monomers, see Table S3 below). The vials were sealed with a septum-lined cap, removed from the glovebox, and cooled to –78 °C with dry ice/acetone.

Two additional stock solutions were prepared in oven-dried 2-dram vials under N_2:

- $SnCl_4$ (0.16 mL, 1.4 mmol) in DCM (4.0 mL)
- pyridine (0.28 mL, 3.5 mmol) in DCM (2.0 mL)

$SnCl_4$ (0.20 mL of DCM stock solution, 0.069 mmol) was added to each reaction vial, and the reactions were stirred at –78 °C for 2 h. The reactions were quenched by adding pyridine (0.20 mL of DCM stock solution, 0.35 mmol), and stirring was continued at –78 °C for an additional 2.5 h. Each solution was separately poured into MeOH (10 mL), resulting in immediate formation of a white precipitate. The solids were isolated by vacuum filtration and dried under vacuum prior to SEC analysis.

Table S3. Yield and SEC data for crude **P5**, **P6**, and **P5-*co*-6**.

Run 1							
polymer	vol **M5** soln (mL)	vol **M6** soln (mL)	**M6** in feed (%)	mass isolated (mg)	yield (%)	M_n (kg/mol)	Đ
P5	0.80	0	0	32.6	35	3.1	2.1
P5-*co*-6a	0.70	0.10	12.5	43.9	42	3.5	1.9
P5-*co*-6b	0.60	0.20	25.0	47.6	42	3.3	1.7
P5-*co*-6c	0.40	0.40	50.0	53.7	40	4.0	1.7
P5-*co*-6d	0.20	0.60	75.0	69.1	45	4.8	1.9
P5-*co*-6e	0.10	0.70	87.5	72.8	44	7.7	1.6
P6	0	0.80	100.0	80.4	46	10.9	1.7
Run 2							
polymer	vol **M5** soln (mL)	vol **M6** soln (mL)	**M6** in feed (%)	mass isolated (mg)	yield (%)	M_n (kg/mol)	Đ
P5	0.80	0	0	31.6	34	3.2	2.2
P5-*co*-6a	0.70	0.10	12.5	45.2	43	3.6	2.0
P5-*co*-6b	0.60	0.20	25.0	47.4	42	3.6	1.7
P5-*co*-6c	0.40	0.40	50.0	65.6	49	3.2	1.8
P5-*co*-6d	0.20	0.60	75.0	78.1	50	4.4	2.0
P5-*co*-6e	0.10	0.70	87.5	80.0	49	6.4	2.0
P6	0	0.80	100.0	87.0	50	12.5	1.7

To purify the polymers, each sample was dissolved in anhydrous DCM with sonication at a concentration of ~100 mg/mL and added dropwise to rapidly stirring ACS-grade MeOH (10 mL). Stirring was continued for 30 min at rt, then each precipitate was isolated by vacuum filtration and dried under vacuum.

For **P5-*co*-6**, the **M6** incorporation was estimated using ^{1}H NMR spectroscopic analysis by setting the integral for the CH_3 resonance at ~3.9–3.5 ppm (in CD_2Cl_2) to 1.5, then integrating the remaining polymer signals at ~8.2–6.0 ppm as *x* and using Eq. S1:

$$\%\mathbf{M6} = 100 \bullet \left[1 - \left(\frac{x - 1}{x + 0.5} \right) \right] \quad \text{(S1)}$$

Table S4. Recovery, composition, SEC, and DSC data for purified **P5**, **P6**, and **P5-*co*-6**.

Run 1								
polymer	**M6** in feed (%)	mass used in purification (mg)	purified mass (mg)	recovery (%)	**M6** in polymer (%)	M_n (kg/mol)	Đ	T_d (ºC)
P5	0	30.7	13.6	44	0	3.6	1.8	111
P5-*co*-6a	12.5	41.9	29.1	69	16.0	3.8	1.7	110
P5-*co*-6b	25.0	47.2	22.4	47	26.0	3.7	1.6	116
P5-*co*-6c	50.0	52.6	19.0	36	49.0	4.6	1.6	138
P5-*co*-6d	75.0	68.5	25.3	37	71.4	6.2	1.7	127
P5-*co*-6e	87.5	71.7	29.0	40	91.5	8.3	1.6	133
P6	100.0	79.3	39.7	50	100	13.2	1.6	147
Run 2								
polymer	**M6** in feed (%)	mass used in purification (mg)	purified mass (mg)	recovery (%)	**M6** in polymer (%)	M_n (kg/mol)	Đ	T_d (ºC)
P5	0	30.5	14.1	46	0	4.0	1.8	106
P5-*co*-6a	12.5	44.6	26.6	60	15.8	4.3	1.8	107
P5-*co*-6b	25.0	45.6	31.8	70	28.5	4.4	1.5	119
P5-*co*-6c	50.0	64.5	38.2	59	47.8	4.6	1.5	124
P5-*co*-6d	75.0	76.2	48.8	64	73.9	6.1	1.7	123
P5-*co*-6e	87.5	76.0	53.0	70	87.7	7.7	1.7	128
P6	100.0	87.2	61.7	71	100	12.2	1.7	140

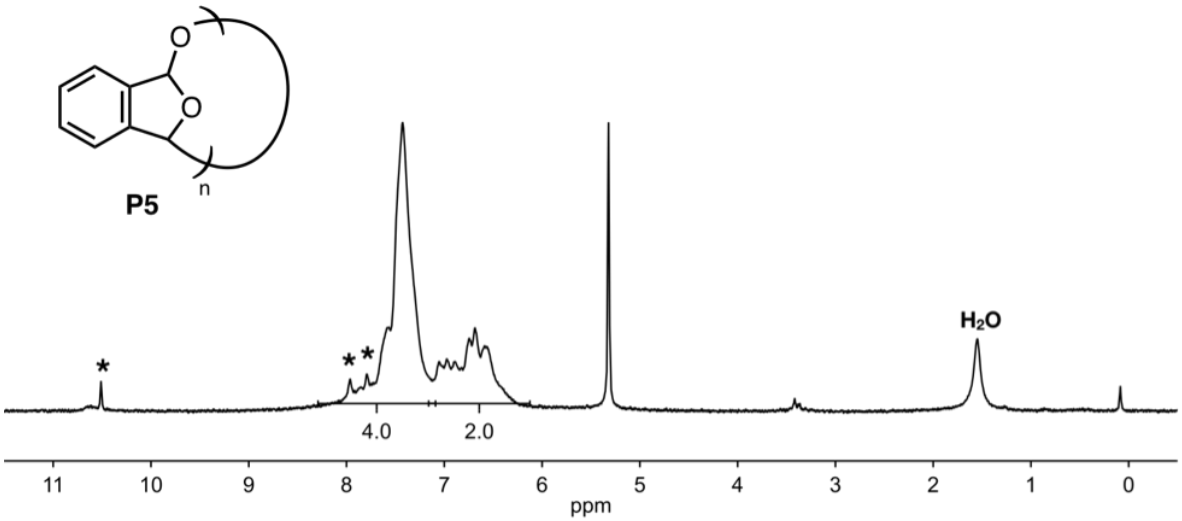

Figure S29. ^{1}H NMR spectrum of purified **P5** (400 MHz, CD_2Cl_2): δ 7.71–7.14 (4H), 7.14–6.29 (2H) ppm. The asterisks denote residual **M5**.

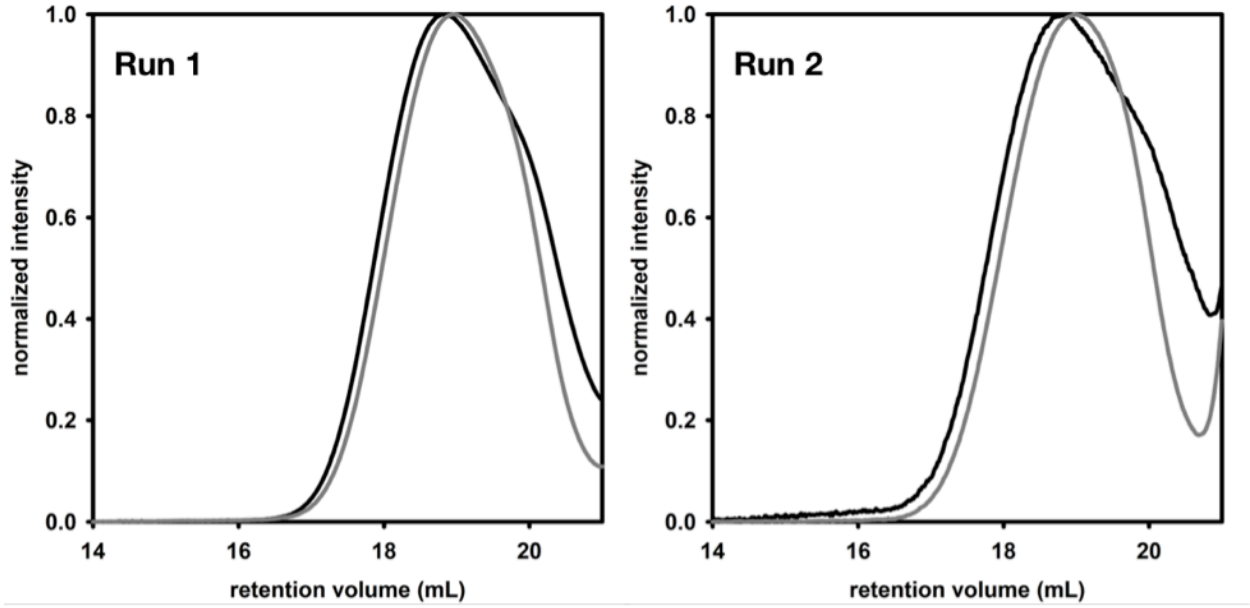

Figure S30. SEC traces for crude (black line) and purified (gray line) **P5**.

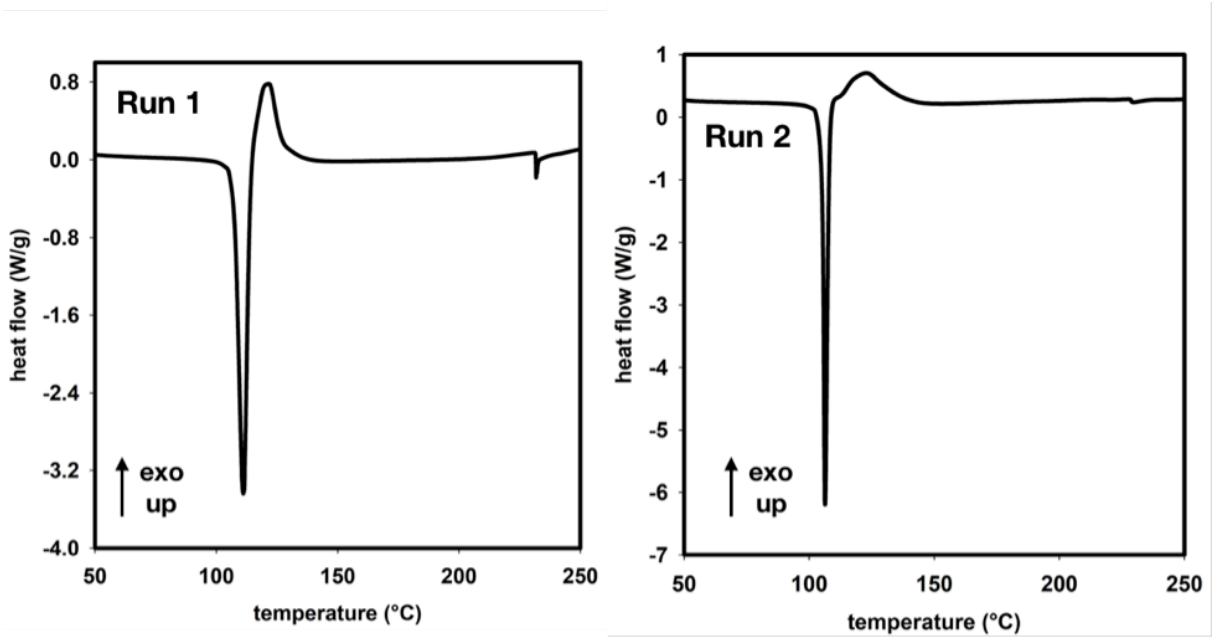

Figure S31. DSC heating thermograms for **P5**.

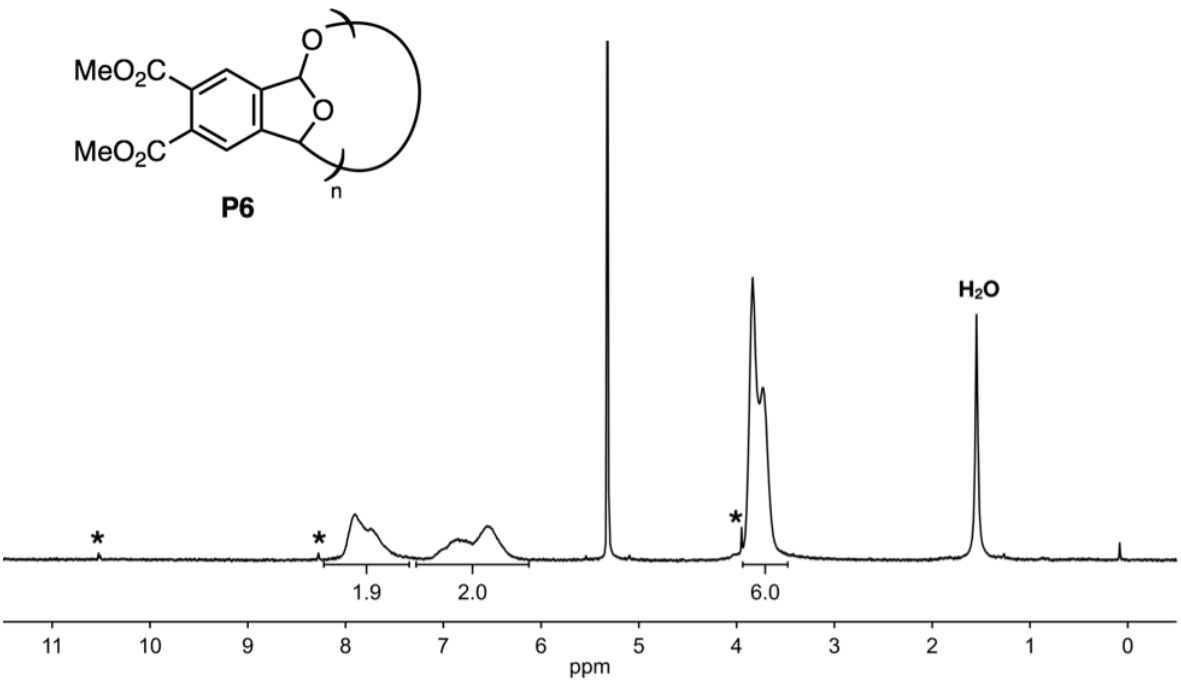

Figure S32. ^{1}H NMR spectrum of purified **P6** (400 MHz, CD_2Cl_2): δ 8.16–7.17 (2H), 7.17–6.10 (2H), 3.93–3.55 (6H) ppm. The asterisks denote residual **M6**.

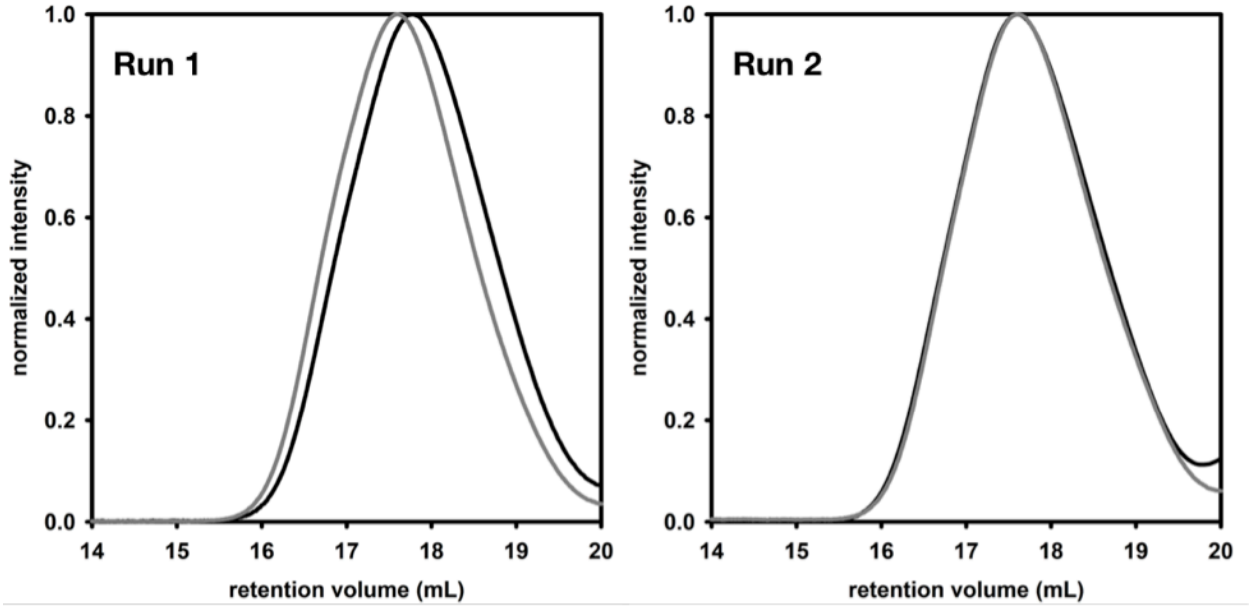

Figure S33. SEC traces for crude (black line) and purified (gray line) **P6**.

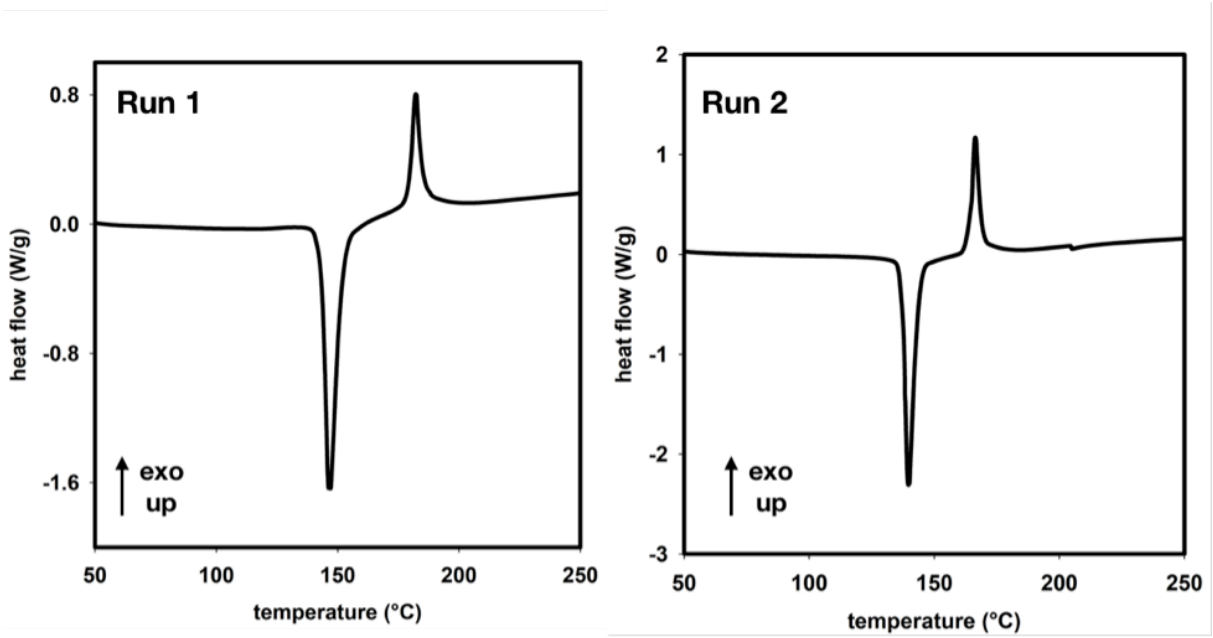

Figure S34. DSC heating thermograms for **P6**.

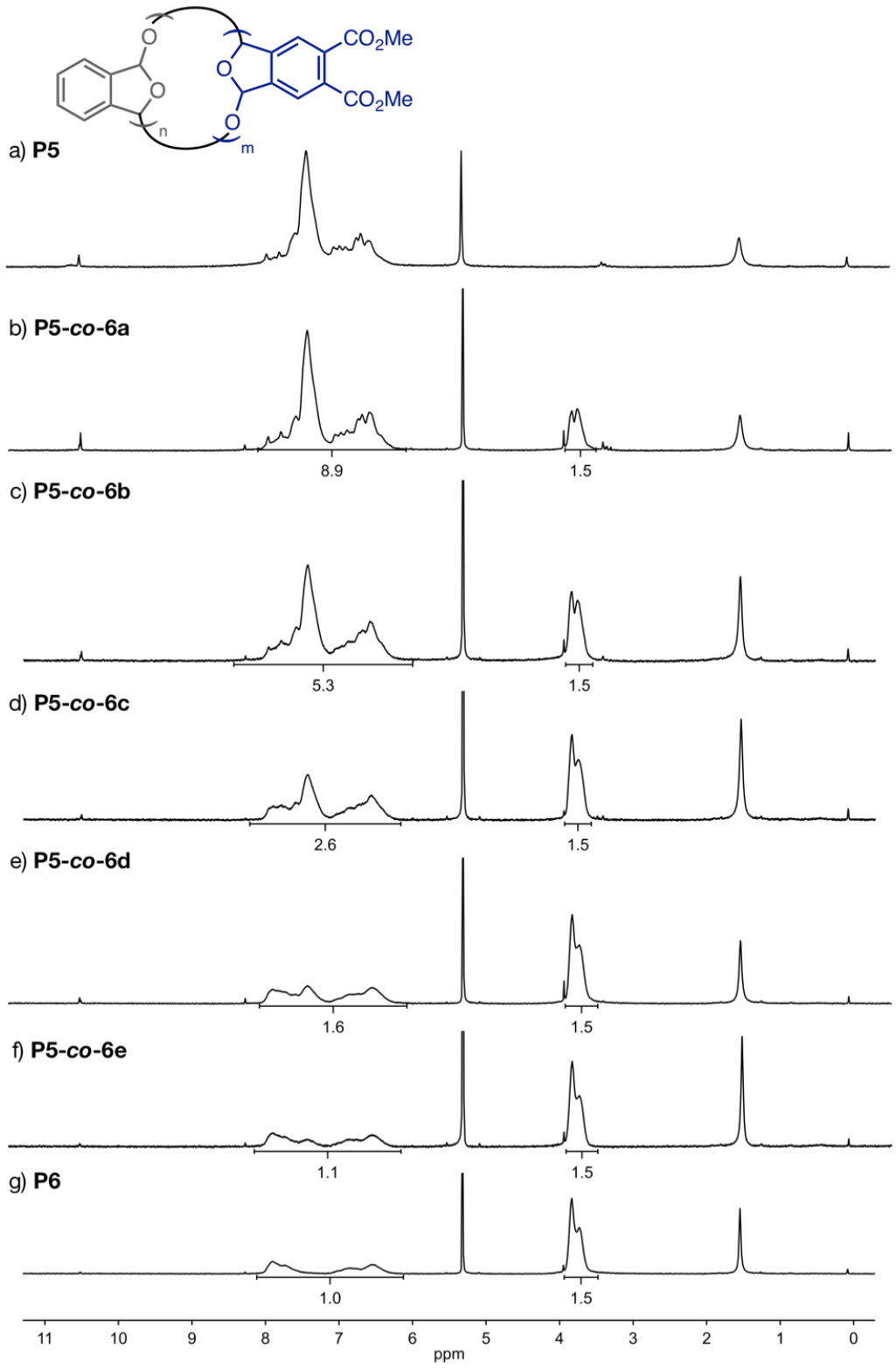

Figure S35. ^{1}H NMR spectra of (a) **P5**, (b–f) **P5-*co*-6a** through **P5-*co*-6e**, and (g) **P6** (400 MHz, CD_2Cl_2).

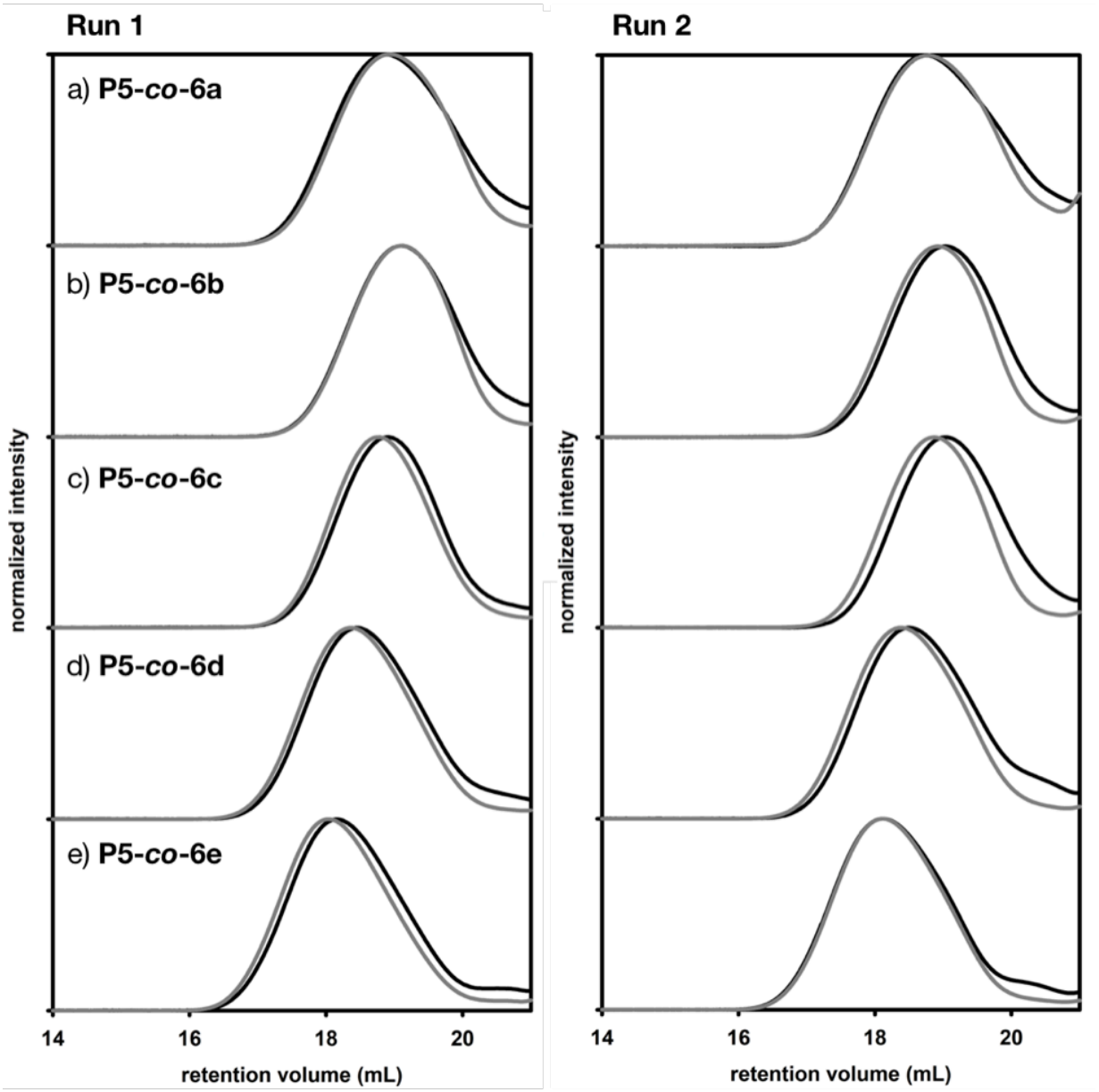

Figure S36. SEC traces for crude (black line) and purified (gray line) **P5-*co*-6a** through **P5-*co*-6e**.

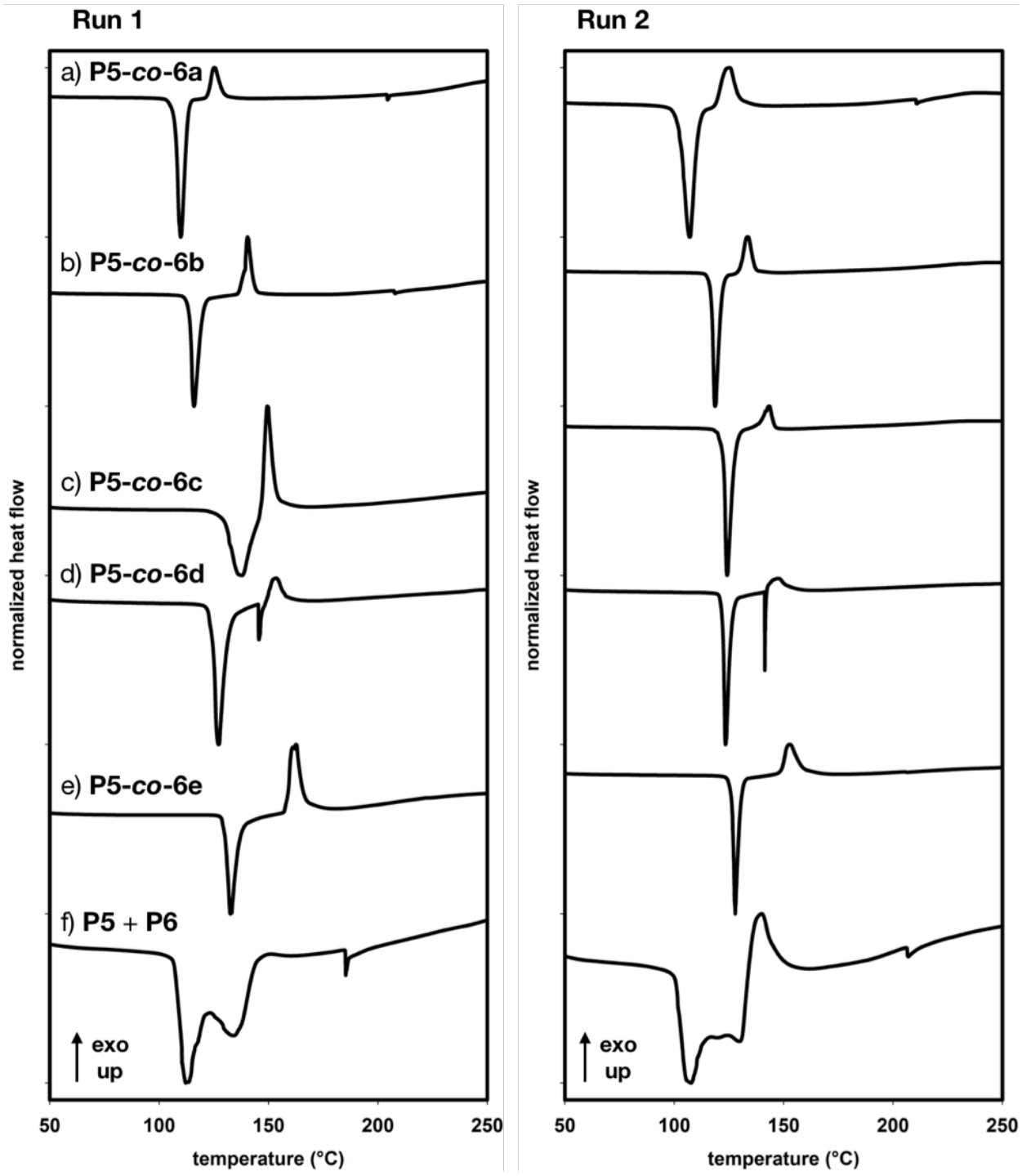

Figure S37. DSC heating thermograms for (a–e) **P5-*co*-6a** through **P5-*co*-6e** and (f) a physical mixture of **P5** and **P6** homopolymers. The presence of two distinct T_d peaks supports the claim that **P5-*co*-6** is a copolymer rather than a mixture of homopolymers.

*Polymerization of **M7***

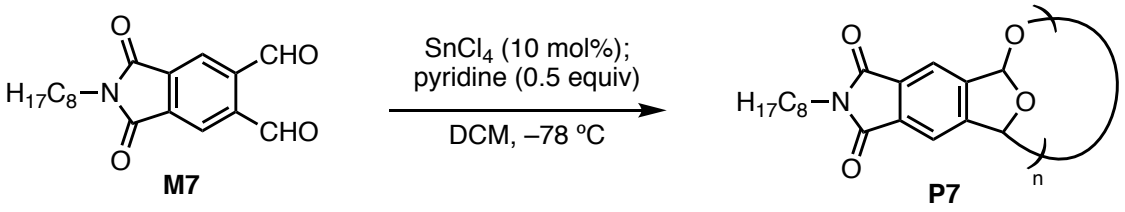

The following stock solutions were prepared in oven-dried 2-dram vials under N_2:

- $SnCl_4$ (0.080 mL, 0.70 mmol) in DCM (2.0 mL)
- pyridine (0.14 mL, 1.7 mmol) in DCM (1.0 mL)

An oven-dried 2-dram vial was charged with a stir bar and **M7** (110.4 mg, 0.3500 mmol), then sealed with a septum-lined cap and evacuated and refilled with N_2 (x3). DCM (0.40 mL) was added, and the solution was cooled to –78 ºC in a dry ice/acetone bath. $SnCl_4$ (0.10 mL of DCM stock solution, 0.035 mmol) was added, and the reaction was stirred at –78 ºC for 2 h. The reaction was quenched by adding pyridine (0.10 mL of DCM stock solution, 0.17 mmol), and stirring was continued at –78 ºC for an additional 2 h. The solution was poured into MeOH (10 mL), and a white precipitate immediately formed. The solid was isolated by vacuum filtration and dried under vacuum prior to SEC analysis.

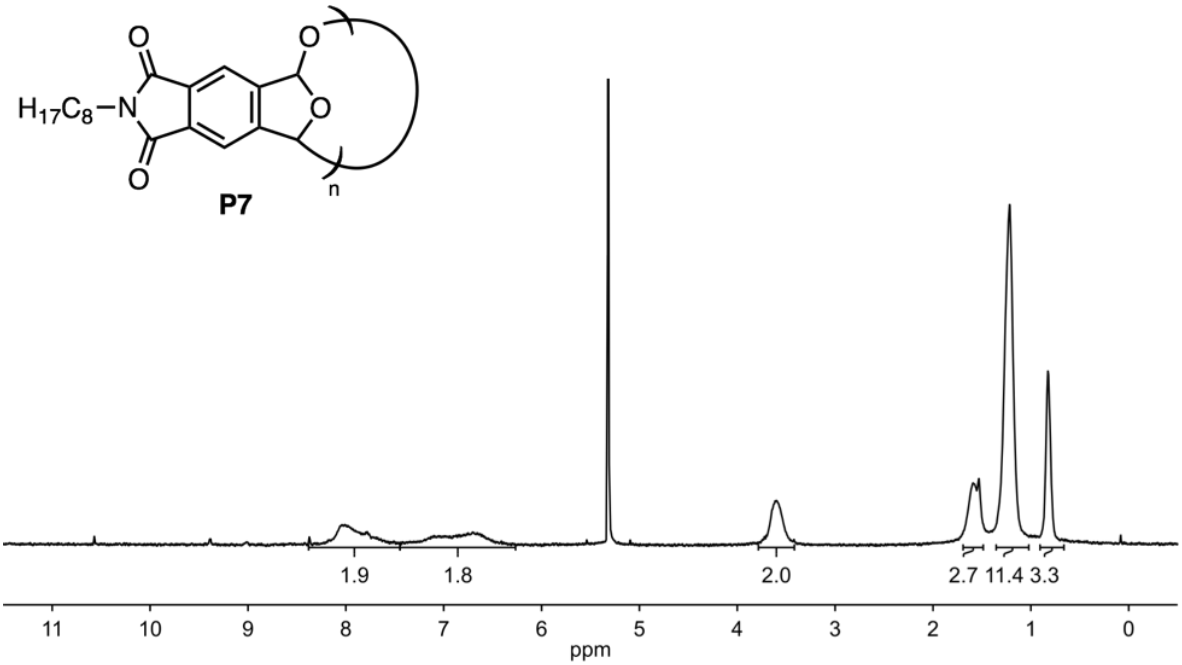

Figure S38. ^{1}H NMR spectrum of **P7** (400 MHz, CD_2Cl_2): δ 8.38–7.45 (2H), 7.45–6.27 (2H), 3.78–3.42 (2H), 1.69–1.49 (2H), 1.35–1.02 (10H), 0.91–0.66 (3H) ppm.

Table S5. Yield and SEC data for crude **P7**.

run	mass isolated (mg)	yield (%)	M_n (kg/mol)	Đ
1	98.1	89	24.8	2.1
2	83.3	76	25.4	1.7

For purification, crude **P7** was dissolved in anhydrous DCM with sonication at a concentration of ~100 mg/mL and added dropwise to rapidly stirring ACS-grade MeOH (10 mL). Stirring was continued for 30 min at rt, then the precipitate was isolated by vacuum filtration and dried under vacuum.

Table S6. Recovery, SEC, and DSC data for purified **P7**.

run	mass used in purification (mg)	purified mass (mg)	recovery (%)	M_n (kg/mol)	Đ	T_d (°C)
1	87.2	75.0	86	30.2	1.8	157
2	77.8	57.8	74	40.7	1.6	166

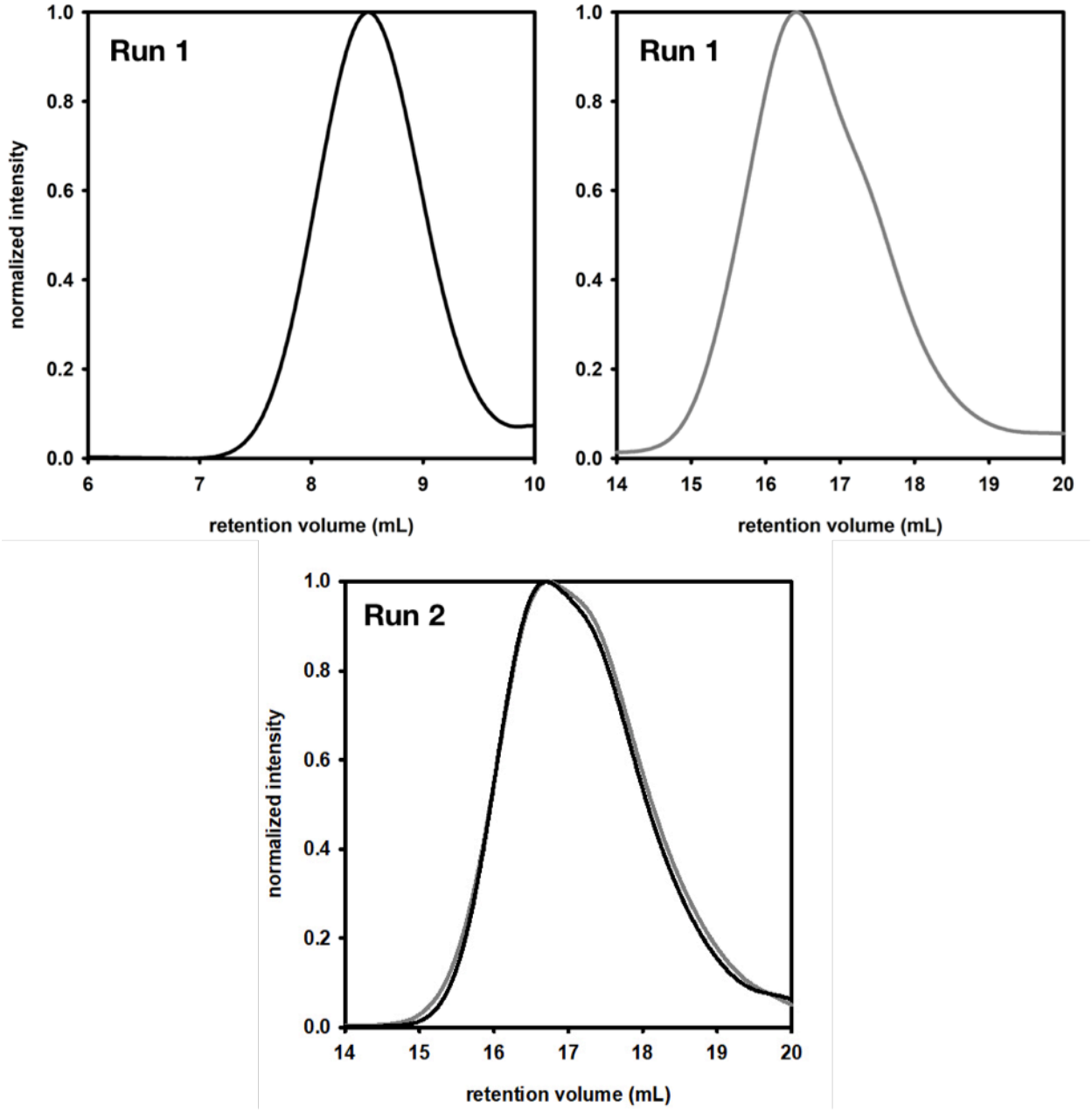

Figure S39. SEC traces for crude (black line) and purified (gray line) **P7**.

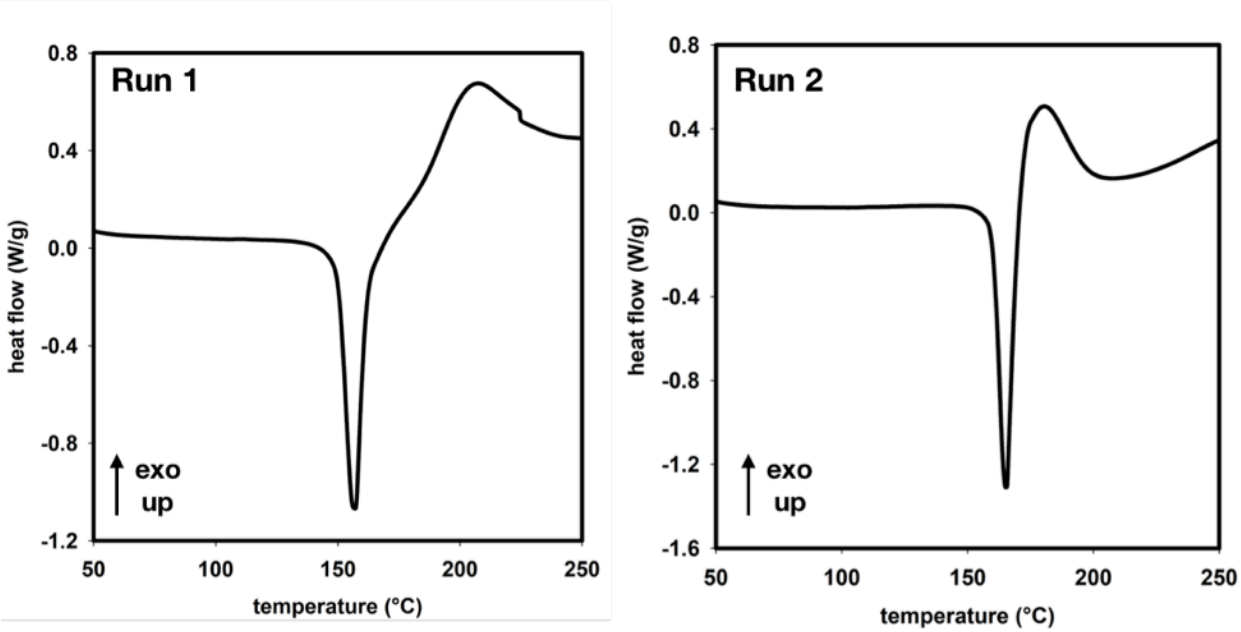

Figure S40. DSC heating thermograms for **P7**.

*Polymerization of **M8***

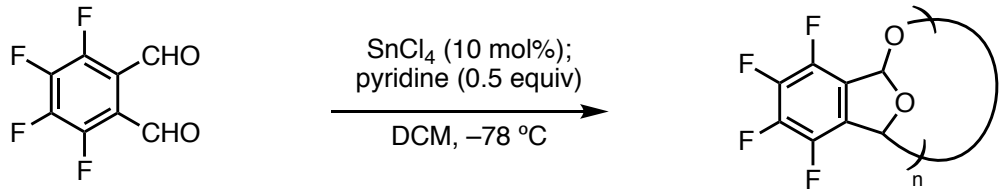

M8 **P8**

The following stock solutions were prepared in oven-dried 2-dram vials under N_2:

- $SnCl_4$ (0.080 mL, 0.70 mmol) in DCM (2.0 mL)
- pyridine (0.14 mL, 1.7 mmol) in DCM (1.0 mL)

In a N_2-filled glovebox, an oven-dried 2-dram vial was charged with a stir bar, **M8** (72.1 mg, 0.350 mmol), and DCM (0.40 mL). The vial was sealed with a septum-lined cap, removed from the glovebox, and cooled to –78 ºC in a dry ice/acetone bath. $SnCl_4$ (0.10 mL of DCM stock solution, 0.035 mmol) was added, and the reaction was stirred at –78 ºC for 2 h. The reaction was quenched by adding pyridine (0.10 mL of DCM stock solution, 0.17 mmol), and stirring was continued at –78 ºC for an additional 2 h. The solution was poured into MeOH (10 mL), and a white precipitate immediately formed. The solid was isolated by vacuum filtration and dried under vacuum prior to SEC analysis.

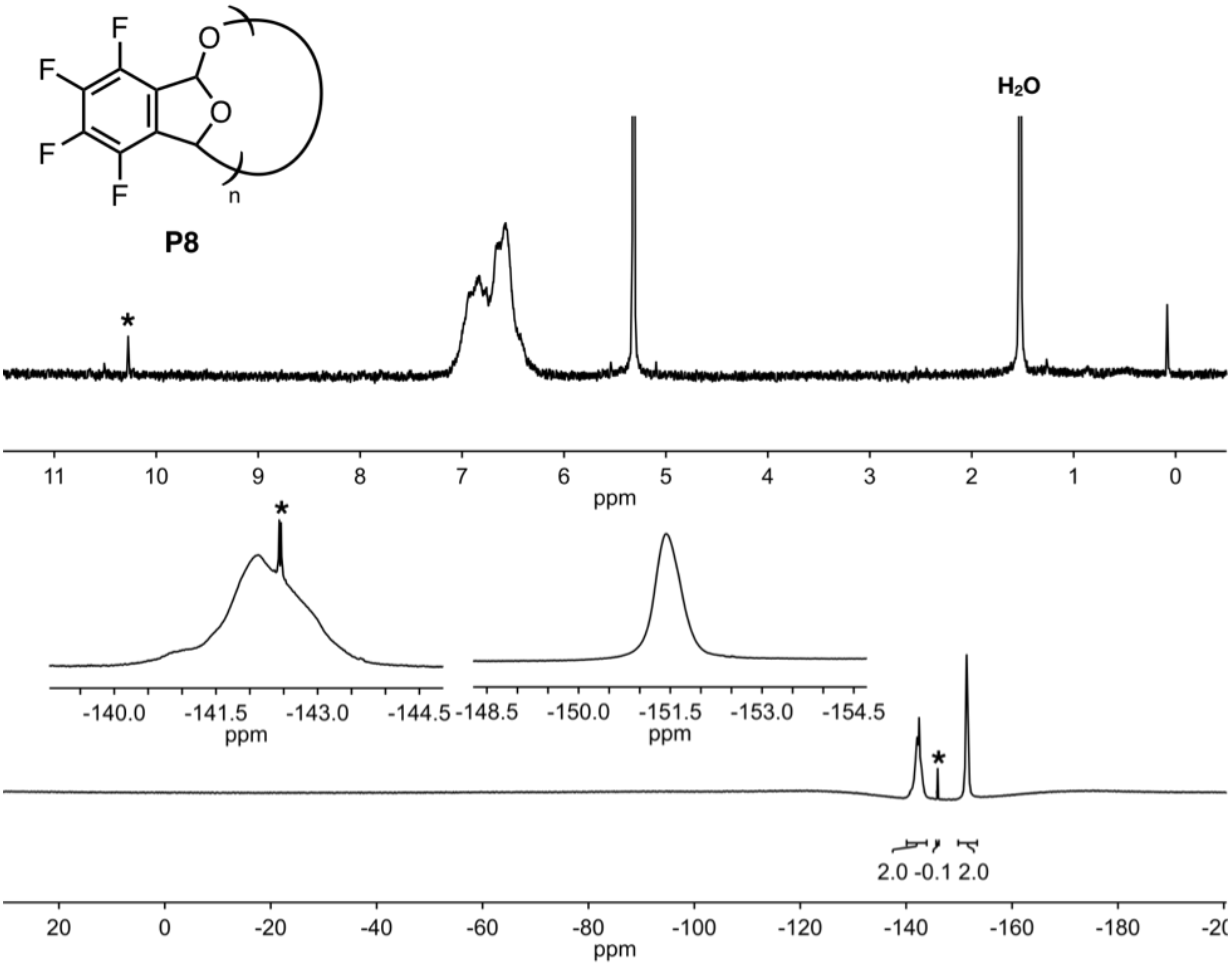

Figure S41. ^{1}H and ^{19}F NMR spectra of **P8**. The asterisks indicate residual **M8**.

^{1}H NMR (400 MHz, CH_2Cl_2): δ 7.26–6.03 (m, 2H) ppm.

^{19}F NMR (471 MHz, CH_2Cl_2): δ –140.13 – –143.93 (m, 2F), –151.43 (broad s, 2F) ppm.

Table S7. Yield and SEC data for crude **P8**.

run	mass isolated (mg)	yield (%)	M_n (kg/mol)	Đ
1	34.3	48	13.7	1.9
2	41.9	58	18.7	2.0

For purification, crude **P8** was dissolved with sonication in anhydrous DCM at a concentration of ~100 mg/mL, then added dropwise to rapidly stirring ACS-grade MeOH (5 mL). Stirring was continued for 30 min at rt, then the precipitate was isolated by vacuum filtration and dried under vacuum.

Table S8. Recovery, SEC, and DSC data for purified **P8**.

run	mass used in purification (mg)	purified mass (mg)	recovery (%)	M_n (kg/mol)	Đ	T_d (ºC)	T_g (ºC)
1	24.4	13.1	54	19.2	1.6	197	146
2	19.4	31.9	61	20.4	1.9	194	154

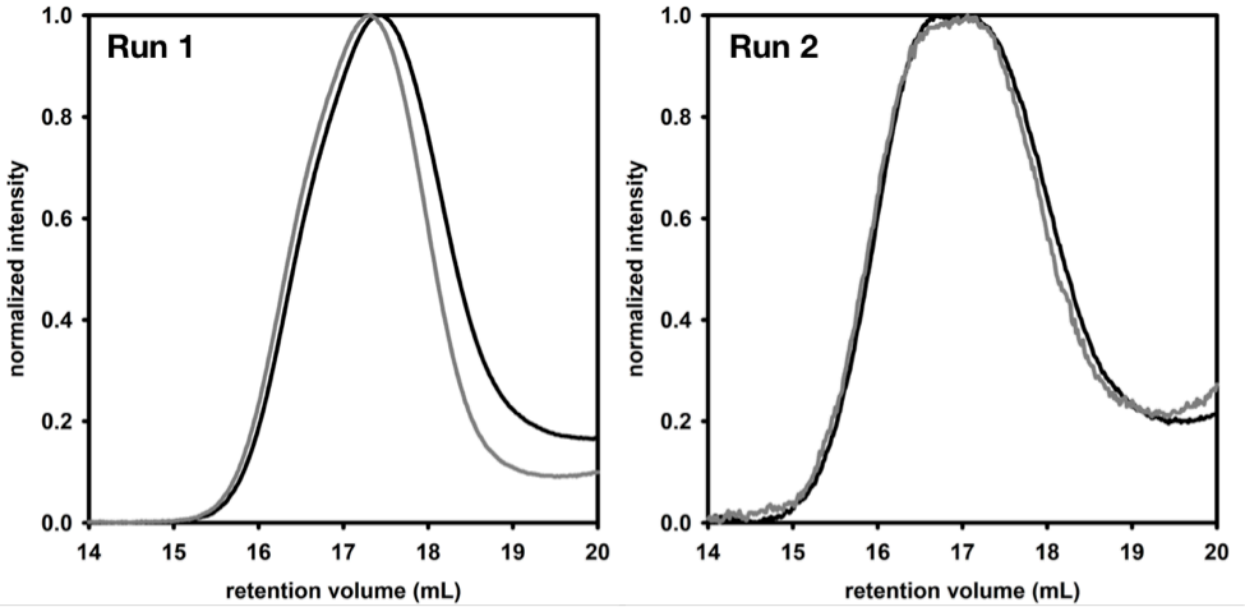

Figure S42. SEC traces for crude (black line) and purified (gray line) **P8**.

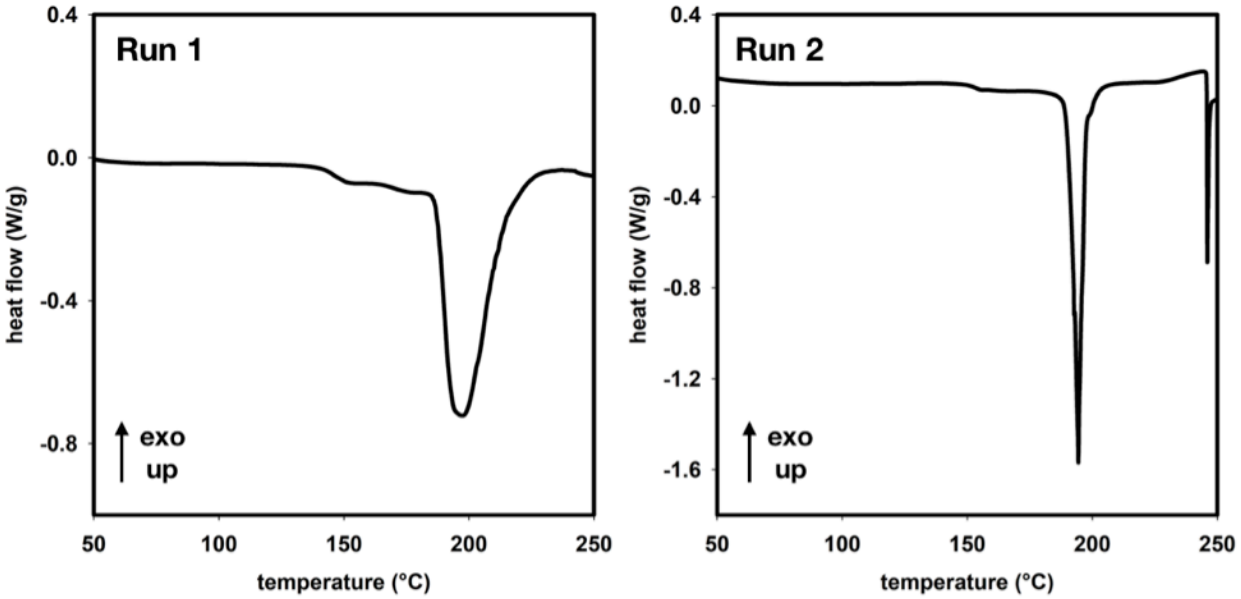

Figure S43. DSC heating thermograms for **P8**.

*Gram-Scale Polymerization of **M6***

On the benchtop, an oven-dried, 20-mL scintillation vial was charged with **M6** (1.11 g, 4.43 mmol, 1.00 equiv) and a stir bar. The vial was sealed with a septum-lined cap and evacuated and refilled with N_2 (x3). DCM (4.4 mL) was added, and the solution was cooled to –78 ºC in a dry ice/acetone bath. Neat $SnCl_4$ (0.050 mL, 0.43 mmol, 10 mol%) was added. The reaction was stirred at –78 ºC for 2 h, then quenched by adding pyridine (0.18 mL, 2.2 mmol, 0.50 equiv). Stirring was continued at –78 ºC for 2 h, then the polymer was precipitated by pouring the reaction mixture into a beaker filled with MeOH (100 mL). The white precipitate that immediately formed was isolated by vacuum filtration and dried under vacuum to afford **P6** (845.6 mg, 76% yield) as a white solid. SEC analysis: M_n = 13.9 kg/mol, Đ = 1.8.

To purify the polymer, a portion of the crude material (810.2 mg) was dissolved in anhydrous DCM (10 mL) with sonication. This polymer solution was added dropwise over ~20 min to a rapidly stirring beaker of ACS-grade MeOH (200 mL) via addition funnel. Following addition, stirring was halted, and the material was allowed to sit in the MeOH for 30 min. The solid was collected via vacuum filtration, then added to a beaker with additional MeOH (100 mL) and allowed to sit for another 30 min. The solid material was collected via vacuum filtration, then dried under vacuum to provide purified **P6** (634.2 mg, 78% recovery) as a white solid. SEC analysis: M_n = 15.5 kg/mol, Đ = 1.8.

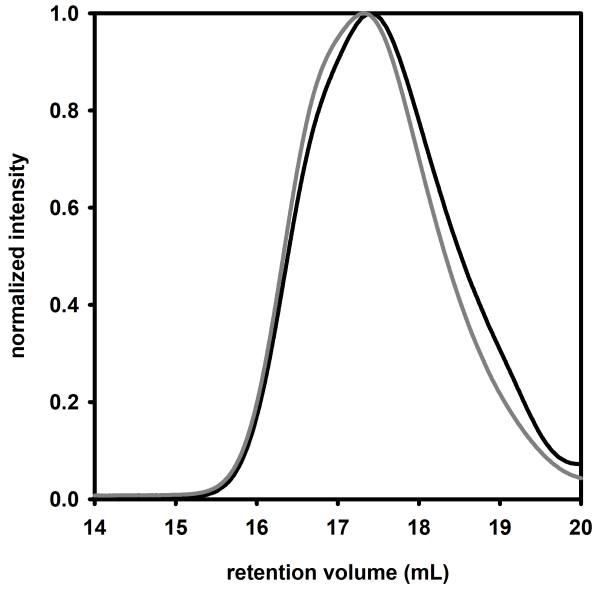

Figure S44. SEC traces for crude (black line) and purified (gray line) **P6** from gram-scale reaction.

VI. Ceiling Temperature Measurements

Temperature Calibration:

The temperature was calibrated according to a literature method.[15] Briefly, ^{1}H NMR spectra of neat, anhydrous MeOH or ethylene glycol were acquired at a range of set temperatures, and the 'tempcal' command in the Vnmrj software was used to determine the observed temperature from the relative spacing of the C–H and O–H resonances. The MeOH calibration curve was used for the ceiling temperature (T_c) measurements for **M1–M6**, and the ethylene glycol calibration curve was used for the T_c measurement for **M7** and **M8**.

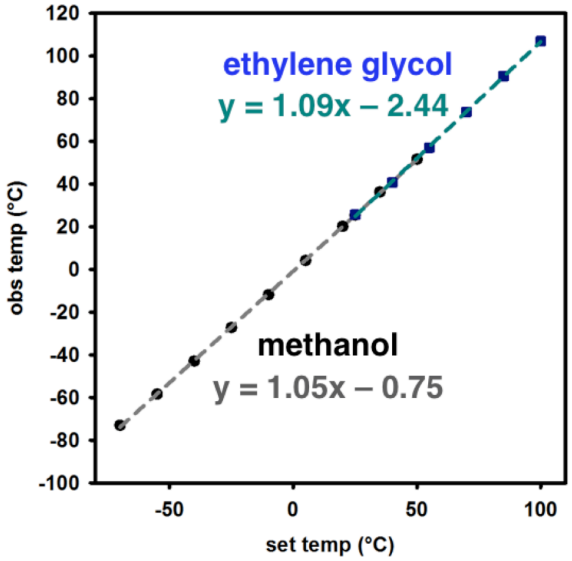

Figure S45. NMR spectroscopic temperature calibration with MeOH and ethylene glycol.

General Procedure:

In a N_2-filled glovebox, an oven-dried 2-dram vial was charged with monomer (0.35 mmol) and durene (~3.5 mg) as an internal standard. The solids were dissolved in deuterated solvent (typically 0.5 mL), then neat $SnCl_4$ (4.1 µL, 0.035 mmol) was added via micropipette. The resulting solution was transferred to a J. Young NMR tube, capped, and removed from the glovebox. The NMR sample was equillibrated in the NMR probe for 10 min at a given temperature before acquiring a ^{1}H NMR spectrum. The monomer concentration was determined for each spectrum by comparing the integration of the aldehyde CH resonance with that of the durene CH_3 resonance.

To determine the T_c, the monomer concentration data were plotted as R•ln[M] versus 1/T, where R is the gas constant. From the slope and y-intercept of a linear regression, the ΔH and ΔS could be obtained, respectively. Using these values in Eq. S2 provided the T_c.[16]

$$T_c = \frac{\Delta H}{\Delta S + R \bullet \ln[\mathrm{M}]_0} \qquad (\mathrm{S2})$$

T_c Measurement for **M1**:

The general procedure was followed with **M1** (87.4 mg, 0.350 mmol) and CD_2Cl_2 (0.50 mL); [**M1**]$_0$ = 0.70 M.

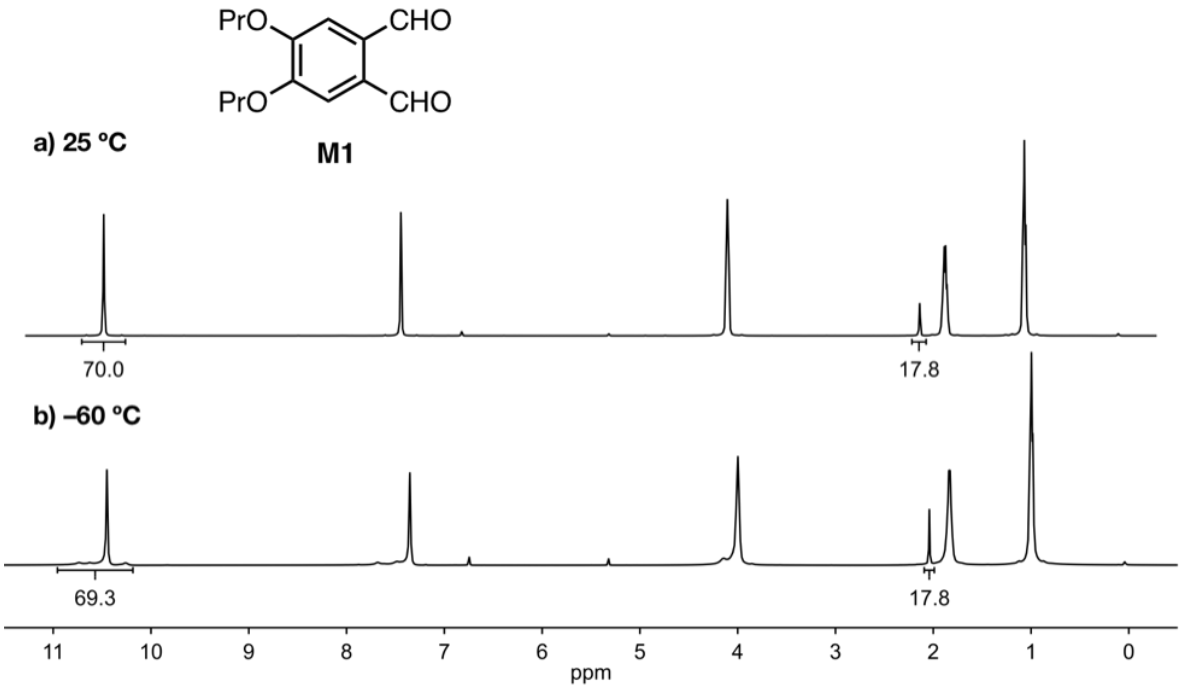

Figure S46. VT-^{1}H NMR spectra of **M1** + $SnCl_4$ (500 MHz, CD_2Cl_2).

Table S9. Concentration data from VT-NMR spectroscopic experiments with **M1**.

set temp (ºC)	corr temp (ºC)	1/T (K^{-1})	[**M1**] (M)	R•ln[**M1**] (cal/mol•K)
25.0	25.4	0.00335	0.70	–0.71
–60.0	–63.5	0.00477	0.69	–0.73

The T_c for **M1** was too low to measure due to temperature limitations of the NMR probe, but –60 ºC provides an upper limit for the T_c.

T_c Measurement for **M2**:

The general procedure was followed with **M2** (108.7 mg, 0.3500 mmol) and CD_2Cl_2 (0.50 mL); $[\mathbf{M2}]_0$ = 0.70 M.

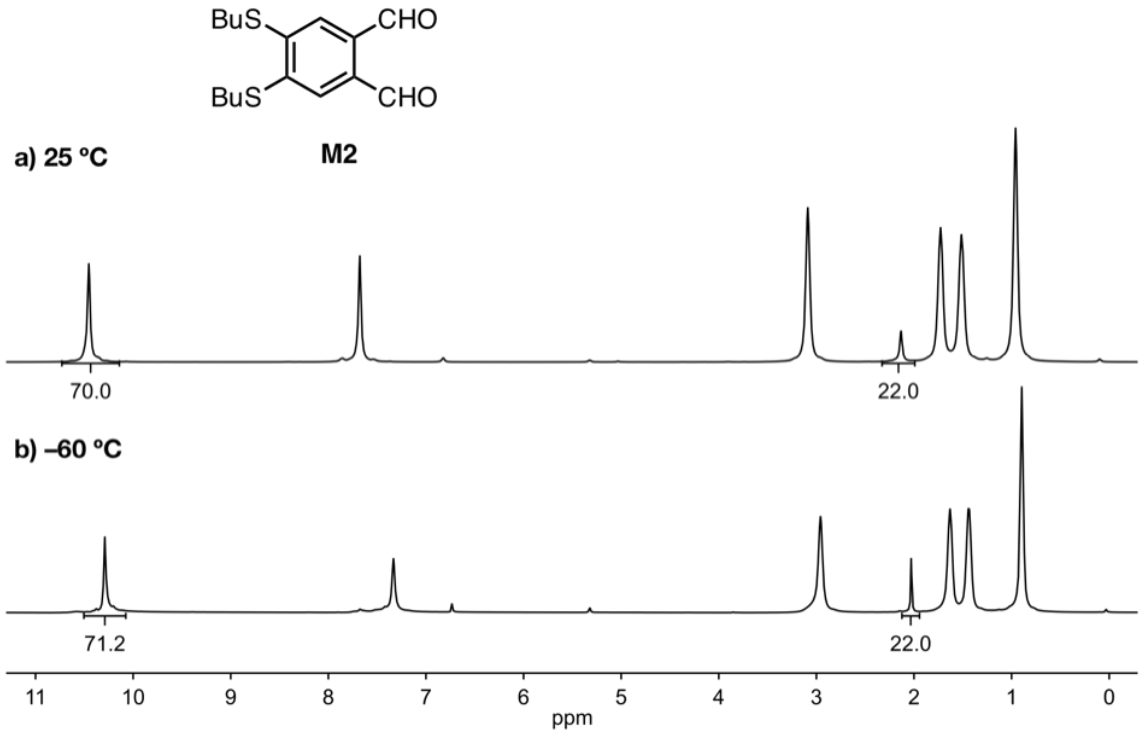

Figure S47. VT-^{1}H NMR spectra of **M2** + $SnCl_4$ (500 MHz, CD_2Cl_2).

Table S10. Concentration data from VT-NMR spectroscopic experiments with **M2**.

set temp (ºC)	corr temp (ºC)	1/T (K^{-1})	[**M2**] (M)	R•ln[**M2**] (cal/mol•K)
25.0	25.4	0.00335	0.70	–0.71
–60.0	–63.5	0.00477	0.71	–0.68

The T_c for **M2** was too low to measure due to temperature limitations of the NMR probe, but –60 ºC provides an upper limit for the T_c.

T_c Measurement for **M3**:

The general procedure was followed with **M3** (105.9 mg, 0.3500 mmol) and CD_2Cl_2 (0.50 mL); $[\mathbf{M3}]_0$ = 0.70 M.

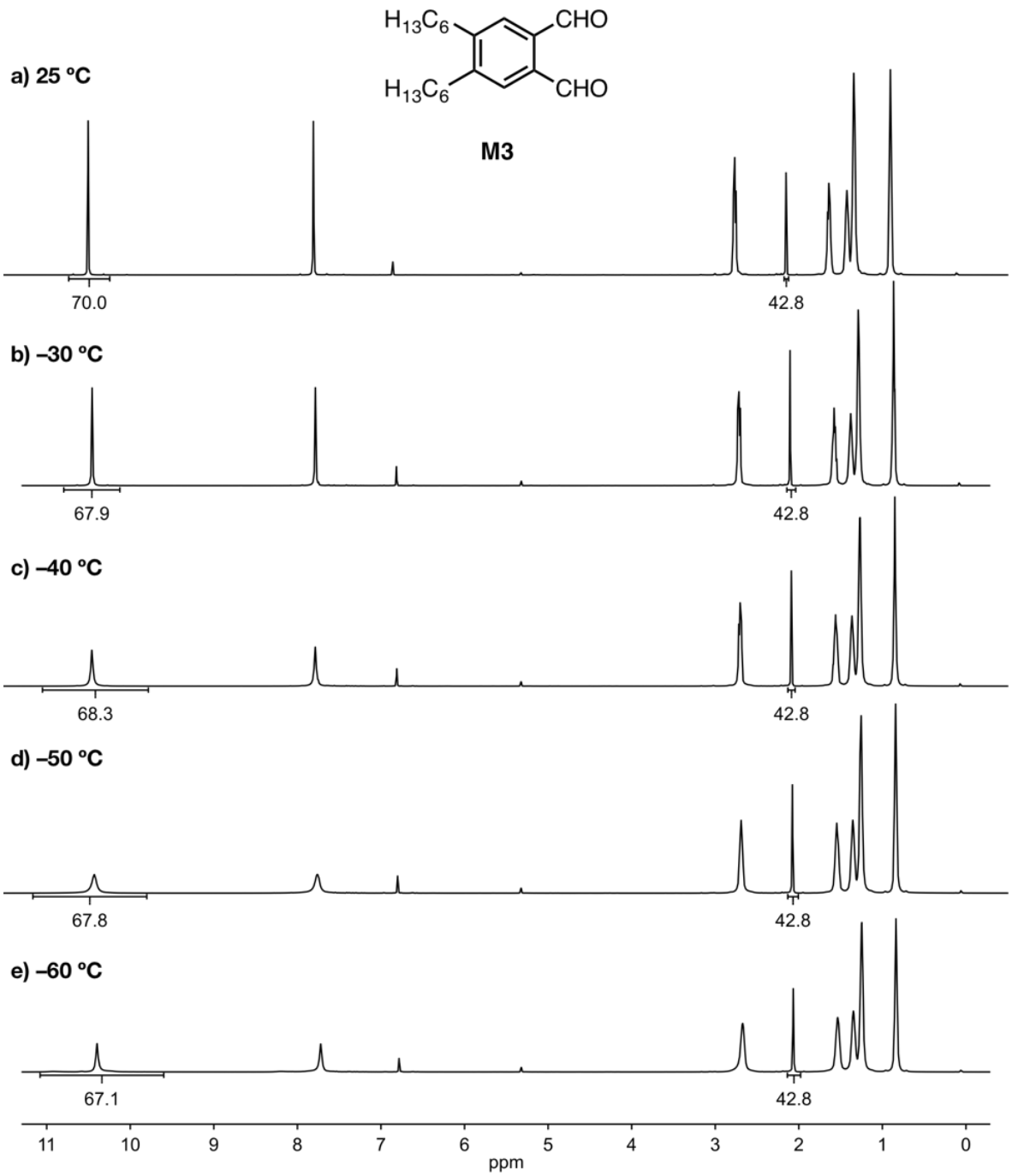

Figure S48. VT-^{1}H NMR spectra of **M3** + $SnCl_4$ (500 MHz, CD_2Cl_2).

Table S11. Concentration data from VT-NMR spectroscopic experiments with **M3**.

set temp (ºC)	corr temp (ºC)	1/*T* (K^{-1})	[**M3**] (M)	R•ln[**M3**] (cal/mol•K)
25.0	25.4	0.00335	0.70	–0.71
–30.0	–32.1	0.00415	0.68	–0.77
-40.0	–42.6	0.00434	0.68	–0.76
–50.0	–53.0	0.00454	0.68	–0.77
–60.0	–63.5	0.00477	0.67	–0.68

The T_c for **M3** was too low to measure due to temperature limitations of the NMR probe, but –60 ºC provides an upper limit for the T_c.

T_c Measurement for **M4**:

The general procedure was followed with **M4** (102.9 mg, 0.3500 mmol) and CD_2Cl_2 (0.50 mL); $[\mathbf{M4}]_0$ = 0.70 M.

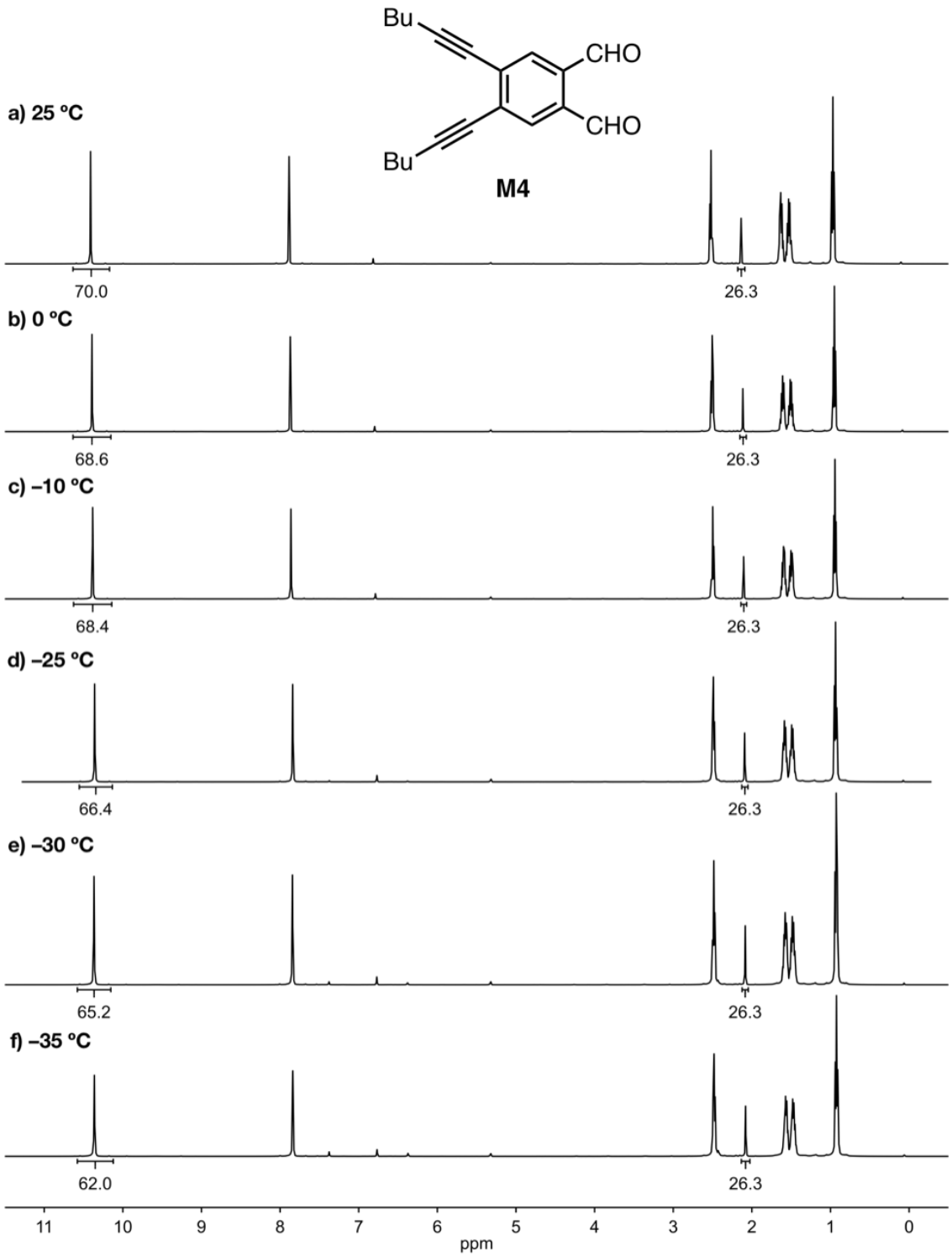

Figure S49. VT-^{1}H NMR spectra of **M4** + $SnCl_4$ (500 MHz, CD_2Cl_2).

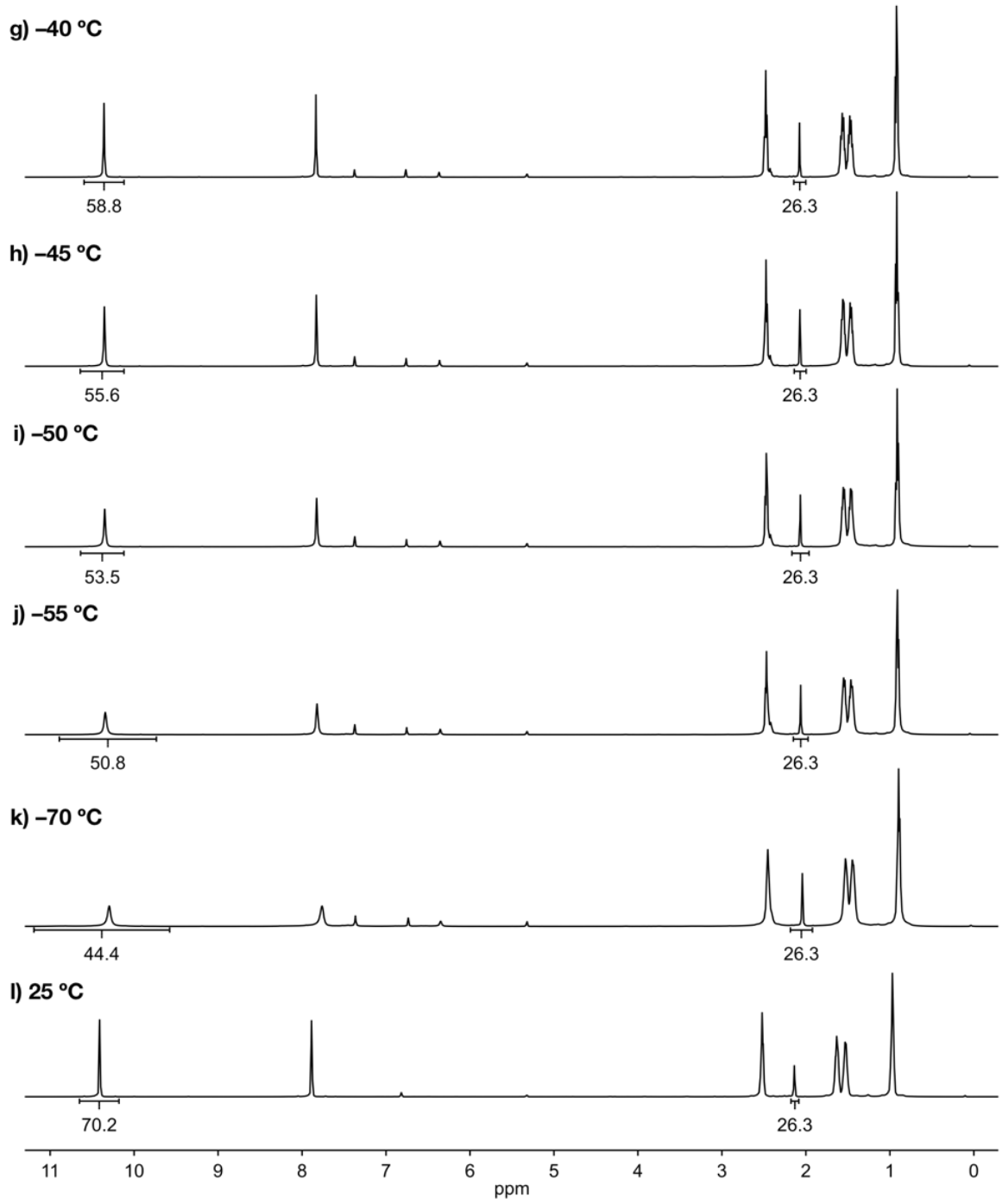

Figure S50. Additional VT-^{1}H NMR spectra of **M4** + $SnCl_4$ (500 MHz, CD_2Cl_2).

Table S12. Concentration data from VT-NMR spectroscopic experiments with **M4**.

set temp (ºC)	corr temp (ºC)	1/*T* (K^{-1})	Run 1		Run 2	
			[**M4**] (M)	R•ln[**M4**] (cal/mol•K)	[**M4**] (M)	R•ln[**M4**] (cal/mol•K)
25.0	25.4	0.00336	0.70	–0.71	0.70	–0.71
0.0	–0.7	0.00367	0.69	–0.75	0.70	–0.70
–10.0	–11.2	0.00382	0.68	–0.75	0.70	–0.71
–20.0	–21.7	0.00398	0.67	–0.79	0.68	–0.76
–25.0	–26.9	0.00406	0.66	–0.81	0.68	–0.77
–30.0	–32.1	0.00415	0.65	–0.85	0.66	–0.83
–35.0	–37.3	0.00424	0.62	–0.95	0.64	–0.89
–40.0	–42.6	0.00434	0.59	–1.1	0.61	–0.97
–45.0	–47.8	0.00444	0.56	–1.2	0.59	–1.1
–50.0	–53.0	0.00454	0.54	–1.2	0.57	–1.1
–55.0	–58.2	0.00465	0.51	–1.3	0.53	–1.3
–70.0	–73.9	0.00502	0.44	–1.6	0.48	–1.5
25.0	25.4	0.00335	0.70	–0.70	0.70	–0.70

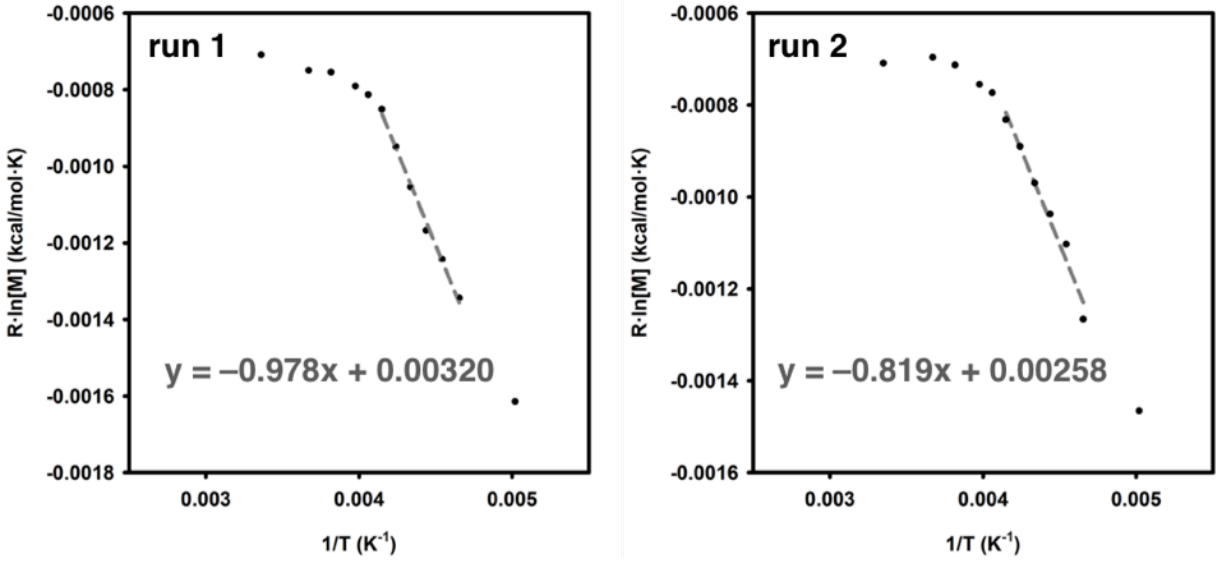

Figure S51. Plots of R•ln[M] versus 1/*T* for **M4**.

Table S13. Thermodynamic parameters for **M4**.

run	ΔH (kcal/mol)	ΔS (cal/mol•K)	T_c (ºC)
1	–0.978	–3.20	–22.6
2	–0.819	–2.58	–24.2

T_c Measurement for **M5**:

The general procedure was followed with **M5** (46.9 mg, 0.350 mmol) and CD_2Cl_2 (0.50 mL); $[\mathbf{M5}]_0$ = 0.70 M.

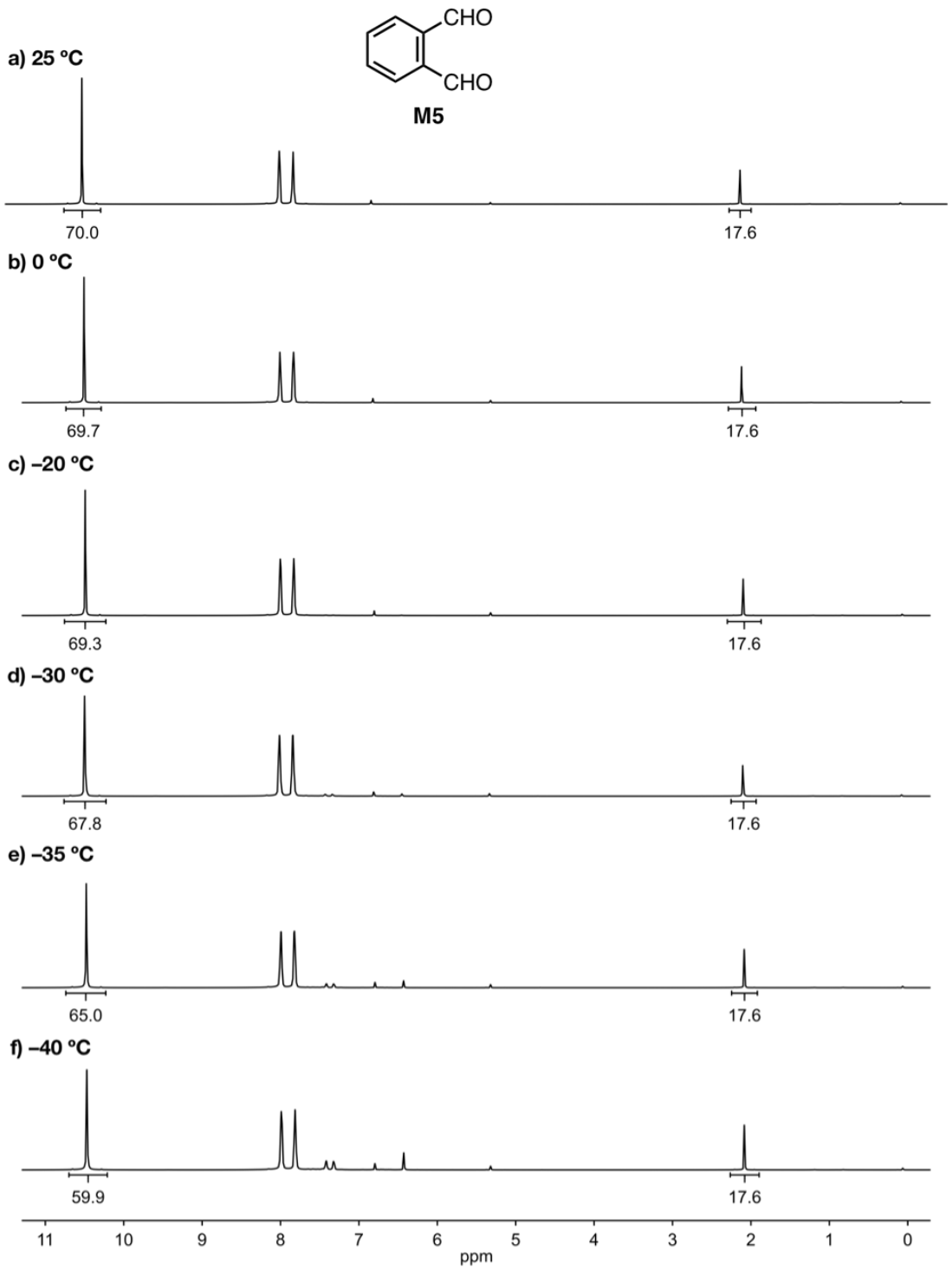

Figure S52. VT-^{1}H NMR spectra of **M5** + $SnCl_4$ (500 MHz, CD_2Cl_2).

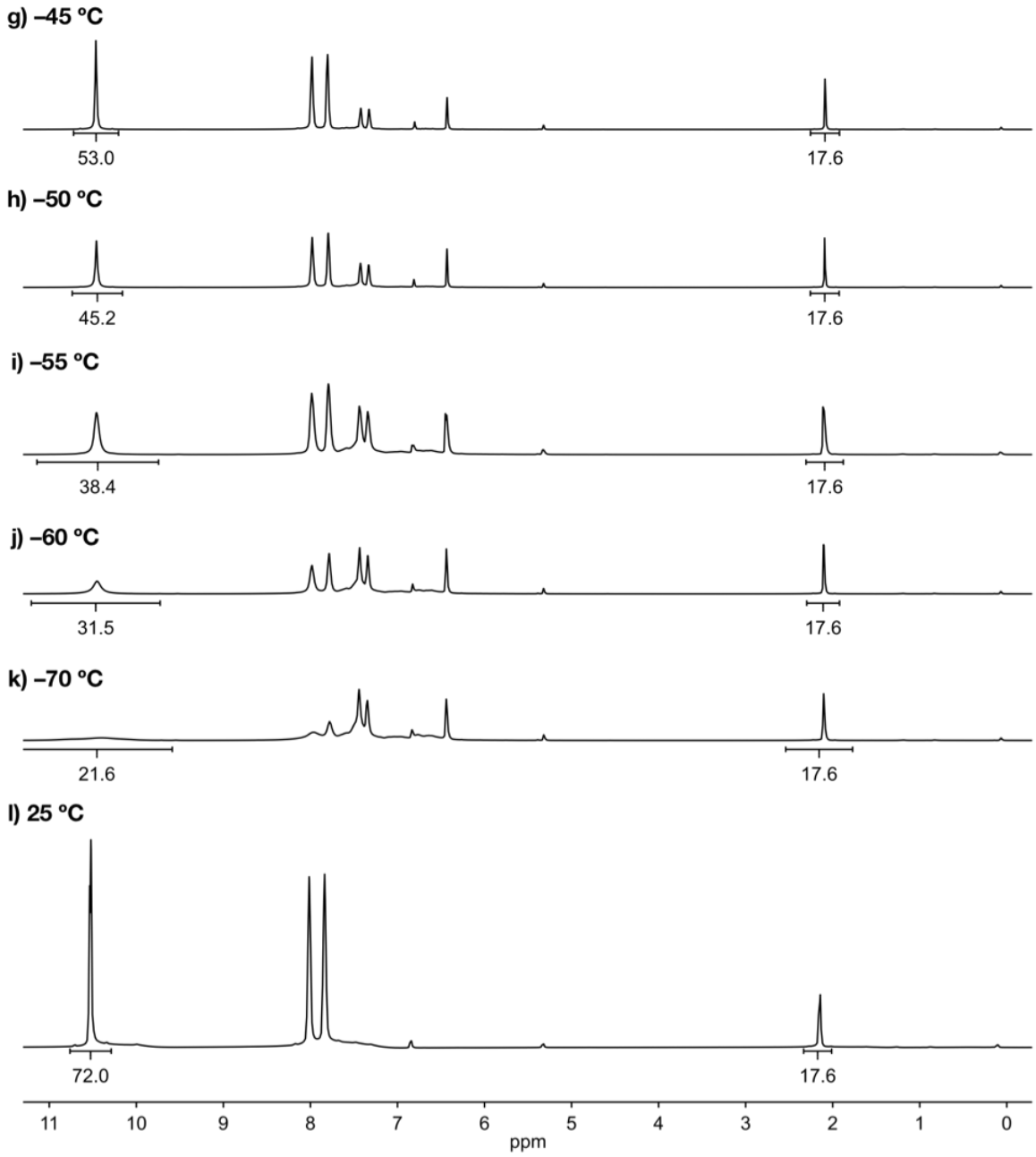

Figure S53. Additional VT-^{1}H NMR spectra of **M5** + $SnCl_4$ (500 MHz, CD_2Cl_2).

Table S14. Concentration data from VT-NMR spectroscopic experiments with **M5**.

set temp (ºC)	corr temp (ºC)	1/*T* (K^{-1})	Run 1		Run 2	
			[**M5**] (M)	R•ln[**M5**] (cal/mol•K)	[**M5**] (M)	R•ln[**M5**] (cal/mol•K)
25.0	25.4	0.00335	0.70	–0.71	0.70	–0.71
0.0	–0.7	0.00367	0.70	–0.72	0.69	–0.73
–20.0	–21.7	0.00398	0.69	–0.73	0.68	–0.76
–25.0	–26.9	0.00406	n/a	n/a	0.68	–0.78
–30.0	–32.1	0.00415	0.68	–0.77	0.66	–0.82
–35.0	–37.3	0.00424	0.65	–0.86	0.63	–0.91
–40.0	–42.6	0.00434	0.60	–1.0	0.60	–1.0
–45.0	–47.8	0.00444	0.53	–1.3	0.52	–1.3
–50.0	–53.0	0.00454	0.45	–1.6	0.46	–1.6
–55.0	–58.2	0.00465	0.38	–1.9	0.37	–2.0
–60.0	–63.5	0.00477	0.31	–2.3	0.28	–2.5
–70.0	–73.9	0.00502	0.22	–3.1	0.20	–3.2
25.0	25.4	0.00335	0.72	–0.65	0.71	–0.69

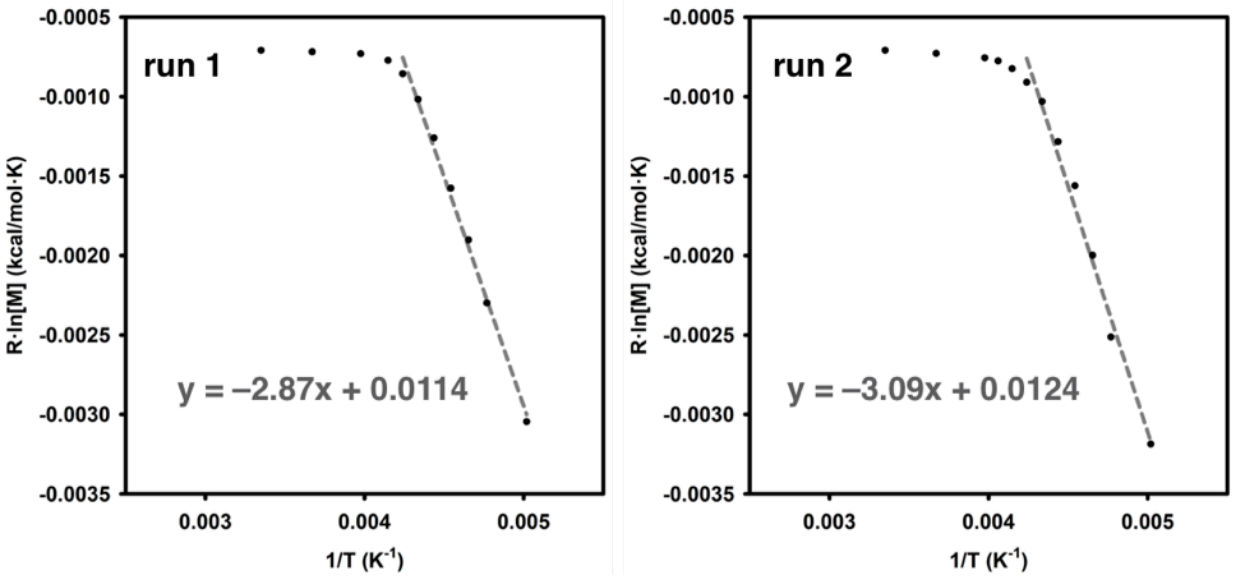

Figure S54. Plots of R•ln[M] versus 1/*T* for **M5**.

Table S15. Thermodynamic parameters for **M5**.

run	ΔH (kcal/mol)	ΔS (cal/mol•K)	T_c (ºC)
1	–2.87	–11.4	–36.4
2	–3.09	–12.4	–36.4

T_c Measurement for **M6**:

The general procedure was followed with **M6** (87.6 mg, 0.350 mmol) and $CDCl_3$ (1.0 mL); $[\mathbf{M6}]_0$ = 0.35 M. This monomer was run at lower $[M]_0$ than the others due to solubility concerns.

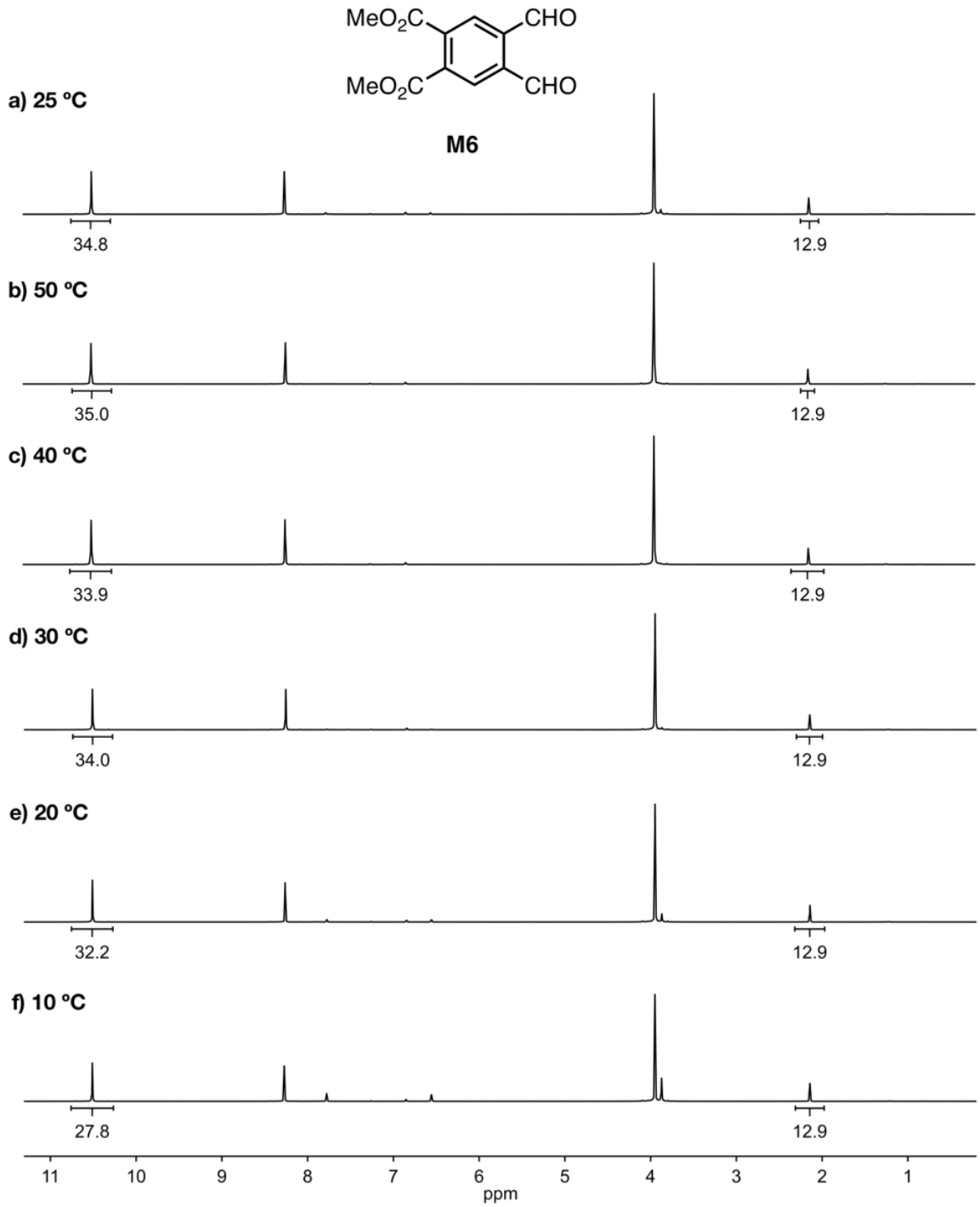

Figure S55. VT-^{1}H NMR spectra of **M6** + $SnCl_4$ (500 MHz, CD_2Cl_2).

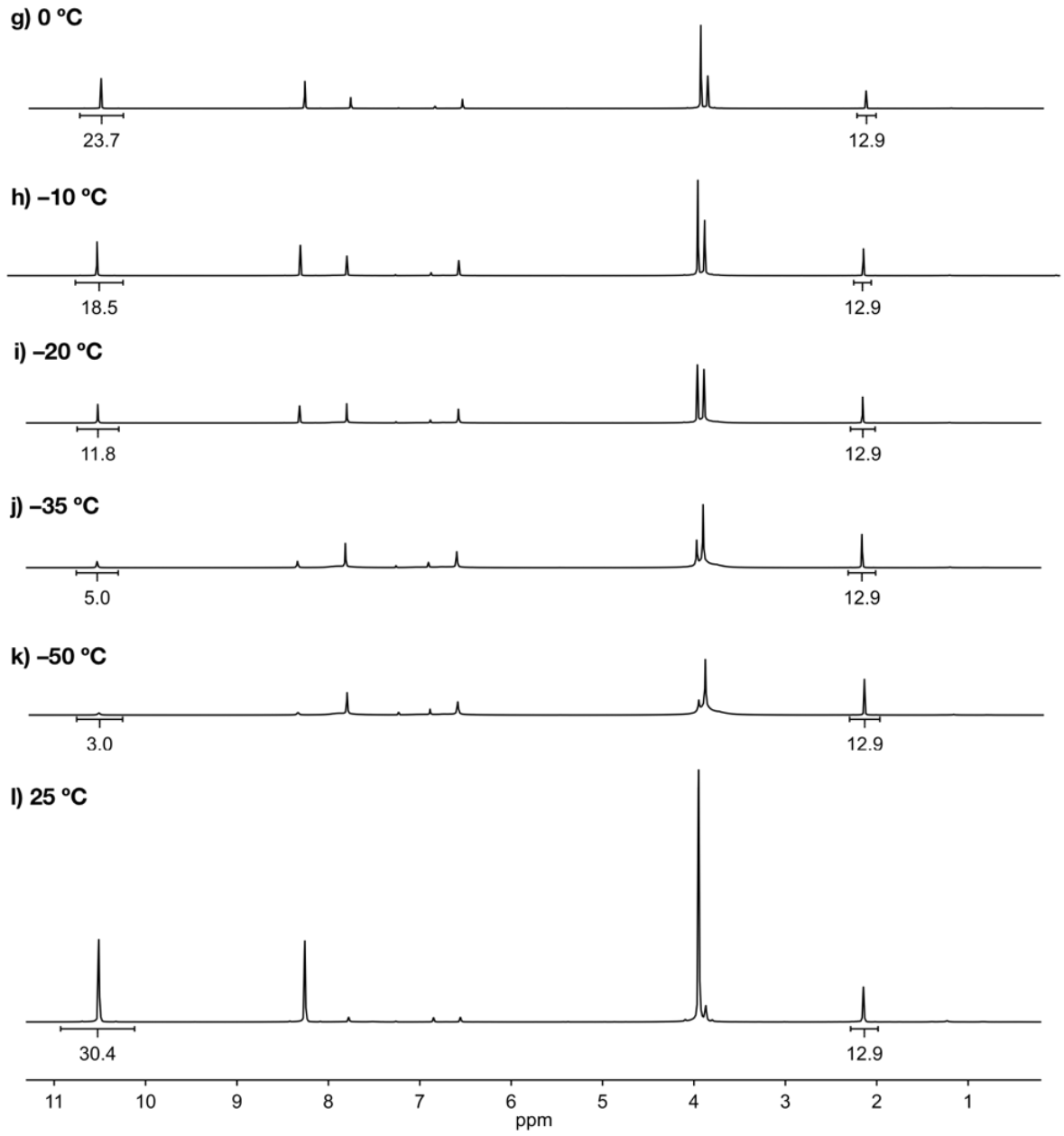

Figure S56. Additional VT-^{1}H NMR spectra of **M6** + $SnCl_4$ (500 MHz, CD_2Cl_2).

Table S16. Concentration data from VT-NMR spectroscopic experiments with **M6**.

set temp (ºC)	corr temp (ºC)	1/*T* (K^{-1})	Run 1		Run 2	
			[**M6**] (M)	R•ln[**M6**] (cal/mol•K)	[**M6**] (M)	R•ln[**M6**] (cal/mol•K)
25.0	25.3	0.00335	0.34	–2.1	0.35	–2.1
50.0	51.5	0.00308	0.35	–2.1	0.35	–2.1
40.0	41.0	0.00318	0.36	–2.0	0.34	–2.2
30.0	30.6	0.00329	0.36	–2.0	0.34	–2.1
20.0	20.1	0.00341	0.33	–2.2	0.32	–2.3
10.0	9.7	0.00354	0.30	–2.4	0.28	–2.5
0.0	–0.7	0.00367	0.24	–2.9	0.24	–2.9
–10.0	–11.2	0.00382	0.17	–3.5	0.18	–3.4
–20.0	–21.6	0.00398	0.11	–4.4	0.12	–4.2
–35.0	–37.3	0.00424	0.045	–6.2	0.050	–5.9
–50.0	–53.0	0.00454	0.028	–7.1	0.030	–7.0
25.0	25.3	0.00335	0.35	–2.1	0.30	–2.4

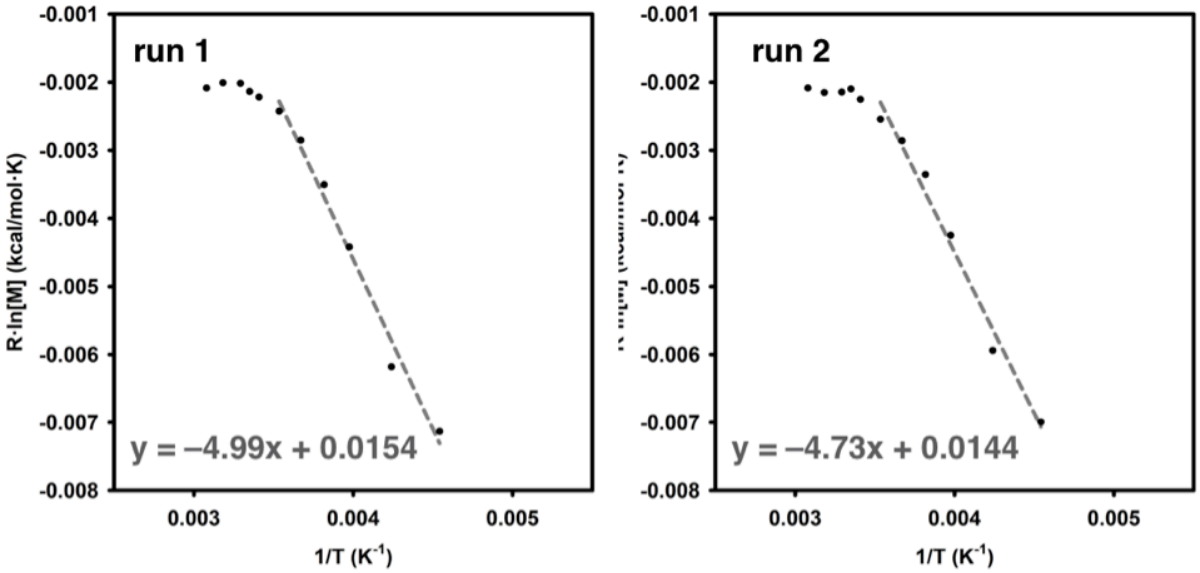

Figure S57. Plots of R•ln[M] versus 1/*T* for **M6**.

Table S17. Thermodynamic parameters for **M6**.

run	Δ*H* (kcal/mol)	Δ*S* (cal/mol•K)	T_c (ºC)
1	–4.99	–15.4	12.9
2	–4.73	–14.4	13.3

T_c Measurement for **M7**:

The general procedure was followed with **M7** (110.4 mg, 0.3500 mmol) and 1,1,2,2-tetrachloroethane-d_2 (0.50 mL); $[\mathbf{M7}]_0$ = 0.70 M.

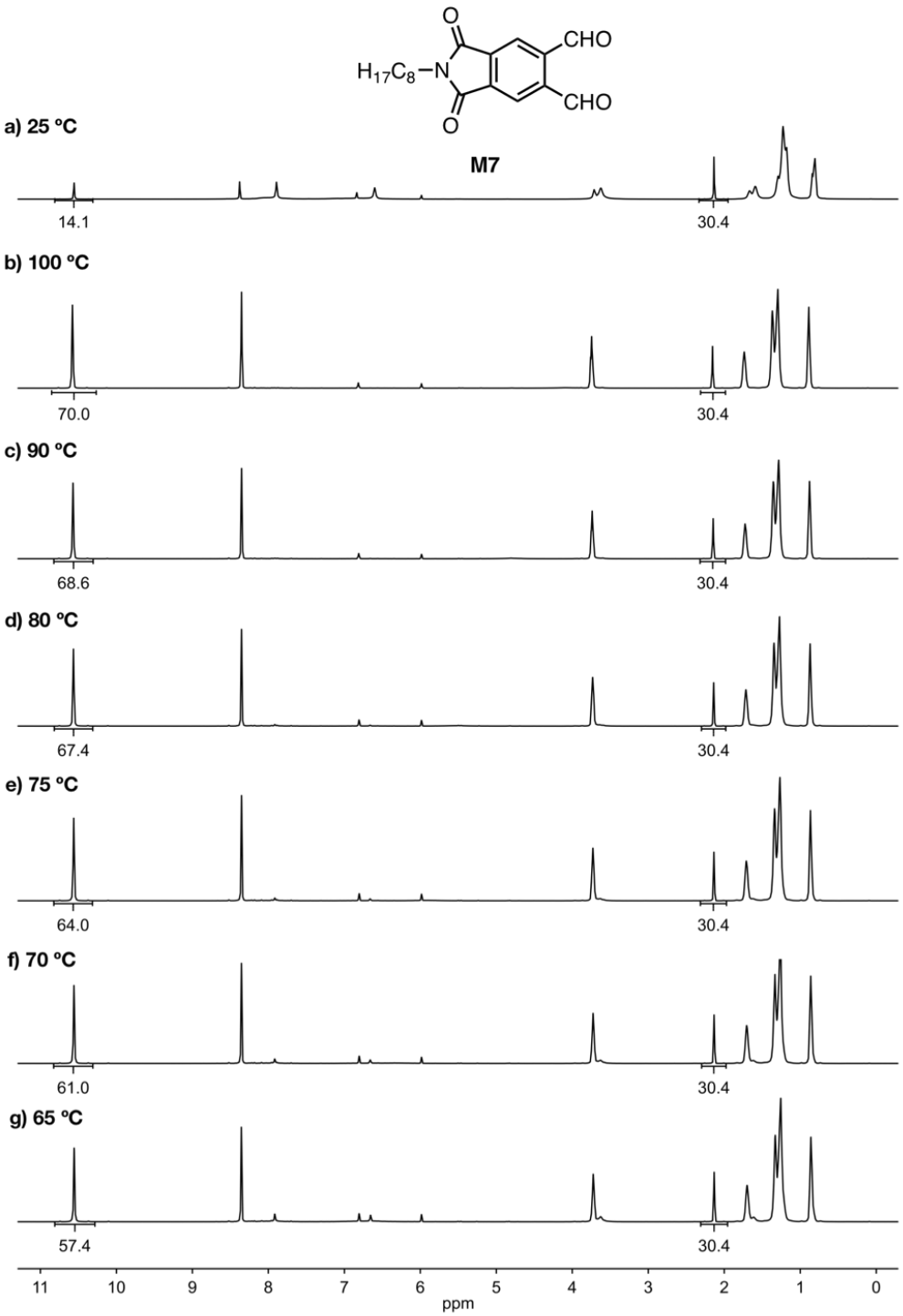

Figure S58. VT-^{1}H NMR spectra of **M7** + $SnCl_4$ (500 MHz, 1,1,2,2-tetrachloroethane-d_2).

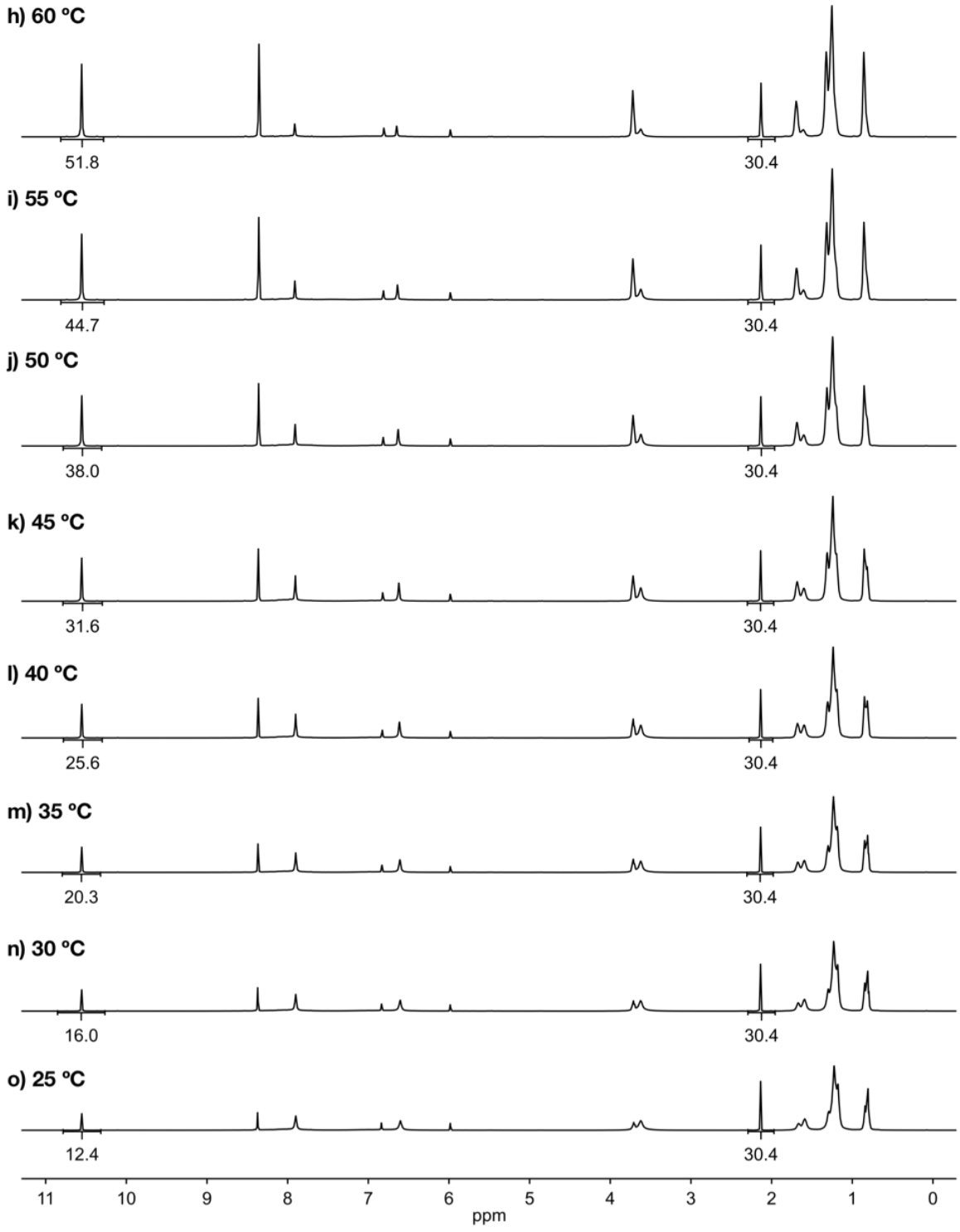

Figure S59. Additional VT-^{1}H NMR spectra of **M7** + $SnCl_4$ (500 MHz, 1,1,2,2-tetrachloroethane-d_2).

Table S18. Concentration data from VT-NMR spectroscopic experiments with **M7**.

set temp (ºC)	corr temp (ºC)	1/*T* (K^{-1})	Run 1		Run 2	
			[**M7**] (M)	R•ln[**M7**] (cal/mol•K)	[**M7**] (M)	R•ln[**M7**] (cal/mol•K)
25.0	24.9	0.00336	0.14	–3.9	0.14	–4.0
100.0	106.7	0.00263	0.70	–0.71	0.70	–0.71
90.0	95.8	0.00271	0.69	–0.75	0.68	–0.76
80.0	84.9	0.00279	0.67	–0.79	0.66	–0.81
75.0	79.4	0.00284	0.64	–0.89	0.64	–0.90
70.0	74.0	0.00288	0.61	–0.98	0.62	–0.94
65.0	68.5	0.00293	0.57	–1.1	0.58	–1.1
60.0	63.1	0.00297	0.52	–1.3	0.54	–1.2
55.0	57.6	0.00302	0.45	–1.6	0.46	–1.5
50.0	52.1	0.00307	0.38	–1.9	0.39	–1.9
45.0	46.7	0.00313	0.32	–2.3	0.32	–2.3
40.0	41.2	0.00318	0.26	–2.7	0.26	–2.7
35.0	35.8	0.00324	0.20	–3.2	0.20	–3.2
30.0	30.3	0.00330	0.16	–3.7	0.16	–3.7
25.0	24.9	0.00336	0.12	–4.2	0.12	–4.2

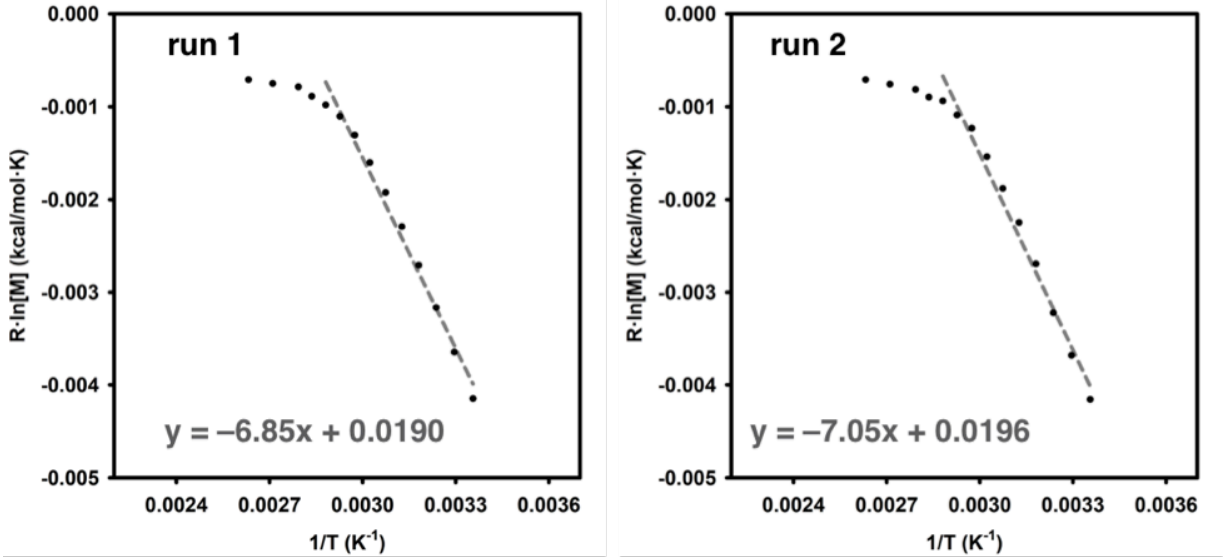

Figure S60. Plots of R•ln[M] versus 1/*T* for **M7**.

Table S19. Thermodynamic parameters for **M7**.

run	ΔH (kcal/mol)	ΔS (cal/mol•K)	T_c (ºC)
1	–6.85	–19.0	74.4
2	–7.05	–19.6	73.3

T_c Measurement for **M8**:

The general procedure was followed with **M8** (72.1 mg, 0.350 mmol) and 1,1,2,2-tetrachloroethane-d_2 (0.50 mL); $[\mathbf{M8}]_0$ = 0.70 M.

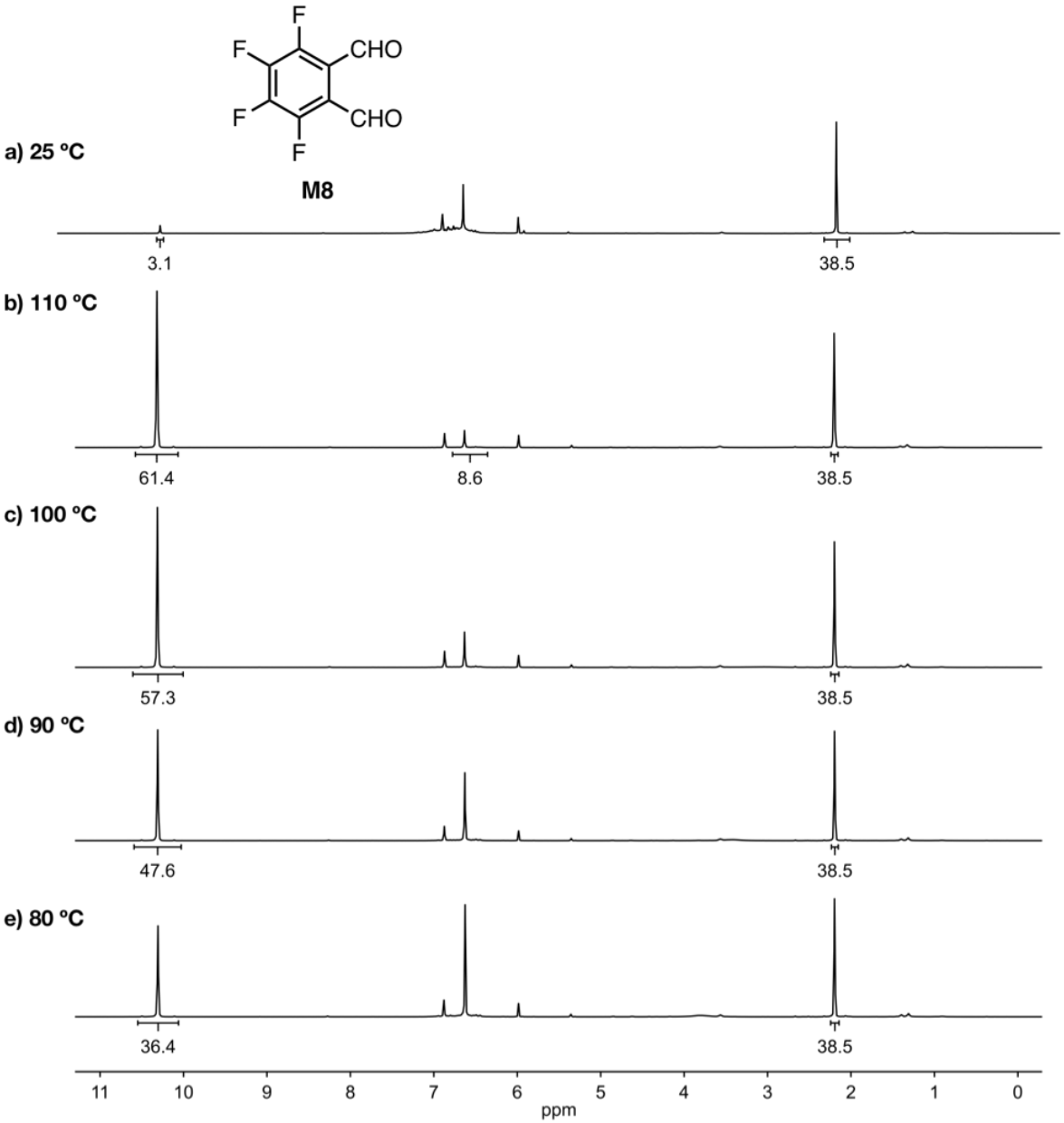

Figure S61. VT-^{1}H NMR spectra of **M8** + $SnCl_4$ (500 MHz, 1,1,2,2-tetrachloroethane-d_2).

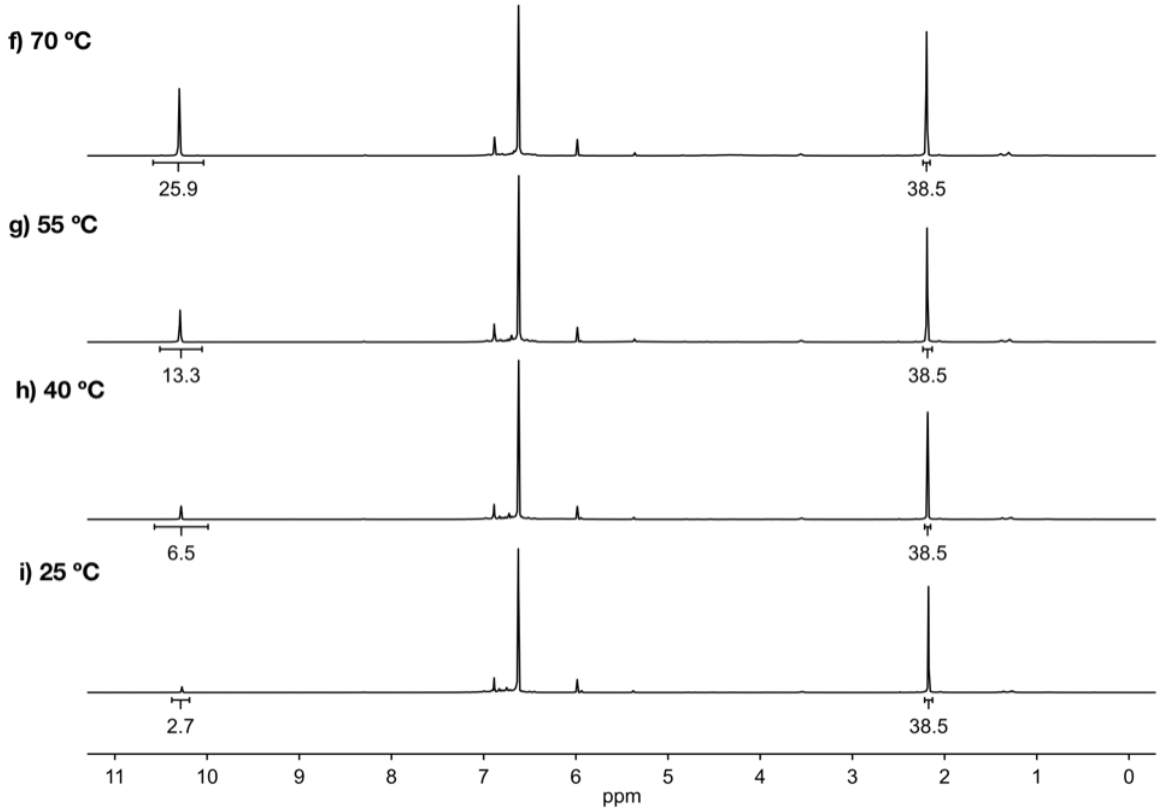

Figure S62. Additional VT-^{1}H NMR spectra of **M8** + $SnCl_4$ (500 MHz, 1,1,2,2-tetrachloroethane-d_2).

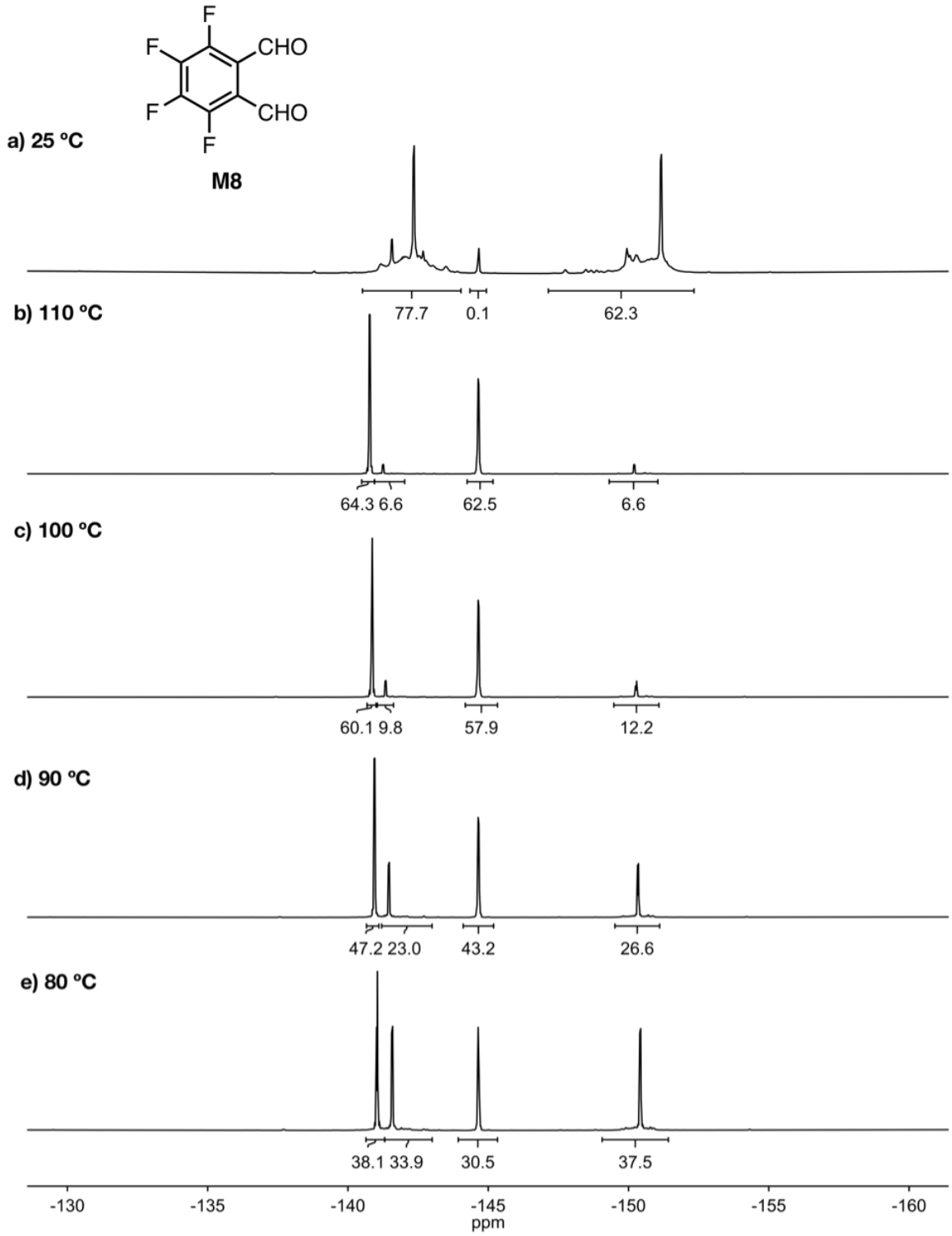

Figure S63. VT-^{19}F NMR spectra of **M8** + $SnCl_4$ (471 MHz, 1,1,2,2-tetrachloroethane-d_2).

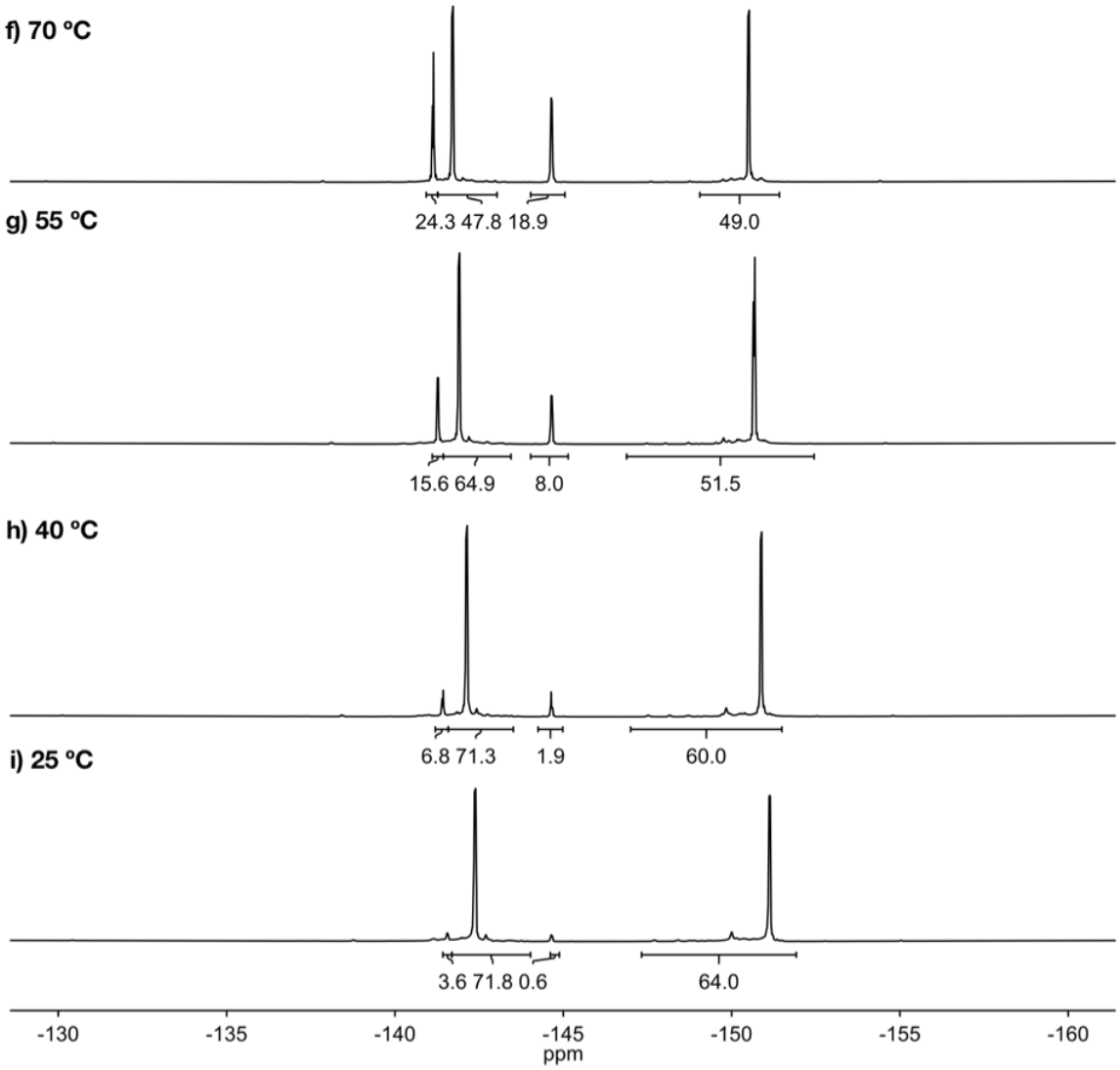

Figure S64. Additional VT-^{19}F NMR spectra of **M8** + $SnCl_4$ (471 MHz, 1,1,2,2-tetrachloroethane-d_2).

Table S20. Concentration data from VT-NMR spectroscopic experiments with **M8**.

set temp (ºC)	corr temp (ºC)	1/*T* (K^{-1})	Run 1		Run 2	
			[**M8**] (M)	R•ln[**M8**] (cal/mol•K)	[**M8**] (M)	R•ln[**M8**] (cal/mol•K)
25.0	24.9	0.00336	0.03	–6.9	0.05	–6.2
110.0	117.6	0.00256	0.61	–1.0	0.61	–0.99
100.0	106.7	0.00263	0.57	–1.1	0.65	–0.87
90.0	95.8	0.00271	0.48	–1.5	0.60	-1.0
80.0	84.9	0.00279	0.36	–2.0	0.53	–1.3
70.0	74.0	0.00288	0.26	–2.7	0.38	–1.9
55.0	57.6	0.00302	0.13	–4.0	0.21	–3.1
40.0	41.2	0.00318	0.06	–5.4	0.10	–4.6
25.0	24.9	0.00336	0.03	–7.1	0.04	–6.3

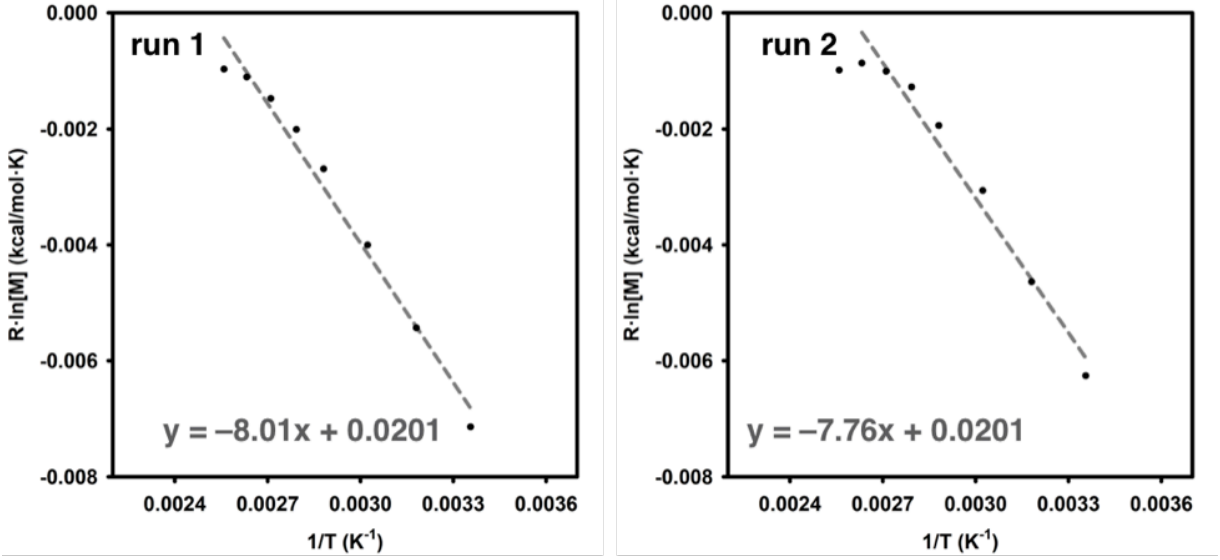

Figure S65. Plots of R•ln[M] versus 1/*T* for **M8**.

Table S21. Thermodynamic parameters for **M8**.

run	Δ*H* (kcal/mol)	Δ*S* (cal/mol•K)	T_c (ºC)
1	–8.01	–20.1	112.5
2	–7.76	–20.1	100.0

VII. Microcapsule Fabrication

Microcapsules were generated following a previously reported procedure that had been optimized for cPPA.[17,18] A solution of **P6** (200 mg) and jojoba oil (200 mg) in DCM (2 mL) was prepared. The solution was passed through a microfluidic flow-focusing device (flow rate = 500 µL/h) into a 2.5 wt% aqueous polyvinyl alcohol solution (50 mL, flow rate = 4000 µL/h). The resulting mixture (30 mL) was diluted with DI water (30 mL) to 1 wt% PVA, then concentrated on the rotary evaporator for 30 min to promote rapid solvent evaporation. The capsules were isolated by vacuum filtration and washed with water (500 mL), then hexanes (250 mL).

For imaging, microcapsules were sputter-coated with Au/Pd using a DESK II TSC sputter coater to remove surface charging effects. Imaging was performed through a scanning electron microscope. ImageJ software was utilized to measure the diameter of the microcapsules (228 ± 5 µm, average of 10 capsules).

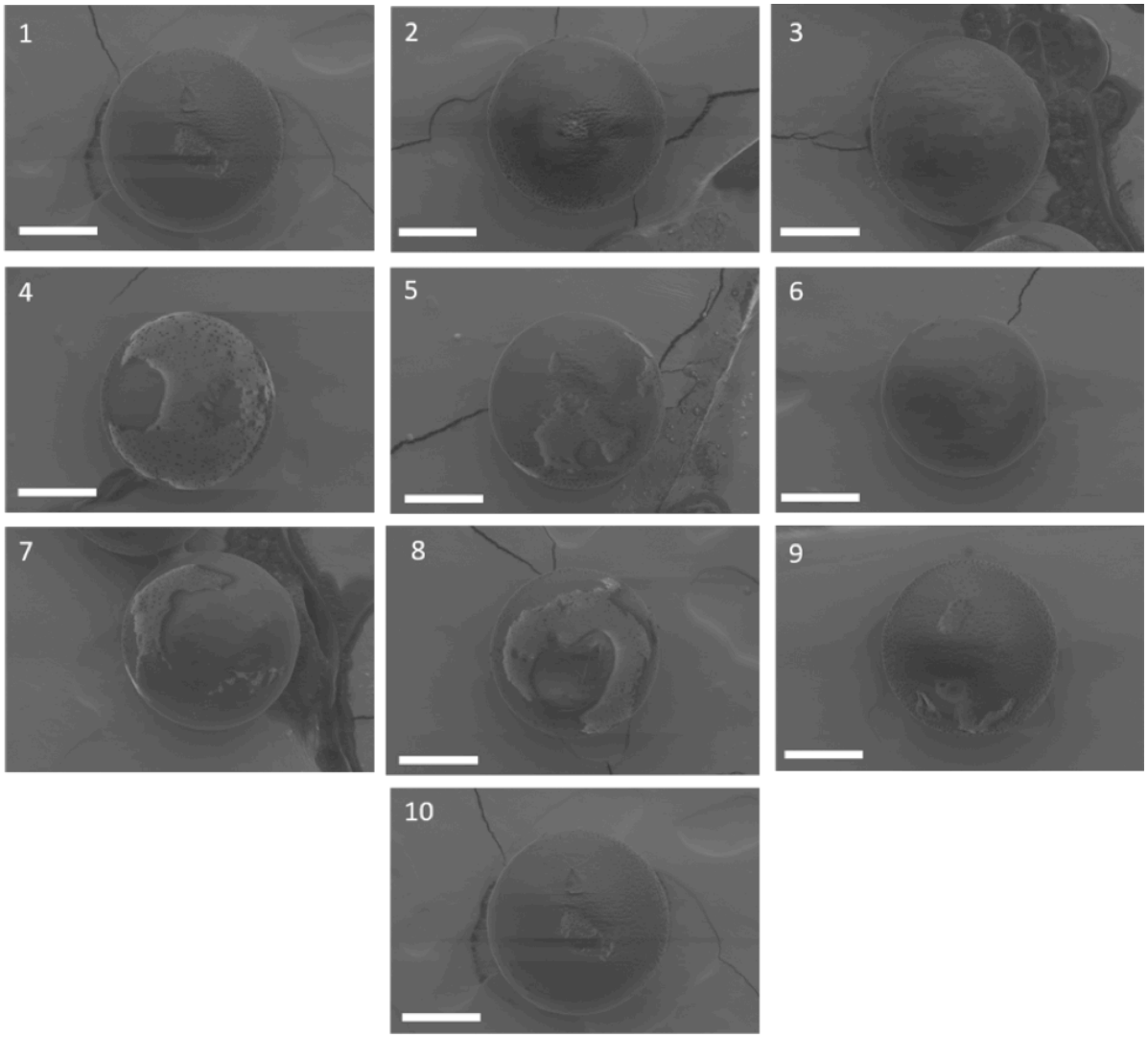

Figure S66. SEM images of **P6** microcapsules. The scale bars represent 100 µm.

Table S22. Microcapsule diameters.

image	diameter (μm)
1	228
2	225
3	224
4	226
5	236
6	237
7	234
8	225
9	223
10	230

Capsules were ruptured using a razor and imaged by SEM to confirm the core–shell morphology. From one of these images, the shell wall thickness was estimated at 11 μm.

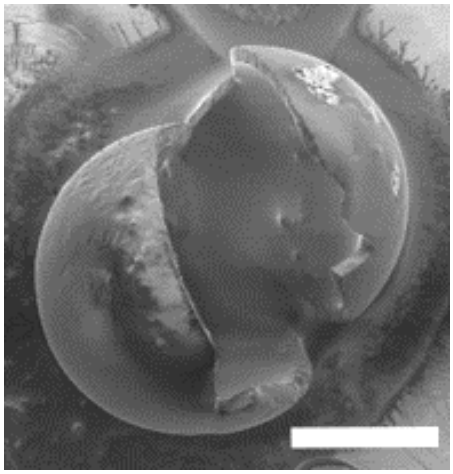

Figure S67. SEM image of a ruptured **P6** microcapsule. The scale bar represents 100 μm.

VIII. Computational Model for Estimating Ceiling Temperatures

Computational Details

Density functional theory computations were carried out using the Q-Chem 4.3 quantum chemistry package.[19] All geometries were optimized using the B3LYP hybrid functional[20] with the 6-31++G** basis set[21] assuming a singlet ground state for all geometries. Vibrational frequency analysis was conducted at the B3LYP/6-3++G** level of theory, and all structures were characterized as stationary points by the absence imaginary vibrational modes. Energies used in the following discussion are the self-consistent field (SCF) electronic energy from the optimization. We found the model deviated further from the experimentally measured T_c values when the electronic energy was corrected with enthalpy and entropy values calculated at 298 K.

*Determining Δ*S *for **M5***

Calculated gas-phase electronic energies for **M5**, **A5$_{meso}$**, **A5$_{rac}$**, H_2O, and MeOH were used to determine Δ*H* for the formation of the two diasteromers of **A5**. Then, the Δ*H* value and the measured T_c for **M5** (–36.4 ºC) were used with Eq. S3 to compute the estimated Δ*S* for the formation of both diastereomers of **A5**.

$$T_c = \frac{\Delta H}{\Delta S} \qquad (S3)$$

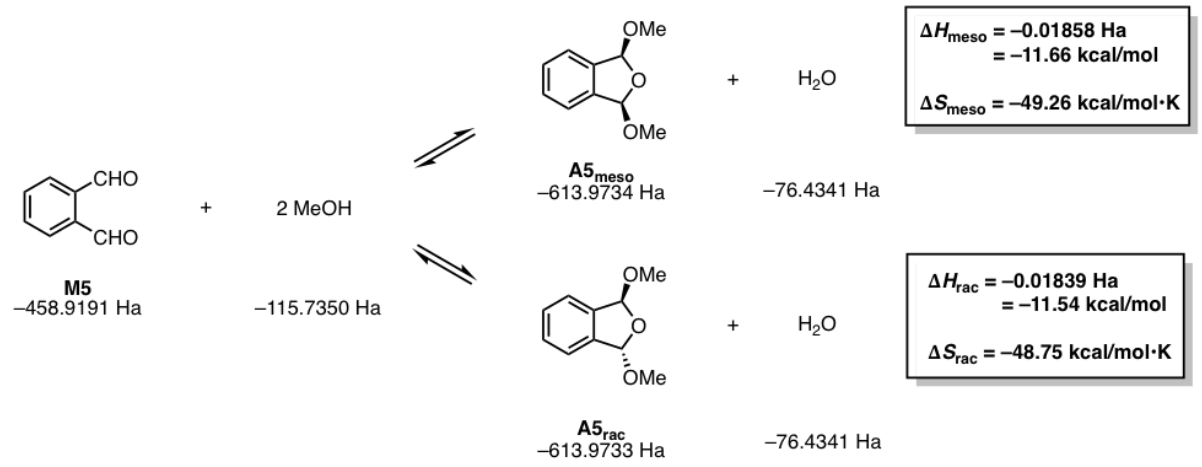

Figure S68. Calculated energies and Δ*S* determination for **M5**.

These values of Δ*S* were assumed to remain constant for the other monomers, enabling the estimation of T_c from their computed Δ*H* values using Eq. 1. The estimated T_c values reported in the manuscript are a simple average of those found for the rac and meso diastereomers

Structure M5

16

C	-0.27734967	2.23958384	-0.00251388
C	1.00106617	2.82075738	-0.00820676

C	2.14252857	1.97506832	-0.00884229
C	-0.44548206	0.85517882	0.00262753
C	1.95685449	0.58662466	-0.00366163
C	0.67886128	0.02630381	0.00205035
H	-1.15014891	2.88770183	-0.00206979
H	2.84218559	-0.04086951	-0.00427179
C	1.02248505	4.30828925	-0.01296980
O	2.00276443	5.03083874	-0.01750870
C	3.55502828	2.48063040	-0.01492504
O	4.51057624	1.72102943	-0.01466226
H	3.69203585	3.57025971	-0.01944720
H	0.00673309	4.75790991	-0.01218618
H	-1.44387072	0.42860093	0.00696540
H	0.56100233	-1.05318752	0.00600204

Structure MeOH

6

C	-2.42918848	1.08846662	-0.02793840
O	-1.30303158	1.95927155	0.03524775
H	-2.17241600	0.11146997	-0.46029343
H	-3.25857301	1.52619566	-0.60055225
H	-2.76220616	0.93483150	1.00074663
H	-0.97741477	2.11918471	-0.85891030

Structure $A5_{meso}$

25

C	0.66176992	0.17883689	-0.03282311
C	1.80925889	0.89436976	0.30097722
C	1.81029863	2.28423776	0.31625180
C	0.66385890	3.00870908	-0.00142734
C	-0.49070689	0.89730432	-0.36686484
C	-0.48971714	2.29954616	-0.35116135
H	0.66164265	4.09418369	0.02942502
H	0.65794621	-0.90705135	-0.02618786
C	3.16681220	0.39578743	0.72014820
O	3.97059042	1.58209477	0.81919316
C	3.16883834	2.77160201	0.74515235
O	3.05941255	-0.30072360	1.93194493
H	3.66460884	-0.24389269	-0.02505555
O	3.06361704	3.44319324	1.97103851
C	4.28615473	-0.87391471	2.37875081
H	5.02593208	-0.09783648	2.60377491
H	4.69863894	-1.55966490	1.62367285
H	4.05432525	-1.43393055	3.28634494
C	4.29115719	4.00682145	2.42777706
H	4.70453886	4.70495813	1.68467661
H	4.06009914	4.55129502	3.34497520
H	5.03008509	3.22610785	2.63929809
H	3.66726290	3.42557599	0.01284142
H	-1.39800482	0.36468102	-0.63679248
H	-1.39624990	2.83939973	-0.60907055

Structure $A5_{rac}$

25

C	0.42372444	-0.04395188	-0.15182775
C	1.55538549	0.60296197	0.33889088
C	1.59167172	1.98555017	0.47206004
C	0.49910978	2.77280794	0.11629716
C	-0.67933276	0.73742444	-0.51103567
C	-0.64171567	2.13296788	-0.37884941
H	0.53500591	3.85386292	0.21048606
H	0.39441352	-1.12529305	-0.24489127
C	2.86523637	0.02549229	0.80550165
O	3.64887194	1.16459001	1.18933274
C	2.93682287	2.39699998	1.00729720
O	3.58090938	3.23281853	0.08336242
H	2.89774328	2.90218932	1.98567292
C	4.83947496	3.72918737	0.53504988
H	5.19011552	4.42665297	-0.22779983
H	5.56492500	2.91688628	0.65359821
H	4.73095221	4.26131014	1.49177544
H	3.42442090	-0.51143221	0.02257200
O	2.64582623	-0.83925676	1.88746831
C	3.82279887	-1.50133764	2.34621030
H	4.30865668	-2.05164804	1.52690130
H	3.50217118	-2.20776557	3.11409921
H	4.53579874	-0.78903314	2.77594814
H	-1.57565869	0.25934491	-0.89542887
H	-1.50749787	2.72238117	-0.66652105

Structure H_2O

3

O	-1.16054528	2.06715998	0.01180078
H	-0.19596376	2.07811263	-0.01835629
H	-1.45181095	2.38132739	-0.85301449

*Estimating T_c for **M1***

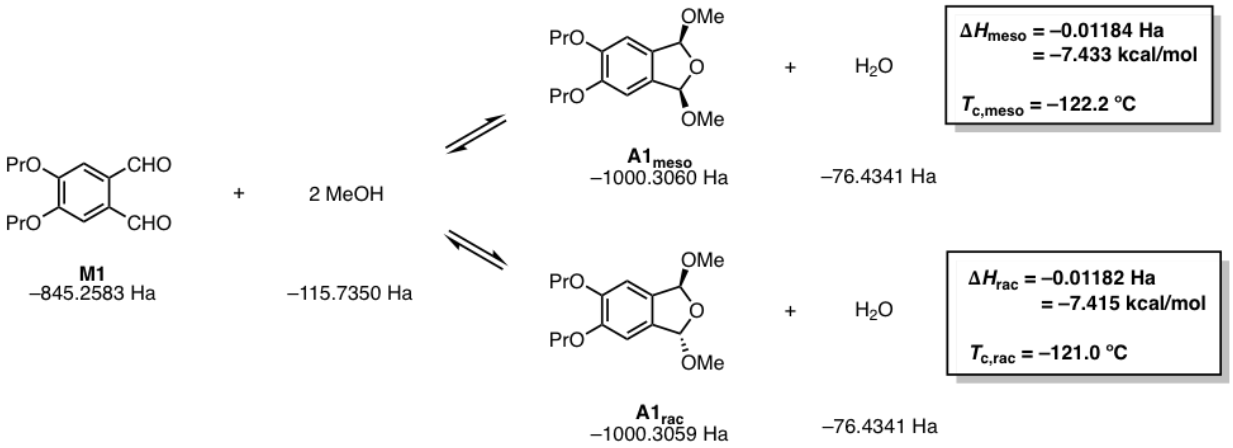

Figure S69. Calculated energies and T_c determination for **M1**.

Structure M1

36

C	-1.72406465	2.35486542	-0.07858191
C	-1.74260581	0.96311631	-0.03861560
H	-2.62196148	2.93291200	0.10212615
C	-0.55155221	3.07534709	-0.35452537
O	-2.83492055	0.20999490	0.21410076
C	-0.53639952	0.24566091	-0.28106772
C	0.64772521	2.36816796	-0.59721683
C	-0.66217404	4.56291592	-0.37833465
C	0.62731098	0.95899996	-0.55485724
C	1.96658910	2.96981827	-0.89901068
H	1.55261957	0.42643806	-0.74353841
O	-0.62922569	-1.10280947	-0.22226025
C	-4.08833522	0.86591749	0.46627668
C	-5.14043792	-0.20880068	0.69191506
H	-4.34970980	1.49668561	-0.39437967
H	-3.98945651	1.51257846	1.34900792
H	-5.18696590	-0.84811012	-0.19744864
C	-6.51967135	0.39360108	0.98387642
H	-4.82086537	-0.84653294	1.52443743
H	-6.86932899	1.02020305	0.15529560
H	-6.50583474	1.01273434	1.88813157
H	-7.26109507	-0.39656741	1.13613466
C	0.53959259	-1.89408092	-0.47228207
C	0.15288810	-3.35912012	-0.33263854
H	1.32542543	-1.62877026	0.24918400
H	0.91379812	-1.68315845	-1.48407395
H	-0.23996880	-3.52367218	0.67725888
C	1.34123886	-4.29054035	-0.59896546
H	-0.66409454	-3.57569686	-1.03038254
H	2.16529304	-4.10094886	0.09862160
H	1.72922743	-4.16685925	-1.61670161

H	1.04564928	-5.33760294	-0.48365699
O	-1.71743553	5.14144034	-0.15689617
H	0.25529325	5.12143355	-0.60763003
O	2.24205074	4.15573758	-0.97853666
H	2.76349199	2.21179250	-1.06290573

Structure A1$_{meso}$

45

C	0.54502634	0.18047774	-0.19978298
C	1.68430977	0.89982378	0.17335950
C	1.68623553	2.27978309	0.18594976
C	0.54878408	3.00918362	-0.17283812
C	-0.59898942	0.88624488	-0.57323221
C	-0.59738129	2.31373868	-0.55881114
H	0.55730592	4.09147773	-0.13547651
H	0.55044350	-0.90233432	-0.18320724
C	3.01768315	0.39620158	0.65054010
O	3.81635796	1.58129751	0.79783501
C	3.02137364	2.77120615	0.67045176
O	2.85845781	-0.31183413	1.85271313
H	3.55279022	-0.23950452	-0.07261259
O	2.86549002	3.46033316	1.88390599
C	4.06525838	-0.88578147	2.34746448
H	4.79404925	-0.11046709	2.60874139
H	4.51144718	-1.56629377	1.60656364
H	3.79692206	-1.45220905	3.24116916
C	4.07431103	4.02367632	2.38599671
H	4.52231472	4.71273439	1.65418016
H	3.80813306	4.57868416	3.28747021
H	4.80087387	3.24265242	2.63627351
O	-1.77087751	0.31209769	-0.96188416
C	-1.88444870	-1.11117231	-0.92519238
H	-1.13670646	-1.56452007	-1.59277071
C	-3.29302962	-1.48124193	-1.37026823
H	-1.69373589	-1.47185693	0.09601995
O	-1.76844704	2.89845708	-0.93399451
C	-1.87907050	4.32083095	-0.86664988
H	-1.68402614	4.65915884	0.16137449
C	-3.28843773	4.70258028	-1.29909571
H	-1.13272372	4.78682659	-1.52699873
H	3.55795028	3.41668434	-0.04293589
H	-3.45480829	4.33852194	-2.31946473
C	-3.51703326	6.21699654	-1.22801234
H	-4.00502309	4.17965525	-0.65522543
H	-2.83087868	6.75951374	-1.88899275
H	-3.36746326	6.59494499	-0.20984944
H	-4.53744878	6.47274620	-1.52952155
H	-3.45536166	-1.09670030	-2.38372675
H	-4.01089340	-0.97003329	-0.71846688
C	-3.52413108	-2.99649386	-1.32991366
H	-2.83781118	-3.52656050	-2.00074067

H	-4.54451275	-3.24452528	-1.63785754
H	-3.37618831	-3.39475083	-0.31931621

Structure A1$_{rac}$

45

C	0.23509206	-0.03633667	-0.16922827
C	1.37965561	0.61587456	0.29891168
C	1.43311924	1.99154170	0.38463339
C	0.34629709	2.78504366	0.00604969
C	-0.86312199	0.73364250	-0.55379269
C	-0.80742769	2.15743111	-0.46497771
H	0.41076085	3.86443973	0.06529518
H	0.20173722	-1.11750293	-0.21787361
C	2.67809076	0.03478376	0.78407905
O	3.48236896	1.17554327	1.11803749
C	2.78276628	2.40867096	0.89557555
O	3.43507222	3.20288871	-0.06255013
H	2.76079033	2.95213875	1.85415898
C	4.70419121	3.69249016	0.36345128
H	5.06221956	4.35732900	-0.42495384
H	5.41701824	2.87264546	0.50572968
H	4.61229790	4.25912151	1.30223383
O	-2.03617040	0.22812793	-1.02458158
C	-2.17082825	-1.18770775	-1.15887297
H	-1.39823787	-1.57146802	-1.84168567
C	-3.56152816	-1.47413519	-1.70748653
H	-2.03057513	-1.66957589	-0.17997051
O	-1.93295554	2.80840720	-0.86824526
C	-1.96771905	4.23379890	-0.78593897
H	-1.81302640	4.54855842	0.25662090
C	-3.32650764	4.70019088	-1.29090478
H	-1.15908216	4.66247830	-1.39579288
H	3.22936251	-0.54628325	0.02701747
O	2.45065515	-0.78029598	1.90573311
C	3.61977186	-1.43718918	2.38853906
H	4.08310726	-2.04726046	1.59863287
H	3.29666030	-2.08871524	3.20277459
H	4.35383271	-0.71587134	2.76480170
H	-3.45502644	4.35672408	-2.32381967
C	-3.47169078	6.22450021	-1.21392197
H	-4.10749815	4.21321568	-0.69546732
H	-3.68083843	-0.93502107	-2.65473604
H	-4.30441646	-1.06263758	-1.01430294
C	-3.80232162	-2.97325605	-1.91747108
H	-3.07949569	-3.40092739	-2.62225014
H	-4.80318504	-3.15198545	-2.32249260
H	-3.72220878	-3.53125728	-0.97721129
H	-2.71334436	6.73128320	-1.82216727
H	-3.36752640	6.58397314	-0.18342889
H	-4.45376490	6.54242391	-1.57734089

*Estimating T_c for **M2***

M2 analogue **M2′** was used for computations, and electron core potential (ECP) was applied due to the presence of many core electrons on sulfur.

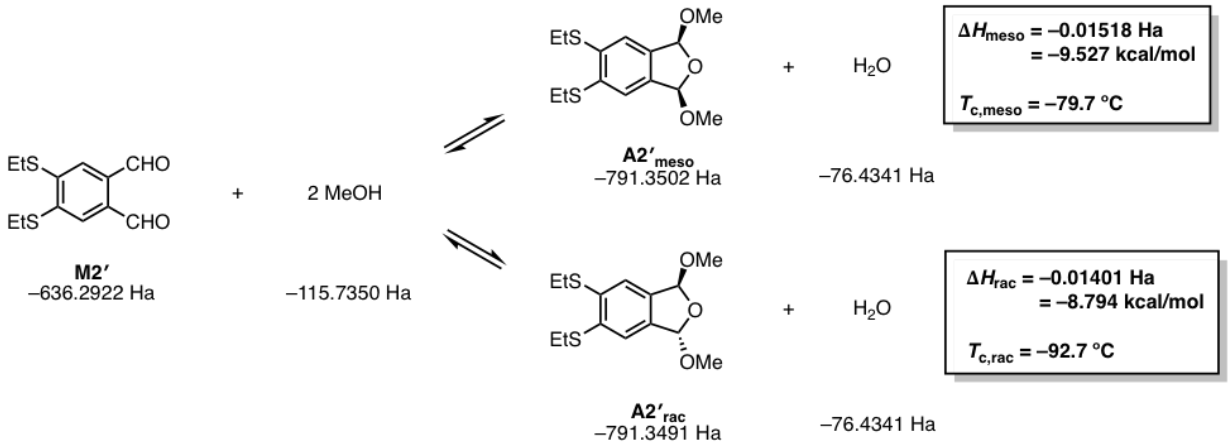

Figure S70. Calculated energies and T_c determination for **M2′**.

Structure M2′

30

C	-0.38268160	1.76055459	0.03256521
C	0.80823531	2.48909285	0.04586810
C	2.01396508	1.84980011	0.43359329
C	-0.43361133	0.40330303	0.39011296
C	1.95899609	0.48986108	0.77860887
C	0.77474631	-0.24571167	0.75434045
H	-1.27469713	2.30047807	-0.25911933
H	2.87265620	-0.01892089	1.07451290
C	0.72322484	3.93367604	-0.35181313
O	-0.32968372	4.44869079	-0.69396468
H	1.65824848	4.50910225	-0.32052220
C	3.35183300	2.48032234	0.50711152
S	-1.93477086	-0.54391776	0.42985479
C	-3.19804667	0.63336566	-0.21784904
H	-3.25611392	1.50308276	0.44306557
C	-4.54730014	-0.08788578	-0.27093531
H	-2.90146408	0.96934980	-1.21573801
S	0.80023616	-1.97063752	1.25965540
C	0.81576002	-2.82067742	-0.39368532
H	-0.04753745	-2.47549343	-0.96832330
C	0.76162834	-4.33310106	-0.18208306
H	1.72953874	-2.52963452	-0.91891229
H	-4.51259773	-0.95494012	-0.93810447
H	-5.31318392	0.59756515	-0.64727582
H	-4.85851015	-0.42968827	0.72126386
H	-0.15484464	-4.63067479	0.33723045
H	1.61766095	-4.68876620	0.40071647

H	0.78056218	-4.84210329	-1.15176905
O	3.63758957	3.63625382	0.24067041
H	4.14596205	1.78159438	0.84643476

Structure A2′$_{meso}$

39

C	0.40037542	-0.10456951	0.60328743
C	1.57087884	0.64407227	0.67030836
C	1.55540722	1.99230733	0.34837366
C	0.38541818	2.64089983	-0.03088030
C	-0.78894863	0.51417259	0.19870369
C	-0.80952052	1.90415436	-0.10302105
H	0.40851834	3.70217170	-0.24455968
H	0.38760988	-1.15843534	0.86279189
C	2.95894180	0.24933327	1.09511874
O	3.75640671	1.41465482	0.82189596
C	2.94057184	2.55758275	0.52813223
O	2.95399571	-0.11012374	2.44959754
H	3.40556808	-0.56474187	0.50365287
O	2.92739299	3.51193029	1.55465469
C	4.21189396	-0.57929104	2.92936794
H	4.96583640	0.21562808	2.90710183
H	4.56678683	-1.43234756	2.33237994
H	4.05027945	-0.90178748	3.95945115
C	4.17876291	4.16387910	1.75801719
H	4.53841960	4.62482291	0.82611275
H	4.00511570	4.94282392	2.50257935
H	4.93512389	3.46333312	2.12914352
S	-2.29620616	-0.46791611	0.14583495
C	-2.40576963	-0.85102129	-1.66635701
H	-2.43406046	0.09193936	-2.21891711
C	-3.66495516	-1.67546453	-1.93449104
H	-1.50723539	-1.40304564	-1.95680642
S	-2.38492650	2.62927218	-0.53981825
C	-1.94032083	4.37776471	-0.91493912
H	-1.49735953	4.83632274	-0.02517945
C	-3.20856686	5.13096608	-1.32355754
H	-1.20350617	4.40307750	-1.72441841
H	3.36694490	3.00786957	-0.38199783
H	-3.66161485	4.69742630	-2.22090062
H	-2.96321295	6.17572569	-1.54074599
H	-3.95578390	5.11952376	-0.52364437
H	-4.56814042	-1.12439730	-1.65296091
H	-3.65237206	-2.61928252	-1.37940874
H	-3.73315861	-1.91270028	-3.00178184

Structure A2′$_{rac}$

39

C	0.86738927	0.35256529	-0.72358648
C	1.87646199	0.95392536	0.02176362
C	1.63602623	2.11582712	0.73781143

C	0.38369250	2.72091625	0.71622361
C	-0.40861680	0.93667335	-0.75302164
C	-0.64818009	2.14186841	-0.03919301
H	0.19673522	3.64286978	1.25705561
H	1.04584935	-0.56926008	-1.26758960
C	3.30320513	0.52275170	0.23588309
O	3.86281459	1.53702913	1.08263109
C	2.89935691	2.54004102	1.43869740
O	3.32594852	-0.73697896	0.85021558
H	3.90838684	0.49031301	-0.68384356
O	3.28603438	3.80939685	0.99008936
H	2.82178238	2.54951607	2.53758349
C	4.63786718	-1.26953304	1.02841414
H	5.21832900	-0.66217016	1.73145156
H	5.17124271	-1.32440079	0.06834939
H	4.51141340	-2.27646362	1.42976152
C	4.43438500	4.33385728	1.65525364
H	4.57562398	5.34731203	1.27581368
H	5.32423684	3.73217843	1.44039716
H	4.27444608	4.37159296	2.74269480
S	-1.66854278	0.13325483	-1.76161218
C	-2.70321397	-0.67094592	-0.45027155
H	-2.08325838	-1.40345397	0.07449707
C	-3.91674998	-1.34089507	-1.09283240
H	-3.01367628	0.10443938	0.25445219
S	-2.25749908	2.95468621	-0.00139973
C	-2.29618789	3.73960702	-1.67914424
H	-1.43125276	4.40353491	-1.76519786
C	-3.60139551	4.51675164	-1.84991632
H	-2.21323559	2.94658786	-2.42650985
H	-4.47123531	3.85560909	-1.77786078
H	-3.62106113	4.99235344	-2.83644332
H	-3.70395501	5.30281204	-1.09453855
H	-3.61953334	-2.09929297	-1.82516912
H	-4.55419910	-0.60748719	-1.59710059
H	-4.51640452	-1.83643870	-0.32161865

*Estimating T_c for **M3***

M3 analogue **M3′** was used for computations.

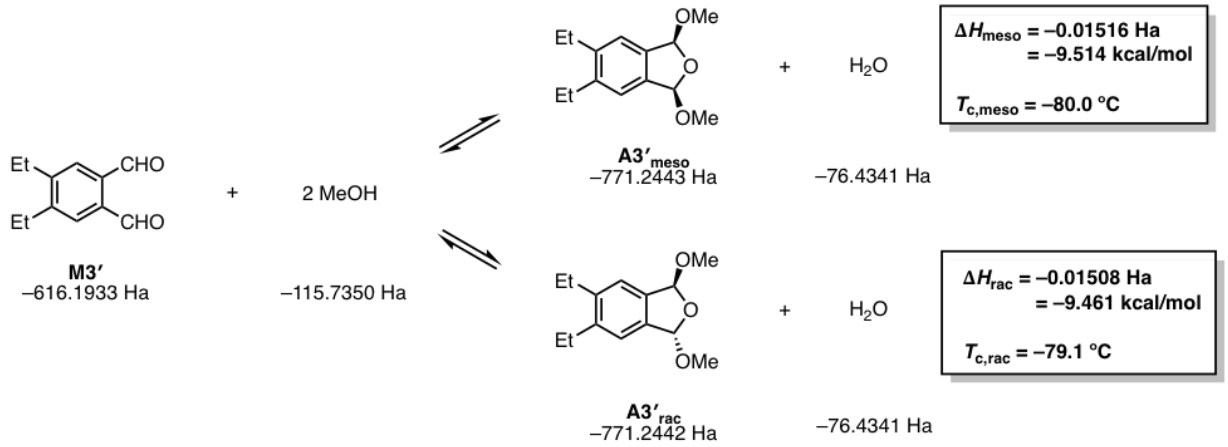

Figure S71. Calculated energies and T_c determination for **M3′**.

Structure M3′

28

C	-0.62167025	1.74477589	0.00046125
C	0.65447527	2.33100994	-0.00587956
C	1.78765668	1.48327857	-0.00628891
C	-0.82433917	0.36282473	0.00638206
C	1.58492694	0.09788498	-0.00043727
C	0.31435895	-0.48477014	0.00577069
H	-1.48284867	2.40591736	0.00076281
H	2.47403827	-0.52211324	-0.00097949
C	0.67409439	3.81500902	-0.01151205
O	1.65291484	4.54171987	-0.01719453
C	3.20041311	1.97602270	-0.01280148
O	4.15503853	1.21293762	-0.01119183
C	-2.21931704	-0.23652770	0.01329211
C	-3.39436153	0.74596105	0.01334965
H	-2.30914992	-0.89631820	0.88742993
H	-2.31494400	-0.90312930	-0.85503189
H	-3.38655877	1.39260267	0.89738751
H	-4.33900816	0.19376849	0.01892093
H	-3.39278591	1.38524250	-0.87605348
C	0.13686180	-1.99231764	0.01153925
C	1.41259124	-2.83840046	0.01075542
H	-0.47636536	-2.27194441	-0.85681036
H	-0.47137429	-2.26596014	0.88528913
H	2.02597144	-2.65344493	-0.87731356
H	1.15113116	-3.90104297	0.01557863
H	2.03144640	-2.64673512	0.89358131
H	3.34327999	3.06532272	-0.01719850
H	-0.34261592	4.26374612	-0.01128778

Structure A3′$_{meso}$

37

C	0.29610750	0.19300119	-0.20817588
C	1.44636422	0.89955715	0.13393562
C	1.44758785	2.28279332	0.14832202
C	0.29856183	2.99842352	-0.17868827
C	-0.87072888	0.88789375	-0.55088765
C	-0.86952320	2.31294748	-0.53574433
H	0.31138778	4.08217132	-0.14586476
H	0.30705333	-0.89121894	-0.19815006
C	2.79648860	0.39732802	0.56735626
O	3.59965761	1.58364752	0.68212173
C	2.79882908	2.77361537	0.59104444
O	2.67627110	-0.30442420	1.77654193
H	3.30564282	-0.24037645	-0.17213352
O	2.68089094	3.45181592	1.81373280
C	3.89891733	-0.87475923	2.23603853
H	4.63391873	-0.09722928	2.47194230
H	4.32298495	-1.55720346	1.48413416
H	3.65875859	-1.43835297	3.13943947
C	3.90461214	4.01201773	2.28281429
H	4.33007180	4.70593300	1.54232610
H	3.66545400	4.56099235	3.19543409
H	4.63824752	3.22938258	2.50585557
C	-2.14157743	0.14445287	-0.93284653
C	-2.07664836	-1.38572955	-0.91787421
H	-2.45540722	0.47233666	-1.93407503
H	-2.95142089	0.46561226	-0.26301890
H	-1.32848207	-1.76972201	-1.61978538
H	-3.04635209	-1.80143745	-1.20989485
H	-1.83751148	-1.77340086	0.07803852
C	-2.13906774	3.06651107	-0.90216717
C	-2.07177232	4.59589667	-0.85352693
H	-2.94994641	2.73188863	-0.24028802
H	-2.45229510	2.76101014	-1.91058982
H	-1.83370084	4.96134081	0.15103718
H	-3.04033746	5.01937443	-1.13805292
H	-1.32182447	4.99403609	-1.54558707
H	3.30884821	3.42455453	-0.13626368

Structure A3′$_{rac}$

37

C	0.26340866	0.14622705	-0.20722907
C	1.38631676	0.84906565	0.22207065
C	1.36735868	2.22936606	0.30417764
C	0.22517366	2.94687405	-0.04188215
C	-0.89964948	0.84263831	-0.55979893
C	-0.91865765	2.26514685	-0.47651772
H	0.23104189	4.02947312	0.01610222
H	0.29268027	-0.93640323	-0.25707098
C	2.73107787	0.34133437	0.66511213

O	3.48007571	1.52578863	0.97684862
C	2.70941390	2.71969528	0.77313819
O	2.58301398	-0.48657192	1.78928680
H	3.28899129	-0.20562312	-0.11176453
O	3.28626462	3.54306042	-0.20668869
H	2.68586982	3.26331241	1.73127805
C	3.80227040	-1.07251582	2.23928409
H	4.49494179	-0.30963495	2.61174166
H	4.28834938	-1.63943941	1.43126117
H	3.53849795	-1.75507229	3.04943454
C	4.53523703	4.11135423	0.18036476
H	4.83236382	4.78690306	-0.62394276
H	5.29860924	3.33645930	0.31182514
H	4.43396711	4.68218500	1.11549152
C	-2.14348896	0.10372697	-1.02880936
C	-2.05688613	-1.42462381	-1.08597846
H	-2.42087658	0.47643616	-2.02505460
H	-2.98434783	0.38172870	-0.37805180
H	-1.27695570	-1.76368108	-1.77628948
H	-3.00845870	-1.83843020	-1.43480363
H	-1.84928460	-1.85761122	-0.10169969
C	-2.18004933	3.02124549	-0.86577823
C	-2.13288905	4.54761305	-0.74752283
H	-3.01616479	2.64856445	-0.25777494
H	-2.44284623	2.75826966	-1.90015941
H	-1.94560821	4.87137886	0.28201937
H	-3.09228029	4.97393669	-1.05769177
H	-1.35635034	4.98268321	-1.38565752

*Estimating T_c for **M4***

M4 analogue **M4′** was used for computations.

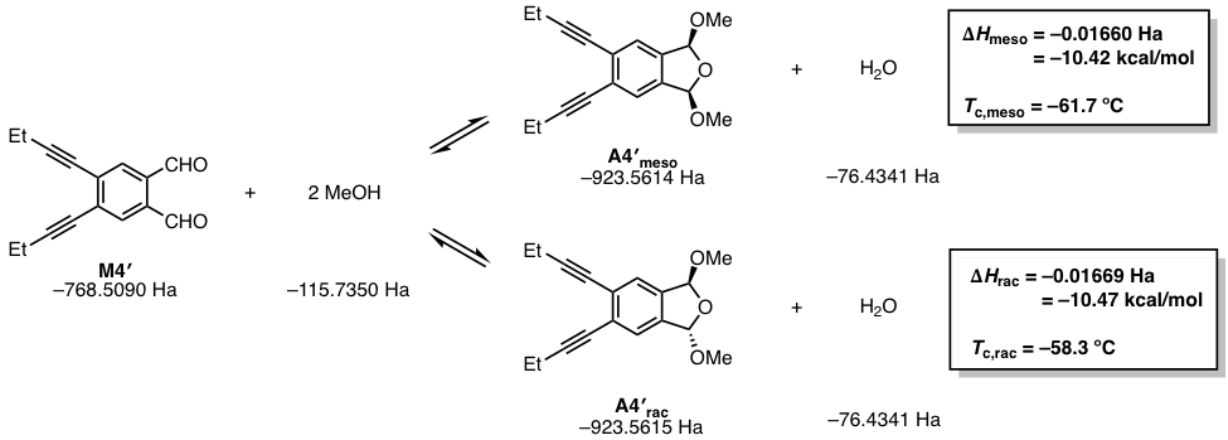

Figure S72. Calculated energies and T_c determination for **M4′**.

Structure M4′

32			
C	-0.74162828	1.55319961	2.67133937
C	0.43585813	2.00706295	3.27501776
C	1.60358198	1.19901919	3.19503701
C	-0.81868538	0.32909036	1.98709902
C	1.53360684	-0.01810860	2.51659556
C	0.35245420	-0.47858419	1.90917603
H	-1.63728790	2.16489466	2.72816841
H	2.43222147	-0.62300092	2.46496909
C	0.33441247	3.32358570	3.95456186
C	2.92194829	1.57428869	3.79930966
O	3.90513844	0.85581378	3.70607879
C	-2.04728649	-0.07928640	1.39247667
C	0.34321898	-1.73309007	1.23482504
H	2.96413029	2.53257592	4.33441333
C	-3.10189332	-0.41789882	0.89336722
C	-4.37342922	-0.81570492	0.28938913
C	0.35545463	-2.80596563	0.66497469
C	0.37883175	-4.10454033	-0.00755927
H	-4.93329155	-1.42324403	1.01318589
H	-4.16957219	-1.47258277	-0.56620949
C	-5.23706476	0.37772884	-0.16253964
H	-5.47630784	1.02894945	0.68323777
H	-6.17519814	0.01957220	-0.59791355
H	-4.71412185	0.97525395	-0.91492019
H	-0.63132776	-4.53398868	0.01455201
C	1.38225602	-5.09646063	0.61246211
H	0.62087286	-3.94896221	-1.06757580
H	1.14575850	-5.28473898	1.66366760

H	2.40225937	-4.70536450	0.55821775
H	1.34859798	-6.04952786	0.07531290
O	1.22024939	3.91650297	4.54552384
H	-0.67913691	3.77327126	3.88742942

Structure A4′$_{meso}$

41

C	0.87599372	0.23451633	0.24255844
C	2.03217266	0.92387753	0.57685474
C	2.05169988	2.31382654	0.61826978
C	0.91539395	3.05457971	0.32913768
C	-0.29192392	0.95724445	-0.07157336
C	-0.27248080	2.38555761	-0.02616648
H	0.92026676	4.13824717	0.38007636
H	0.84999049	-0.84995505	0.22643953
C	3.38495860	0.39984660	0.97941756
O	4.20630795	1.57404548	1.08116936
C	3.41973629	2.77581904	1.04394002
O	3.27465210	-0.30414606	2.18639341
H	3.86759791	-0.24050796	0.22512600
O	3.33469916	3.41922685	2.28589286
C	4.49598852	-0.89629242	2.62362399
H	5.24579785	-0.13111882	2.85262002
H	4.89716306	-1.58057446	1.86120768
H	4.26006903	-1.46110158	3.52718010
C	4.57213206	3.96191982	2.74190125
H	4.98624369	4.66879988	2.00763592
H	4.35419877	4.49234934	3.67047081
H	5.30490126	3.17021973	2.93339325
C	-1.48177521	0.25137582	-0.42567419
C	-1.44361243	3.14453003	-0.32891399
H	3.91889972	3.43975912	0.32134284
C	-2.42942691	3.80836608	-0.57933443
C	-3.61954450	4.60635071	-0.87672455
C	-2.48308160	-0.36801748	-0.72397026
C	-3.69068759	-1.11415790	-1.08009012
H	-4.49688820	4.11588945	-0.43425760
H	-3.78773456	4.60701025	-1.96229323
C	-3.52609728	6.05769726	-0.36825803
H	-3.39330888	6.08268120	0.71746793
H	-4.44047204	6.60642723	-0.61654401
H	-2.67826819	6.57696251	-0.82506909
C	-3.51024795	-2.64256709	-1.01026165
H	-4.00234933	-0.82616920	-2.09324624
H	-4.50824666	-0.80874901	-0.41324571
H	-2.72019929	-2.97317941	-1.69116188
H	-4.44066478	-3.14682297	-1.29100041
H	-3.23935329	-2.95756632	0.00183570

Structure A4′$_{rac}$

41

C	1.13252408	0.66342209	-1.12016193
C	2.04560081	1.10094358	-0.17237243
C	1.79271409	2.22754763	0.60169127
C	0.62091705	2.95345331	0.44656311
C	-0.06930749	1.37591030	-1.30084716
C	-0.32745498	2.53690846	-0.50837359
H	0.42488180	3.84110912	1.03868556
H	1.32093135	-0.22256440	-1.71721954
C	3.37832770	0.51965540	0.21650487
O	3.86702933	1.39202770	1.24579836
C	2.95667810	2.46561202	1.52588924
O	3.20724061	-0.78938464	0.68664069
H	4.12249896	0.51810491	-0.59593595
O	3.53198537	3.71525615	1.25398521
H	2.70142453	2.40983956	2.59627790
C	4.42885179	-1.45686169	0.99812235
H	4.93639461	-0.97958951	1.84370302
H	5.10337001	-1.46807225	0.12909670
H	4.16298278	-2.48229412	1.26101998
C	4.60254871	4.06057847	2.13094269
H	4.89761329	5.07936849	1.87355381
H	5.45498385	3.38525112	1.99889723
H	4.27484138	4.03090148	3.18054105
C	-1.01368922	0.92639134	-2.27302332
C	-1.53504688	3.28122768	-0.67182119
C	-2.55514421	3.92779287	-0.80106355
C	-3.78908342	4.70094235	-0.94567195
C	-1.79781364	0.52764028	-3.11058119
C	-2.75700739	0.03652604	-4.10076065
H	-4.55798469	4.06271959	-1.40066266
H	-3.61684991	5.52251526	-1.65409985
C	-4.31166786	5.27148646	0.38715050
H	-4.52029267	4.46770565	1.09938380
H	-5.23573871	5.83516542	0.22203674
H	-3.57496132	5.94229047	0.83906980
H	-3.55432044	0.78087771	-4.22465463
C	-3.37422432	-1.32578430	-3.72643999
H	-2.25803702	-0.04282929	-5.07585890
H	-3.91188006	-1.26169093	-2.77587390
H	-2.59824614	-2.09033658	-3.62523611
H	-4.07786984	-1.64828321	-4.50101539

*Estimating T_c for **M6***

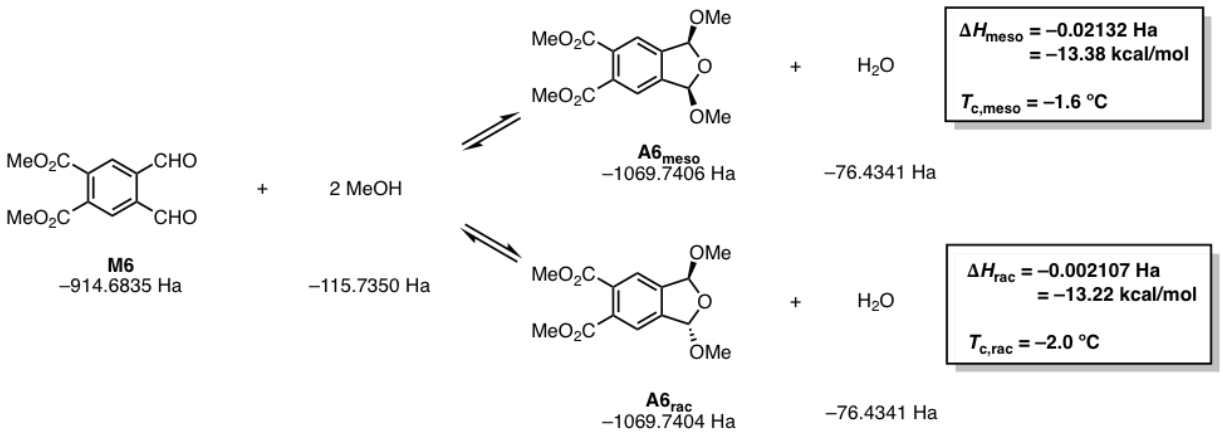

Figure S73. Calculated energies and T_c determination for **M6**.

Structure M6

28

C	-0.47673263	1.53267987	-0.18905039
C	0.76161302	2.18252983	-0.12864378
C	1.93017790	1.41173954	0.09786524
C	-0.59295355	0.14531343	-0.05073867
C	1.80770362	0.02679850	0.24237546
C	0.57103084	-0.61775483	0.15642422
H	-1.37763806	2.11589869	-0.34739891
H	2.71025046	-0.54717831	0.42566480
C	0.72267949	3.65690738	-0.32902002
O	1.67930956	4.40519423	-0.40792105
C	3.30971484	1.99593481	0.22533772
O	4.29799182	1.28730127	0.30598745
C	-1.93476893	-0.51738119	-0.06807139
O	-2.91189271	0.31742045	-0.47472538
C	0.56061898	-2.11659238	0.32772457
O	0.35037591	-2.74299877	-0.83894630
C	0.26958964	-4.18349187	-0.77173787
H	3.38475119	3.09137857	0.24915281
H	-0.30760659	4.06100998	-0.41753771
O	0.80201498	-2.66258265	1.38210108
O	-2.13074896	-1.67068676	0.26076458
C	-4.24492102	-0.23584761	-0.49189044
H	0.15040325	-4.51251133	-1.80312078
H	-0.59380311	-4.47331563	-0.16855754
H	1.18107229	-4.59567431	-0.33383087
H	-4.88685108	0.57302545	-0.83819611
H	-4.53193680	-0.55922380	0.51106699
H	-4.29046436	-1.08707256	-1.17460773

Structure A6$_{meso}$

37

C	0.83426168	-0.16362544	-0.01454376
C	1.86853613	0.72686699	0.24924053
C	1.67603936	2.09781436	0.14616228
C	0.44024799	2.62195039	-0.21099873
C	-0.40754277	0.34334459	-0.41448511
C	-0.61295001	1.73980198	-0.49703541
H	0.27277849	3.69185794	-0.25123955
H	0.97001531	-1.23591785	0.07999831
C	3.28361865	0.45877208	0.69468468
O	3.91363182	1.74918681	0.65844943
C	2.95046477	2.80533369	0.52883468
O	3.26820975	-0.11985050	1.96759371
H	3.86028200	-0.17646470	0.00524381
O	2.74320552	3.52235647	1.71329095
C	4.55451232	-0.50841584	2.44710226
H	5.19603924	0.36433079	2.61270440
H	5.04676151	-1.19245546	1.74061166
H	4.38758500	-1.02512216	3.39359874
C	3.87401655	4.28060281	2.13907046
H	4.20364976	4.97235748	1.35005239
H	3.55166697	4.85287219	3.01049266
H	4.70632204	3.62474750	2.41711603
C	-1.46023140	-0.66897145	-0.76883624
O	-1.94626934	-0.47184476	-2.00881613
C	-3.01724736	-1.35000450	-2.40714946
C	-1.97933991	2.28618602	-0.76372772
O	-1.93627189	3.53146806	-1.28749045
C	-3.21379146	4.16115348	-1.50628281
H	3.34650339	3.47941889	-0.24597247
O	-3.01725249	1.70718353	-0.50836128
O	-1.76602690	-1.60260720	-0.05594222
H	-3.25516749	-1.06804600	-3.43236590
H	-3.88037665	-1.19956707	-1.75430561
H	-2.69622754	-2.39283518	-2.35564048
H	-2.98412202	5.14260321	-1.92002213
H	-3.75756151	4.25445326	-0.56325757
H	-3.81005948	3.57491560	-2.20927391

Structure A6$_{rac}$

37

C	0.32737148	-0.17259611	-0.49331652
C	1.47254487	0.56829763	-0.22387568
C	1.41511654	1.94718834	-0.08211604
C	0.21051008	2.62942994	-0.19730699
C	-0.89356754	0.49759758	-0.63172490
C	-0.95791813	1.90031056	-0.46572109
H	0.15689020	3.70455602	-0.07305188
H	0.36117007	-1.25228120	-0.59419044
C	2.89057392	0.10482998	-0.01406842

O	3.63158746	1.31187367	0.22220724
C	2.79708198	2.47844060	0.19269797
O	3.17236362	3.35958910	-0.82849258
H	2.89821982	2.98271893	1.16688128
C	4.43755912	3.98624059	-0.61765025
H	4.56487500	4.70523026	-1.42861337
H	5.25094336	3.25300910	-0.64345490
H	4.45571204	4.51655898	0.34548598
C	-2.08622414	-0.34931419	-0.97895538
O	-2.68557671	0.06913343	-2.10909337
C	-3.88824875	-0.63536268	-2.47552594
C	-2.28185978	2.59584265	-0.45260531
O	-2.17143797	3.90887025	-0.75074101
C	-3.39496700	4.66797880	-0.69618123
H	3.33602351	-0.39024563	-0.89158779
O	2.93951033	-0.75871764	1.08541124
C	4.22921414	-1.32370276	1.32236345
H	4.11288685	-2.01883284	2.15523717
H	4.58421100	-1.87138280	0.43733353
H	4.95635818	-0.54833982	1.58635943
O	-2.41017575	-1.34175301	-0.35985387
O	-3.33782714	2.06433410	-0.16859679
H	-4.20344840	-0.19592856	-3.42145852
H	-4.65044805	-0.48710230	-1.70680861
H	-3.68676571	-1.70268081	-2.59128657
H	-3.11166847	5.68882051	-0.95054913
H	-3.82720276	4.62260692	0.30631701
H	-4.11631728	4.27626242	-1.41704771

*Estimating T_c for **M7***

M7 analogue **M7′** was used for computations.

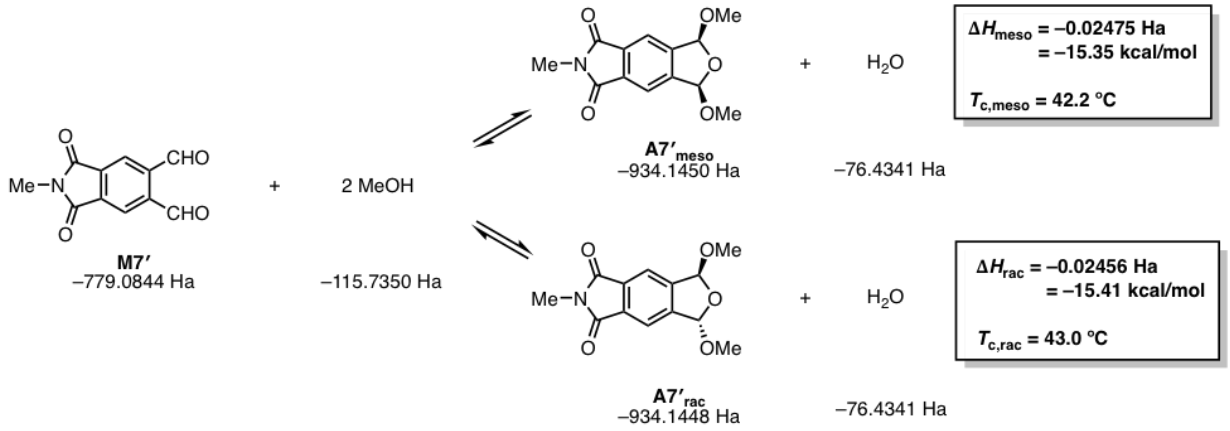

Figure S74. Calculated energies and T_c determination for **M7′**.

Structure M7′

23

C	-0.28504444	1.23709056	-0.17765554
C	0.80984322	2.11010536	-0.01746858
C	2.12118035	1.58426746	0.15944926
C	-0.05568246	-0.12738527	-0.15675882
C	2.32537957	0.19217411	0.17592979
C	1.22995381	-0.64040601	0.01832754
H	-1.28986684	1.62732140	-0.31312724
H	3.33027556	-0.19437458	0.30958766
C	0.46071249	3.56186821	-0.04830232
O	1.22314394	4.49981060	0.08486596
C	3.34467911	2.44501107	0.33073728
O	4.44874770	1.95248299	0.48375843
C	-1.00727744	-1.27375119	-0.29859342
C	1.13823249	-2.13636028	-0.00675600
N	-0.22008120	-2.42951653	-0.19801345
C	-0.74334099	-3.78511631	-0.28402933
H	3.19673390	3.53219721	0.31007555
H	-0.62153752	3.74528231	-0.21124951
O	2.02373641	-2.95914752	0.10922909
H	-1.82214617	-3.71496375	-0.42561073
H	-0.52169228	-4.33345605	0.63503136
H	-0.28920467	-4.31166272	-1.12732724
O	-2.21077453	-1.24356105	-0.46640974

Structure A7′$_{meso}$

32

C	1.21205686	-0.50685943	-0.12300755
C	2.07945158	0.54009813	0.20003023
C	1.69923231	1.87740009	0.09307196
C	0.42712155	2.25541772	-0.34541557
C	-0.04588974	-0.12974529	-0.57506452
C	-0.42774622	1.21437345	-0.68367050
H	0.11742394	3.29300923	-0.41456234
H	1.49278086	-1.55031266	-0.02462608
C	3.48855520	0.47179291	0.73195352
O	3.93092346	1.83695072	0.74809477
C	2.84062011	2.74891640	0.55299881
O	3.47538758	-0.12642238	1.99640757
H	4.19037924	-0.06488783	0.07557563
O	2.46188886	3.42465598	1.71787184
C	4.77167961	-0.32259656	2.56081852
H	5.26411826	0.63558452	2.75821033
H	5.40323709	-0.92670119	1.89349202
H	4.62127243	-0.85855062	3.49925498
C	3.44668410	4.33508177	2.20687507
H	3.72152266	5.06834080	1.43495063
H	2.99442825	4.85300537	3.05398554
H	4.34483323	3.80199658	2.53672426
C	-1.19783793	-0.97422166	-1.01489655
N	-2.21837158	-0.08006555	-1.36643546
C	-3.52202513	-0.49827690	-1.85562540
C	-1.83100178	1.25884959	-1.19579874
H	3.18514880	3.47397394	-0.20027245
O	-1.28018961	-2.18692021	-1.07627319
H	-4.10694316	0.40187550	-2.04757825
H	-4.02559008	-1.11875283	-1.10965586
H	-3.41382793	-1.07564687	-2.77782061
O	-2.52670280	2.22899725	-1.43088262

Structure A7′$_{rac}$

32

C	0.56838839	-0.31909116	-0.70504985
C	1.63446520	0.49540586	-0.31258897
C	1.48336727	1.86555318	-0.10924200
C	0.25838648	2.51392193	-0.29022610
C	-0.64885966	0.32558263	-0.88324665
C	-0.80000450	1.70425183	-0.68116128
H	0.13623338	3.58214234	-0.14465097
H	0.67479303	-1.38846567	-0.85443384
C	3.06027631	0.10653776	-0.01659145
O	3.71002770	1.33832000	0.32377662
C	2.81214686	2.45553394	0.28838253
O	3.19933550	3.40456732	-0.66358095
H	2.81426895	2.91569119	1.28920536
C	4.40550243	4.09731778	-0.33932188

H	4.53825154	4.86051737	-1.10763092
H	5.26412211	3.41727519	-0.34199045
H	4.32587156	4.58074495	0.64489295
C	-1.97411739	-0.23221342	-1.29199974
N	-2.85785148	0.85885162	-1.31277206
C	-2.22567352	2.05812697	-0.95647822
H	3.59591380	-0.32332216	-0.87792051
O	3.07658955	-0.80500590	1.04517772
C	4.37662725	-1.30396699	1.36323290
H	4.23530903	-2.06280204	2.13431422
H	4.84526421	-1.76317495	0.48100703
H	5.02252876	-0.50551537	1.74375055
O	-2.26756207	-1.38220436	-1.55954453
O	-2.77161738	3.14415173	-0.89721337
C	-4.26620425	0.76507193	-1.66232374
H	-4.48826568	-0.28420712	-1.85915242
H	-4.47779591	1.36333265	-2.55282624
H	-4.88463744	1.13073095	-0.83853376

*Estimating T_c for **M8***

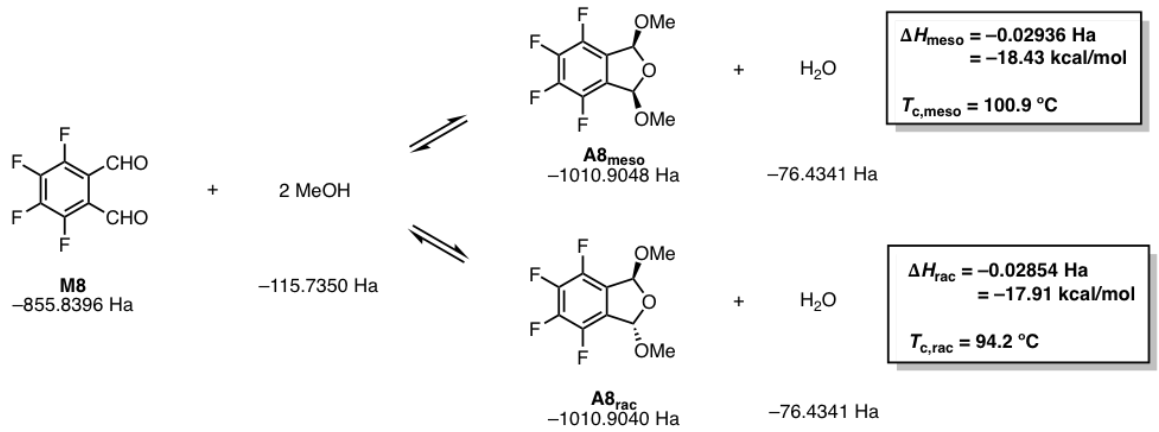

Figure S75. Calculated energies and T_c determination for **M8**.

Structure M8

16

C	-0.27749672	2.24255637	0.01415355
C	0.98939025	2.83283925	0.01113526
C	2.14095422	2.00375323	-0.00909691
C	-0.43990004	0.85920547	-0.00147185
C	1.96500639	0.62174602	-0.02503167
C	0.68874125	0.04721070	-0.02534367
F	-1.38803634	3.00173061	0.05612429
F	3.00620901	-0.21644516	-0.08831935
C	1.09638032	4.31253608	0.07868774
O	2.14995116	4.89727648	0.25891115
C	3.54052233	2.57150511	-0.07540297
O	4.44621658	2.14132614	0.60393608
H	3.69618071	3.37317046	-0.81504853
H	0.15152058	4.86836107	-0.04319968
F	-1.65999580	0.31645739	0.01136865
F	0.54961611	-1.27846922	-0.05504209

Structure $A8_{meso}$

25

C	0.68963006	0.19324522	-0.03868440
C	1.83942645	0.89341606	0.28523694
C	1.84072455	2.28464478	0.30091382
C	0.69223563	2.99409954	-0.00701225
C	-0.47179975	0.89985318	-0.35531959
C	-0.47054102	2.29701391	-0.33939463
F	0.66788230	4.33896080	-0.00591608
F	0.66279737	-1.15124043	-0.06828212
C	3.20018709	0.39529633	0.70670890
O	4.00715768	1.58220824	0.72138010
C	3.20270530	2.77091110	0.73218144
O	3.09019819	-0.22287917	1.95303498

H	3.67551696	-0.28461996	-0.01425366
O	3.09524885	3.36321001	1.99114403
C	4.29736067	-0.83591768	2.40798450
H	5.07686282	-0.08697370	2.58485883
H	4.65878922	-1.57622766	1.68029733
H	4.05161931	-1.33927153	3.34395413
C	4.30259450	3.96903843	2.45528837
H	4.66093535	4.72418418	1.74147441
H	4.05836531	4.45350085	3.40156516
H	5.08395201	3.21825238	2.61553820
H	3.67873744	3.46478473	0.02509072
F	-1.59545547	0.24552422	-0.68102901
F	-1.59296082	2.96068618	-0.64992014

Structure A8$_{rac}$

25

C	0.48756050	-0.02640449	-0.19351185
C	1.60594788	0.60266921	0.32825060
C	1.62369307	1.98152304	0.50846998
C	0.51661997	2.74951567	0.18661381
C	-0.62935501	0.74019027	-0.52948901
C	-0.61755523	2.12346648	-0.33291350
F	0.49939307	4.08190650	0.36673945
F	0.44805510	-1.35566898	-0.39228831
C	2.90688348	0.01945242	0.82037999
O	3.68414806	1.16327883	1.19776819
C	2.97906535	2.39895650	1.02057794
O	3.59571483	3.21151923	0.06688998
H	2.95454817	2.91325332	1.99268286
C	4.84575699	3.75839127	0.49179321
H	5.17200809	4.43138127	-0.30228248
H	5.59102431	2.96915436	0.63766568
H	4.72530573	4.32722556	1.42451943
H	3.47132730	-0.53236905	0.05420745
O	2.64819207	-0.81203018	1.91217043
C	3.79192010	-1.52773119	2.38254230
H	4.22932348	-2.13540358	1.57792490
H	3.43677860	-2.18443014	3.17790441
H	4.54974654	-0.84351757	2.77926338
F	-1.72304609	0.15687208	-1.03922494
F	-1.70322638	2.84249917	-0.65046391

IX. References

(1) Kaitz, J.A.; Diesendruck, C.E.; Moore, J.S. End Group Characterization of Poly(phthalaldehyde): Surprising Discovery of a Reversible, Cationic Macrocyclization Mechanism. *J. Am. Chem. Soc.* **2013**, *135*, 12755–12761.

(2) Percec, V.; Rudick, J.G.; Peterca, M.; Wagner, M.; Obata, M.; Mitchell, C.M.; Cho, W.-D.; Balagurusamy, V.S.K.; Heiney, P.A. Thermoreversible Cis–Cisoidal to Cis–Transoidal Isomerization of Helical Dendronized Polyphenylacetylenes *J. Am. Chem. Soc.* **2005**, *127*, 15257–15264.

(3) Bisai, V.; Suneja, A.; Singh, V.K. Asymmetric Alkynylation/Lactamization Cascade: An Expeditious Entry to Enantiometrically Enriched Isoindolinones. *Angew. Chem. Int. Ed.* **2014**, *3*, 10737–10741.

(4) Hert, J.; Hunziker, D.; Mattei, P.; Mauser, H.; Tang, G.; Wang, L. New Octahydro-Pyrrolo[3,4-C]-Pyrrole Derivatives and Analogs Thereof as Autotaxin Inhibitors. Patent WO/2014/139978. March 11, 2014.

(5) DiLauro, A.M.; Lewis, G.G.; Phillips, S.T. Self-Immolative Poly(4,5-dichlorophthalaldehyde) and its Applications in Multi-Stimuli-Responsive Macroscopic Plastics. *Angew. Chem. Int. Ed.* **2015**, *54*, 6200–6205.

(6) Hennessy, E.J.; Buchwald, S.L. Synthesis of 4,5-Dianilinophthalimide and Related Analogues for Potential Treatment of Alzheimer's Disease via Palladium-Catalyzed Amination. *J. Org. Chem.* **2005**, *70*, 7371–7375.

(7) Murata, M.; Buchwald, S.L. A General and Efficient Method for the Palladium-Catalyzed Cross-Coupling of Thiols and Secondary Phosphines. *Tetrahedron* **2004**, *60*, 7397–7403.

(8) Reddy, V.K.; Valasinas, A.; Sarkar, A.; Basu, H.S.; Marton, L.J.; Frydman, B. Conformationally Restricted Analogues of 1*N*,12*N*-Bisethylspermine: Synthesis and Growth Inhibitory Effects on Human Tumor Cell Lines. *J. Med. Chem.* **1998**, *41*, 4723–4732.

(9) Kleijn, H.; Westmijze, H.; Meijer, J.; Vermeer, P. A Convenient Synthesis of Specifically Substituted Conjugated Dienes *via* Organocopper(I) Induces S_N2' Reactions. An Attractive Route to Myrcene. *Recl. Trav. Chim. Pays-Bas,* **1980**, *99*, 340–343.

(10) Levick, M.T.; Coote, S.C.; Grace, I.; Lambert, C.; Turner, M.L.; Procter, D.J. Phase Tag-Assisted Synthesis of Benzo[*b*]carbazole End-Capped Oligothiophenes. *Org. Lett.* **2012**, *14*, 5744–5747.

(11) Gelman, D.; Buchwald, S.L. Efficient Palladium-Catalyzed Coupling of Aryl Chlorides and Tosylates with Terminal Alkynes: Use of a Copper Cocatalyst Inhibits the Reaction. *Angew. Chem. Int. Ed.* **2003**, *42*, 5993–5996.

(12) Brown, H.C.; Narasimham, S.; Choi, Y.M. Selective Reductions. 30. Effect of Cation and Solvent on the Reactivity of Saline Borohydrides for Reduction of Carboxylic Esters. Improved Procedures for the Conversion of Esters to Alcohols by Metal Borohydrides. *J. Org. Chem.* **1982**, *47*, 4702–4708.

(13) Song, D.; Sun, S.; Tian, Y.; Huang, S.; Ding, Y.; Yuan, Y.; Hu, A. Maleimide-Based Acyclic Enediyne for Efficient DNA-Cleavage and Tumor Cell Suppression. *J. Mater. Chem. B* **2015**, *3*, 3195–3200.

(14) Naganawa, A.; Matsui, T.; Ima, M.; Saito, T.; Murota, M.; Aratani, Y.; Kijima, H.; Yamamoto, H.; Maruyama, T.; Ohuchida, S.; Nakai, H.; Toda, M. Further Optimization of Sulfonamide Analogs as EP1 Receptor Antagonists: Synthesis and Evaluation of Bioisosteres for the Carboxylic Acid Group. *Bioorg. Med. Chem.* **2006**, *14*, 7121–7137.

(15) Ammann, C.; Meier, P.; Merbach, A.E. A Simple Multinuclear NMR Thermometer. *J. Mag. Res.* **1982**, *46*, 319–321.

(16) Schwartz, J.M.; Engler, A.; Phillips, O.; Lee, J.; Kohl, P.A. Determination of Ceiling Temperature and Thermodynamic Properties of Low Ceiling Temperature Polyaldehydes. *J. Polym. Sci. Part A: Polym. Chem.* **2017**, *56*, 221–228.

(17) Tang, S.; Yourdkhani, M.; Possanza Casey, P.M.; Sottos, N.R.; White, S.R.; Moore, J.S. Low–Ceiling-Temperature Polymer Microcapsules with Hydrophobic Payloads via Rapid Emulstion-Solvent Evaporation. *ACS Appl. Mater. Interfaces* **2017**, *9*, 20115–20123.

(18) Tang, S.; Tang, L.; Lu, X.; Liu, H.; Moore, J.S. Programmable Payload Release from Transient Polymer Microcapsules Triggered by a Specific Ion Coactivation Effect. *J. Am. Chem. Soc.* **2018**, *140*, 94–97.

(19) Shao, Y.; Gan, Z.; Epifanovsky, E.; Gilbert, A.T.B.; Wormit, M.; Kussmann, J.; Lange, A.W.; Behn, A.; Deng, J.; Feng, X.; Ghosh, D.; Goldey, M.; Horn, P.R.; Jacobson, L.D.; Kaliman, I.; Khaliullin, R.Z.; Kús, T.; Landau, A.; Liu, J.; Proynov, E.I.; Rhee, Y.M.; Richard, R.M.; Rohrdanz, M.A.; Steele, R.P.; Sundstrom, E.J.; Woodcock III, H.L.; Zimmerman, P.M.; Zuev, D.; Albrecht, B.; Alguire, E; Austin, B.; Beran, G.J.O.; Bernard, Y.A.; Berquist, E.; Brandhorst, K.; Bravaya, K.B.; Brown, S.T.; Casanova, D.; Chang, C.-M.; Chen, Y.; Chien, S.H.; Closser, K.D.; Crittenden, D.L.; Diedenhofen, M.; DiStasio Jr., R.A.; Dop, H.; Dutoi, A.D.; Edgar, R.G.; Fatehi, S.; Fusti-Molnar, L.; Ghysels, A.; Golubeva-Zadorozhnaya, A.; Gomes, J.; Hanson-Heine, M.W.D.; Harbach, P.H.P.; Hauser, A.W.; Hohenstein, E.G.; Holden, Z.C.; Jagau, T.-C.; Ji, H.; Kaduk, B.; Khistyaev, K.; Kim, J.; Kim, J.; King, R.A.; Klunzinger, P.; Kosenkov, D.; Kowalczyk, T.; Krauter, C.M.; Lao, K.U.; Laurent, A.; Lawler, K.V.; Levchenko, S.V.; Lin, C.Y.; Liu, F.; Livshits, E.; Lochan, R.C.; Luenser, A.; Manohar, P.; Manzer, S.F.; Mao, S.-P.; Mardirossian, N.; Marenich, A.V.; Maurer, S.A.; Mayhall, N.J.; Oana, C.M.; Olivares-Amaya, R.; O'Neill, D.P.; Parkhill, J.A.; Perrine, T.M.; Peverati, R.; Pieniazek, P.A.; Prociuk, A.; Rehn, D.R.; Rosta, E.; Russ, N.J.; Sergueev, N.; Sharada, S.M.; Sharmaa, S.; Small, D.W.; Sodt, A.; Stein, T.; Stück, D.; Su, Y.-C.; Thom, A.J.W.; Tsuchimochi, T.; Vogt, L.; Vydrov, O.; Wang, T.; Watson, M.A.; Wenzel, J.; White, A.; Williams, C.F.; Vanovschi, V.; Yeganeh, S.; Yost, S.R.; You, Q.-Z.; Zhang, I.Y.; Zhang, X.; Zhou, Y.; Brooks, B.R.; Chan, G.K.L.; Chipman, D.M.; Cramer, C.J.; Goddard III, W.A.; Gordon, M.S.; Hehre, W.J.; Klamt, A.; Schaefer III, H.F.; Schmidt, M.W.; Sherrill, C.D.; Truhlar, D.G.; Warshel, A.; Xua, X.; Aspuru-Guzik, A.; Baer, R.; Bell, A.T.; Besley, N.A.; Chai, J.-D.; Dreuw, A.; Dunietz, B.D.; Furlani, T.R.; Gwaltney, S.R.; Hsu, C.-P.; Jung, Y.; Kong, J.; Lambrecht, D.S.; Liang, W.; Ochsenfeld, C.; Rassolov, V.A.; Slipchenko, L.V.; Subotnik, J.E.; Van Voorhis, T.; Herbert, J.M.; Krylov, A.I.; Gill, P.M.W.; Head-Gordon, M. Advances in Molecular Quantum Chemistry Contained in the Q-Chem 4 Program Package. *Mol. Phys.* **2015**, *113*, 184–215.

(20) Becke, A.D. A New Mixing of Hartree–Fock and Local Density-Functional Theories. *J. Chem. Phys.* **1993**, *98*, 1372–1377.

(21) (a) Hehre, W. J., Ditchfield, R., Pople, J. A. Self-Consistent Molecular Orbital Methods. XII. Further Extensions of Gaussian-Type Basis Sets for Use in Molecular Orbital Studies of Organic Molecules. *J. Chem. Phys.* **1972**, *56*, 2257–2261. (b) Clark, T.; Chandrasekhar, J.; Spitznagel, G.W.; Schleyer, P.V.R. Efficient Diffuse Function-Augmented Basis Sets for Anion Calculations. III. The 3-21+G Basis Set for First-Row Elements, Li–F. *J. Comput. Chem.* **1983**, *4*, 294–301. (c) Spitznagel, G. W.; Clark, T.; Schleyer, P.V.R.; Hehre, W.J. An Evaluation of the Performance of Diffuse Function-Augmented Basis Sets for Second Row Elements, Na–Cl. *J. Comput. Chem.* **1987**, *8*, 1109–1116. (d) Hariharan, P.C.; Pople, J.A. The Influence of Polarization Functions on Molecular Orbital Hydrogenation Energies. *Theor. Chim. Acta.* **1973**, *28*, 213–222. (e) Francl, M.M.; Pietro, W.J.; Hehre, W.J.; Brinkley, S.; Gordon, M.S.; DeFrees, D.J.; Pople, J.A. Self-Consistent Molecular Orbital Methods. XXIII. A Polarization-Type Basis Set for Second-Row Elements. *J. Chem. Phys.* **1982**, *77*, 3654–3665.